

**EPIGENETIC MECHANISMS OF ANTI-CANCER EFFECTS OF DIETARY  
STILBENOIDS**

by

Megan Beetch

B.Sc., The University of Saint Thomas, 2015

A THESIS SUBMITTED IN PARTIAL FULFILLMENT OF  
THE REQUIREMENTS FOR THE DEGREE OF

DOCTOR OF PHILOSOPHY

in

THE FACULTY OF GRADUATE AND POSTDOCTORAL STUDIES  
(Human Nutrition)

THE UNIVERSITY OF BRITISH COLUMBIA  
(Vancouver)

April 2020

© Megan Beetch, 2020

The following individuals certify that they have read, and recommend to the Faculty of Graduate and Postdoctoral Studies for acceptance, the dissertation entitled:

Epigenetic mechanisms of anti-cancer effects of dietary stilbenoids

submitted by Megan Beetch in partial fulfillment of the requirements for

the degree of Doctor of Philosophy

in Human Nutrition

**Examining Committee:**

Dr. Barbara Stefanska (Human Nutrition)

Supervisor

Dr. Carolyn Brown (Medical Genetics)

Supervisory Committee Member

Supervisory Committee Member

Dr. Simone Castellarin (Plant Science)

University Examiner

Dr. Michael Kobor (Medical Genetics)

University Examiner

**Additional Supervisory Committee Members:**

Supervisory Committee Member

Supervisory Committee Member

## Abstract

Epigenetics refers to control of gene expression without changes to the underlying DNA sequence. DNA methylation, a dynamic epigenetic modification responsive to environmental factors, underlies genomic instability, silencing of tumor suppressor genes (TSGs), and activation of genes driving cancer development. Reversing DNA methylation patterns established during carcinogenesis constitutes a promising anti-cancer strategy. Interestingly, certain dietary polyphenols, such as stilbenoids abundantly found in grapes and blueberries, have been shown to exert anti-cancer effects through epigenetic gene regulation. The overarching objective of my research is to understand epigenetic mechanisms of stilbenoids' anti-cancer effects. We hypothesize that dietary stilbenoids, resveratrol (RSV) and pterostilbene (PTS), modulate DNA methylation patterns and thereby gene transcription via modifying expression and activity of epigenetic enzymes such as DNA methyltransferases (DNMTs) and transcriptional machinery such as transcription factors (TFs). Stilbenoid-induced changes in DNA methylation and transcriptional machinery could, in turn, lead to reactivation of methylation-silenced TSGs and downregulation of epigenetically-activated oncogenes leading to reduced cancer development.

Upon treatment with RSV (15  $\mu$ M, 9 days), DNA methylation levels in MCF10CA1a breast cancer cells were altered as assessed by genome-wide DNA methylation analysis. Hypermethylated CpG sites corresponded to genes predominantly associated with oncogenic functions, whereas hypomethylated sites were located in genes with potential tumor suppressor roles. Changes in methylation and expression of candidate oncogenes and TSGs were examined using pyrosequencing and qPCR, respectively, upon treatment with RSV or PTS. Further, chromatin immunoprecipitation (ChIP) sequencing assessed DNA binding events, including

occupancy of DNMTs and TFs at stilbenoid-mediated differentially methylated sites. Specific putative roles for *de novo* DNMTs in mediating changes in DNA methylation patterns upon exposure to stilbenoids were established. Based on our findings in cell lines, we turned to an *in vivo* model of methyl donor deficiency to assess the contribution of methyl donors, another important factor for maintaining normal DNA methylation patterns, to carcinogenesis. Collectively, these findings provide evidence that dietary stilbenoids may exert their anti-cancer effects, at least partially, by impacting DNA methylation machinery, and as a result, this line of evidence has potential to be used to develop novel anti-cancer approaches.

## **Lay Summary**

Epigenetics refers to control of gene expression without changes to the underlying DNA sequence. DNA methylation, a dynamic epigenetic modification that is responsive to environmental factors including diet, is altered during cancer development. The goal of my thesis research is to understand how natural compounds derived from the diet, namely a class of polyphenols found abundantly in grapes and blueberries, can act as safe agents with the capacity to reverse aberrant DNA methylation patterns that underlie cancer. More specifically, providing insights into mechanistic players governing DNA methylation events in cancer will inform chemopreventive strategies and support anti-cancer efforts. As a whole, this work will contribute to advancing the knowledgebase surrounding the anti-cancer effects attributed to bioactive compounds.

## **Preface**

Contributions to design of research program: Together, Dr. Barbara Stefanska and I conceived the research plan and experiments.

Contributions to various parts of the research: Processing of genome-wide data was undertaken in collaboration with various collaborators, as explained in the next section. I performed all analyses of processed genome-wide data and wet lab work. CRISPR-Cas9 knockout of *DNMT3B* from MCF10CA1a breast cancer cells was performed in collaboration with Dr. Carolyn Brown from the Department of Medical Genetics at UBC, and Thomas Dixon-McDougall, a PhD candidate from Dr. Brown's group, was directly involved in the experiment. Conception and planning for the year-long rat feeding project was completed prior to my joining the lab in 2015, but I was involved in blood draws, sacrifice, and assessing endpoints during the last 4 months of the study and beyond. Rat housing, handling, feeding and weighing throughout the 52-week timeline was done in collaboration with the Biological Evaluation Shared Resource within the Purdue University Center for Cancer Research (previous location of Dr. Stefanska's lab). Histopathological analysis by H&E staining was conducted by board-certified animal pathologist Dr. Abigail Cox from Purdue University. Liquid chromatography-mass spectroscopy (LC-MS) to measure SAM and SAH levels in rat livers was performed in collaboration with Dr. Tao Huan from the Department of Chemistry at UBC.

Contributions to analysis of genome-wide data: Processing of genome-wide data was performed by Dr. Stefanska's group in collaboration with other researchers. Illumina 450K DNA methylation microarray was processed by Dr. Stefanska and Dr. Katarzyna Lubecka (a previous

postdoc in Dr. Stefanska's lab) prior to my joining the lab. Chromatin immunoprecipitation (ChIP) sequencing (calling peaks, aligning to genome, assigning peaks with gene names and chromatin states) was performed in collaboration with Dr. LeAnn Howe from the Department of Biochemistry at UBC, and Dr. Benjamin Martin, a PhD candidate in Dr. Howe's group at that time, was directly involved in the analyses. Following generation of the ChIP sequencing data files, I performed analyses to identify candidate genes, etc. Initially, RNA sequencing data was processed by Dr. Nadia Atallah from the Purdue University Center for Cancer Research Bioinformatics Core. However, I re-analyzed the data using an online bioinformatics platform called Galaxy ([usegalaxy.org](http://usegalaxy.org)).

Chapter 1 Figures. Figures in Chapter 1 are my original work published in **Beetch M**, Harandi-Zadeh S, Shen K, Lubecka K, Kitts DD, O'Hagan HM, Stefanska B. (2020) Dietary antioxidants remodel DNA methylation patterns in chronic disease. *Br J Pharmacol.* Mar;177(6):1382-1408. The British Journal of Pharmacology is published by Wiley, which gives contributors permission to reuse figures in theses.

Chapter 2. A version of this material has been published as **Beetch M**, Lubecka K, Shen K, Flower K, Harandi-Zadeh S, Suderman M, Flanagan JM, Stefanska B. (2019) Stilbenoid-mediated epigenetic activation of Semaphorin 3A in breast cancer cells involves changes in dynamic interactions of DNA with DNMT3A and NF1C transcription factor. *Mol Nutr Food Res.* Oct;63(19):e1801386. I conducted the analyses and experiments, wrote the manuscript with Dr. Stefanska, and addressed edits and revision from both my supervisor (Stefanska B) and reviewers. The other authors on this paper assisted with initial analysis of the Illumina 450K

DNA methylation microarray (Lubecka K, Flower K, Suderman M, Flanagan JM, Stefanska B)  
and some experimental work (Lubecka K, Shen K, Harandi-Zadeh S).

# Table of Contents

<b>Abstract.....</b>	<b>iii</b>
<b>Lay Summary .....</b>	<b>v</b>
<b>Preface.....</b>	<b>vi</b>
<b>Table of Contents .....</b>	<b>ix</b>
<b>List of Tables .....</b>	<b>xv</b>
<b>List of Figures.....</b>	<b>xvi</b>
<b>List of Abbreviations .....</b>	<b>xx</b>
<b>Acknowledgements .....</b>	<b>xxiii</b>
<b>Dedication .....</b>	<b>xxiv</b>
<b>Chapter 1: Introduction and Literature Review.....</b>	<b>1</b>
1.1    The epigenome.....	1
1.1.1    A focus on DNA methylation .....	1
1.1.2    The DNA methylation machinery.....	2
1.1.2.1    DNA methyltransferases.....	2
1.1.2.2    TET demethylating enzymes and DNA demethylation .....	4
1.1.2.3    Sites of DNA methylation.....	4
1.1.2.4    Relationship between DNA methylation machinery and transcription factors ..	6
1.1.3    Biological functions of DNA methylation.....	6
1.1.3.1    Functions of 5-mC .....	7
1.1.3.2    Functions of 5-hmC and further oxidized derivatives 5-fC and 5-caC.....	7
1.2    Dysregulation of DNA methylation during carcinogenesis.....	8

1.2.1	Global changes in DNA methylation in cancer .....	9
1.2.2	Loci-specific changes in DNA methylation in cancer .....	10
1.2.3	Changes in the DNA methylation machinery during carcinogenesis .....	10
1.2.4	DNMT inhibitors in cancer therapy .....	11
1.3	Dietary bioactive compounds as regulators of the cancer methylome .....	12
1.3.1	Antioxidants .....	12
1.3.2	Polyphenols .....	13
1.3.3	A focus on stilbenoid compounds .....	17
1.4	Stilbenoids alter DNA methylation landscapes in cancer .....	17
1.4.1	The stilbenoid class .....	17
1.4.2	Stilbenoid metabolism .....	18
1.4.3	Anti-cancer effects described for stilbenoids .....	19
1.4.4	Stilbenoids and epigenetic regulation .....	20
1.4.5	Current state of mechanistic studies of stilbenoid-mediated DNA methylation alterations in cancer .....	21
1.5	Research goal and hypothesis .....	26
 <b>Chapter 2: Stilbenoid-mediated epigenetic activation of Semaphorin 3A in breast cancer cells involves changes in dynamic interactions with DNMT3A and NF1C transcription factor .....</b>		
<b>28</b>		
2.1	Introduction .....	28
2.2	Materials and Methods .....	31
2.2.1	Cell culture and treatment with resveratrol (RSV) and pterostilbene (PTS) .....	31

2.2.2	Treatment with epigallocatechin gallate (EGCG), genistein (GEN), and chlorogenic acid (CGA).....	32
2.2.3	Cell viability assay.....	32
2.2.4	Invasion and anchorage-independent growth assay.....	33
2.2.5	Illumina Infinium Human Methylation 450K BeadChip microarray.....	33
2.2.6	DNA isolation and pyrosequencing.....	34
2.2.7	RNA isolation and qPCR.....	34
2.2.8	Chromatin immunoprecipitation (ChIP) and qChIP.....	35
2.2.9	Cell transfection with siRNA.....	36
2.2.10	Statistical analysis.....	38
2.3	Results.....	39
2.3.1	Resveratrol (RSV) and pterostilbene (PTS) decrease breast cancer cell growth and invasive properties.....	39
2.3.2	Exposure to resveratrol (RSV) leads to time-dependent genome-wide changes in the DNA methylation patterns in breast cancer cells.....	42
2.3.2.1	Time-dependent hypermethylation in response to RSV treatment.....	42
2.3.2.2	Time-dependent hypomethylation in response to RSV treatment.....	44
2.3.3	RSV-mediated loci-specific hypomethylation in lowly and highly invasive breast cancer cells.....	46
2.3.4	Tumor suppressor gene SEMA3A is epigenetically activated upon exposure to resveratrol (RSV) or pterostilbene (PTS) in breast cancer cells.....	51
2.3.5	Decreased DNMT3A occupancy within SEMA3A promoter in response to resveratrol (RSV) or pterostilbene (PTS).....	55

2.3.6	DNMT3A knockdown mimics the effects of stilbenoid compounds on DNA methylation and expression of SEMA3A .....	56
2.3.7	Nuclear factor 1C (NF1C) occupancy at SEMA3A promoter increases upon resveratrol (RSV) and pterostilbene (PTS) treatment.....	59
2.3.8	DNMT3A inhibitor SALL3 is upregulated upon stilbenoid treatment.....	60
2.4	Discussion.....	62
<b>Chapter 3: Roles for OCT1 transcription factor and DNMT3B in pterostilbene-mediated epigenetic regulation of oncogenes in breast cancer cells.....</b>		
3.1	Introduction.....	69
3.2	Materials and Methods.....	73
3.2.1	Cell culture and pterostilbene (PTS) treatment.....	73
3.2.2	Chromatin immunoprecipitation (ChIP) sequencing and qChIP .....	73
3.2.3	DNA isolation and pyrosequencing.....	74
3.2.4	RNA isolation and qPCR.....	75
3.2.5	CRISPR-Cas9 knockout of <i>DNMT3B</i> in MCF10CA1a cells .....	76
3.2.6	Statistical analysis.....	76
3.3	Results.....	77
3.3.1	Overview of genome-wide changes in OCT1 binding in response to PTS .....	77
3.3.2	Genes associated with reduced OCT1 peaks in regulatory regions overlap with genes exhibiting increased DNMT3B binding in response to PTS .....	81
3.3.3	Protein kinase C alpha (PRKCA) modulates several oncogenic signaling pathways .....	84

3.3.4	<i>PRKCA</i> silencing through hypermethylation in response to PTS is associated with decreased OCT1 binding at DNMT3B-occupied site .....	86
3.3.5	Knockout of <i>DNMT3B</i> indicates that PTS-mediated hypermethylation of <i>PRKCA</i> is DNMT3B-dependent .....	89
<b>Chapter 4: Epigenetic activation of oncogenes in rat hepatocellular carcinoma triggered by choline-deficiency is attenuated by pterostilbene supplementation .....</b>		<b>96</b>
4.1	Introduction.....	96
4.2	Materials and Methods.....	99
4.2.1	Rat model .....	99
4.2.1.1	Animals and experimental timeline .....	99
4.2.1.2	Diets .....	100
4.2.1.3	Histopathological analysis .....	100
4.2.2	RNA isolation and qPCR.....	100
4.2.3	RNA sequencing.....	103
4.2.4	Measurement of SAM/SAH levels by LC-MS .....	103
4.2.5	DNA isolation and pyrosequencing .....	105
4.2.6	Statistical analysis.....	105
4.3	Results.....	106
4.3.1	CDAA diet leads to fully developed HCC after 52 weeks .....	106
4.3.2	Profound gene dysregulation occurs in the liver of rats exposed to the CDAA diet .....	109
4.3.3	One carbon metabolism and DNA methylation machinery are altered in CDAA rat livers.....	117

4.3.4 Robust upregulation of oncogenes accompanies dysregulation liver functions in CDAA rats .....	121
4.3.5 DNA hypomethylation in regulatory regions of candidate oncogenes corresponds with gene upregulation and may contribute to the potent HCC phenotype in CDAA livers .....	123
4.3.6 Supplementation of CDAA diet with pterostilbene leads to hypermethylation and reduced expression of <i>Mmp12</i> oncogene .....	126
4.4 Discussion .....	129
<b>Chapter 5: Conclusions and Discussion .....</b>	<b>133</b>
<b>References .....</b>	<b>144</b>
<b>Appendices .....</b>	<b>166</b>
Appendix A .....	166
Appendix B .....	170
Appendix C .....	172
Appendix D .....	174
Appendix E .....	175
Appendix F .....	178

## List of Tables

<b>Table 2.1.</b> Primer sequences used in methylation analysis by pyrosequencing (A) and in gene expression analysis by qPCR and analysis by qChIP (B). Target sequences of siRNAs used in DNMT3A knockdown experiment (C).....	36
<b>Table 2.2.</b> A list of CpG loci highly hypomethylated in invasive MCF10CA1a cells in response to 9-day exposure to 15µM resveratrol (RSV), as measured by Illumina Infinium Human Methylation 450K BeadChip microarray.....	47
<b>Table 3.1.</b> Primer sequences used in analysis by qChIP, methylation analysis by pyrosequencing, and gene expression analysis by qPCR.....	74
<b>Table 4.1.</b> Primer sequences used in gene expression analysis by qPCR and methylation analysis by pyrosequencing.....	100

## List of Figures

<b>Figure 1.1.</b> DNA methylation in regulation of gene expression.....	5
<b>Figure 1.2.</b> Currently proposed mechanisms of polyphenol-mediated alterations in DNA methylation machinery.....	15
<b>Figure 2.1.</b> Resveratrol (RSV) and pterostilbene (PTS) inhibit cell growth, invasive capacities and anchorage independent growth in breast cancer cells with negligible effects in mammary epithelial cells. . . . .	40
<b>Figure 2.2.</b> Landscape of changes in the DNA methylation patterns in breast cancer cells in response to resveratrol (RSV). . . . .	49
<b>Figure 2.3.</b> Quantitative analysis of methylation state of the selected genes, <i>SEMA3A</i> , <i>UACA</i> , <i>FAM49A</i> , <i>TMEM91</i> , and <i>EPN2</i> , which contain CpG loci highly hypomethylated in invasive MCF10CA1a breast cancer cells exposed to resveratrol (RSV) based on the Illumina 450K microarray. . . . .	52
<b>Figure 2.4.</b> <i>SEMA3A</i> tumor suppressor gene is hypomethylated and reactivated upon treatment of highly invasive MCF10CA1a breast cancer cells with pterostilbene (PTS). . . . .	54

<b>Figure 2.5.</b> Binding of DNMT3A and modifications of histone tails within <i>SEMA3A</i> promoter in breast cancer cells in response to resveratrol (RSV) or pterostilbene (PTS).....	57
<b>Figure 2.6.</b> Occupancy of transcription factor NF1C within <i>SEMA3A</i> promoter and potential role for <i>SALL3</i> in breast cancer cells in response to resveratrol (RSV) or pterostilbene (PTS).....	60
<b>Figure 2.7.</b> Epigallocatechin gallate (EGCG), genistein (GEN), and chlorogenic acid (CGA) inhibit cell growth but have varying effects on expression of <i>SEMA3A</i> , <i>DNMT3A</i> , <i>NF1C</i> and <i>SALL3</i> . . . . .	66
<b>Figure 3.1.</b> Overview of genome-wide changes of OCT1 binding in response to PTS.....	79
<b>Figure 3.2.</b> Genes associated with OCT1 peaks in regulatory regions overlap with genes exhibiting differential DNMT3B binding in response to PTS. ....	82
<b>Figure 3.3.</b> Oncogenic roles of protein kinase C alpha ( <i>PRKCA</i> ). ....	85
<b>Figure 3.4.</b> DNMT3B-mediated hypermethylation is linked to OCT1-dependent transcriptional silencing in response to PTS in breast cancer cells. ....	87
<b>Figure 3.5.</b> DNMT3B-dependent regulation of PTS-mediated hypermethylation of <i>PRKCA</i> upon DNMT3B knockout.....	90

<b>Figure 4.1.</b> Macroscopic and histopathological analyses of rat livers upon methyl donor deficient diets. ....	106
<b>Figure 4.2.</b> Rat liver weights at earlier time-points and lobe-specific nodule analysis.....	107
<b>Figure 4.3.</b> Overview of RNA sequencing data: functional and pathway analysis.....	109
<b>Figure 4.4.</b> Overview of genes involved in metabolism-related alterations in livers of CDAA rats. ....	112
<b>Figure 4.5.</b> Choline and associated lipid distribution pathways are dysregulated upon methyl donor deficiency. ....	115
<b>Figure 4.6.</b> Alterations in one carbon metabolism (OCM) in response to methyl donor deficiency-driven liver carcinogenesis. ....	118
<b>Figure 4.7.</b> <i>Dnmt</i> and <i>Tet</i> expression in CSAA versus CDAA livers.....	119
<b>Figure 4.8.</b> Upregulated oncogenes and oncogenic pathways in CDAA livers.....	121
<b>Figure 4.9.</b> Expression of candidate oncogenes that were found to be upregulated in CDAA livers. ....	123

**Figure 4.10.** DNA hypomethylation of promoter regions of candidate oncogenes evaluated by pyrosequencing. .... 124

**Figure 4.11.** Attenuation of HCC by PTS supplementation..... 127

## List of Abbreviations

5-caC: 5-carboxylcytosine

5-fC: 5-formylcytosine

5-hmC: 5-hydroxymethylcytosine

5-mC: 5-methylcytosine

AML: acute myeloid leukemia

ATRA: all-trans retinoic acid

AZA: 5-azacytidine

BER: base excision repair

CD: choline deficient

CDAA: choline-deficient L-amino acid-defined

CGA: chlorogenic acid

CGI: CpG island

ChIP: chromatin immunoprecipitation

CSAA: choline-sufficient L-amino acid-defined

DNMT: DNA methyltransferase

DNMTi: DNMT inhibitor

E2: 17 $\beta$ -estradiol

EGCG: epigallocatechin gallate

FE: fold enrichment

GEN: genistein

GP: grape powder

GPCR: G-protein coupled receptor

GSI: gamma-secretase inhibitor

H&E: hematoxylin and eosin

HCC: hepatocellular carcinoma

HDAC: histone deacetylase

HLM: human liver microsomes

IGV: integrative genome viewer

LC-MS: liquid chromatography-mass spectrometry

LINE-1: long interspersed nuclear element 1

MAPK: mitogen-activated protein kinase

MDD: methyl donor deficiency

MMP: matrix metalloproteinase

mTOR: mammalian target of rapamycin

NF1C: nuclear factor 1C

NF $\kappa$ B: nuclear factor kappa-light-chain-enhancer of activated B cells

NICD: Notch intracellular domain

OCM: one carbon metabolism

PC: phosphatidylcholine

PCNA: proliferating cell nuclear antigen

PRC: polycomb repressive complex

PTS: pterostilbene

RSV: resveratrol

SAM: S-adenosyl-methionine

SAH: S-adenosyl-homocysteine

SIRT: sirtuin

TET: ten-eleven translocation methylcytosine dioxygenase

TF: transcription factor

TNBC: triple-negative breast cancer

TSG: tumor suppressor gene

TSS: transcription start site

UGT: UDP-glucuronosultransferase

VLDL: very low density lipoprotein

For full list of specific gene names, please see **Appendix F**.

## Acknowledgements

I offer my gratitude to the people I have worked alongside day in and day out, Dr. Stefanska, Sadaf, Lucy and Kasia, and several undergrads. I appreciate everything you have contributed to my work and my life.

I thank the faculty and UBC for all of the opportunities.

I thank my supervisory committee for keeping me on track in a productive and friendly way.

I thank Thomas Dixon-McDougall and Benjamin Martin for their science wizardry, generosity and for kindly responding to all of my silly questions and emails.

I thank Mom, Dad, Jessee and Andrew for celebrating the accomplishments and letting me complain during the stressful times over the last almost 5 years of hard work.

I thank my UBC friends, and beer club in particular, who welcomed me into their circle during a time of change and transition.

## **Dedication**

*To my friends and family, near and far.*

# **Chapter 1: Introduction and Literature Review**

## **1.1 The epigenome**

Epigenetics refers to the control of gene expression without changes to the underlying DNA sequence by coordinated components such as DNA methylation, covalent histone modifications, non-coding RNA mechanisms, and chromatin-remodeling complexes (Cheishvili, Boureau & Szyf, 2015; Jones, Issa & Baylin, 2016; Liu & Gao, 2016; Stefanska et al., 2011). Epigenetic components work together to activate or repress regions of the genome. DNA hypomethylation and histone acetylation within gene regulatory regions have been associated with open, active chromatin, whereas DNA hypermethylation and histone deacetylation are typically associated with a closed chromatin state (Jones, 2012; Stefanska et al., 2011). An intricate crosstalk facilitates the recruitment of enzymes that catalyze these epigenetic processes. While all components of the epigenetic machinery are important to influence gene expression, our group specifically focuses on regulation by DNA methylation.

### **1.1.1 A focus on DNA methylation**

DNA methylation has long been considered to have a crucial role in marking regions and mediating accessibility of DNA to transcription factors (TFs) for transcriptional control (Luo, Hajkova & Ecker, 2018). DNA methylation is thought to provide stable, long-term regulation by sustaining gene expression over time (Cedar & Bergman, 2009). However, tissue- and cell type-specific DNA methylation patterns have been observed during development and disease, indicating a dynamic nature for DNA methylation. Indeed, DNA methylation has been deemed heritable, dynamic and responsive to environmental influence. Lifestyle factors such as diet, alcohol consumption,

smoking, physical inactivity, and stress levels have all been associated with changes in the DNA methylation landscape. In addition, DNA methylation has important biological functions during embryonic development and is dysregulated in several diseases during childhood and adulthood (Andersen & Tost, 2018). Considering the dynamic nature of DNA methylation states and its definitive role in disease, this component of the epigenome is of particular interest when investigating preventive and therapeutic strategies.

### **1.1.2 The DNA methylation machinery**

DNA methylation is a covalent modification catalyzed by DNA methyltransferases (DNMTs) in mammalian cells. Most often, DNMTs transfer a methyl group from the universal methyl donor S-adenosyl-methionine (SAM) to the fifth position of the cytosine pyrimidine ring within CpG dinucleotides (Gruenbaum, Stein, Cedar & Razin, 1981). DNA methylation can also occur at non-CpG sites such as CpA, CpT, and CpC. Functions of non-CpG methylation are still unknown but researchers have proposed that hyperactive DNMTs play a role (Jang, Shin, Lee & Do, 2017). Mammals have three active DNMTs that are classified into two categories: maintenance (DNMT1) and *de novo* DNA methyltransferases (DNMT3A and DNMT3B).

#### **1.1.2.1 DNA methyltransferases**

DNMT1, the most abundant DNMT in mammalian cells, preferentially targets hemimethylated DNA to maintain methylation patterns from mother to daughter strand during replication; thus propagating methylation patterns to the next generation (Berkyurek et al., 2014). In order for this process to occur, ubiquitin like with PHD and ring finger domains 1 (UHRF1) is required to recognize and bind hemimethylated DNA leading to DNMT1 recruitment to those sites (Liu et al.,

2013). UHRF1 can also target DNMT1 to regions for maintenance DNA methylation by binding to di- or tri-methylated histone 3 lysine 9 (H3K9me<sub>2/3</sub>) associated with heterochromatin (Liu et al., 2013). In addition, interaction between DNMT1 and proliferating cell nuclear antigen (PCNA), a factor associated with DNA replication forks, has been observed, further emphasizing the role of DNMT1 during replication to maintain DNA methylation patterns.

*De novo* DNMTs, DNMT3A and DNMT3B, catalyze methylation of new, previously unmethylated regions of the DNA (Chen & Li, 2004). DNMT3A and DNMT3B are expressed mainly during early embryonic development to establish patterns of methylation that are then faithfully copied with each cell cycle. *De novo* DNMTs may also participate in a crosstalk with DNMT1 during maintenance DNA methylation (Kim, Ni, Kelesoglu, Roberts & Pradhan, 2002). DNMT3L is catalytically inactive but is required for establishing maternal genomic imprinting. DNMT3L co-localizes with *de novo* DNMTs and may be cooperating in transcriptional repression but does not possess methylating activity. Specifically, DNMT3 enzymes, including DNMT3L, possess an ADD domain, which targets *de novo* DNMTs to unmethylated histone H3 lysine 4 (H3K4) associated with repressed transcription. In response, catalytically active DNMT3A and DNMT3B are recruited to the transiently silenced region to mark it for long-term repression through stable DNA methylation (Ooi et al., 2007). *De novo* DNMTs also function in complexes containing H3K9 methyltransferases and histone deacetylases (HDACs) to form heterochromatin (Greenberg & Bourc'his, 2019). DNMT3B canonically deposits methyl marks at promoters and repetitive sequences to regulate long-term gene silencing. DNMT3B also associates with distal regulatory regions called enhancers through H3K36 tri-methylation to further control corresponding gene transcription (Rinaldi et al., 2016).

### **1.1.2.2 TET demethylating enzymes and DNA demethylation**

Demethylation of DNA occurs either passively or actively. Passive demethylation happens across cell divisions by a replication-dependent mechanism in the absence of the activity of DNA methylating enzymes. Active demethylation is regulated by ten-eleven translocation methylcytosine dioxygenase (TET) enzymes. During TET-mediated demethylation, a methylated cytosine (5-mC) can be the substrate for oxidation that converts 5-mC to 5-hydroxymethylcytosine (5-hmC), and further oxidized products 5-formylcytosine (5-fC) and 5-carboxylcytosine (5-caC). Oxidized derivatives are then removed by thymine-DNA-glycosylase (TDG) and replaced by an unmodified cytosine via the base excision repair (BER) pathway (Rasmussen & Helin, 2016). Expression of TETs and levels of 5-hmC are tissue- and cell type-specific, with highest 5-hmC levels detected in the brain and embryonic stem cells (Nestor et al., 2012). Even in tissues with high levels of 5-hmC, levels are approximately ten-fold lower than that of 5-mC. Some studies report that 5-hmC correlates with open chromatin and active transcription (Nestor et al., 2012), whereas other studies report increased 5-hmC density in gene bodies is associated with active transcription (Bhattacharyya et al., 2017). 5-fC and 5-caC are barely detectable in the human genome.

### **1.1.2.3 Sites of DNA methylation**

The human genome contains approximately  $3 \times 10^7$  CpG dinucleotide sites, each of which can be in a methylated or unmethylated state. Transposons are abundant throughout the genome and are highly methylated, while the methylation status of the rest of the genome is more variable. Upwards of 80% of CpG sites are methylated, with the exception of regions densely populated with CpGs that are termed CpG islands (CGIs) (Lister et al., 2009). The human genome contains

roughly 30,000 CGIs. Among CGIs, the majority remain unmethylated and lie within promoter regions, while about 9,000 CGIs found in gene bodies and intergenic regions have greater chance to become methylated (Jeziorska et al., 2017). Promoter-associated CGIs, and those associated with enhancers, are more likely to regulate transcriptional activity of associated genes, whereas the biological function of intergenic CGI methylation is less well understood (**Figure 1.1**).

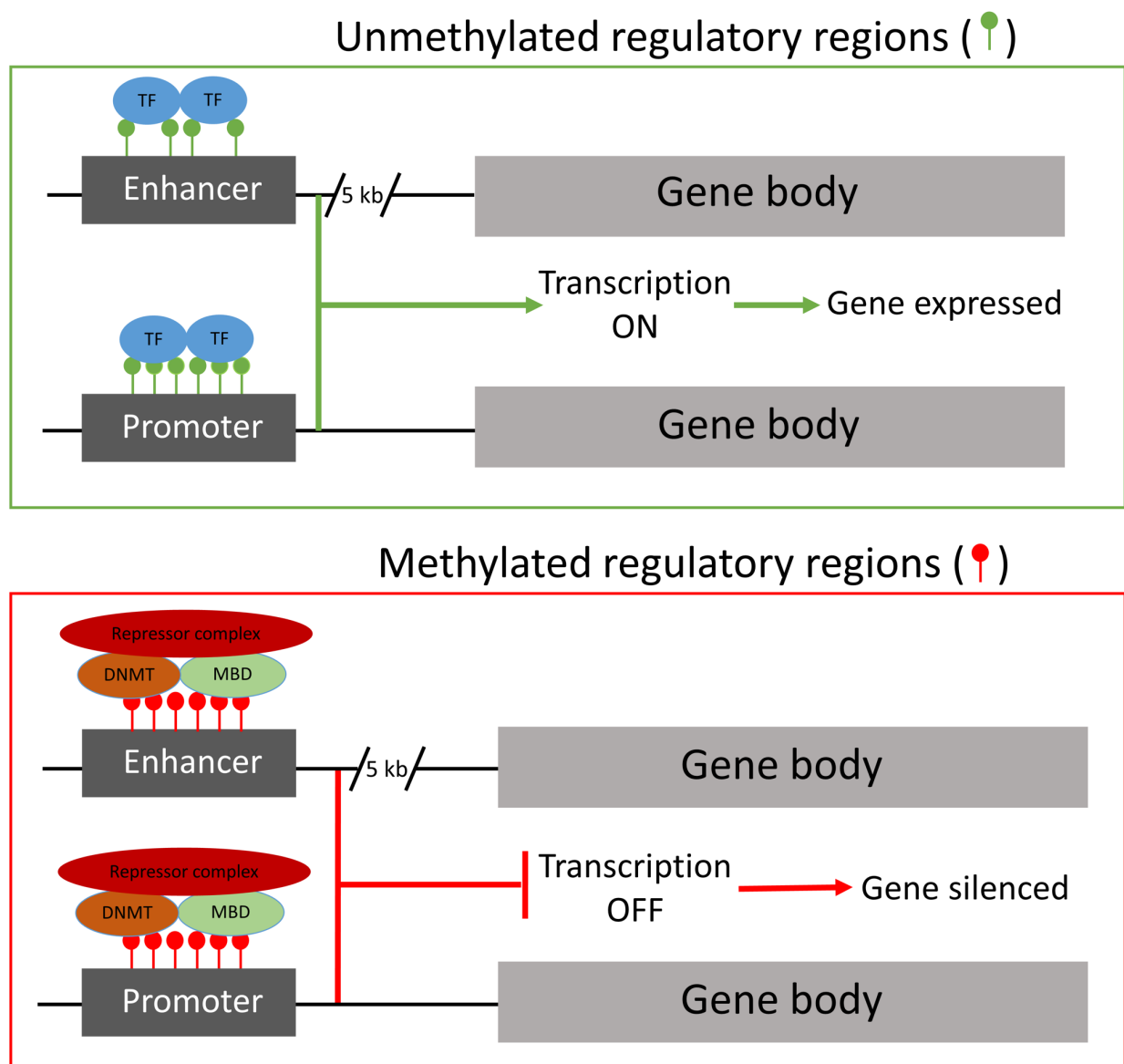


**Figure 1.1. DNA methylation in regulation of gene expression.** Transcriptional machinery, such as transcription factors, RNA polymerase II, and other proteins access and bind to gene promoters and enhancers to enable gene transcription to occur. Unmethylated CpG sites within these regulatory regions enable binding of the transcriptional machinery and the gene is actively transcribed, whereas methylated CpG sites in these regulatory regions leads to recruitment of repressive complexes that prevent binding of the transcriptional machinery resulting in gene silencing. Figure published in Beetch M, Harandi-Zadeh S, Shen K, Lubecka K, Kitts DD, O'Hagan HM, Stefanska B. (2020) Dietary antioxidants remodel DNA methylation patterns in chronic disease. *Br J Pharmacol.* Mar;177(6):1382-1408.

#### **1.1.2.4 Relationship between DNA methylation machinery and transcription factors**

DNA methylation has been shown to both control accessibility of gene regulatory regions to TFs and be controlled by the presence of certain TFs and chromatin-remodeling complexes. On the one hand, DNA methylation as a repressive mark in regulatory elements can block TF binding to disallow transcriptional activation. However, a subset of TFs prefers to bind to methylated DNA, indicating a range of sensitivity of TFs to 5-mC. On the other hand, depletion of 5-mC in promoter-associated CGIs can be protected by CXXC domain-containing proteins such as components of the histone H3 lysine 4 (H3K4) methyltransferase complex leading to inhibition of DNMT3A-mediated methylation. In addition, 5-mC deposition at enhancer regions is determined by insulator protein CCCTC-binding factor (CTCF), transcriptional repressor RE1-silencing transcription factor (REST), and other TFs (Luo, Hajkova & Ecker, 2018). Altogether, components of the DNA methylation and transcriptional machinery cooperate in order to control gene expression and consequently affect biological functions within the cell.

#### **1.1.3 Biological functions of DNA methylation**

DNA methylation serves a variety of biological functions including maintaining monoallelic expression of imprinted genes, X chromosome inactivation, transcriptional silencing of

retrotransposons and maintaining genome stability, and modifying sites within gene regulatory regions for transcriptional machinery to access and activate transcription (Andersen & Tost, 2018).

### **1.1.3.1 Functions of 5-mC**

Methylated CpGs create genome stability via silencing retrotransposons, repetitive DNA sequences, and other mobile genetic elements. There is evidence for 5-mC in maintaining genome stability based on findings that global loss of DNA methylation in diseases lead to chromosomal rearrangements and aneuploidy (Baylin & Jones, 2016). Another classical role for 5-mC is in imprinting, which is established in maternal gametes by DNMT3A and cofactor DNMT3L as well as other epigenetic modifications such as histone deacetylation and methylation. Additionally, X chromosome inactivation occurs to silence one of the two X chromosomes in females for dosage compensation. Following activation of the non-coding RNA called XIST, changes in histones and DNA methylation are coordinated to induce gene silencing and form an inactive X (Gendrel & Heard, 2014). Lastly, presence of 5-mC in regulatory regions of genes is correlated with corresponding gene silencing, as previously discussed. However, the inverse association between DNA methylation and gene expression is not always the case.

### **1.1.3.2 Functions of 5-hmC and further oxidized derivatives 5-fC and 5-caC**

The role of 5-hmC and other oxidized derivatives of active demethylation is not well understood. It has been reported that 5-hmC levels are enriched in open chromatin of regulatory regions (promoters and enhancers) and correlate with actively transcribed genes (Bhattacharyya et al., 2017). Increased 5-hmC over gene bodies has also been suggested to correspond with active transcription of associated genes (Bhattacharyya et al., 2017; Gao et al., 2019b). While these

functional consequences have been proposed, the role of 5-hmC may go beyond gene regulatory functions. For example, 5-hmC may be involved in alternative splicing during cell differentiation (Gao et al., 2019b). Detection of 5-fC and 5-caC during TET3-mediated demethylation of the paternal genome in pre-implantation development may indicate a possible biological function for these oxidized derivatives (Wossidlo et al., 2011). However, the role of 5-fC and 5-caC as simple intermediates of DNA demethylation has not been ruled out. Studies beyond early development or in pathological states have yet to describe biological functions of 5-fC or 5-caC.

## **1.2 Dysregulation of DNA methylation during carcinogenesis**

Thousands of studies have sought to define DNA methylation landscapes in many cancer types using *in vitro* and *in vivo* models as well as human clinical samples. Genome-wide investigations, assessment of candidate genes, and mechanistic studies have yielded a wealth of evidence distinguishing DNA methylation alterations as strong drivers of carcinogenesis. Tumor suppressor genes are hypermethylated most commonly at their promoters and silenced (Pfeifer, 2018). Simultaneously, DNA methylation levels decrease globally which occurs mainly in repetitive sequences and transposons and results in chromosomal rearrangements and genome instability (Baylin & Jones, 2016). In addition, a more recently discovered phenomenon involving loci-specific hypomethylation and activation of genes associated with oncogenic and pro-metastatic functions has been observed in cancer (Stefanska et al., 2014; Stefanska et al., 2011; Stefanska, Suderman, Machnes, Bhattacharyya, Hallett & Szyf, 2013).

### **1.2.1 Global changes in DNA methylation in cancer**

Many years ago, a global loss of DNA methylation was observed in cancer (Feinberg & Vogelstein, 1983), and since that time has been considered a hallmark epigenetic driver of tumor formation. On average, there is 5-20% loss of 5-mC in tumor genomes. This shift in 5-mC levels has been proposed to induce genome instability and chromosomal rearrangements, increase transcriptional noise, influence the three-dimensional cancer genome, and activate cancer-promoting genes via loci-specific hypomethylation (Pfeifer, 2018).

As mentioned previously, transposons and repetitive sequences are typically methylated. Therefore, these regions are particularly susceptible to loss of 5-mC. Upon loss of 5-mC, these elements become mobile and contribute to aberrant activation or silencing of genes and transcriptional noise. For example, disrupted methylation of LINE-1 and Alu repeats, which are often used as surrogate markers of global DNA methylation status, contribute to chromosomal rearrangements and genome instability characteristic of cancer development (Baylin & Jones, 2011).

In addition, a global decrease in 5-hmC levels has been observed in cancer cells. Studies have shown cancer-specific mutations in TET2 induce significantly diminished 5-hmC levels. In fact, TET2 mutations are thought to be one of the first genetic aberrations in hematological cancers, indicating the early and impactful role DNA methylation patterns play in malignancy. Although alterations in TET enzymes are less well understood in solid tumors, downregulation of TET expression and reduced 5-hmC levels are associated with gastric, liver, lung and breast tumors (Rasmussen & Helin, 2016).

### **1.2.2 Loci-specific changes in DNA methylation in cancer**

Methylation-induced inactivation of genes associated with tumor suppressive functions occurs during stages of carcinogenesis. Increasing evidence indicates that DNA hypermethylation within promoter regions of tumor suppressor genes leading to their silencing is another epigenetic hallmark of human cancer. Classical tumor suppressor genes such as *BRCA1*, *MLH1* and *MGMT* (DNA repair and genome stability), *APC* (potent negative regulator of WNT signaling), and *RB* have been reported to be aberrantly silenced by DNA methylation (Michailidi et al., 2015). Disabled apoptosis by decreased expression of *DAPK* and *RASSF1A*, as well as silencing of cell cycle regulators (*CDKN2A*, *p14*, *p16*) through DNA hypermethylation mechanisms have also been described in cancer (Guo et al., 2015). Methylation status of other candidate genes has been used as prognostic markers of certain cancers such as *FANCF* (Ding, Wang, Shi, Zhou & Zhao, 2016) and *CHFR* (Guo et al., 2015). Genes found to be hypomethylated and upregulated in cancers include *MMP2*, *PLAU*, *S100A5*, *MYCN*, *BCL2L10*, and *CTNNB1* (Saghafinia, Mina, Riggi, Hanahan & Ciriello, 2018; Stefanska et al., 2011). Together, aberrant methylation patterns associated with these genes and others likely contribute to cancer-promoting properties.

### **1.2.3 Changes in the DNA methylation machinery during carcinogenesis**

Maintenance and *de novo* DNMTs have been presented as vital players in pathology of many diseases, including cancer, as their presence at the DNA dictates transcriptional activity of genes. Across many cancers, upregulation of DNMTs has been observed (Esteller, 2008). In fact, DNMT expression and activity can even increase with cancer stage (Gravina et al., 2013). DNMT1 and DNMT3B were the first DNA methylating enzymes to be heavily implicated in carcinogenesis.

Overexpression of DNMT3B is detected in 30% of breast tumors. DNMT3A mutations are present at a rate of approximately 20% in acute myeloid leukemia (AML).

As a whole, aberrant DNA methylation patterns play a major role in carcinogenesis through epigenetic regulation of transcription and reprogramming gene expression profiles. Thus, reversing DNA methylation patterns established during different stages of carcinogenesis, including initiation and progression, constitutes a promising strategy to prevent cancer and support existing cancer therapies.

#### **1.2.4 DNMT inhibitors in cancer therapy**

At this time, there is a lack of suitable and effective tools to modify DNA methylation patterns during carcinogenesis. Molecules have been synthesized that inhibit DNMT activity by incorporating into the DNA and covalently binding with DNMTs. DNMT inhibitors such as 5-azacytidine (AZA) and 5-aza-2'-deoxycytidine also known as decitabine have been around for decades. AZA was approved for treatment of myelodysplastic syndrome in 2004, but success in treatment of solid tumors is under ongoing investigation.

In theory, DNMT inhibitors have unidirectional effects on DNA methylation patterns to reactivate methylation-silenced tumor suppressor genes. DNMT inhibitors are replication-dependent and impart only transient effects. Additionally, the efficacy of DNMT inhibitors is often dependent on other genetic and epigenetic layers. For example, sensitivity of leukemia cells to AZA treatment has been shown to be modulated by expression of mixed lineage leukemia 5 gene (*MLL5*), which has lysine methyltransferase activity (Yun et al., 2014). In breast cancer, DNMT protein levels and degradation have recently been suggested as biomarkers for DNMT inhibitor response (Yu et al.,

2018). Altered levels of enzymes that participate in AZA metabolism, such as cytidine deaminase (CDA) and deoxycytidine kinase (DCK), have also been shown to contribute to AZA resistance of cancer cells (Qin et al., 2011). Alternatively, to target TET enzymes would involve oxidized 5-mC derivatives that are currently poorly understood in terms of their biological functions. Therefore, a need for other preventive or therapeutic options targeting this hallmark molecular event is evident.

### **1.3 Dietary bioactive compounds as regulators of the cancer methylome**

Epigenetics at least partially explains the relationship between environmental influence on a given phenotype. In this case, DNA methylation is modified by environmental factors, such as diet and more specifically dietary compounds, which can further modify cancer risk and tumor behavior. Individual dietary nutrients and bioactive food components may alter DNA methylation machinery or may change the availability of substrate for methylation reactions. Evidence for antioxidants and polyphenols defining ways in which these bioactive compounds lead to altered DNA methylation status is discussed.

#### **1.3.1 Antioxidants**

Vitamin C has been found to increase 5-hmC levels via enhancing TET protein functions (Minor, Court, Young & Wang, 2013). The connection between vitamin C and TET protein activity lies in the antioxidant capacity of vitamin C. Vitamin C reduces ferric iron to ferrous iron, making it into the necessary form for the catalytic center of TET enzymes (Yin et al., 2013). In bladder cancer, genome-wide mapping of 5-hmC levels showed a loss of 5-hmC in cancer-related genes that was attenuated when cells were exposed to vitamin C. The vitamin C-mediated shift in 5-hmC levels corresponded with an altered transcriptomic profile and anti-cancer effects (Peng et al., 2018).

In response to vitamin E, DNMTs were suppressed in a mouse model of prostate cancer (Huang et al., 2012). In another study, vitamin E resulted in increased methylation of LINE-1 in cancer cells, which is used as a proxy for global methylation status (Zappe et al., 2018). These seemingly contradictory findings emphasize a need for further studies to assess the connection between vitamin E and DNA methylation.

Treatment of breast cancer cells with *all-trans* retinoic acid (ATRA), a form of vitamin A, resulted in DNA hypomethylation and reactivation of tumor suppressor genes (*PTEN* and *RAR $\beta$ 2*) (Stefanska, Rudnicka, Bednarek & Fabianowska-Majewska, 2010; Stefanska, Salame, Bednarek & Fabianowska-Majewska, 2012). Downregulation of DNMTs in response to ATRA was found to potentially be through a microRNA-related mechanism (Das et al., 2010).

### **1.3.2 Polyphenols**

Stilbenoid compounds, resveratrol (RSV) and pterostilbene (PTS), are present most abundantly in grapes and blueberries, respectively. Stilbenoids remodel DNA methylation patterns in cancer cells (Beetch, Lubecka, Kristofzski, Suderman & Stefanska, 2018; Beetch et al., 2019b; Lubecka et al., 2016; Medina-Aguilar et al., 2016; Papoutsis, Borg, Selmin & Romagnolo, 2012; Stefanska, Rudnicka, Bednarek & Fabianowska-Majewska, 2010; Stefanska, Salame, Bednarek & Fabianowska-Majewska, 2012). Past studies by our group and others indicate that exposure to dietary stilbenoids modifies DNA methylation patterns in cancer cells leading to differential changes in thousands of CpG loci. Targets of these compounds constitute tumor suppressor genes that are often silenced by methylation and oncogenes that undergo demethylation and activation during cancer development. In addition, stilbenoids have been shown to increase

expression of PTEN and p21 tumor suppressor genes and have direct and indirect effects on DNA methylation machinery (**Figure 1.2A and B**).

Epigallocatechin gallate (EGCG) is a polyphenol found in green tea. Studies have reported reduced expression and/or activity of DNMTs by direct binding of EGCG to the catalytic pocket of DNMT1 (Fang et al., 2003; Lee, Shim & Zhu, 2005) and predicted docking in DNMT3B (Khan et al., 2015). Another way in which EGCG may decrease DNMT activity is through catechol-O-methyltransferase (COMT). COMT catalyzes the transfer of SAM to EGCG as a substrate, which is shuttling SAM to non-DNA methylation reactions. In addition, utilizing SAM for COMT reactions produces S-adenosyl-homocysteine (SAH), a potent non-competitive inhibitor of DNMTs (Lee, Shim & Zhu, 2005). Increased p21 expression upon EGCG treatment may decrease DNMT1 activity due to p21 competition for binding of PCNA during replication (Chuang, Ian, Koh, Ng, Xu & Li, 1997) (**Figure 1.2B**). These mechanisms of DNMT activity downregulation contribute to demethylation and transcriptional activation of methylation-silenced tumor suppressor genes eliciting anti-cancer effects (Fang et al., 2003; Khan et al., 2015; Lee, Shim & Zhu, 2005; Morris et al., 2016).

Genistein is a soy isoflavone. Genistein treatment of cancer cells is linked to reactivation of tumor suppressor genes through DNA methylation mechanisms (Adjakly et al., 2011; Fang, Chen, Sun, Jin, Christman & Yang, 2005; Majid et al., 2010; Xie et al., 2014). For example, reactivation of *ATM*, *APC* and *PTEN* tumor suppressor genes in breast cancer cells by DNA hypomethylation of their promoter regions has been observed (Xie et al., 2014). Like curcumin and EGCG, studies

have also shown that genistein can bind directly into the catalytic pocket of DNMT1 to reduce its activity (Xie et al., 2014) (**Figure 1.2A and B**).

Curcumin is a compound present in the spice turmeric. A mechanism of direct inhibition of DNMT1 activity by covalent binding within the catalytic pocket has been described for curcumin (Liu et al., 2009) (**Figure 1.2B**). Other studies have revealed decreased expression of DNMT1 in response to curcumin (Liu, Zhou, Hu, Wang & Yuan, 2017; Yu et al., 2013). These studies have all reported anti-cancer effects of curcumin treatment.

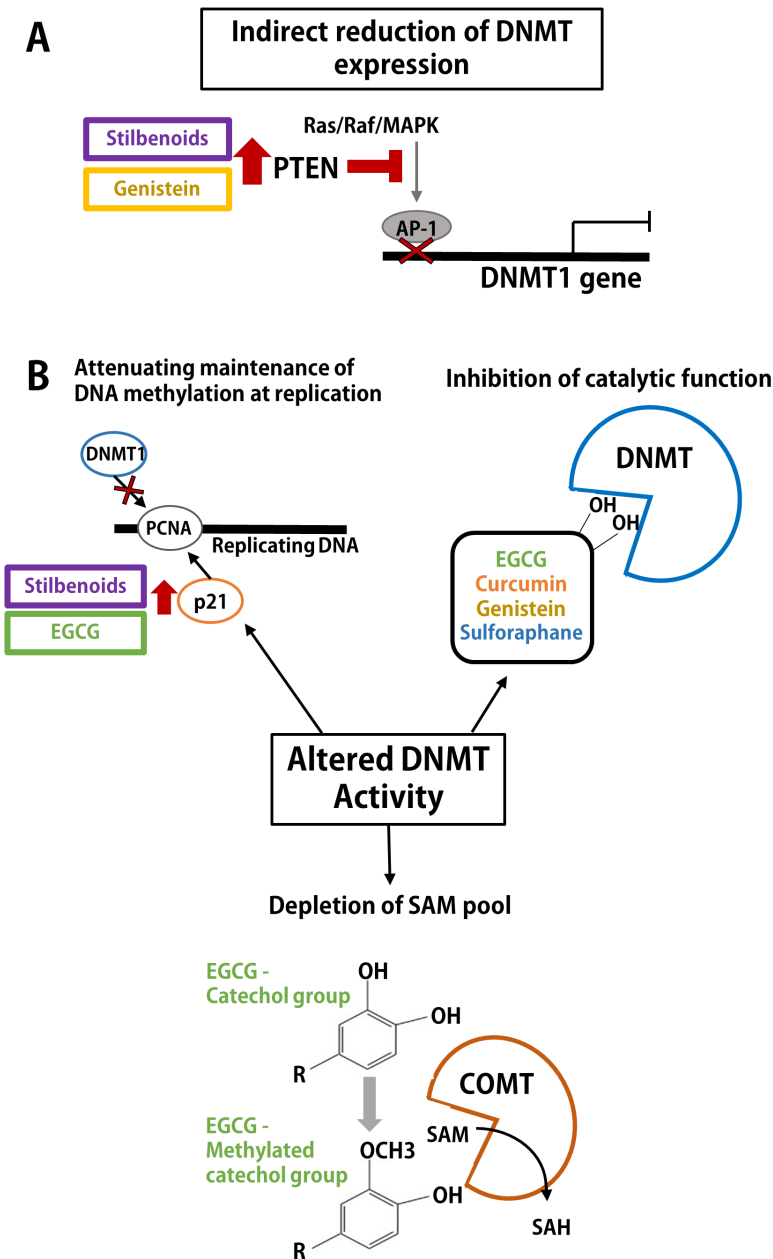


**Figure 1.2. Currently proposed mechanisms of polyphenol-mediated alterations in DNA methylation machinery.** (A) Indirect reduction in expression of DNMT1 by polyphenol-mediated increase in phosphatase and tensin homologue (PTEN) to inhibit AP-1 transcription factor binding to the DNMT1 promoter. (B) DNMT activity is altered through mechanisms associated with attenuation of DNMT1 binding to replicating DNA, inhibition of catalytic activity of DNMTs, and

depletion of the SAM pool. Figure published in Beetch M, Harandi-Zadeh S, Shen K, Lubecka K, Kitts DD, O'Hagan HM, Stefanska B. (2020) Dietary antioxidants remodel DNA methylation patterns in chronic disease. *Br J Pharmacol.* Mar;177(6):1382-1408.

### **1.3.3 A focus on stilbenoid compounds**

Altogether, numerous dietary compounds have been shown to alter DNA methylation patterns in cancer. To date, DNA hypomethylation and reactivation of tumor suppressor genes have been described as a major factor underlying the anti-cancer action of these compounds. RSV and PTS are compounds found in natural sources, whose effects on inhibiting growth of cancer cells is robust, even at low doses, which underscores the attractiveness of studying these compounds. In addition, the bidirectional effect (i.e. hypomethylation of tumor suppressor genes and hypermethylation of oncogenes) exerted by stilbenoids appears to be unique, but mechanistic underpinnings have not yet been fully elucidated.

## **1.4 Stilbenoids alter DNA methylation landscapes in cancer**

### **1.4.1 The stilbenoid class**

Stilbenoids are a class of polyphenols whose health benefits range from antioxidant, anti-inflammatory, and anti-aging effects, anti-cancer action, and neuro- and cardio-protective properties. RSV is the most well-studied stilbenoid compound to date. RSV is found in highest quantities in grapes and red wine, mulberries, legumes and peanuts (Walle, 2011). PTS, a dimethoxyl analog of RSV, is most abundantly present in blueberries (Kapetanovic, Muzzio, Huang, Thompson & McCormick, 2011). These stilbenoids have differing bioavailabilities (RSV, 20%; PTS, 80%), likely due to their slightly different chemical structure and capacity to be converted to metabolites (Dellinger, Garcia & Meyskens, 2014; Kapetanovic, Muzzio, Huang, Thompson & McCormick, 2011). Despite having a higher bioavailability than RSV, a relatively

limited body of research on PTS has surfaced in regard to its anti-cancer effects, especially in relation to epigenetic mechanisms.

#### **1.4.2 Stilbenoid metabolism**

Upon absorption, RSV and PTS are transported to the liver where the main routes of stilbenoid metabolism are glucuronidation and sulfation, both of which facilitate elimination from the body (Brill et al., 2006; Miksits et al., 2005). Glucuronidation is catalyzed by UDP-glucuronosyltransferase (UGT) enzymes, which metabolize RSV and PTS by conjugating a glucuronic acid to the hydroxyl group(s) of RSV or PTS. RSV has 2 hydroxyl groups (3-hydroxyl and 4-hydroxyl) available for glucuronidation, whereas PTS has only 1 hydroxyl group (4-hydroxyl) for conjugation reactions. In addition, the specific UGT enzymes that catalyze this modification on 3-hydroxyl and 4-hydroxyl groups of RSV (UGT1A1 and UGT1A9) have reduced activity for the 4-hydroxyl group on PTS (Brill et al., 2006; Dellinger, Garcia & Meyskens, 2014; Kapetanovic, Muzzio, Huang, Thompson & McCormick, 2011). Therefore, RSV has been shown to be a better substrate for UGT than PTS. Another route of metabolizing stilbenoids is through sulfation of hydroxyl groups. The 3-hydroxyl position, which PTS does not possess, is preferable and most efficient for sulfation enzymes (Miksits et al., 2005), making RSV a more suitable substrate for sulfation as well. A third route to metabolize stilbenoids is biotransformation by the gut microbiota. Dihydroresveratrol and 2 other dihydro derivatives, characterized by a reduced carbon-carbon double bond, have been discovered to be formed upon metabolism of RSV by gut microbial transformation (Bode et al., 2013). There is no evidence, however, of PTS metabolites with a reduced carbon-carbon double bond. In fact, demethylation pathways to metabolize PTS are more prominent (Shao, Chen, Badmaev, Ho & Sang, 2010). Pinostilbene, a derivative with a

hydroxyl group at the 5-position as opposed to a methoxyl group, was identified as major microbial metabolite of PTS. Microbial demethylases were proposed to be responsible for this transformation (Sun et al., 2016). In recent years, increasing evidence on the topic of microbial biotransformation to produce potentially biologically important metabolites has surfaced but further studies are needed.

Inter-individual variability is a limitation to studying stilbenoid metabolism. One example is gender differences observed in metabolizing stilbenoid compounds. Dellinger and colleagues measured glucuronidation profiles of human liver microsomes (HLMs) from males and females. The study reported that female HLMs were more efficient than male HLMs at glucuronidation of RSV and PTS, and attributed this difference to variation in UGT1A1 expression, the most highly expressed UGT in human livers (Dellinger, Garcia & Meyskens, 2014). Whether or not the parent compound or the metabolites of RSV and PTS are the prominent bioactive or beneficial compounds is under investigation.

### **1.4.3 Anti-cancer effects described for stilbenoids**

Several lines of evidence indicate the anti-cancer potential of RSV and PTS. In recent years, many research groups have comprehensively reviewed RSV and PTS as anti-cancer agents in numerous cancer types (Ma et al., 2019; Rauf, Imran, Butt, Nadeem, Peters & Mubarak, 2018). Among processes impacted by stilbenoid treatment of cancer cells are increased apoptosis through a Bcl-2 and Bax-related mechanism (Ma et al., 2015; Mohapatra, Satapathy, Siddharth, Das, Nayak & Kundu, 2015), inhibition of angiogenesis and metastasis, modulation of pathways to handle oxidative stress and suppress inflammation such as NRF2 (Singh et al., 2014), downregulation of oncogenic signaling (NOTCH, Hedgehog, Wnt, mTORC1) (Gao, Yuan, Gan

& Peng, 2015; Mohapatra, Satapathy, Siddharth, Das, Nayak & Kundu, 2015; Zhang et al., 2014), reprogramming cancer cell metabolism (Li et al., 2016; Saunier et al., 2017), and improved sensitivity to chemotherapy or repression of chemoresistance upon combination treatment (i.e. doxorubicin or cisplatin in combination with RSV) (Rezk, Balulad, Keller & Bennett, 2006). The vast body of evidence delineating ways in which stilbenoid compounds exert their anti-cancer action also includes epigenetic regulation of gene expression.

#### **1.4.4 Stilbenoids and epigenetic regulation**

Studies have indicated that RSV and PTS exert anti-cancer effects through epigenetic regulation of gene expression. Historically, polyphenols such as RSV were shown to directly and indirectly activate histone deacetylase sirtuin 1 (SIRT1) to elicit cellular responses to manage environmental and pro-inflammatory signals. Deacetylation of histones and modulation of acetylated proteins by activated SIRT1 contribute to anti-inflammatory, anti-aging, and metabolism responses of polyphenols (Chung et al., 2010).

In more recent studies, stilbenoid compounds have been shown to reverse hypermethylation and silencing of several established tumor suppressor genes, and inhibited cancer growth (Beetch et al., 2019b; Papoutsis, Borg, Selmin & Romagnolo, 2012; Stefanska, Rudnicka, Bednarek & Fabianowska-Majewska, 2010; Stefanska, Salame, Bednarek & Fabianowska-Majewska, 2012). To date, studies have provided proof of principle for targeting hypermethylated tumor suppressor genes in response to bioactive compounds as an effective approach in cancer prevention and/or therapy, but they neglect to address underlying mechanisms. Moreover, the effects of stilbenoid compounds on epigenetic events occurring at oncogenes is severely understudied.

#### **1.4.5 Current state of mechanistic studies of stilbenoid-mediated DNA methylation alterations in cancer**

Pre-clinical studies have evaluated the effectiveness of stilbenoids in chemoprevention and in support of anti-cancer therapies using *in vitro* and *in vivo* models with focus on DNA methylation. Genome-wide investigations of *in vitro* cancer models have identified altered DNA methylation landscapes upon treatment with RSV or PTS (Beetch et al., 2019b; Lubecka et al., 2016; Medina-Aguilar et al., 2016). Other studies define genes or signaling pathways modulated by DNA methylation in response to stilbenoid treatment leading to anti-cancer effects (Kala, Shah, Martin & Tollefsbol, 2015; Kala & Tollefsbol, 2016; Lubecka et al., 2016). A large portion of studies with a goal of understanding DNA methylation-related effects of RSV and PTS utilize models of breast cancer. However, more recent research on epigenetic regulation of cancer-related genes in response to stilbenoid compounds has surfaced in other types of solid tumors.

Upon treatment with RSV, the expression levels of *DNMT1*, *DNMT3A*, and *DNMT3B*, as well as other epigenetic regulators (*HDAC1* and *MeCP2*), were decreased in breast cancer cells (Mirza, Sharma, Parshad, Gupta, Pandya & Ralhan, 2013). It was hypothesized that anti-cancer effects exerted by RSV were at least partially through downregulation of DNMTs leading to hypomethylation and subsequent transcriptional activation of methylation-silenced tumor suppressor genes. This hypothesis resulted in a body of work assessing loci-specific DNA hypomethylation and reactivation of tumor suppressor genes in response to RSV. Established tumor suppressor genes such as *BRCA1*, *RASSF1A*, *PTEN*, *APC*, and *RAR $\beta$ 2* were used as candidates to examine DNA methylation patterns in breast cancer cell lines upon RSV treatment.

These candidate tumor suppressor genes were shown to lose methyl marks in their promoter regions and become transcriptionally activated in response to RSV (Papoutsis, Borg, Selmin & Romagnolo, 2012; Stefanska, Rudnicka, Bednarek & Fabianowska-Majewska, 2010; Stefanska, Salame, Bednarek & Fabianowska-Majewska, 2012; Zhu et al., 2012). While findings were promising, these studies lacked mechanistic insight and were confined to gene candidates.

Since that time, genome-wide technologies have provided a more thorough understanding of the widespread action of RSV on the DNA methylation landscape in cancer cells. Our group was the first to use a DNA methylation microarray to report bidirectional DNA methylation alterations in breast cancer cells treated with 15  $\mu$ M RSV for 9 days. We found that a majority of RSV-mediated changes in DNA methylation manifested as increased methylation at loci associated with oncogenes and genes with pro-metastatic functions (Lubecka et al., 2016). A smaller portion of changes persisted as loss of methylation in genes related to tumor suppressive functions (Lubecka et al., 2016). Others have used the DNA methylation microarray to further support our observation that RSV exerts broad, bidirectional effects on DNA methylation patterns in breast cancer cells (Medina-Aguilar et al., 2016).

We went on to show that oncogenic NOTCH signaling was a target for DNA hypermethylation upon treatment with either 15  $\mu$ M RSV or 7  $\mu$ M PTS treatment of breast cancer cells. Specifically, DNA methylation within an enhancer region of mastermind-like transcriptional co-activator 2 (*MAML2*), a co-activator of NOTCH signaling, was significantly increased upon treatment with RSV or PTS, which coincided with transcriptional downregulation. Within the hypermethylated *MAML2* enhancer, DNMT3B binding was enriched in response to RSV, and was accompanied by

diminished occupancy of oncogenic transcription factor OCT1. Epigenetic silencing of *MAML2* was associated with inhibition of the NOTCH pathway activity, as evidenced by decreased expression of NOTCH target genes *HEY1*, *HES1* and *NOTCH1*. These findings suggest that stilbenoid compounds may alter DNA methylation and transcriptional machinery to exert anti-cancer responses through inhibition of oncogenic signaling pathways (Lubecka et al., 2016).

Contrary to our findings in cell lines, a rodent study to understand the effect of RSV on estrogen-dependent breast cancer found that 21-week high dose RSV treatment resulted in decreased *Dnmt3b* expression in tumors but increased *Dnmt3b* expression in normal tissue. Expression level of *Dnmt1* did not change in response to RSV treatment. Both high dose and low dose RSV treatment led to delayed mammary tumor formation (Qin, Zhang, Clarke, Weiland & Sauter, 2014). Singh and colleagues also used a rat study to characterize mechanisms of RSV-mediated protection against estrogen-induced breast cancer with underlying oxidative stress. Specifically, 8-month treatment of 17 $\beta$ -estradiol (E2), RSV or both E2 and RSV revealed that RSV reduced E2-induced cell proliferation and tumor development. RSV upregulated the master regulator NRF2 through promoter hypomethylation and led to subsequent activation of NRF2-controlled antioxidant genes that protected cells against E2-induced oxidative stress (Singh et al., 2014).

Combinatorial RSV and PTS treatment has shown enhanced beneficial anti-cancer effects in triple negative breast cancer (TNBC) *in vitro* models. Combinatorial stilbenoid treatment at physiologically relevant doses (15  $\mu$ M RSV and 5  $\mu$ M PTS) restored estrogen receptor alpha (ER $\alpha$ ) at least partially by reducing DNA methylation and reverting back to a transcriptionally active state. DNMT enzyme activity and global DNA methylation were significantly decreased upon

either PTS only or combination stilbenoid treatment. Stilbenoid-mediated reactivation of ER $\alpha$  resulted in sensitization of TNBC cells to traditional hormone-targeted therapy (Kala & Tollefsbol, 2016). DNA damage response is another process influenced by combinatorial stilbenoid treatment of TNBC cells. Combinatorial RSV and PTS treatment downregulated all 3 catalytically active DNMTs, diminished overall DNA methylation activity, and reduced expression and activity of histone deacetylase sirtuin 1 (SIRT1), which contributed to decreased DNA repair (Kala, Shah, Martin & Tollefsbol, 2015). In addition to combinatorial stilbenoid treatment, combining RSV with other polyphenolic compounds present in red wine called proanthocyanidins, yields similarly promising anti-cancer results. RSV and proanthocyanidins caused synergistic anti-cancer effects on breast cancer cells by inducing apoptosis through upregulation of pro-apoptotic *Bax* and downregulation of anti-apoptotic *Bcl-2*. These changes in gene expression may be at least partially modulated by epigenetic mechanisms, as evidenced by reduction of DNMT and HDAC activities in response to combination polyphenol treatment (Gao & Tollefsbol, 2018).

As other studies have suggested, RSV and PTS impact several facets of the epigenetic machinery and not only DNA methylation. A recent report discussed upregulation of *ATP2A3* in breast cancer cell lines (MCF-7 and MDA-MB-231) upon treatment with 100  $\mu$ M RSV. The study found that DNMT activity was reduced and expression of methyl-DNA binding proteins MeCP2 and MBD2 was decreased in response to RSV but those changes did not correspond with a hypomethylated *ATP2A3* promoter region. However, RSV decreased HDAC expression and activity, and led to enrichment of active histone mark H3K27 acetylation within the *ATP2A3* promoter (Izquierdo-Torres, Hernandez-Oliveras, Meneses-Morales, Rodriguez, Fuentes-Garcia & Zarain-Herzberg, 2019). While these findings highlight the contribution of histone acetylation changes to this RSV-

mediated mechanism, the role for DNA methylation should not be ruled out based on null findings in one regulatory region.

RSV studies investigating DNA methylation changes in other cancer types are on the rise. Like in breast cancer models, the DNA methylation alterations being described in other solid tumors involve reactivation of genes by RSV-mediated hypomethylation. For example, RSV epigenetically reactivated *ZNF36* expression in non-small cell lung cancer cells lines leading to an anti-cancer effect. In cancer, downregulation of *ZNF36* is associated with aberrant stabilization of mRNA transcripts (Fudhaili et al., 2019). RSV treatment of thyroid cancer cells resulted in reversal of retinoic acid resistance by demethylation and upregulation of cellular retinoic acid binding protein 2 (*CRABP2*). Slightly varying findings were reported for DNMT expression in the two thyroid cancer cell lines used in response to RSV. In one cell line, all 3 DNMTs were reduced, whereas in the other cell line, only DNMT1 and DNMT3A were reduced upon RSV treatment. Another interesting study compared anti-cancer and DNA methylation-related effects of RSV, PTS and synthetic analog called RSVN by a newly developed workflow called Comparative Profiling of Analog Targets. In melanoma cells, RSV and PTS could suppress cell migration by targeting HDAC1 and DNMT3A but the inhibitory effect was lost with modified RSVN indicating epigenetic regulation in controlling cell migration. Focal adhesion kinase (*FAK*) was targeted by HDAC1 and DNMT3A in response to RSV and PTS but not RSVN, leading to epigenetic downregulation of *FAK* and suppression of cell migration (Chen et al., 2018).

In terms of studying stilbenoid-mediated hypermethylation events in other cancers, the evidence base is lacking. Short term RSV treatment of bladder cancer cells harboring different TP53 status

yielded decreased cell proliferation and colony formation in all cell lines except TP53 wild type cells. There was an RSV-mediated increase in apoptosis and downregulation of AKT, mTOR and SRC (Almeida et al., 2019). A slight decrease in *DNMT1* expression suggests a role for DNA methylation contributing to anti-cancer effects, but many additional experiments would be needed to confirm the mechanism.

Interestingly, the body of research surrounding PTS-associated epigenetic effects compared to RSV-mediated effects is quite limited in cancer models. Only a handful of studies investigate PTS either alone or in combination with RSV, despite its higher bioavailability. In addition, evidence describing stilbenoid-mediated hypermethylation to impede oncogenic signaling is in its infancy, whereas hypomethylation and transcriptional activity triggered by RSV or PTS is well-studied. In all cases, more in-depth mechanistic evidence would increase application of polyphenols in preventive strategies and presumably as support of anti-cancer therapy.

## **1.5 Research goal and hypothesis**

The **goal of my thesis research** is to capitalize on dietary stilbenoids as safe agents with the capacity to activate methylation-silenced tumor suppressor genes and repress epigenetically-activated oncogenes in cancer, and to delineate underlying mechanisms governing DNA methylation events in cancer. **My hypothesis** is that dietary stilbenoids, like RSV and PTS, have effects on DNA methylation patterns and thereby gene transcription via modulation of the DNA methylation and transcriptional machinery, such as DNMTs and TFs. Changes in DNMTs lead to an altered DNA methylation profile and, in coordination with TFs and other epigenetic modifiers, influence transcription of cancer-related genes. While alterations in tumor suppressor

genes make up the bulk of the existing evidence delineating stilbenoid-mediated effects on DNA methylation, comprehensive mechanistic understanding of these processes is lacking in the literature. In addition, based on previous findings generated by our group, stilbenoid compounds induce loci-specific alterations with a large portion being increases in DNA methylation levels within regulatory regions of oncogenes. A role for stilbenoids in inhibiting overactive oncogenic pathways through epigenetic mechanisms has yet to be extensively explored.

## **Chapter 2: Stilbenoid-mediated epigenetic activation of Semaphorin 3A in breast cancer cells involves changes in dynamic interactions with DNMT3A and NF1C transcription factor**

### **2.1 Introduction**

The breast is the leading site of new cancer cases in women (Ly, Forman, Ferlay, Brinton & Cook, 2013). Even more striking, 1 in 8 women in North America will develop breast cancer in her lifetime (Ly, Forman, Ferlay, Brinton & Cook, 2013; Siegel, Miller & Jemal, 2015). Furthermore, 85% of women who are diagnosed with breast cancer have no family history of breast cancer, meaning that the majority of cases are sporadic (Siegel, Miller & Jemal, 2015). Although gender and age are strong predictors of diagnosis, modifiable factors such as environmental exposures and lifestyle factors, including alcohol, smoking, poor diet, physical inactivity, overweight/obesity, appear to play an important role in development of breast cancer, indicating a potential role for epigenetics as a driving force of the disease (Toska et al., 2017).

Epigenetics is the study of heritable gene expression changes that are not due to a change in the DNA sequence. Epigenetic modifications, particularly DNA methylation, have attracted a significant amount of attention for the prevention and treatment of different illnesses with cancer at the forefront, mainly due to the inherent reversibility of epigenetic states (Jones, Issa & Baylin, 2016). In mammals, DNA methylation occurs mainly on the cytosine of CpG dinucleotide and is catalyzed by DNA methyltransferases (DNMTs). The promoters of approximately 80% of genes contain dense regions of CpGs called CpG islands (CGIs). In normal cells, these islands are

typically unmethylated, allowing expression of the associated gene. In cancer cells, certain CpG islands in gene promoters become hypermethylated (Jones, Issa & Baylin, 2016). It occurs mostly within tumor suppressor genes (TSGs) leading to their silencing, which can participate in tumor formation. In contrast, promoters of certain genes functionally linked to processes accelerating carcinogenesis become hypomethylated, which leads to their up-regulation and contributes to cancer (Mayol et al., 2012; Rao et al., 2013; Shao et al., 2011; Stefanska et al., 2013; Stefanska et al., 2014; Stefanska et al., 2011; Stefanska, Suderman, Machnes, Bhattacharyya, Hallett & Szyf, 2013; Vizoso et al., 2015). Thus, reversing alterations in DNA methylation constitutes an excellent anti-cancer approach.

Certain dietary constituents have been shown to exert beneficial effects in cancer, including polyphenols from grapes and blueberries, namely resveratrol (RSV) and its dimethylated analog pterostilbene (PTS) (Carter, D'Orazio & Pearson, 2014; Jeyabalan, Aqil, Munagala, Annamalai, Vadhanam & Gupta, 2014a; Jeyabalan, Aqil, Munagala, Annamalai, Vadhanam & Gupta, 2014b; McCormack & McFadden, 2012; Wang, Cheng, Zhang, Mu & Wu, 2010; Wen et al., 2017). These compounds were shown to have anti-cancer properties, however studies to date have been exploratory and limited without direct mechanistic input (Bishayee, Politis & Darvesh, 2010; Carter, D'Orazio & Pearson, 2014; Jeyabalan, Aqil, Munagala, Annamalai, Vadhanam & Gupta, 2014b; McCormack & McFadden, 2012; Wen et al., 2017). Several pieces of evidence indicate that modifying the epigenome, specifically DNA methylation patterns, and subsequently gene expression may be a mediator of anti-cancer effects of dietary polyphenols (Fang, Chen, Sun, Jin, Christman & Yang, 2005; Lee & Zhu, 2006; Stefanska, Rudnicka, Bednarek & Fabianowska-Majewska, 2010; Stefanska, Salame, Bednarek & Fabianowska-Majewska, 2012). Previous

studies have found that RSV reversed hypermethylation and silencing of several established TSGs such as *BRCA1*, *PTEN*, *APC* and *RAR $\beta$ 2*, and inhibited breast cancer growth (Papoutsis, Borg, Selmin & Romagnolo, 2012; Stefanska, Rudnicka, Bednarek & Fabianowska-Majewska, 2010; Stefanska, Salame, Bednarek & Fabianowska-Majewska, 2012). Although these studies provide proof of principle for targeting hypermethylated TSGs by polyphenols, they are limited to candidate genes and do not address underlying mechanisms.

Our recent genome-wide investigation into DNA methylation patterns demonstrates that loci-specific increases and decreases in DNA methylation occur in breast cancer cells in response to RSV (Lubecka et al., 2016). We specifically described genes that gain methylation and are enriched with oncogenic pathways (Lubecka et al., 2016). In the present study, we extended our investigation by performing Illumina Infinium Human Methylation 450K BeadChip microarray to test time-dependent genome-wide effects and focused on genes that lose methylation upon exposure to RSV and fall into a category of potential TSGs, in lowly invasive MCF10CA1h and highly invasive MCF10CA1a breast cancer cells.

We found changes characteristic of early and late response to RSV, indicating that RSV treatment often targets for differential methylation the same genes but at different CpG loci, the same gene families or the same functional categories of genes upon 9-day compared with 4-day exposure. Among all genes containing CpG loci hypomethylated upon exposure to stilbenoids, we identified a group of 113 genes that lose methylation in both lowly MCF10CA1h and highly MCF10CA1a invasive breast cancer cells, and are associated with functions attenuating cancerous properties. One of the highest differences was located within *SEMA3A*, a gene found to have a potential tumor

suppressor role in breast cancer (Mishra et al., 2015; Wallerius et al., 2016). DNA hypomethylation of the semaphorin 3A (*SEMA3A*) promoter as confirmed quantitatively by pyrosequencing coincided with increase in gene expression upon exposure to stilbenoids. Mechanistic studies indicated the presence of DNMT3A binding at *SEMA3A* promoter in cancer cells, which is diminished in response to stilbenoids. Decrease in DNMT3A binding is associated with increased occupancy of nuclear factor 1C (NF1C) transcription factor, which may contribute to active *SEMA3A* transcription. In addition, we detected increased expression of sal-like 3 (*SALL3*), a negative regulator of DNMT3A activity, upon treatment with stilbenoids (Shikauchi et al., 2009). Our results indicate that stilbenoids target specific genes that are hypermethylated and silenced in cancer. Reversal of methylation-mediated silencing of these genes by stilbenoids is potentially linked to anti-cancer properties of these compounds.

## **2.2 Materials and Methods**

### **2.2.1 Cell culture and treatment with resveratrol (RSV) and pterostilbene (PTS)**

Human mammary epithelial MCF10A cell line and human breast cancer MCF10CA1h and MCF10CA1a cell lines were cultured in DMEM/F12 (1:1) medium (Gibco) supplemented with 5% horse serum (Gibco), 1U/ml penicillin and 1 $\mu$ g/ml streptomycin (Gibco). Medium for MCF10A cells (ATCC, CRL-10317, USA) was additionally supplemented with 20 ng/ml epidermal growth factor (Sigma-Aldrich, St. Louis, MO, USA), 100 ng/ml cholera toxin (Calbiochem, EMD Millipore, Billerica, MA, USA), 0.01 mg/ml insulin (Sigma-Aldrich, St. Louis, MO, USA), and 500 ng/ml hydrocortisone (Sigma-Aldrich, St. Louis, MO, USA). MCF10CA1h and MCF10CA1a breast cancer cells used in our experiments were derived from tumor xenografts of MCF10A cells transformed with constitutively active Harvey-*ras* oncogene,

and represent respectively well- and poorly-differentiated malignant tumors. All cell lines were routinely verified by morphology, invasion and growth rate. Cell lines were authenticated by DNA profiling using the short tandem repeat (ATCC). Cells, grown in a humidified atmosphere of 5% carbon dioxide at 37°C, were treated with resveratrol (RSV, Sigma-Aldrich, St. Louis, MO, USA) or pterostilbene (PTS, Cayman Chem., Ann Arbor, MI, USA) freshly resuspended in ethanol. 24 h prior to treatments, cells were plated at a density of  $2-3 \times 10^5$  followed by exposure to RSV or PTS at 0-20  $\mu\text{M}$  concentrations for 4 days. Cells were then passaged 1:50 and exposed for additional 4 days (9-day exposure).

### **2.2.2 Treatment with epigallocatechin gallate (EGCG), genistein (GEN), and chlorogenic acid (CGA)**

MCF10CA1a cells were cultured and grown as described above. Cells were treated with epigallocatechin gallate (EGCG, Cayman Chem., Ann Arbor, MI, USA), genistein (GEN, Cayman Chem., Ann Arbor, MI, USA) or chlorogenic acid (CGA, Cayman Chem., Ann Arbor, MI, USA) freshly resuspended in ethanol. 24 h prior to treatments, cells were plated at a density of  $2 \times 10^5$  followed by exposure to EGCG at 10, 50 and 100  $\mu\text{M}$  dose, GEN at 10, 30, and 50  $\mu\text{M}$  dose, or CGA at 0.1, 0.5, 1, and 5  $\mu\text{M}$  dose for 4 days. Cells were then passaged and exposed for additional 4 days (9-day exposure). Cells were counted at 4-day and 9-day time points.

### **2.2.3 Cell viability assay**

Trypan blue exclusion test (Sigma-Aldrich, St. Louis, MO, USA) was used to determine cell viability. Cells were harvested on day 4 and day 9 during treatments with RSV or PTS and

incubated with Trypan blue for 3-5 minutes. Viable and dead cells were counted under the microscope.

#### **2.2.4 Invasion and anchorage-independent growth assay**

Anchorage-independent growth in a 3D format that resembles an in vivo cellular environment was determined by soft agar assay (de Larco & Todaro, 1978). 6,000-12,000 live cells treated with vehicle (ethanol) or compounds (RSV or PTS) were seeded into soft agar and plated in triplicate in a 6-well plate for 21 days. The number of colonies (>10 cells/colony) in five random fields (40×) per well, throughout all planes of the triplicate wells, was counted under the microscope.

The ability of treated cells to invade through extracellular matrix was evaluated by the Cell Invasion Assay Kit (Chemicon Int.). The kit utilizes a reconstituted basement membrane matrix of proteins derived from Engelbreth-Holm-Swarm (EHS) mouse tumor. Briefly, 50,000 cells resuspended in serum-free media were added to the inserts dipped in the lower chamber containing complete media. Following 24-48 h-incubation at 37°C, invasive cells were stained and counted under the microscope.

#### **2.2.5 Illumina Infinium Human Methylation 450K BeadChip microarray**

DNA from cells treated with ethanol as a vehicle control and from cells exposed to RSV was isolated using standard phenol:chloroform extraction protocol and subjected to genome-wide DNA methylation analysis using Infinium HumanMethylation 450K BeadChip, as described previously in detail (Lubecka et al., 2016). Hybridization and scanning were performed in the Genomics Facility of University of Chicago, IL. Raw data were processed using the Methylation module (version 1.9.0) of the GenomeStudio software (Illumina; version 2011.1) followed by

preprocessing using R Bioconductor minfi package and the analysis of differential methylation in R Bioconductor limma package. The microarray data are available from Gene Expression Omnibus (accession numbers: GSE80794 for MCF10CA1h and MCF10CA1a breast cancer cells; and GSE113299 for MCF10A mammary epithelial cells).

### **2.2.6 DNA isolation and pyrosequencing**

DNA, isolated using standard phenol:chloroform extraction protocol, was treated with sodium bisulfite as previously described (Colella, Shen, Baggerly, Issa & Krahe, 2003; Lubecka et al., 2016). HotStar Taq DNA polymerase (Qiagen) and biotinylated primers were used to amplify bisulfite converted promoter sequences of the selected genes (please see **Table 2.1A** for primer sequences). Pyrosequencing of the biotinylated DNA strands was performed in the PyroMarkTMQ24 instrument (Qiagen) as previously described (Tost & Gut, 2007). Percentage of methylation at a single CpG site resolution was calculated using PyroMarkTMQ24 software.

### **2.2.7 RNA isolation and qPCR**

TRIzol (Invitrogen) was used to isolate total RNA which served as a template for cDNA synthesis with AMV reverse transcriptase (Roche Diagnostics), according to the manufacturer's protocol. Amplification reaction was performed in CFX96 Touch Real-Time PCR Detection System (Bio-Rad) using 2 µl of cDNA, 400 nM forward and reverse primers (please see **Table 2.1B** for sequences), and 10 µl of SsoFast EvaGreen Supermix (Bio-Rad) in a final volume of 20 µl. The following cycles were used in the amplification reaction: denaturation at 95 °C for 10 min, amplification for 60 cycles at 95 °C for 10s, annealing temperature for 10s, 72 °C for 10s, and final extension at 72 °C for 10 min. The CFX Maestro Software (Bio-Rad) was used to quantify gene

expression with a standard curve-based analysis. qPCR data is presented as gene of interest/REF. REF is a reference gene factor consisting of expression of 3 reference genes (GAPDH, RPS17, and 18S). Analysis of the QPCR results was performed according to Pfaffl's method (Pfaffl, Horgan & Dempfle, 2002; Taylor, Nadeau, Abbasi, Lachance, Nguyen & Fenrich, 2019), where so-called relative level of expression (relative to geometric mean of expression level of reference genes) is calculated. Briefly, the quantitative cycle (Cq) values of each reference gene (GAPDH, RPS17, and 18S) were determined for each sample. The Cq values for all samples in the control group were averaged for each reference gene.  $\Delta Cq$  values comparing averaged control Cq values for each reference gene to each control and treatment sample were calculated.  $\Delta Cq$  values of reference genes were averaged together to produce a combination  $\Delta Cq$  value for each sample. Combination  $\Delta Cq$  values were then changed to relative quantities ( $2^{-\Delta Cq}$ ). For each control or treatment group, a normalization factor or reference gene factor (REF) was determined from the geometric mean of the combination reference gene relative quantities ( $2^{-\Delta Cq}$ ). Comparison of relative quantities ( $2^{-\Delta Cq}$ ) for gene of interest over geometric mean of relative quantity ( $2^{-\Delta Cq}$ ) for combination of reference genes yielded the  $\Delta\Delta Cq$  value of the gene of interest for each sample.

### **2.2.8 Chromatin immunoprecipitation (ChIP) and qChIP**

Chromatin immunoprecipitation was performed as previously described in detail (Brown, Suderman, Hallett & Szyf, 2008; Lubecka et al., 2016; Peng & Chen, 2013). Briefly, one sub-sample was maintained as an input. The second sub-sample was incubated with anti-acetyl-Histone H3 Lys9 rabbit antibody (H3K9ac, Millipore, 07-352), anti-trimethyl-Histone H3 Lys27 rabbit antibody (H3K27me3, Millipore, 07-449), anti-DNA methyltransferase 3A rabbit antibody (DNMT3A, Abcam ab2850), and anti-nuclear factor 1/C rabbit antibody (NF1C, Millipore Sigma

ABE1387). The third sub-sample was incubated with rabbit IgG non-specific antibody (negative control, Santa-Cruz Biotechnology, sc-2027). Fraction of DNA bound to antibodies was washed, eluted and used as a template for QPCR (qChIP). 25ng of input, antibody bound and IgG bound DNA was used as starting material in all conditions. Levels of H3K9ac, H3K27me3, DNMT3A, and NF1C binding were expressed as (Bound-IgG)/Input. Primers used in qChIP are listed in **Table 2.1B**.

### **2.2.9 Cell transfection with siRNA**

MCF10CA1a cells were plated at a density of  $4-6 \times 10^5$  per 10-cm tissue culture dish, 24 h prior to treatment with small interfering RNAs (siRNAs). All siRNA sequences were obtained from Dharmacon, including control siRNA (siCtrl) and human DNMT3A siRNA (siDNMT3A) (see **Table 2.1C** for sequences). Using Lipofectamine RNAiMAX (Invitrogen, Carlsbad, CA, USA) in serum free Opti-MEM, cells were transfected with siRNA. Specifically, 15  $\mu$ l of lipofectamine were incubated in 500  $\mu$ l of Opti-MEM for 45 minutes at room temperature. siRNA was added to the Opti-MEM-lipofectamine solution to a final concentration of 56 nM. The mixture was incubated for 15 min at the same conditions. Opti-MEM was added to a final volume of 5 ml and was then applied to the plates. The transfection solution was removed from the cells and replaced with standard medium after 4 h. The cells were split 1:2 after 48 h and transfected again 24 h later. The transfection sequence was repeated 3 times in total.

<b>Table 1A.</b> Primer sequences used in methylation analysis by pyrosequencing.			
<b>Gene</b>	<b>Primer sequences for pyrosequencing</b>	<b>Annealing temperature [°C]</b>	<b>Amplicon length [bp]</b>
SEMA3A	FW 5'-GGGGGATTTTTAAAAGGATATTTAGA-3' RVBio 5'-AAAACCACAACCAACTACTTATTT-3' Seq 5'-GGTATTAATTTTTTGTGGG -3'	50	321
TMEM91	FW 5'-GGAAAAAGTAGAAGTTGTAATTGTATG-3' RVBio 5'-ACTCCTAACCTCAAATAATCCTATTAC-3' Seq1 5'-GTAGAAGTTGTAATTGTATGTT-3' (CpG 1) Seq2 5'-GTTTTAAGTTTGAATTATTTAATTA-3' (CpG 2)	50	212
UACA	FW 5'-AGGTAATTTATATAGGATGATAGTAAAA-3' RVBio 5'-CTCCTAAACTCAAATAATCCCAAATAC-3' Seq1 5'-GTTTAAAGTTAAGAGGAGTTAT-3' (CpG 1) Seq2 5'-TAGGGTGTGGTGGTT-3' (CpG 2)	53	197
FAM49A	FW 5'-GTGGTTATTTTAGTGTGTTGGTATT-3' RVBio 5'-ACCTAATATAACTAACATTCCTCCTAAA-3' Seq 5'-TTTTTATATTGGGTTT-3'	54	159
EPN2	FW 5'-GGAAAAGTGGGAGTTTTTAGGGATAGA-3' RVBio 5'-AAAACCCACAATCCTACCCACTCA-3' Seq1 5'-TTGAGTTGAGTAAGGAG-3' (CpG 1) Seq2 5'-TTGATTAGATTTTTTAGGTAGG-3' (CpGs 2-4)	54	241
<b>Table 1B.</b> Primer sequences used in gene expression analysis by qPCR and analysis by qChIP.			
<b>Gene</b>	<b>Primer sequences</b>	<b>Annealing temperature [°C]</b>	<b>Amplicon length [bp]</b>
<b>qPCR</b>			
SEMA3A	FW 5'-TAGGCTGTATGTTGGAGCAAAG-3' RV 5'-AGCCCACTTGCAATTCATCTC-3'	59	118
DNMT3A	FW 5'-AAGGAGGAGCGCCAAGA-3' RV 5'-TCACCGCAGGGTCCTTT-3'	59	112
NF1C	FW 5'-CCTGGCATAACGACCTGAAC-3' RV 5'-CCATCGAGCCCGATTTGT-3'	59	98
SALL3	FW 5'-CAAAGCGAGCTCAGAAACAG-3' RV 5'-CCTGATGCTCCAACCTCAA-3'	59	136
GAPDH	FW 5'-TGCACCACCAACTGCTTA-3' RV 5'-AGAGGCAGGGATGATGTTCC-3'	59	177
RPS17	FW 5'-AAGCGCGTGTGCGAGGAGATC-3' RV 5'-TCGCTTCATCAGATGCGTGACATAACCTG-3'	59	87
18S	FW 5'-TCGGAAGTGGGCCATGATT-3' RV 5'-CTTTCGCTCTGGTCCGTCTT-3'	59	101

qChIP			
SEMA3A	FW 5'-ATCTCTGTGTCTTCATGAGCTG-3' RV 5'-TCAGAAGGAACTAATGGTGTCATA-3'	59	101
<b>Table 1C.</b> Target sequences of Ctrl and DNMT3A siRNAs.			
siRNA	Target sequences		
siCtrl	5'-UCGCCUAGGCUGCCAAGGCUU-3'		
siDNMT3A 1	5'-GCAUUCAGGUGGACCGCUA-3'		
siDNMT3A 2	5'-GCACUGAAAUGGAAAGGGU-3'		
siDNMT3A 3	5'-CUCAGGCGCCUCAGAGCUA-3'		
siDNMT3A 4	5'-GGGACUUGGAGAAGCGGAG-3'		

**Table 2.1.** Primer sequences used in methylation analysis by pyrosequencing (A) and in gene expression analysis by qPCR and analysis by qChIP (B). Target sequences of siRNAs used in DNMT3A knockdown experiment (C).

### 2.2.10 Statistical analysis

Human Methylation 450K microarray data were pre-processed using GenomeStudio and IMA (Illumina Methylation Analyzer for 450K, R/Bioconductor), including quality control, background correction, normalization, probe scaling, and adjustment for batch effect. Linear modelling in R Bioconductor package limma was applied to calculate differential methylation between sample groups. Limma uses an empirical Bayes moderated t-test, computed for each probe, with standard errors moderated using information from the full set of probes (Wilhelm-Benartzi et al., 2013). Probes with a methylation difference of beta value greater than 0.05 (5%) and with moderated t-test  $P < 0.05$  were considered as statistically significant.

Unpaired *t*-test with two-tailed distribution was used for statistical analysis of pyrosequencing, QPCR, qChIP, and cell growth assays. Each value represents the mean  $\pm$  S.D. of three independent

experiments, unless otherwise stated. The results were considered statistically significant when  $P < 0.05$ .

## 2.3 Results

### 2.3.1 Resveratrol (RSV) and pterostilbene (PTS) decrease breast cancer cell growth and invasive properties

In order to examine the effects of increasing concentrations of stilbenoid compounds, RSV and PTS, on the number of viable and dead cells, we used trypan blue exclusion test. Breast cancer cells, MCF10CA1h and MCF10CA1a, as well as MCF10A mammary epithelial cells, used as a normal cell model, were treated with RSV or PTS at 0-20 $\mu$ M concentrations for 4 or 9 days to determine time- and concentration-dependent effects on cell growth. MCF10CA1h and MCF10CA1a cells are derived from mice xenografts of MCF10A-*ras* cells that were generated by transfecting MCF10A mammary epithelial cells with constitutively active T24 Harvey-*ras* oncogene. MCF10CA1h and MCF10CA1a cells form well-differentiated and poorly differentiated tumors in xenograft models, respectively. Thus, MCF10CA1h cells have low invasive properties, whereas MCF10CA1a cells have characteristics of highly invasive cancer phenotype. This isogenic cell model appears to be attractive for studying epigenetic effects that arise during breast carcinogenesis without genetic differences as a confounding factor.

Stilbenoid treatment of MCF10CA1h and MCF10CA1a breast cancer cells resulted in significant inhibition of cell growth compared to cells treated with ethanol as a vehicle control (**Figure 2.1A and 2.1B**). These effects were dose- and time-dependent in both breast cancer cell lines treated with RSV or PTS. The compounds caused approximately 50% decrease in cell number ( $IC_{50}$ ) at

doses of 15 $\mu$ M for RSV and 7 $\mu$ M for PTS on day 9-exposure (**Figure 2.1A and 2.1B**), which confirms our previous findings (Lubecka et al., 2016). At the same time, the number of dead cells did not exceed 10% indicating non-cytotoxic mode of action at these concentrations (**Figure 2.1C**). In accordance with what we previously reported, invasive capacity and anchorage independent growth were attenuated by 15 $\mu$ M RSV and 7 $\mu$ M PTS (**Figure 2.1D and 2.1E**). Additionally, these doses did not cause significant differences in cell number in MCF10A mammary epithelial cells (**Figure 2.1F**). For these reasons, doses of 15 $\mu$ M for RSV and 7 $\mu$ M for PTS were chosen for further experiments.

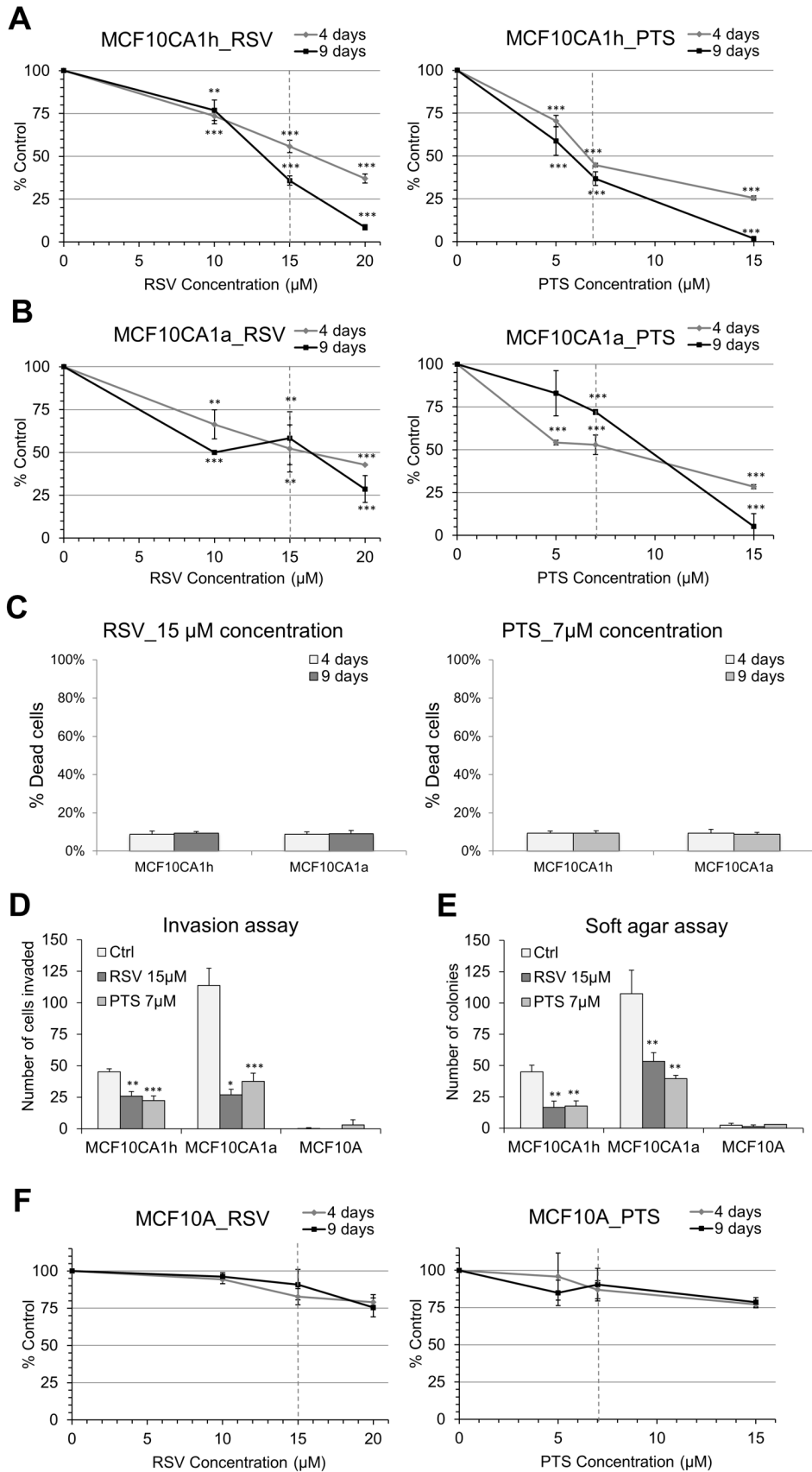


**Figure 2.1. Resveratrol (RSV) and pterostilbene (PTS) inhibit cell growth, invasive capacities and anchorage independent growth in breast cancer cells with negligible effects in mammary epithelial cells.** Effect on cell viability after 4-day and 9-day exposure of MCF10CA1h lowly invasive (A) and MCF10CA1a highly invasive breast cancer cells (B), as well as in MCF10A mammary epithelial cells (F) to RSV and PTS at 0–20  $\mu$ M concentration range, as determined by trypan blue exclusion test. Dashed line indicates 50% decrease in the number of viable cells as compared with control (cells treated with ethanol as a vehicle control); (C) Number of dead cells upon 9-day exposure of MCF10CA1h and MCF10CA1a breast cancer cells to 15  $\mu$ M RSV and 7  $\mu$ M PTS, as measured by trypan blue exclusion test. (D, E) MCF10CA1h and MCF10CA1a breast cancer cells as well as MCF10A mammary epithelial cells were treated with 15  $\mu$ M RSV or 7  $\mu$ M PTS for 9 days. Cell invasion (D) and anchorage-independent growth (E) were measured by Boyden chamber invasion assay and soft agar assay, respectively, upon exposure to RSV or PTS as compared with cells treated with ethanol as a vehicle control. All results represent mean  $\pm$  SD of three independent experiments; \*\*\* $P < 0.001$ , \*\* $P < 0.01$ , \* $P < 0.05$ .

### **2.3.2 Exposure to resveratrol (RSV) leads to time-dependent genome-wide changes in the DNA methylation patterns in breast cancer cells**

Using the Illumina Infinium Human Methylation 450K BeadChip microarray, we delineated the DNA methylation patterns upon 4-day and 9-day exposure of MCF10CA1h breast cancer cells to 15 $\mu$ M RSV. We identified 364 hypomethylated CpG sites at day 4 of RSV treatment compared to 990 hypomethylated CpG sites at day 9 of treatment ( $P < 0.05$ , limma  $t$ -test) (**Figure 2.2A**). While the number of hypomethylated loci increased after longer exposure, the opposite occurred for hypermethylated loci (**Figure 2.2A**). Although the number of differentially methylated CpG sites varied between 4- and 9-day treatment, similar genes and gene families were affected in terms of biological functions.

#### **2.3.2.1 Time-dependent hypermethylation in response to RSV treatment**

Functional analysis of genes corresponding to hypermethylated CpG loci upon 4-day RSV exposure revealed important players, silencing of which could at least partially contribute to anti-cancer effects of RSV. We identified genes from the WNT (*WNT16*, *WNT7A*) and NOTCH

(*NOTCH3*, *NOTCH4*) oncogenic signaling pathways, transcriptional regulators of gene expression (*JMJD1C*, *POU1F1*, *POU3F2*, *PRDM16*), genes regulating cell adhesion and migration (*MMP28*, *PTPRN2*), brain-specific genes (several SNORD members of small nucleolar RNAs, *GRIA4*, *MYTIL*), pluripotency genes (*NANOG*, *TCF15*), and serine/threonine protein kinase *ACVR1C*. The latter phosphorylates cytoplasmic SMAD transcription factors facilitating their translocation to the nucleus where SMADs regulate transcription of genes associated with differentiation, growth and apoptosis. RSV-mediated increase in methylation of the genes described above could potentially decrease their expression and consequently attenuate cancerous properties of cells.

We found 299 genes which were hypermethylated at exactly the same CpG positions at both time points of exposure ( $P < 9 \times 10^{-124}$ , Fisher's exact test). Additional 637 genes were identified where hypermethylation occurred at different loci on day 4 as compared with day 9 of treatment. Interestingly, 9-day RSV exposure often targeted different CpG loci within the same gene, the same gene family or the same functional gene category, as compared with a short-term exposure (**Figure 2.2B**). For instance, among overlapped genes, we detected hypermethylation within members of WNT (*WNT11*, *WNT5A*) and NOTCH (*NOTCH4*) signaling pathways, within metalloproteinase family (*MMP12*), SNORD members of small nucleolar RNAs, *PRDM16* and other members of PRDM family of transcription factors, and serine/threonine protein kinase *ACVR1*. *JMJD1C* was hypermethylated at exactly the same CpG locus on day 4 and day 9, showing a time-dependent increase in methylation and becoming the most robustly hypermethylated gene on day 9 of RSV treatment. *JMJD1C* is a histone demethylase that regulates activity of many transcription factors and has a potential oncogenic role in cancer (Chen et al., 2015). Another interesting example is protein tyrosine phosphatase *PTPRN2* which was hypermethylated at

different loci on day 4 compared with day 9 of RSV exposure. *PTPRN2* regulates localization of cofilin and phosphatidylinositol 4,5-diphosphate level in the plasma membrane impacting actin dynamics related to cell migration and metastasis. Indeed, *PTPRN2* was shown to promote metastatic breast cancer cell migration (Sengelaub, Navrazhina, Ross, Halberg & Tavazoie, 2016). There were also changes characteristic of only 9-day exposure. Additional activators of oncogenic signaling pathways were hypermethylated including Hedgehog (*GLI2*), MAPK (*MAPK12*), and mTOR (*RPS6KA3*, *RPTOR*). We also found additional well established oncogenes among hypermethylated genes such as *BRAF* from Ras/Raf oncogenic signal transduction and *TERT* that maintains telomere ends delaying programmed cell death. Many members of calcium ion channels family *CACNA* that regulate cellular functions, including mitogenesis, proliferation, differentiation, apoptosis and metastasis were hypermethylated on day 9 of RSV treatment.

### **2.3.2.2 Time-dependent hypomethylation in response to RSV treatment**

Genes encompassing CpG sites hypomethylated upon RSV treatment on day 4 were functionally linked to pathways and processes that inhibit cancer development suggesting their potentially tumor suppressive role. We identified *LIFR* cytokine receptor that inhibits cancer and suppresses metastasis (Chen et al., 2012a), *CSMD1* whose loss contributes to high proliferation, migration and invasion of breast cancer cells (Kamal, Holliday, Morrison, Speirs, Toomes & Bell, 2017), *PAX9* transcription factor whose suppression is linked to cancer development, G protein-coupled receptors (GPCRs) from LPHN family (*LPHN1*, *LPHN3*) regulating cell adhesion and frequently inhibited in cancer (Maiga et al., 2016), cadherins *CDH13* and *CDH18* promoting cell adhesion, imprinted gene *PEG3* that induces apoptosis and possesses a tumor suppressing role in glioma (Jiang, Yu, Yang, Agar, Frado & Johnson, 2010), and *BRMS1* that promotes binding of histone

deacetylase HDAC1 to gene promoters followed by transcriptional inhibition of pro-metastatic genes (Liu et al., 2016). *PBRM1* and *PHF20* that are negative regulators of cell proliferation and invasion were also among hypomethylated genes on day 4 (Tang et al., 2015). Both *PBRM1* and *PHF20* are involved in epigenetic regulation of gene transcription. *PBRM1* is a subunit of chromatin remodeling complexes while methyllysine-binding protein *PHF20* is a component of the MOF histone acetyltransferase protein complex and is involved in acetylation of histone H4. Interestingly, among RSV hypomethylated genes we found other epigenetic regulators such as *SMARCA4*, *MLL5*, *HDAC5*, and *CDKN2BAS*. *SMARCA4* is part of the large ATP-dependent chromatin remodeling complex SNF/SWI, which is required for transcriptional activation. Similarly, lysine methyltransferase *MLL5* is associated with activation of gene transcription upon methylation of histone H4 and is implicated in regulation of cell cycle progression (Rabello Ddo, de Moura, de Andrade, Motoyama & Silva, 2013). On the other hand, histone deacetylase *HDAC5* and *CDKN2BAS* are responsible for gene silencing. *HDAC5* promotes condensed chromatin structure by decrease in acetylation at histone proteins while *CDKN2BAS* encodes functional RNA molecule that interacts with polycomb repressive complexes (PRCs) leading to epigenetic silencing of target genes.

A comparison of 4-day vs. 9-day treatment shows that RSV treatment often targets for hypomethylation the same genes but at different CpG loci, the same gene families or the same functional categories of genes at both time points, which was earlier noted for hypermethylated genes (**Figure 2.2B**). Altogether 28 genes, including 15 genes with the same location of hypomethylated loci, overlapped between both treatments ( $P < 1 \times 10^{-14}$ , Fisher's exact test). For instance, cell adhesion promoter *LPHN3*, lysine methyltransferase *MLL5*, and long non-coding

RNA *CDKN2BAS* were hypomethylated at exactly the same site at 4- and 9-day treatment. Tumor suppressor *CSMD1*, and cadherins *CDH13* and *CDH18* were hypomethylated on day 9 at different CpG loci compared with day 4. *PHF* family of genes regulating histone acetylation and HDAC family of histone deacetylases were found to be hypomethylated upon 9-day exposure however different members of the families were targeted compared with 4-day treatment. In addition to epigenetic regulators mentioned above (i.e., *PHF*, *HDAC*, *MLL5*, *CDKN2BAS*), we identified *MBD4* and *SUV39H1* among hypomethylated genes that were affected specifically on day 9. *MBD4* is a methyl-CpG binding domain protein and has thymine glycosylase activity important for G:T mismatches. Methylated cytidine in CpG dinucleotides can be deaminated to thymidine that is then excised by MBD4 resulting in DNA demethylation. *SUV39H1* is a histone modifying enzyme with methyltransferase activity specifically for trimethylation of Lys-9 of histone H3 which recruits HP1 proteins and leads to transcriptional repression. Genes implicated in RNA maturation and epigenetic regulation of RNA, such as pre-mRNA alternative splicing regulator *BRUNOL4* and RNA methyltransferase *METTL3*, were also specific to 9-day exposure. In addition, 9-day exposure resulted in hypomethylation of known tumor suppressor genes, *BRCA2* and *HOXA9*.

### **2.3.3 RSV-mediated loci-specific hypomethylation in lowly and highly invasive breast cancer cells**

Next, we compared DNA methylation changes in response to 9-day treatment with 15 $\mu$ M RSV in lowly invasive MCF10CA1h to highly invasive MCF10CA1a breast cancer cells. We previously described genes containing CpG sites that are hypermethylated in response to RSV in both cell lines (Lubecka et al., 2016). In the present study, we focus on CpG sites that are hypomethylated

in cells treated with RSV to deliver mechanistic input on diet-mediated epigenetic activation of genes (diff. methylation  $\leq -0.05$ ,  $P < 0.05$ , limma  $t$ -test). Genes hypomethylated in response to RSV would be expected to become expressed and contribute to anti-cancer effects of dietary stilbenoids. Similar amount of hypomethylated CpG sites were detected after RSV treatment in both breast cancer cell lines (**Figure 2.2C**). The magnitude of average hypomethylation across all hypomethylated sites reached approximately -0.25 (delta beta) in MCF10CA1a cells compared to maximum magnitude of hypomethylation of less than -0.20 in MCF10CA1h cells (**Figure 2.2D**). More specifically, the majority of CpG sites with the most robust hypomethylation in MCF10CA1a cells showed lower extent of changes in MCF10CA1h cells, demonstrating a stronger effect of RSV in highly invasive breast cancer cells (**Table 2.2**). The loci listed in **Table 2.2** are located in gene regulatory regions, including promoters and 5'UTRs of *AGTPBP1*, *SEMA3A*, *FOXP3*, *UACA*, *FAM49A*, *TMEM91*, *CSMD1*, *WFDC3*, *EPN2*, and *HAT1*. Interestingly, *SEMA3A*, *FOXP3*, and *CSMD1* were shown to be implicated in regulation of invasiveness of cancer cells. Increased expression of *SEMA3A* lowered the ability of cancer cells to invade through extracellular matrix (Herman & Meadows, 2007) while loss of *FOXP3* promoted growth and migration of cancer cells (Dai, Wang, Wu, Xiao, Liu & Zhang, 2017). In addition, breast cancer patients with low levels of *CSMD1* showed a significantly shorter overall survival (Escudero-Esparza et al., 2016).

Gene name	CpG #	CpG location	Differential methylation in MCF10CA1h (delta beta)	Differential methylation in MCF10CA1a (delta beta)
AGTPBP1	cg14079243	TSS1500	-0.03	-0.16
SEMA3A	cg05081033	TSS1500	-0.01	-0.14
FOXN3	cg14843872	5'UTR	0.01	-0.12
UACA	cg10177766	Body	-0.01	-0.12
FAM49A	cg07091529	5'UTR	-0.08	-0.11
TMEM91	cg13736811	5'UTR	-0.13	-0.11
CSMD1	cg25114299	Body	-0.04	-0.11
WFDC3	cg07982740	Body	-0.14	-0.11
EPN2	cg25132536	5'UTR	0.01	-0.10
CSMD3	cg00417291	5'UTR	-0.03	-0.10
CDKN2BAS	cg14069088	Body	-0.07	-0.08
HIST1H2BK	cg23155468	3'UTR	-0.05	-0.08
SEMA3D	cg26801812	Body	-0.01	-0.08
HAT1	cg04507121	TSS1500	-0.01	-0.08

**Table 2.2.** A list of CpG loci highly hypomethylated in invasive MCF10CA1a cells in response to 9-day exposure to 15 $\mu$ M resveratrol (RSV), as measured by Illumina Infinium Human Methylation 450K BeadChip microarray.

In order to identify loci with the highest probability to be specifically targeted by RSV in breast cancer, we searched for overlap between CpG sites and genes hypomethylated in MCF10CA1h and MCF10CA1a breast cancer cells (**Figure 2.2E**). We found 116 CpG sites hypomethylated in response to RSV in both cell lines (**Appendix A**) ( $P < 4 \times 10^{-150}$ , Fisher's exact test). The majority of these CpG sites were lowly methylated in MCF10A mammary epithelial cells and were gaining high levels of methylation in breast cancer cells (**Figure 2.2F**), which could suggest methylation-mediated silencing of corresponding genes in cancer. Exposure to RSV resulted in a similar degree of hypomethylation across all the sites without substantial differences between lowly and highly invasive cells (**Figure 2.2G**). Loci whose initial methylation level was higher than 0.3 in MCF10A

mammary epithelial cells were coming back to normal levels upon RSV exposure in both cancer cell lines (**Figure 2.2G**).

Out of 116 common CpG sites, 75 were assigned to genes. Additional 38 genes were identified to be hypomethylated in both cell lines although different CpG locus was affected in response to RSV (**Appendix B**). The 113 genes identified from the overlap would be considered as strongest targets of RSV and their appearance in both breast cancer cell lines would limit the possibility of cell line-specific artifact. We refer to these genes as “hypomethylated RSV targets”. Biological function and signaling pathway analysis for “hypomethylated RSV targets” revealed that the majority of these genes are implicated in increase in cell adhesion, apoptosis, and cell cycle arrest, in regulation of gene transcription and p53 signaling, and in inhibition of WNT oncogenic pathway; functions that indicate tumor suppressive roles of these genes (**Figure 2.2H and 2.2I**). “Hypomethylated RSV targets” include inhibitors of cell migration and invasion such as *CSMD1*, cadherin *CDH6*, and G protein-coupled receptor *LPHN3*. Epigenetic regulators such as *CDKN2BAS* and *METTL3*, and potential tumor suppressors *SEMA3A* and *WFDC3* are also present among 113 “hypomethylated RSV targets”. *RBPJ* is another important candidate present among genes hypomethylated in both cancer cell lines. *RBPJ* acts as a transcriptional repressor by recruitment of chromatin remodeling complexes which consequently suppresses oncogenic NOTCH signaling (Xu et al., 2017).

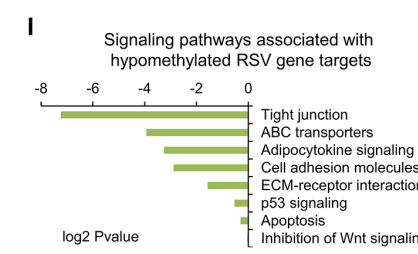
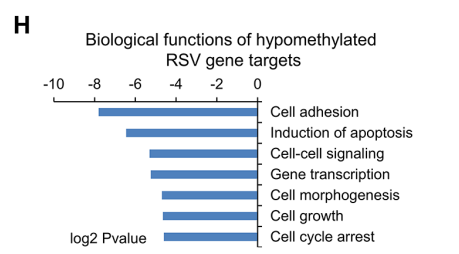
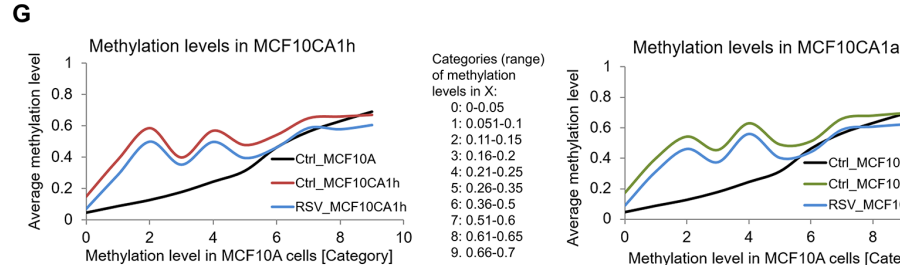
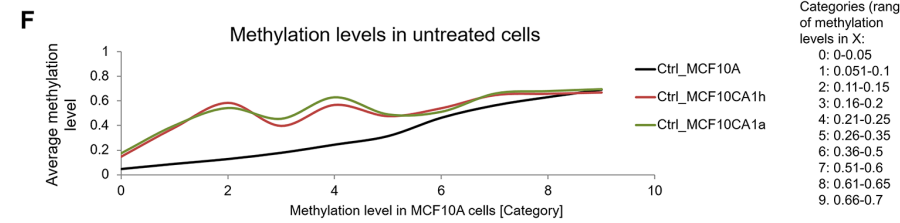
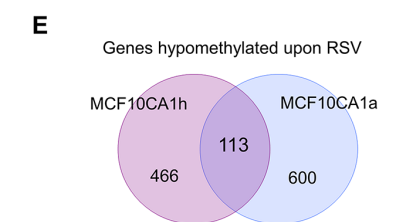
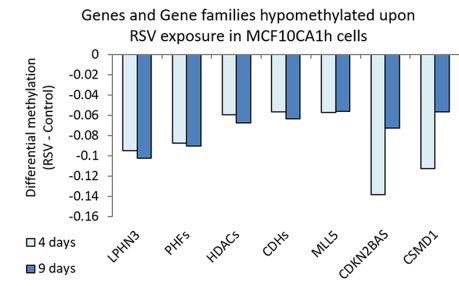
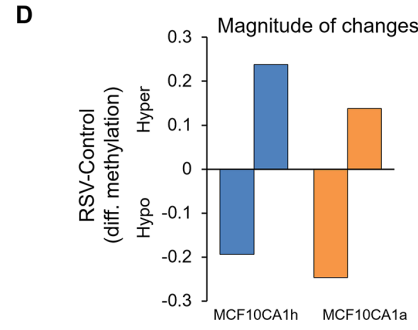
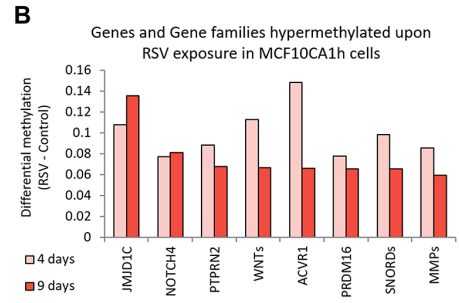
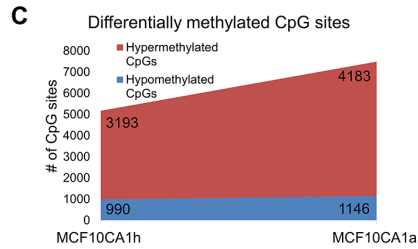
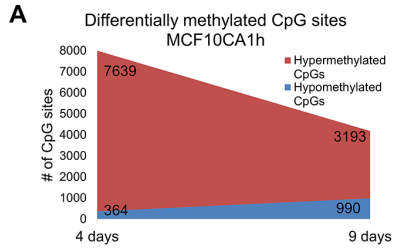


**Figure 2.2. Landscape of changes in the DNA methylation patterns in breast cancer cells in response to resveratrol (RSV).** (A) A comparison of the number of differentially methylated CpG sites with statistically significant difference of at least 0.05 between RSV-treated and control cells (i.e., delta beta) on day 4 and day 9 exposure to 15 $\mu$ M RSV in MCF10CA1h lowly invasive breast cancer cells, as determined by Illumina 450K microarray ( $P < 0.05$ , limma  $t$ -test). (B) Magnitude of methylation difference between RSV-treated and control cells at genes and gene families differentially methylated as indicated by the microarray data upon 4-day and 9-day exposure of MCF10CA1h breast cancer cells. (C) A comparison of the number of differentially methylated CpG sites with statistically significant difference of at least 0.05 between RSV-treated and control cells on day 9 exposure to 15 $\mu$ M RSV in MCF10CA1h lowly invasive and MCF10CA1a highly invasive breast cancer cells, as determined by Illumina 450K microarray ( $P < 0.05$ , limma  $t$ -test). (D) Magnitude of overall methylation changes upon treatment of MCF10CA1h and MCF10CA1a breast cancer cells with RSV. (E) Venn diagram for genes containing CpG sites hypomethylated in response to RSV in MCF10CA1h and MCF10CA1a breast cancer cells, showing overlap between both cell lines. (F,G) Basal levels of methylation of “hypomethylated RSV targets” as determined by the genome-wide microarray data in untreated MCF10A mammary epithelial cells, MCF10CA1h lowly invasive and MCF10CA1a highly invasive breast cancer cells (F), as well as in breast cancer cells exposed to 15 $\mu$ M RSV for 9 days (G). The basal level of methylation at CpG loci commonly hypomethylated in MCF10CA1h lowly invasive and MCF10CA1a highly invasive breast cancer cells upon 9-day RSV treatment is compared to the methylation levels at these loci in MCF10A cells. (H, I) Functional analyses using GO, KEGG and DAVID knowledgebase indicate biological functions (H) and signaling pathways (I) associated with genes corresponding to CpG sites hypomethylated in response to RSV in both MCF10CA1h and MCF10CA1a breast cancer cells (“hypomethylated RSV targets”).

### **2.3.4 Tumor suppressor gene *SEMA3A* is epigenetically activated upon exposure to resveratrol (RSV) or pterostilbene (PTS) in breast cancer cells**

Our genome-wide DNA methylation analysis of breast cancer cells treated with 15 $\mu$ M RSV revealed a group of genes containing CpG loci at which the magnitude of hypomethylation in response to stilbenoids rises with increasing invasive potential of cancer cells (**Figure 2.3A**). Methylation levels at five out of these CpG sites corresponding to *SEMA3A*, *UACA*, *FAM49A*, *TMEM91*, and *EPN2* were quantitatively measured by pyrosequencing in highly invasive MCF10CA1a breast cancer cells exposed to RSV (**Figure 2.3B**). The exact location of the CpG loci is visualized in the gene map in **Figure 2.3B** with the tested region blue shaded. Fragments tested in pyrosequencing encompassed a CpG site covered on Illumina (marked in square in

**Figure 2.3B**) and neighboring CpG loci so that a broader region was investigated. Pyrosequencing confirmed 10-20% hypomethylation within sites located in promoters of *SEMA3A*, *TMEM91*, and *EPN2*, and within gene body of *UACA* and *FAM49A* (**Figure 2.3B**, right panel). One of the five genes, *SEMA3A*, was previously shown to exert a tumor suppressor function in breast cancer. One study reported that *SEMA3A* regulates phosphorylation of phosphatase and tensin homolog (PTEN), which in turn activates a chain of tumor suppressor genes to inhibit breast cancer growth, invasiveness and angiogenic capacity (Mishra et al., 2015). Another study demonstrated a role for *SEMA3A* in proliferative control of tumor-associated macrophages (Wallerius et al., 2016). Silencing of *SEMA3A* in many types of cancer, including breast cancer, was found in publicly available gene expression data in clinical samples, which further supports a tumor suppressor role of *SEMA3A* (**Figure 2.4A**). Using publicly available methylation datasets of breast cancer patients, we also confirmed hypermethylation of *SEMA3A* promoter region in tumors at the same CpG locus as the site affected by RSV (**Figure 2.4B**, the locus marked in square). *SEMA3A* hypermethylation could at least partly explain downregulation of the gene observed in tumors versus normal tissue. Taken together, this evidence indicates that *SEMA3A* may act as a tumor suppressor regulated by DNA methylation, however epigenetic regulation of *SEMA3A* has not yet been explored. We therefore selected *SEMA3A* for further studies on mechanisms associated with hypomethylation mediated by stilbenoids.

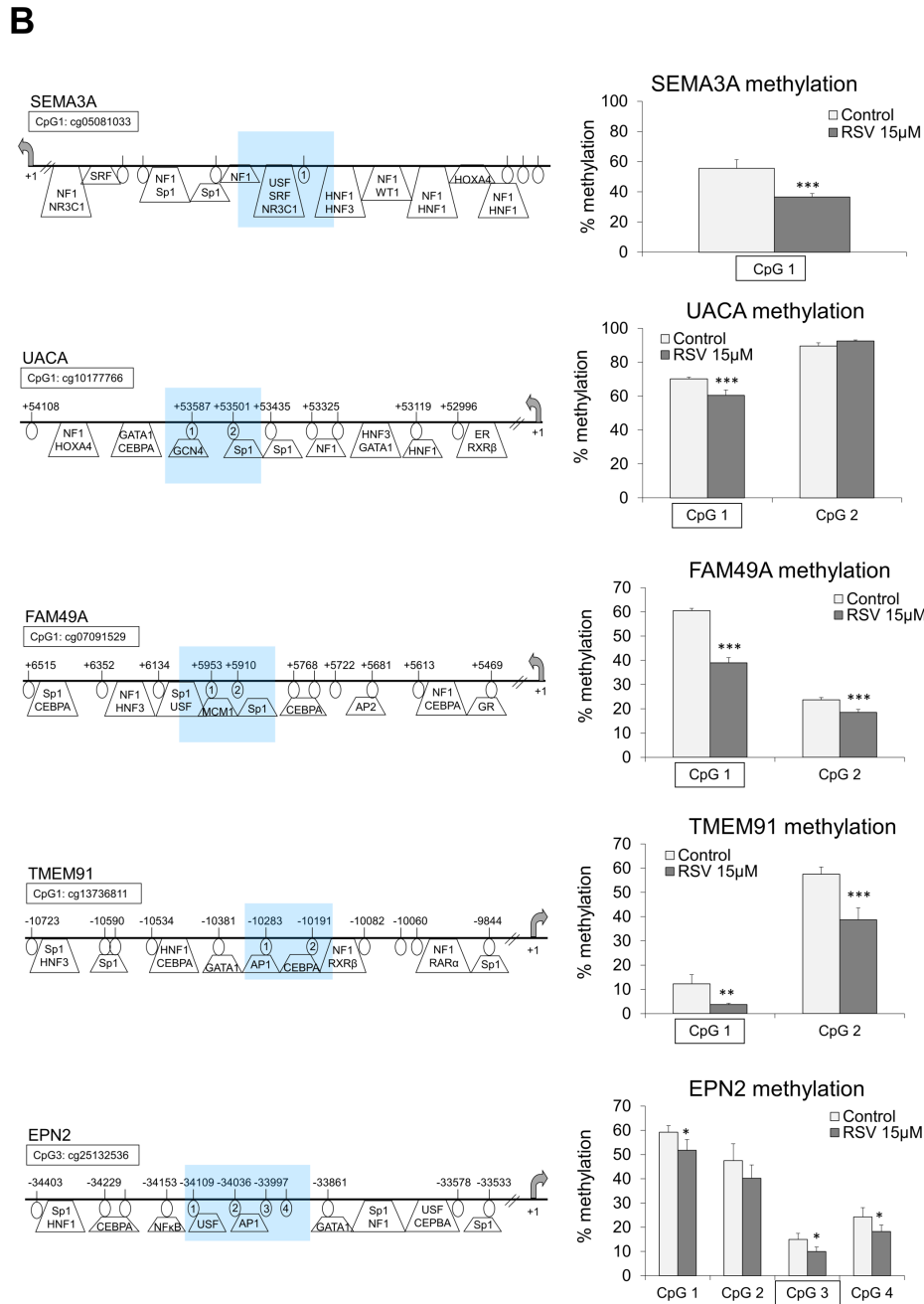
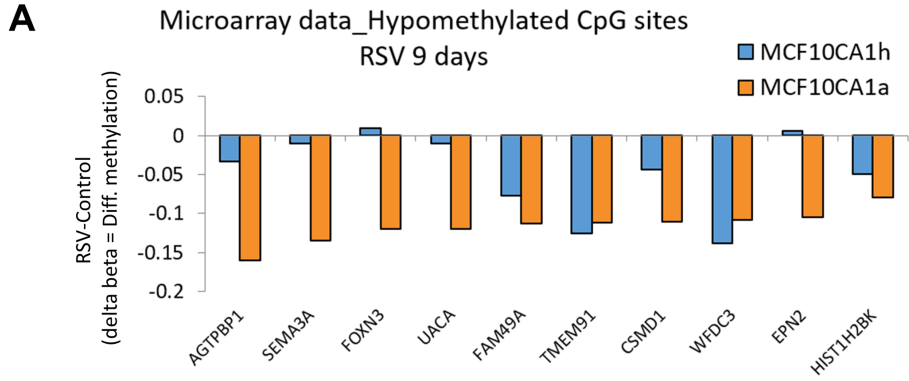


**Figure 2.3. Quantitative analysis of methylation state of the selected genes, SEMA3A, UACA, FAM49A, TMEM91, and EPN2, which contain CpG loci highly hypomethylated in invasive MCF10CA1a breast cancer cells exposed to resveratrol (RSV) based on the Illumina 450K microarray.** Using Illumina 450K microarray, the DNA methylation landscape was determined in lowly and highly invasive breast cancer cells exposed to 15  $\mu$ M RSV for 9 days. Based on the microarray data, 5 hypomethylated CpG sites corresponding to 5 genes (probes) were chosen for validation of the methylation difference by pyrosequencing. The difference in DNA methylation, statistical significance, location of the CpG site in gene regulatory region, consistency of the change between the cell lines, and the function of a corresponding gene as a potential tumor suppressor gene were taken into account in the selection. (A) Magnitude of methylation difference between RSV-treated and control cells at CpG loci corresponding to 10 genes that are highly hypomethylated in response to RSV in invasive MCF10CA1a breast cancer cells upon 9-day treatment, as indicated by the microarray data. (B) Right panel shows the average methylation state at single CpG sites within the selected probes in control MCF10CA1a cells (treated with ethanol as a vehicle control) and MCF10CA1a cells exposed to 15 $\mu$ M RSV for 9 days. Each region encompasses a differentially methylated CpG site covered on Illumina 450K microarray (marked in square) along with neighboring CpG loci. Gene maps in the left panel show the exact position of the tested CpG sites relative to transcription start site (TSS). The tested region is shaded and pyrosequenced CpG sites are circled and numbered. The putative transcription factor binding sites are indicated as predicted by TransFac. All results represent mean  $\pm$  SD of three independent experimental exposures; \*\*\*P < 0.001, \*\*P < 0.01, \*P < 0.05.

Exposure of MCF10CA1a breast cancer cells to another stilbenoid compound, pterostilbene (PTS), led to hypomethylation of *SEMA3A* promoter at the same RSV target site (**Figure 2.4C**). Decrease in *SEMA3A* methylation was linked to increase in gene expression in response to both RSV and PTS (**Figure 2.4D**), which further supports epigenetic regulation of transcriptional activity of *SEMA3A*. Importantly, although the microarray indicated just slight hypomethylation at the studied CpG site (cg05081033) within *SEMA3A* promoter in lowly invasive MCF10CA1h cells, we detected a strong 25% hypomethylation using pyrosequencing and confirmed gene upregulation in response to RSV (**Figure 2.4E and 2.4F**). This further strengthens the role for DNA methylation in regulation of *SEMA3A* expression.

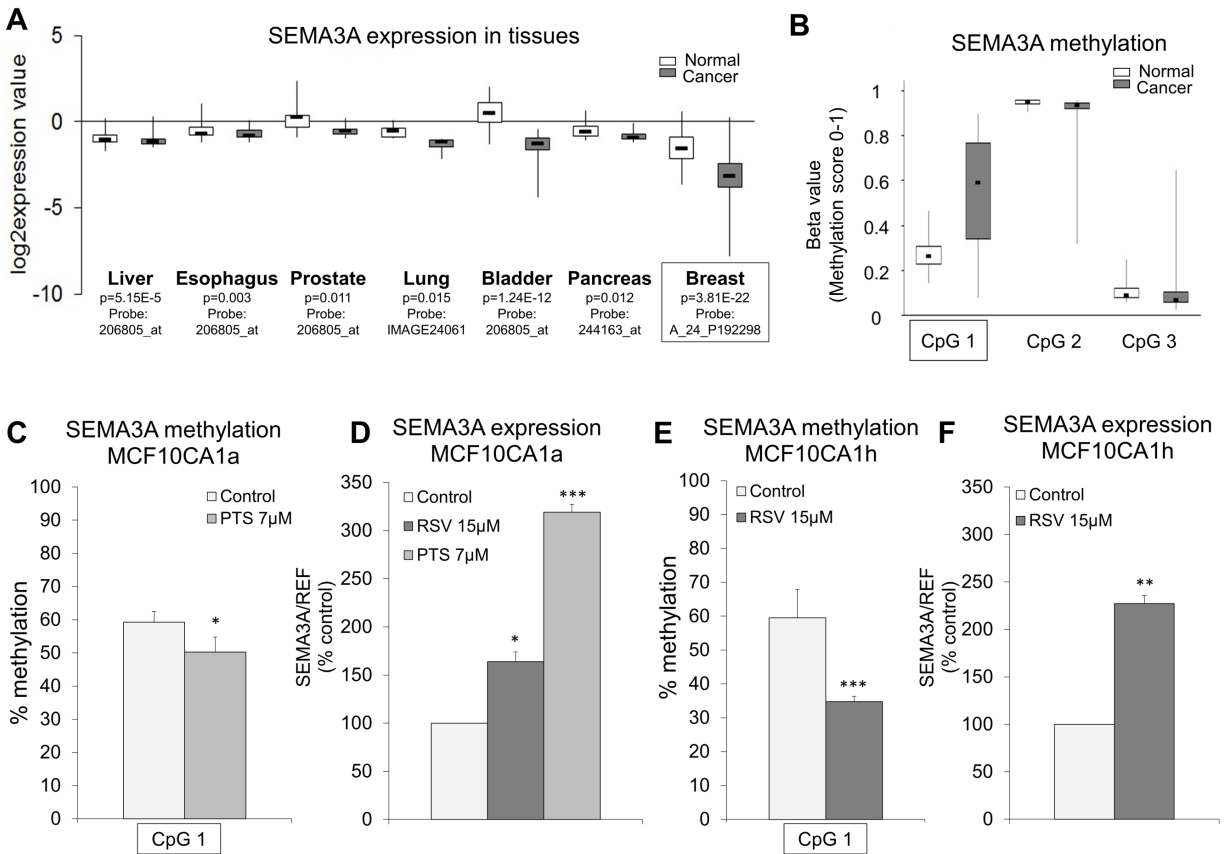


**Figure 2.4. *SEMA3A* tumor suppressor gene is hypomethylated and reactivated upon treatment of highly invasive MCF10CA1a breast cancer cells with pterostilbene (PTS).** (A) *SEMA3A* expression in normal and cancer tissues based on microarray data from Oncomine database. Expression values are presented as log<sub>2</sub>-transformed median centered per array, and SD-normalized to 1 per array. (B) *SEMA3A* methylation state expressed as beta value in normal and cancer tissues based on microarray data from TCGA database. (C) Hypomethylation of *SEMA3A* promoter upon 9-day exposure to 7 $\mu$ M PTS in MCF10CA1a breast cancer cells, as measured by pyrosequencing. (D) Increased expression of *SEMA3A* upon 9-day exposure to 15 $\mu$ M RSV or 7 $\mu$ M PTS in MCF10CA1a breast cancer cells, as measured by qPCR. (E) Hypomethylation and increased expression of *SEMA3A* in response to 9-day exposure to 15 $\mu$ M RSV in lowly invasive MCF10CA1h breast cancer cells, as measured by pyrosequencing and qPCR, respectively. All results represent mean  $\pm$  SD of three independent experiments; \*\*\* $P < 0.001$ , \*\* $P < 0.01$ , \* $P < 0.05$ .

### 2.3.5 Decreased DNMT3A occupancy within *SEMA3A* promoter in response to resveratrol (RSV) or pterostilbene (PTS)

After validation of DNA hypomethylation and increased expression of *SEMA3A* upon stilbenoid

treatment, we sought to delve into the mechanism underlying these effects. As the magnitude of changes in the DNA methylation patterns in response to stilbenoids was higher in highly invasive than in lowly invasive cells, we proceed with highly invasive MCF10CA1a cell line as an experimental model in further investigations. DNA methyltransferases (DNMTs) are enzymes that catalyze the transfer of a methyl group to the 5th position of the cytosine ring on the DNA; thereby they are central players in the DNA methylation reaction. While DNMT1 is mainly responsible for maintenance of the DNA methylation patterns during replication, DNMT3A and DNMT3B are categorized as *de novo* methyltransferases (Jones, Issa & Baylin, 2016). We found that treatment of MCF10CA1a breast cancer cells with RSV or PTS caused a reduction of *DNMT3A* expression (**Figure 2.5A**). DNMT3A binding at the hypomethylated CpG site within the *SEMA3A* promoter was diminished upon RSV or PTS treatment (**Figure 2.5B**). Reduction in *DNMT3A* expression and DNMT3A occupancy at the *SEMA3A* promoter in response to stilbenoids suggests a connection between loss of DNMT3A and hypomethylation. In addition to hypomethylation and lower occupancy of DNMT3A, we observed increased enrichment of active histone mark, acetylation of histone H3 lysine 9 (H3K9ac), and decreased enrichment of repressive histone mark, trimethylation of histone H3 lysine 27 (H3K27me3). Such changes in occupancy of histone modifications are indicative of open chromatin structure and increased transcriptional activity of *SEMA3A* upon exposure to RSV or PTS (**Figure 2.5C and 2.5D**).

### **2.3.6 *DNMT3A* knockdown mimics the effects of stilbenoid compounds on DNA methylation and expression of *SEMA3A***

We further established the role of DNMT3A in mediating hypomethylation of the *SEMA3A* promoter in response to stilbenoid compounds by knocking down the *DNMT3A* gene using small

interfering RNAs (siRNAs). MCF10CA1a cells were transfected with one of four siRNAs targeting DNMT3A (siDNMT3A 1-4) or siCtrl. Measurement of cell growth revealed that all DNMT3A siRNAs led to robust reduction in cell growth after 3 rounds of transfection (**Figure 2.5E**). Expression of *DNMT3A* was knocked down most effectively by siDNMT3A 1 and siDNMT3A 3 (**Figure 2.5F**), therefore we present further data using those DNMT3A siRNAs. Upon knocking down *DNMT3A*, expression of *SEMA3A* was significantly increased (**Figure 2.5G**), mimicking the effect of stilbenoids on expression of this TSG. In addition, *DNMT3A* knockdown resulted in a 12% decrease in DNA methylation at the same CpG site identified and validated as differentially methylated in response to RSV and PTS treatment (**Figure 2.5H**). These findings suggest that DNMT3A is an important mechanistic player in hypomethylation of *SEMA3A* in response to RSV and PTS.

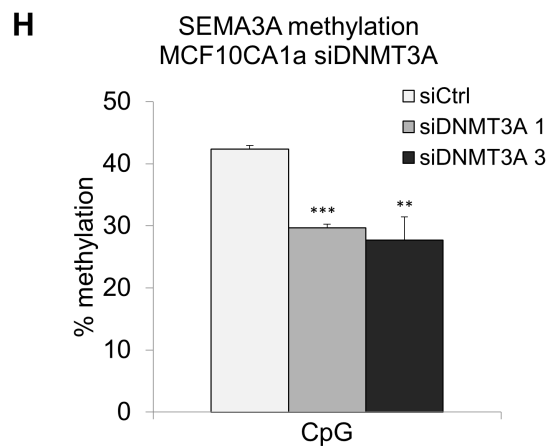
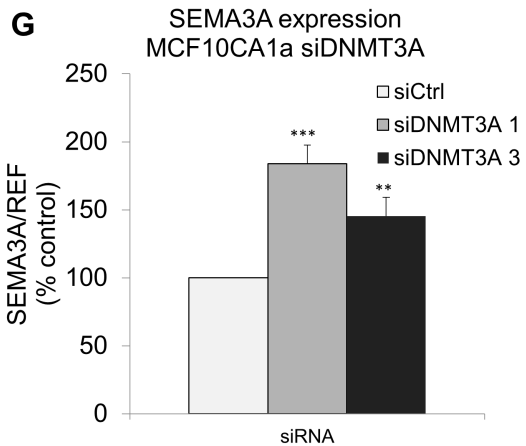
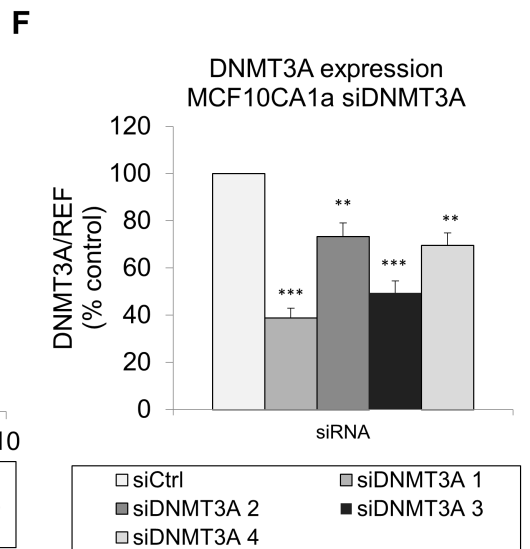
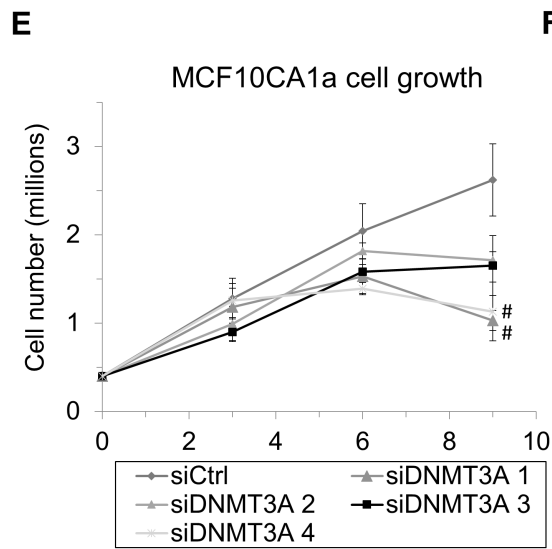
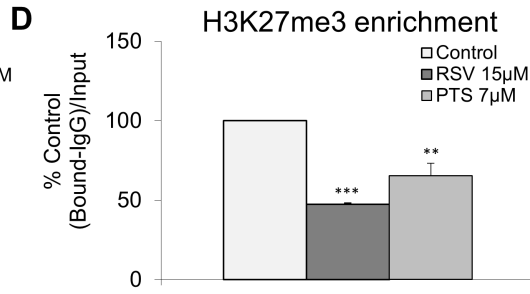
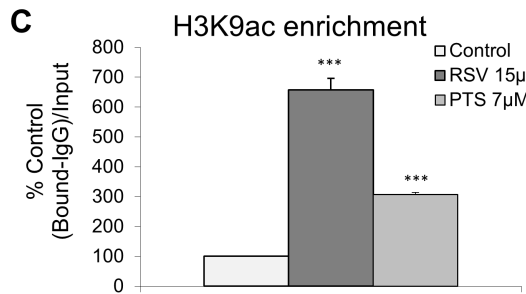
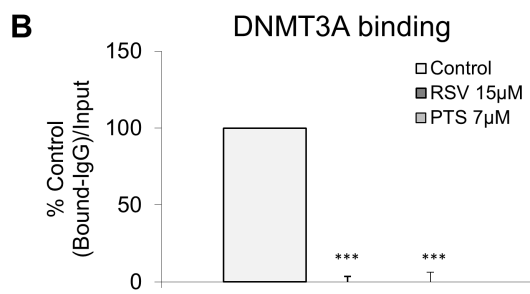
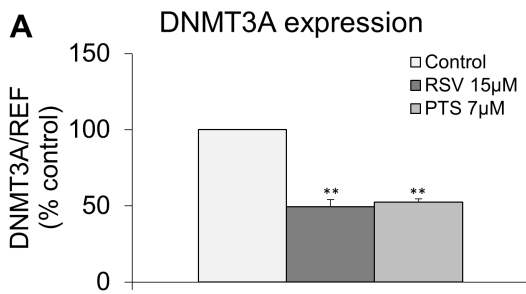


**Figure 2.5. Binding of DNMT3A and modifications of histone tails within *SEMA3A* promoter in breast cancer cells in response to resveratrol (RSV) or pterostilbene (PTS).** (A) Expression of *DNMT3A* upon 9-day exposure to 15  $\mu$ M RSV or 7  $\mu$ M PTS in MCF10CA1a breast cancer cells, as measured by qPCR. (B) Binding of DNMT3A within the *SEMA3A* promoter in MCF10CA1a cells in response to 9-day treatment with 15  $\mu$ M RSV or 7  $\mu$ M PTS, as assessed by qChIP and expressed as a percentage of the binding level in control cells. (C,D) Enrichment of histone H3 acetylation at lysine 9 (H3K9ac, activating mark) (C) and histone H3 trimethylation at lysine 27 (H3K27me3, repressive mark) (D) within the *SEMA3A* promoter in MCF10CA1a cells in response to 9-day treatment with 15  $\mu$ M RSV or 7  $\mu$ M PTS, as assessed by qChIP and expressed as a percentage of the binding level in control cells. (E) Effect on MCF10CA1a cell growth after first (day 3), second (day 6) and third (day 9) transfection with siCtrl or siDNMT3A 1-4. (F) *DNMT3A* expression quantified by qPCR after third transfection with siCtrl or siDNMT3A 1-4. (G) Increased *SEMA3A* expression quantified by qPCR after third transfection with siDNMT3A 1 or siDNMT3A 3 compared to siCtrl. (H) Hypomethylation of *SEMA3A* quantified by pyrosequencing after third transfection with siDNMT3A 1 or siDNMT3A 3 compared to siCtrl. All results represent mean  $\pm$  SD of three independent experiments, except siRNA results represent three technical replicates; \*\*\* $P < 0.001$ , \*\* $P < 0.01$ , \* $P < 0.05$ , # $P < 0.1$ .

### **2.3.7 Nuclear factor 1C (NF1C) occupancy at *SEMA3A* promoter increases upon resveratrol (RSV) and pterostilbene (PTS) treatment**

Changes in DNA methylation are known to affect binding of transcription factors to a gene regulatory region (Yin et al., 2017). We used TransFac to compute putative transcription factor binding elements encompassing the hypomethylated CpG site in *SEMA3A* promoter. We found several candidates including nuclear factor 1C (NF1C). A response element for NF1C was further found in 80% of hypomethylated loci within “hypomethylated RSV targets”, a group of genes hypomethylated in both MCF10CA1h and MCF10CA1a cells (**Appendix B**). Additionally, transcription factors from NF1 family have been implicated as key epigenetic regulators in cancer possibly through regulating chromatin accessibility (Fane, Harris, Smith & Piper, 2017). NF1C was specifically reported to have a tumor suppressor role in breast cancer (Lee, Lee & Park, 2015). For these reasons, we proceeded with experimentally testing whether stilbenoid-mediated changes in DNA methylation near predicted NF1C binding site within the *SEMA3A* promoter affected

binding of this potentially important transcription factor. Interestingly, we found that RSV or PTS treatment of highly invasive MCF10CA1a breast cancer cells increased occupancy of NF1C at the *SEMA3A* promoter (**Figure 2.6A**). This enrichment in binding was accompanied by increased *NF1C* expression in PTS-treated breast cancer cells, while expression of *NF1C* was unchanged in response to RSV (**Figure 2.6B**). Such changes in *NF1C* expression and binding observed in stilbenoid-treated MCF10CA1a breast cancer cells may be linked to transcriptional reactivation of *SEMA3A*.

### **2.3.8 DNMT3A inhibitor SALL3 is upregulated upon stilbenoid treatment**

To introduce an upstream element to the proposed mechanism of stilbenoid-mediated epigenetic reactivation of *SEMA3A*, we identified a protein called sal-like 3 (SALL3) that has been reported to directly inhibit DNMT3A activity and impose subsequent DNA hypomethylation (Shikauchi et al., 2009). We found that *SALL3* expression was significantly increased by 2.5- and 1.5-fold upon 9-day treatment of MCF10CA1a cells with 15 $\mu$ M RSV or 7 $\mu$ M PTS, respectively (**Figure 2.6C**). While further work is needed to confirm SALL3 as a player in this mechanism, the upregulation of this gene may be related to decreased DNMT3A activity by direct binding which consequently results in DNA hypomethylation at the *SEMA3A* promoter (**Figure 2.6D**). We propose a mechanism wherein stilbenoid treatment of breast cancer cells results in sequestration of DNMT3A via direct inhibition by SALL3 followed by subsequent DNA hypomethylation at the *SEMA3A* promoter. Decreased methylation at the *SEMA3A* promoter allows NF1C transcription factor to bind and promote a transcriptionally active state (**Figure 2.6D**).

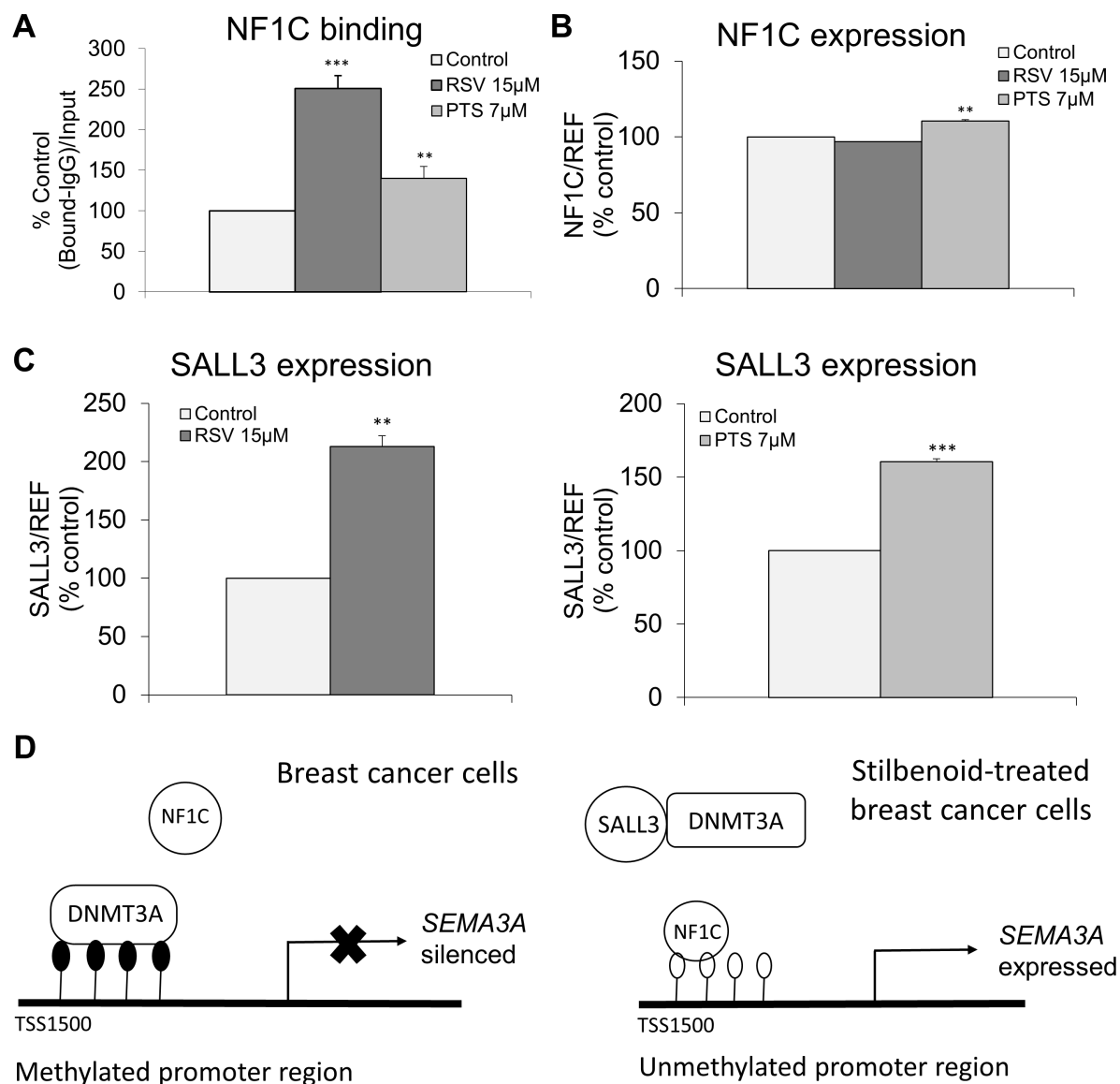


**Figure 2.6. Occupancy of transcription factor NF1C within *SEMA3A* promoter and potential role for SALL3 in breast cancer cells in response to resveratrol (RSV) or pterostilbene (PTS).** (A) Binding of NF1C within the *SEMA3A* promoter in MCF10CA1a cells in response to 9-day treatment with 15  $\mu$ M RSV or 7  $\mu$ M PTS as assessed by qChIP and expressed as a percentage of the binding level in control cells. (B) Expression of *NF1C* upon 9-day exposure to 15  $\mu$ M RSV or 7  $\mu$ M PTS in MCF10CA1a breast cancer cells, as measured by qPCR. (C) *SALL3* expression quantified by qPCR in MCF10CA1a cells in response to 9-day treatment with 15  $\mu$ M RSV or 7  $\mu$ M PTS. (D) Schematic of proposed mechanism of stilbenoid-mediated epigenetic reactivation of *SEMA3A* involving direct inhibition of DNMT3A by SALL3 to impose DNA hypomethylation and allow NF1C to bind at the *SEMA3A* promoter and drive gene transcription. All results represent mean  $\pm$  SD of three independent exposures; \*\*\* $P$  < 0.001, \*\* $P$  < 0.01, \* $P$  < 0.05.

## 2.4 Discussion

Functions of tumor suppressor genes (TSGs) are commonly lost during the course of cancer development which is often associated with inactivating mutations or epigenetic silencing (Jones, Issa & Baylin, 2016). The latter phenomenon plays an important role in majority of cancer cases without family history. Transcriptionally silenced TSGs as a result of epigenetic alterations, specifically increased DNA methylation within gene regulatory regions, have been shown as a hallmark of cancer (Jones, Issa & Baylin, 2016). Epigenetic drugs such as DNA methyltransferase inhibitors (DNMTi) target DNMTs to lead to passive DNA hypomethylation with the goal to re-express TSGs that have been silenced by DNA methylation in cancer (Jones, Issa & Baylin, 2016). However, the effects of DNMTi such as decitabine (5-aza-2'-deoxycytidine) are non-specific which may lead to activation of other genes responsible for side-effects or resistance to therapy. Indeed, the initial patterns of gene expression in patients treated with decitabine may influence the efficacy of this drug. For example, patients with low levels of lysine methyltransferase *MLL5* were developing resistance to low-doses of decitabine (Yun et al., 2014). In addition, expression levels of two enzymes involved in decitabine metabolism, namely cytidine deaminase (CDA) and deoxycytidine kinase (DCK), differ between non-responders and responders (Qin et al., 2011). Hence, alternative more specific methods of reactivating epigenetically-silenced tumor suppressor genes are needed. As DNA methylation is responsive to environmental stimuli (Jones, Issa & Baylin, 2016), dietary compounds could possibly comprise a novel approach in anti-cancer epigenetic strategies. A genome-wide DNA methylation study where curcumin, a bioactive compound from a spice Turmeric, was compared with decitabine, shows that curcumin caused loci-specific both hyper- and hypomethylation, predominantly in partially-methylated CpG sites, while decitabine treatment led to non-selective hypomethylation (Link et al., 2013). This evidence

opens the door to investigating whether other dietary polyphenols can exert specific epigenetic effects and what mechanisms are involved in such an action.

Herein, we were investigating polyphenols from stilbenoid class, such as resveratrol (RSV) and its natural dimethylated analog pterostilbene (PTS), and their epigenetic effects in breast cancer cells. Stilbenoids were shown to exert anti-cancer effects in cell lines and *in vivo* models however without a clear molecular mechanism demonstrated (Carter, D'Orazio & Pearson, 2014; Jeyabalan, Aqil, Munagala, Annamalai, Vadhanam & Gupta, 2014b; McCormack & McFadden, 2012; Wen et al., 2017). There are a few reports by us and others on the involvement of epigenetics and specifically DNA methylation in the action of stilbenoids (Gracia et al., 2014; Lou, Wang, Xia, Skog & Sun, 2014; Lubecka et al., 2016; Papoutsis, Borg, Selmin & Romagnolo, 2012; Stefanska, Rudnicka, Bednarek & Fabianowska-Majewska, 2010; Stefanska, Salame, Bednarek & Fabianowska-Majewska, 2012). Briefly, RSV treatment reversed methylation-mediated silencing of TSGs, *BRCA1*, *PTEN*, *APC*, and *RAR $\beta$ 2*, in breast cancer (Papoutsis, Borg, Selmin & Romagnolo, 2012; Stefanska, Rudnicka, Bednarek & Fabianowska-Majewska, 2010; Stefanska, Salame, Bednarek & Fabianowska-Majewska, 2012). Furthermore, both RSV and PTS were shown to increase methylation at specific CpG loci located in pro-inflammatory cytokines and fatty acid synthase gene, respectively, which resulted in gene suppression (Gracia et al., 2014; Lou, Wang, Xia, Skog & Sun, 2014). In our recent genome-wide study using methylation microarray technology, we further confirmed hyper- and hypomethylation upon treatment with stilbenoids and epigenetic silencing of oncogenic pathways in response to the compounds (Lubecka et al., 2016). Our results confirm what was observed for curcumin (Link et al., 2013) and clearly suggest a bidirectional mode of epigenetic effects, whereby the compounds induce DNA hypomethylation

and activation of TSGs, with simultaneous DNA hypermethylation and silencing of oncogenes.

In our present study, we demonstrate that stilbenoids at non-cytotoxic concentrations slow down growth of cancer cells by 50% (**Figure 2.1**) and change DNA methylation patterns causing remodeling rather than robust turn on/off changes on day 4 and day 9 of treatment (**Figure 2.2**). Interestingly, similar effects are observed at both time points where often the same genes but at different CpG loci, the same gene families or the same functional categories of genes are differentially methylated (**Figure 2.2B**). One excellent example of targeted genes is those involved in epigenetic regulation of gene transcription. For instance, histone demethylase *JMJD1C* with potential oncogenic role (Chen et al., 2015) is hypermethylated by RSV which would indicate potential repression of this oncogene. A methyllysine-binding protein family of *PHF* genes encoding for components of the MOF histone acetyltransferase protein complex, lysine methyltransferase *MLL5*, and long non-coding RNA *CDKN2BAS* are involved in epigenetic regulation of gene transcription and become hypomethylated and potentially activated in response to RSV upon 4-day and 9-day exposure (**Figure 2.2B**). Additional epigenetic enzymes are affected after 9-day treatment, including *MBD4*, *SUV39H1*, and *METTL3*, which modify DNA, histones, and RNA, respectively. Hence, stilbenoids may exert a very broad effect on transcription of other genes through these epigenetic regulators.

We further compared patterns of changes in DNA methylation in response to RSV in lowly and highly invasive breast cancer cells. We found a group of 113 genes that were hypomethylated in both cancer cell lines. Interestingly, the basal methylation level at CpG loci located in these genes was low in MCF10A mammary epithelial cells (**Figure 2.2F**). It would suggest that the genes are

expressed in normal cells and become silenced during carcinogenesis through gain of methylation. This would indicate their tumor suppressor role in cancer. Indeed, the genes are involved in inhibition of main pathways associated with oncogenic properties (**Figure 2.2H and 2.2I**) (Herman & Meadows, 2007; Kamal, Holliday, Morrison, Speirs, Toomes & Bell, 2017; Maiga et al., 2016; Wu et al., 2017; Xu et al., 2017). Among genes that were the most robustly hypomethylated in invasive MCF10CA1a cells, we observed a progressive RSV-mediated hypomethylation from lowly invasive to highly invasive stages (**Table 2.2, Figure 2.3A**). One of the highest changes was identified within a promoter region of *SEMA3A*, a gene with reported tumor suppressor functions (**Table 2.2, Figure 2.3B**) (Mishra et al., 2015; Wallerius et al., 2016). Publicly available clinical data show methylation of the studied CpG locus within *SEMA3A* and gene downregulation in tumors vs. normal tissue. In our study, the same locus loses methylation upon exposure to RSV which could at least partially be associated with observed increase in *SEMA3A* expression (**Figure 2.4**). Importantly, similar effects are observed upon treatment with another stilbenoid, PTS, which is an analog of RSV abundantly present in blueberries (**Figure 2.4**). The latter compound is of high interest in future studies due to its high bioavailability compared with RSV which is reflected in a much lower dose of PTS needed to inhibit cancer cell proliferation (**Figure 2.1**). High PTS bioavailability is likely linked to its chemical structure and slower conversion rate to metabolites (Dellinger, Garcia & Meyskens, 2014).

Although activation of methylation-silenced TSGs in response to dietary polyphenols was reported before (Fang, Chen, Sun, Jin, Christman & Yang, 2005; Lee & Zhu, 2006; Lubecka et al., 2016; Papoutsis, Borg, Selmin & Romagnolo, 2012; Stefanska, Rudnicka, Bednarek & Fabianowska-Majewska, 2010; Stefanska, Salame, Bednarek & Fabianowska-Majewska, 2012), mechanistic

studies investigating players involved in this phenomenon are lacking. We therefore elucidated the effects of stilbenoids on gene-protein interactions at *SEMA3A* promoter to enhance our knowledge on epigenetic enzymes, transcription factors and other proteins involved in epigenetic effects imposed by stilbenoid compounds. Among DNA methylating enzymes, DNMTs, we found downregulation of *DNMT3A* leading us to a hypothesis that DNMT3A may be implicated in stilbenoid-mediated loss of methylation at *SEMA3A* promoter. Indeed, decrease in DNMT3A binding at *SEMA3A* in response to stilbenoids was confirmed by chromatin immunoprecipitation (**Figure 2.5B**). Enrichment of active histone mark and reduction of repressive histone mark further illustrated a transcriptionally active chromatin state at *SEMA3A* (**Figure 2.5C and 2.5D**). Using TransFac, we predicted NF1C as a candidate transcription factor that binds to regions hypomethylated in response to stilbenoids, including a promoter region of *SEMA3A*. This binding was confirmed experimentally indicating that NF1C is associated with transcriptionally active status of *SEMA3A* after stilbenoid treatment (**Figure 2.6A**). Finally, we propose SALL3 as an upstream regulator of loci-specific DNA hypomethylation observed upon exposure to stilbenoids (**Figure 2.6D**). SALL3 was shown to directly inhibit DNMT3A binding to promote DNA hypomethylation (Shikauchi et al., 2009). We observed an increase in *SALL3* expression in response to stilbenoids (**Figure 2.6C**), which may contribute to sequestration of DNMT3A to result in DNA hypomethylation at *SEMA3A* promoter (**Figure 2.6D**). It appears that the epigenetic regulation of *SEMA3A* by stilbenoids is not common to polyphenols as a class of bioactive compounds. We tested expression of the mechanistic players proposed in response to epigallocatechin gallate (EGCG), genistein (GEN) and chlorogenic acid (CGA). We found that while treatment of MCF10CA1a breast cancer cells with these polyphenols slowed cancer cell growth (**Figure 2.7A**), expression of *SEMA3A*, *DNMT3A*, *NF1C*, and *SALL3* was not uniformly

changed compared to control-treated cells and did not show the same pattern of gene expression change compared to RSV and PTS treatment (**Figure 2.7B**).

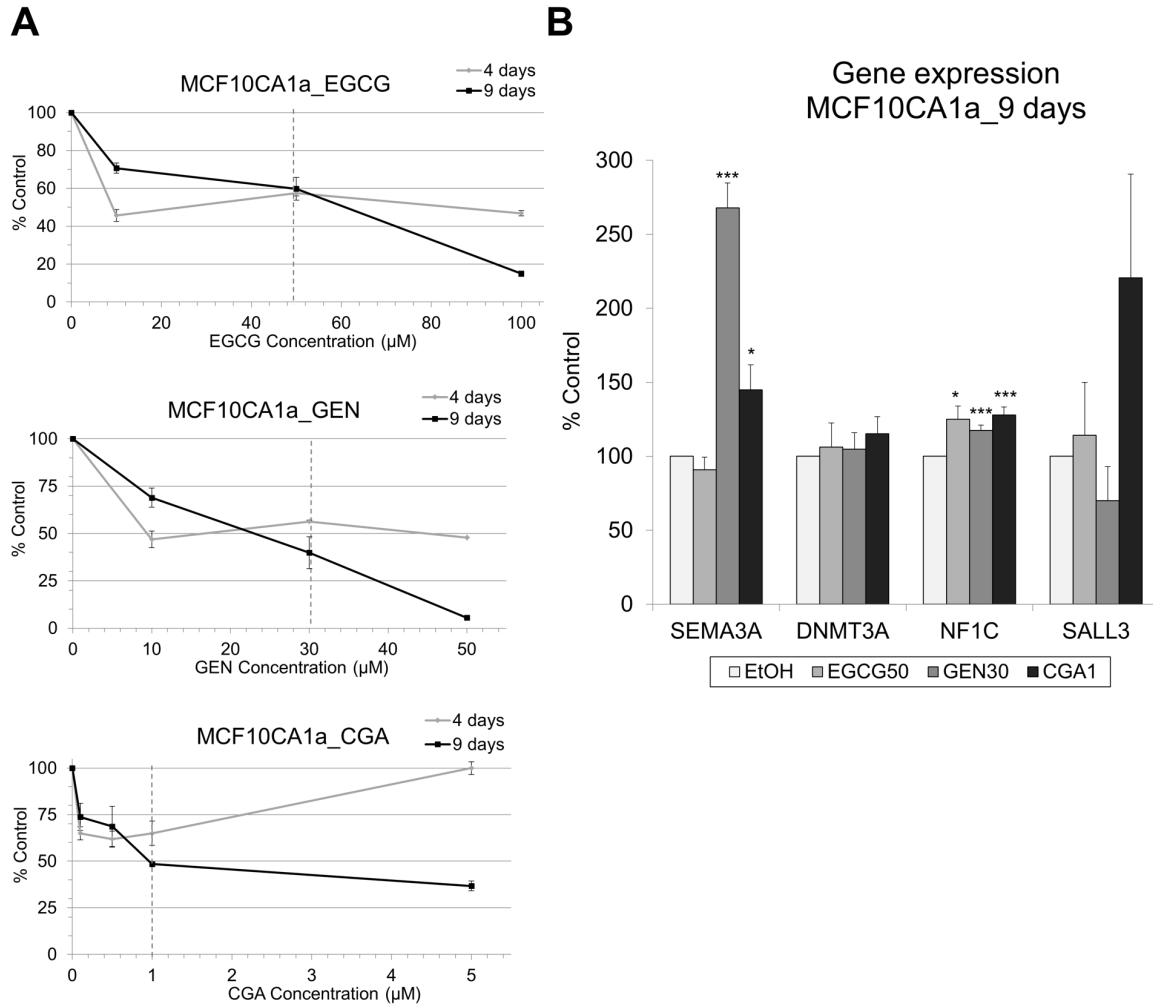


**Figure 2.7. Epigallocatechin gallate (EGCG), genistein (GEN), and chlorogenic acid (CGA) inhibit cell growth but have varying effects on expression of *SEMA3A*, *DNMT3A*, *NF1C* and *SALL3*.** (A) Effect on cell growth after 4-day and 9-day exposure of MCF10CA1a highly invasive breast cancer cells to EGCG at 10, 50 and 100 μM, GEN at 10, 30 and 50 μM, and CGA at 0.1, 0.5, 1 and 5 μM concentrations. Dashed line indicates the IC50 concentration at which qPCR experiments were performed (i.e., a dose that leads to decrease in cell growth by 50% with low cytotoxicity). (B) Expression of *SEMA3A*, *DNMT3A*, *NF1C* and *SALL3* upon 9-day exposure of

MCF10CA1a breast cancer cells to polyphenols, as measured by qPCR. All results represent mean  $\pm$  SD of three independent experimental exposures; \*\*\* $P < 0.001$ , \*\* $P < 0.01$ , \* $P < 0.05$ .

The proposed series of events may comprise an anti-cancer mechanism prompted by treatment with RSV or PTS. Our findings propose several proteins such as DNMT3A, NF1C and SALL3 as key players in the effects on DNA methylation within potential tumor suppressor genes upon stilbenoid treatment with a goal to use this mechanistic knowledge to implement these compounds into cancer prevention and support of anti-cancer therapies. Importantly, the present study along with our earlier reports indicate that these bioactive compounds exert bidirectional effects on DNA methylation in cancer cells without affecting normal cells which constitutes advantages over standard epigenetic therapies (Link et al., 2013; Lubecka et al., 2016; Stefanska, Rudnicka, Bednarek & Fabianowska-Majewska, 2010; Stefanska, Salame, Bednarek & Fabianowska-Majewska, 2012).

## **Chapter 3: Roles for OCT1 transcription factor and DNMT3B in pterostilbene-mediated epigenetic regulation of oncogenes in breast cancer cells**

### **3.1 Introduction**

Epigenetics refers to heritable changes in gene expression without changes to the underlying DNA sequence (Tsai & Baylin, 2011). DNA methylation of CpG dinucleotides is one component of the epigenome whose presence or absence may dictate availability for transcriptional machinery, including transcription factors (TFs), to bind DNA and instigate transcription. Specifically, increased methylation of regulatory regions of tumor suppressor genes (TSGs) or decreased methylation of regulatory regions of oncogenes has been found to result in corresponding changes in expression, namely silencing of TSGs or upregulation of oncogenes in many cancer types including breast cancer (Baylin & Jones, 2011; Beetch et al., 2019b; Lubecka et al., 2016; Stefanska et al., 2011). Several groups have identified TFs that are sensitive to DNA methylation status of cancer-related genes. For example, TFs such as NRF1, CTCF, NF $\kappa$ B, CREB, and OCT1 have impaired binding to DNA when cytosines are methylated around their respective TF binding sites (Domcke, Bardet, Adrian Ginno, Hartl, Burger & Schubeler, 2015; Maurano et al., 2015; Murayama et al., 2006; Sunahori, Juang & Tsokos, 2009; Wang et al., 2017). Numerous pieces of evidence show that changes in gene expression during carcinogenesis are often related to genes with differentially methylated regions and those regions are enriched for binding sites of methylation-sensitive TFs. Hence, the interplay between DNA methylation and TF binding within regulatory regions of cancer-related genes is of great interest and may at

least partially explain the transcriptional dysregulation occurring during carcinogenesis (Haney et al., 2016).

Bioactive dietary compounds have been shown to remodel DNA methylation patterns and impact regulation of DNA methylation machinery in cancer models (Beetch et al., 2019b; Kala & Tollefsbol, 2016; Lubecka et al., 2016). Specifically, stilbenoid polyphenols, resveratrol (RSV) and its dimethylated analogue pterostilbene (PTS), present abundantly in grapes and blueberries, respectively, have been shown to elicit bidirectional effects on DNA methylation status, change binding of DNA methyltransferases (DNMTs), and alter TF occupancy within differentially methylated regions (Beetch et al., 2019b; Lubecka et al., 2016). A classic example is the capacity of RSV to effectively reverse cancer-specific hypermethylation and silencing of a number of TSGs such as *BRCA1*, *RASSF1A*, and *PTEN* (Papoutsis, Borg, Selmin & Romagnolo, 2012; Stefanska, Salame, Bednarek & Fabianowska-Majewska, 2012; Zhu et al., 2012). Additionally, a study evaluating the effects of PTS on DNA methylation in obesogenic rats showed changes in DNA methylation patterns in the *Fasn* gene promoter whereby *Fasn* regained normal methylation levels and deterred gene upregulation in response to PTS (Gracia et al., 2014). Furthermore, using genome-wide technology, we have recently identified differentially methylated genes in response to RSV and followed up with mechanistic studies to describe epigenetic and transcriptional regulators associated with remodeling DNA methylation patterns in response to polyphenols (Beetch et al., 2019b; Lubecka et al., 2016). In fact, we were the first group to show that treatment of breast cancer cells with stilbenoid polyphenols results in DNA hypermethylation of regulatory regions of numerous genes with oncogenic and pro-metastatic functions and silences them. Taking into account the epigenetic and transcriptional regulators,

we specifically showed that 80% of regions hypermethylated in response to stilbenoids encompass a putative binding site for OCT1 (Lubecka et al., 2016).

OCT1 is a ubiquitous transcription factor that controls a wide range of target genes including genes involved in immune response, metabolic regulation, and stem cell function (Zhao, 2013). Expression of *OCT1*, also known as *POU2F1*, is increased in certain malignancies such as gastric, breast, lung, and thyroid cancer and has been suggested to have a role in tumor initiation and progression (Vazquez-Arreguin & Tantin, 2016). Moreover, regions across the genome that are implicated in cancer malignancies have also been shown to be enriched with OCT1 binding sites, and elevated OCT1-mediated transcription in different cancers is associated with poor prognosis (Hwang-Verslues et al., 2013; Kalamohan, Periasamy, Bhaskar Rao, Barnabas, Ponnaiyan & Ganesan, 2014). Analysis of regulatory regions in the *IL2* gene in lymphoma cells demonstrated that methylation of OCT1 binding site inhibits binding and subsequent *IL2* transcription, but demethylation in the same region allows for OCT1 to be recruited and remain bound in a readily inducible state (Murayama et al., 2006). The sensitivity of OCT1 to DNA methylation within its binding region has also been shown in other gene targets such as *DAPK* and *HSPA2* promoters (Han, Shi & Spivack, 2013; Kisliouk, Cramer & Meiri, 2017). A more recent study in acute myeloid leukemia (AML) determined that aberrant expression of *CDX2*, which plays a prominent role in the disease, is associated with OCT1 regulation in *CDX2* promoter (Jafek et al., 2019). Bisulfite sequencing analysis of the OCT1 binding region of samples taken from AML patients revealed complete absence of methylation in the *CDX2* promoter, whereas healthy human samples showed substantial methylation in the same region; thus, suggesting that demethylation of the region surrounding the OCT1 site within *CDX2* is

associated *CDX2* overexpression and AML malignancy (Jafek et al., 2019). Thus, DNA methylation status appears to be a driving factor in dictating the activity of OCT1 due to its sensitivity to methylation in proximity of the OCT1 binding region. However, whether the same mechanism takes place in breast cancer remains unknown.

Previously, we have shown that stilbenoid treatment restores normal DNA methylation levels in *MAML2* regulatory region and this subsequently inhibits tumorigenic properties of breast cancer cells (Lubecka et al., 2016). These changes corresponded with increased binding of DNMT3B, a *de novo* DNMT, and decreased binding of OCT1 within *MAML2* enhancer region. Of note, PTS exerted those effects at lower concentrations (7  $\mu$ M) compared with RSV (15  $\mu$ M), which supports the higher bioavailability and metabolic stability of PTS observed by others in *in vivo* studies (Wang & Sang, 2018). These results have given us the basis for focusing on PTS and suggesting that epigenetically activated oncogenes may be silenced through a mechanism whereby stilbenoid compounds recruit DNMT3B to regulatory regions of oncogenes to increase methylation and consequently reduce the binding of OCT1 and impose transcriptional silencing. To further investigate these mechanistic players and their roles in modulating expression of genes with potential oncogenic functions, we have utilized chromatin immunoprecipitation (ChIP) followed by next-generation sequencing to analyze binding events of OCT1 and DNMT3B at a genome-wide scale. We hypothesized that regions with decreased occupancy of OCT1 and increased binding of DNMT3B in response to PTS correspond to genes associated with cancer-driving processes, which may constitute a mechanism of hypermethylation and silencing of oncogenes and contribute to the anti-cancer effects of stilbenoid polyphenols.

## **3.2 Materials and Methods**

### **3.2.1 Cell culture and pterostilbene (PTS) treatment**

Human breast cancer MCF10CA1a and DNMT3B KO cell lines cells were cultured in DMEM/F12 (1:1) medium (Gibco) supplemented with 5% horse serum (Gibco), 1U/ml penicillin and 1µg/ml streptomycin (Gibco). MCF10CA1a breast cancer cells used in our experiments were obtained from Dr. Dorothy Teegarden (Purdue University, USA). They were derived from tumor xenografts of MCF10A cells transformed with constitutively active Harvey-*ras* oncogene, and represent poorly-differentiated malignant tumors. Cell lines were routinely verified by morphology, invasion and growth rate as well as authentication by DNA profiling using the short tandem repeat (ATCC). Cells, grown in a humidified atmosphere of 5% carbon dioxide at 37°C, were treated with pterostilbene (PTS, Cayman Chem., Ann Arbor, MI, USA) freshly resuspended in ethanol. 24 h prior to treatments, cells were plated at a density of 2-3 x 10<sup>5</sup> followed by exposure to PTS at 7µM concentration for 4 days. Cells were then passaged 1:50 and exposed for additional 4 days (9-day exposure). 7µM concentration of PTS for a total of 9 days was determined in our previous studies to be the IC<sub>50</sub> concentration (Beetch et al., 2019b; Lubecka et al., 2016).

### **3.2.2 Chromatin immunoprecipitation (ChIP) sequencing and qChIP**

Chromatin immunoprecipitation was performed as previously described in detail (Lubecka et al., 2016). Briefly, one sub-sample was maintained as an input. The second sub-sample was incubated with anti-OCT1 mouse antibody (Millipore, MAB5434), and anti-DNMT3B rat antibody (Millipore, MABE305). A third sub-sample was incubated with mouse or rat IgG non-specific antibody (negative control, Santa-Cruz Biotechnology, sc-2027). Fraction of DNA

bound to antibodies was washed, eluted and used as a template for sequencing and qPCR (qChIP).

ChIP sequencing reads obtained using the HiSeq2500 were aligned to the GRCh37/hg19 human reference genome using Bowtie2 after quality control and filtering. MACS2 peak calling software was used to identify enrichment patterns in control-treated versus PTS-treated samples (Zhang et al., 2008; Thomas, Thomas, Holloway & Pollard, 2017). Differential binding was assessed through occupancy analysis and visualized on genome browser. CHIPSeeker Bioconductor package was used to assign peaks to closest gene. Broad ChromHMM data from human mammary epithelial cells (HMEC) were used to assign peaks to chromatin states (Ernst & Kellis, 2012).

ChIP DNA at an amount of 25ng of input, antibody bound and IgG bound DNA was used as starting material in all conditions. Levels of OCT1 and DNMT3B binding were expressed as (Bound-IgG)/Input. Primers used in qChIP are listed in **Table 3.1**.

### **3.2.3 DNA isolation and pyrosequencing**

DNA, isolated using standard phenol:chloroform extraction protocol, was treated with sodium bisulfite as previously described (Lubecka et al., 2016). HotStar Taq DNA polymerase (Qiagen) and biotinylated primers were used to amplify bisulfite converted promoter sequences of the selected genes (please see **Table 3.1** for primer sequences). Pyrosequencing of the biotinylated DNA strands was performed in the PyroMarkTMQ48 instrument (Qiagen). Percentage of methylation at a single CpG site resolution was calculated using PyroMarkTMQ48 software.

### 3.2.4 RNA isolation and qPCR

TRIzol (Invitrogen) was used to isolate total RNA which served as a template for cDNA synthesis with AMV reverse transcriptase (Roche Diagnostics), according to the manufacturer's protocol. Amplification reaction was performed in CFX96 Touch Real-Time PCR Detection System (Bio-Rad) using 2 µl of cDNA, 400 nM forward and reverse primers (please see **Table 3.1** for sequences), and 10 µl of SsoFast EvaGreen Supermix (Bio-Rad) in a final volume of 20 µl. The following cycles were used in the amplification reaction: denaturation at 95 °C for 10 min, amplification for 60 cycles at 95 °C for 10s, annealing temperature for 10s, 72 °C for 10s, and final extension at 72 °C for 10 min. The CFX Maestro Software (Bio-Rad) was used to quantify gene expression with a standard curve-based analysis. qPCR data is presented as gene of interest/REF. REF is a reference gene factor consisting of expression of 5 reference genes (GAPDH, BMG, RPS17, H3F3A and 18S).

<b>Table 3.1.</b> Primer sequences used in qChIP, methylation and qPCR analysis.			
<b>Gene</b>	<b>Primer sequences</b>	<b>Annealing temperature [°C]</b>	<b>Amplicon length [bp]</b>
<b>qChIP</b>			
PRKCA	FW 5'-GAGGAGGAGAGGCCCTAA-3' RV 5'-GGAAGCACAAACACAACCC-3'	59	150
<b>Pyrosequencing</b>			
PRKCA	FW 5'-AGGTGGAGAAGGGGATTTTTT-3' RVBio 5'-TTACCCCTTAAAACCTCT-3' Seq 5'-TTTAGGGTAGGGTTTTTTATTTT -3'	53.5	139
<b>qPCR</b>			
PRKCA	FW 5'-CGAGGTGAAGGACCACAAAT-3' RV 5'-TGGAAGCCTTGTTTCCCAA-3'	59	102
BMG	FW 5'-TGAGTGCTGTCTCCATGTTTGA-3' RV 5'-TCTGCTCCCCACCTCTAAGTTG-3'	59	88

GAPDH	FW 5'-TGCACCACCAACTGCTTA-3' RV 5'-AGAGGCAGGGATGATGTTC-3'	59	177
RPS17	FW 5'-AAGCGCGTGTGCGAGGAGATC-3' RV 5'-TCGCTTCATCAGATGCGTGACATAACCTG-3'	59	87
H3F3A	FW 5'-AGGACTTTAAAACAGATCTGCGCTTCCA-3' RV 5'-ACCAGATAGGCCTCACTTGCCTCCTGC-3'	59	76
18S	FW 5'-TCGGAAGTGGAGCCATGATT-3' RV 5'-CTTTCGCTCTGGTCCGTCTT-3'	59	101

**Table 3.1.** Primer sequences used in analysis by qChIP, methylation analysis by pyrosequencing, and gene expression analysis by qPCR.

### 3.2.5 CRISPR-Cas9 knockout of *DNMT3B* in MCF10CA1a cells

Online tool E-Crisp was used to design gRNAs targeting the first or second exon of the *DNMT3B* gene. The gRNA was cloned into pSPgRNA (Plasmid #47108), and transformed into Subcloning Efficiency™ DH5α™ Competent Cells (Life Technologies). The transfection protocol was performed with Lipofectamine 3000 according to the instructions using pCAS9-mCherry-Frame+0 from Addgene (Plasmid #66939) and a CRISPaint plasmid pCRISPaint-TagGFP2-PuroR from the CRISPaint Gene Tagging Kit (Addgene, #1000000086). MCF10CA1a cells were transfected with a 1:1:2 mass ratio of gRNA, Cas9 and donor into 24 well plates. Selection in puromycin for 5 days was initiated 48 hours after transfection at a concentration of 1.5ug/ml (Tian et al., 2003). Cells were then picked and grown before being tested by PCR.

### 3.2.6 Statistical analysis

Unpaired *t*-test with two-tailed distribution was used for statistical analysis of pyrosequencing, qPCR, and qChIP in MCF10CA1a cells. Each value represents the mean ± S.D. of three independent experiments. The results were considered statistically significant when  $P < 0.05$ . *DNMT3B* KO results represent technical triplicates. One-way ANOVA with Tukey's post-hoc test was used when comparing more than 2 groups.

### 3.3 Results

#### 3.3.1 Overview of genome-wide changes in OCT1 binding in response to PTS

In order to understand OCT1-dependent loci-specific hypermethylation in response to polyphenols, we performed ChIP for OCT1 followed by next-generation sequencing in MCF10CA1a breast cancer cells upon exposure to 7  $\mu$ M PTS for 9 days. This specific PTS concentration was determined as the IC<sub>50</sub> concentration for MCF10CA1a cells in our previous work which refers to a dose leading to 50% inhibition in cell growth compared with control (cells treated with ethanol as vehicle) with less than 10% dead cell count (Beetch et al., 2019b; Lubecka et al., 2016). OCT1 binding changed in 7,112 loci throughout the genome in response to PTS. Those peaks correspond with 1,754 genes, of which 49% encompass peaks with statistically significant decrease in OCT1 binding upon PTS treatment. The other 51% correspond with significantly enriched OCT1 sites in response to PTS. Since our interest was to elucidate the role of OCT1 in PTS-mediated epigenetic silencing of potential oncogenes, we focused on regions where OCT1 occupancy decreased upon treatment.

Chromosomal view of sites of reduced OCT1 binding in response to PTS was plotted using Integrative Genome Viewer (IGV) visualization tool in **Figure 3.1A**. Each bar represents a single peak that was called using MACS2 peak calling method. Peaks were aligned to the closest gene using the hg19 human genome. Based on location in the genome, peaks were assigned to chromatin states based on Broad ChromHMM tracks from human mammary epithelial cells (HMEC). A total of 2,819 OCT1 peaks with statistically significant depletion upon PTS treatment were identified and corresponded to 857 unique genes. A majority of depleted OCT1 peaks were situated within heterochromatin (28%) and repetitive regions (23%), whereas 19% of

them were within regulatory regions of genes (promoters and enhancers). The 527 peaks depleted within regulatory regions were associated with 311 genes. Among those 311 genes, 112 had OCT1 peaks in their promoter regions only, 38 had OCT1 peaks in both promoter and enhancer regions, and 161 genes had OCT1 peaks only in enhancer regions (**Figure 3.1B**). As promoters and enhancers are directly associated with transcriptional regulation and OCT1, as a transcription factor, binds to the octamer motif (ATGCAAAT) or closely related sequences in promoters and enhancers of a variety of genes, we further explored these regions and corresponding genes. We refer to this group of genes as “PTS-mediated OCT1-depleted target genes” in the following sections.

Using gene ontology (GO) and KEGG tools, we performed functional and pathway analyses of the 311 PTS-mediated OCT1-depleted target genes. We found that these genes are enriched in signaling pathways commonly upregulated in cancer (Wnt signaling, Ras signal transduction, Hippo pathway), kinase-related cascades (intracellular signal transduction, GTPase activity), transport (protein, mitochondrial), and pathways leading to transcriptional misregulation in cancer (**Figure 3.1C**). Thorough analysis of those target genes revealed candidates with oncogenic functions. Several genes involved in DNA damage and immune response (*FCGR2A*, *NOS1AP*, *PRDX6*, *ASCC1*, and *HAUS6*), protein folding/trafficking (*DNAJB12*, *FBXW11*, *ANKHD1*, and *SH3RF2*), and mitochondria/metabolism (*MCU*, *SIGMAR1*, *SHMT1*, and *MICU1*) were discovered to have reduced OCT1 binding upon PTS. A variety of genes associated with transcriptional activity such as *MYC*, *MLLT3*, *DDX46*, *GLIS3*, *KDM4C*, *JADE2*, *ANP32E*, *UBE2B*, *CXXC5*, *NR3C1*, *CHD1L*, *ZBTB20*, *PVT1*, and *TLE1* were also detected. Furthermore, many genes with roles in cellular signalling cascades such as *PRKCA*, *RACK1*, *G3BP1*, *SMCR8*,

*MPZL1, RASD1, GAPVD1, MAP2K3, RRAGA, FRMPD1, and LAMTOR2* were identified as well. These findings support our hypothesis that target genes at which OCT1 binding is reduced in response to PTS are mostly associated with cancer-driving functions. The reduction in OCT1 binding within regulatory regions of these oncogenes could contribute to the anti-cancer effects of PTS via decreased transcriptional activation of these cancer-promoting genes.

In line with our findings regarding OCT1 targeting of oncogenes, OCT1 overexpression has been observed in several cancer types such as esophageal (4.1-fold), cervical (2-fold), gastric (2-fold), liver (1.6-fold) and breast (1.4-fold), according to Oncomine data depicting OCT1 expression levels in human tissues shown in **Figure 3.1D**. Several other pieces of evidence have confirmed OCT1 as an oncogenic transcription factor (Vazquez-Arreguin & Tantin, 2016). Additionally, our past studies show that depletion of OCT1 in MCF10CA1a invasive breast cancer cells using siRNA leads to significant reduction in cancer cell growth (Lubecka et al., 2016). Taking into account the oncogenic nature of OCT1 and its gene targets, understanding ways to reverse OCT1-related changes in cancer and potentially correct cancer-related transcriptional aberrations is important.

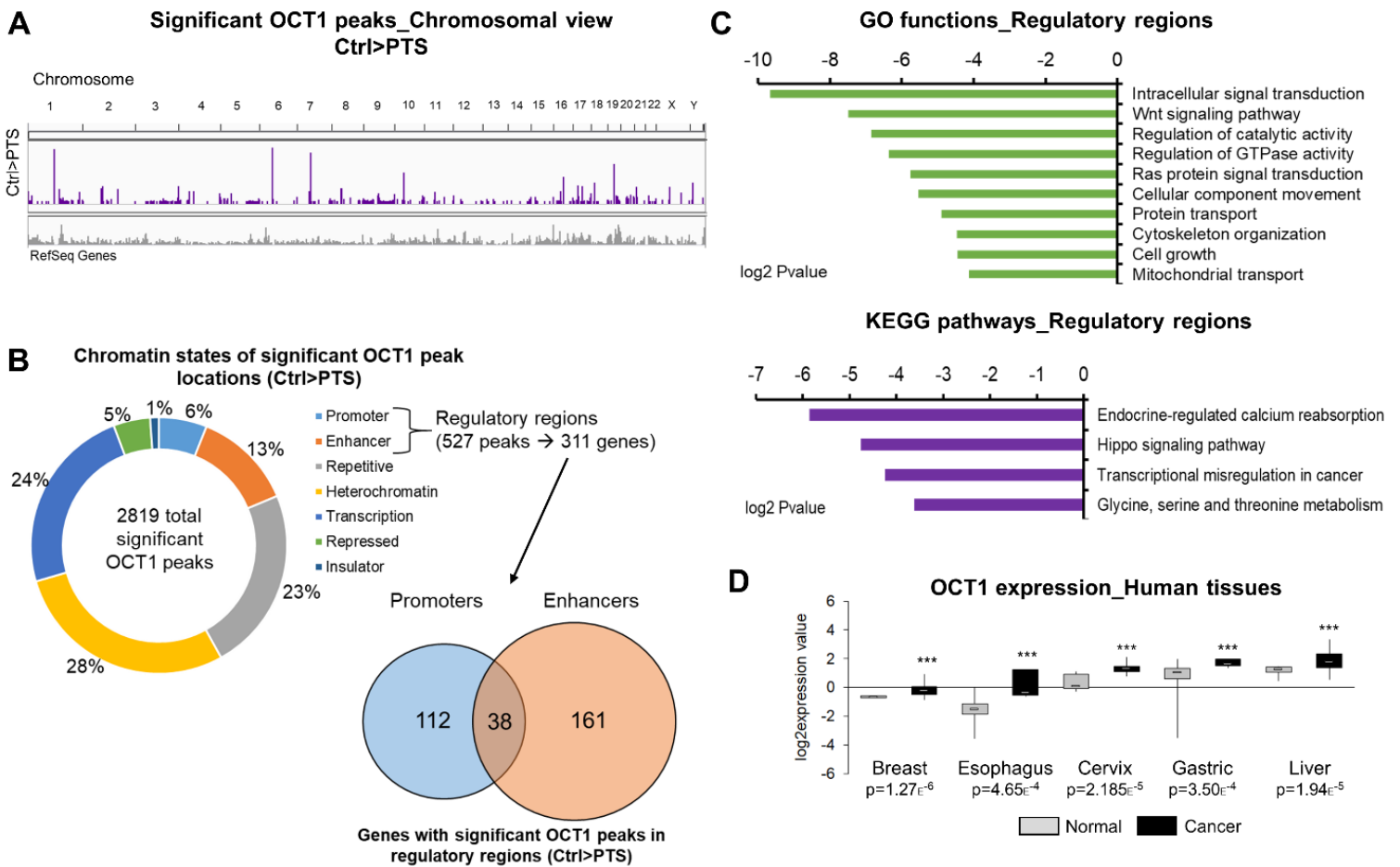


**Figure 3.1. Overview of genome-wide changes of OCT1 binding in response to PTS.** (A) Chromosomal view of depleted OCT1 peaks in response to PTS treatment. Each bar represents a single peak that was called using MACS2 peak calling software. (B) Chromatin states associated with depleted OCT1 peaks were determined using Broad ChromHMM HMEC sequencing data available on UCSC Genome Browser (hg19). Peaks could correspond with promoters, enhancers, repetitive regions, heterochromatin, regions associated with transcription, repressed regions, or insulator regions. Regulatory regions were defined as those corresponding to promoters and enhancers. Peaks within regulatory regions assigned to genes were categorized into genes containing promoter peaks only, promoter and enhancer peaks, or enhancer peaks only as depicted by the Venn diagram. (C) The 311 genes with depleted OCT1 peaks in regulatory regions upon PTS were subjected to Gene Ontology (GO) function and Kyoto Encyclopedia of Genes and Genomes (KEGG) pathway analysis using DAVID Knowledgebase. (D) OCT1 expression in normal and cancer tissues based on microarray data from Oncomine database. Expression is presented as  $\log_2$ -transformed median centered per array, and SD-normalized to 1 per array.

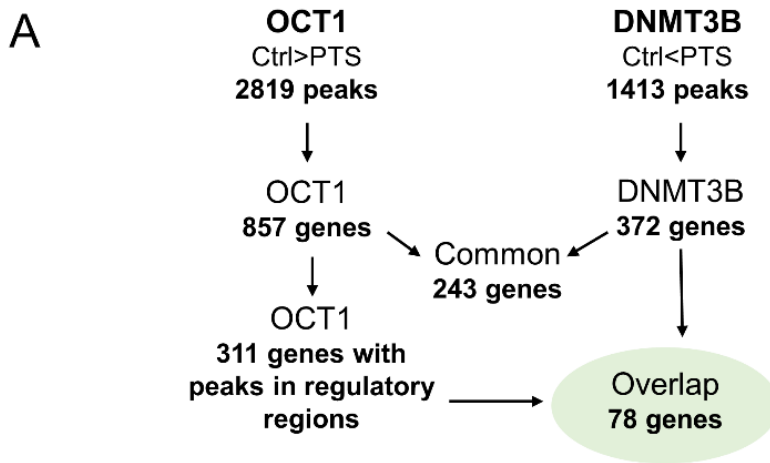
### **3.3.2 Genes associated with reduced OCT1 peaks in regulatory regions overlap with genes exhibiting increased DNMT3B binding in response to PTS**

As mentioned previously, binding of TFs to regulatory regions of genes can be altered by the DNA methylation status at the TF binding site or at a surrounding region. We previously found that DNMT3B-mediated deposition of methyl marks in an OCT1 binding site upon PTS treatment was associated with DNA hypermethylation and silencing of the *MAML2* oncogene (Lubecka et al., 2016). Therefore, we aligned genes with PTS-mediated decreased OCT1 occupancy with DNMT3B-enriched target genes. The latter group was identified upon ChIP sequencing analysis of DNMT3B-bound DNA in response to PTS. We found a total of 1,413 significant DNMT3B-enriched peaks upon PTS, corresponding to 372 genes. There were 243 common genes associated with decreased OCT1 binding and enriched DNMT3B binding. The differential occupancy of OCT1 and DNMT3B, namely decreased OCT1 and increased DNMT3B occupancy, occurred within promoters and enhancers of 78 of those genes (**Figure 3.2A**).

Among the 78 overlap genes, 19 genes had OCT1 peaks within their promoters only, while 20 genes contained OCT1 peaks in both promoters and enhancer regions. Another 39 genes had OCT1 peaks only in enhancer regions (**Figure 3.2B**). Thorough analysis of these overlap genes revealed many genes associated with oncogenic or pro-metastatic functions and narrowed down OCT1-target genes to those possibly regulated by DNA methylation and DNMT3B specifically. In fact, approximately 35 of the 78 genes were associated with established or potential oncogenic functions (**Figure 3.2B**), whereas only 7 with putative tumor suppressor role. Remaining 36 genes have undetermined or unknown roles in cancer. *NOTCH2NL*, an oncogene found to have

OCT1 peaks in both promoter and enhancer regions, activates Notch signaling by direct interaction with NOTCH2; thereby promoting proliferation and self-renewal (Suzuki et al., 2018). *PVT1* is a long non-coding RNA that is commonly overexpressed in breast cancer and has been implicated in regulation of MYC (Sarver, Murray, Temiz, Tseng & Bagchi, 2016; Wang, Zhou, Wang, Wang & Li, 2017). *MCU*, an important player in mitochondrial adaptation to metabolic demands during cell cycle (Koval et al., 2019), and *ASCCI*, which is involved in DNA damage repair (Soll, Brickner, Mudge & Mosammaparast, 2018), are other oncogenes with OCT1 peaks within both promoter and enhancer. Very strong cancer-related genes were found to have OCT1-depleted peaks and DNMT3B-enriched peaks in response to PTS in their promoters, namely *MYC* and *PRKCA*. *MYC* is a pervasive proto-oncogene and transcription factor commonly dysregulated in many cancer types (Gabay, Li & Felsher, 2014). *PRKCA* encodes for a kinase responsible for phosphorylation of many protein targets and activation of various cancer-promoting pathways such as the MAPK cascade and the PI3K-AKT pathway (Kolch et al., 1993). Lastly, genes with OCT1 peaks only in enhancer regions include *CCAT1*, a long non-coding RNA upregulated in breast cancer and associated with activation of WNT signaling (Tang et al., 2019), and *CPLX2*, which is upregulated and used as a prognostic marker in various cancer types (Komatsu et al., 2013; Makuuchi et al., 2017). *SREBF1*, a gene involved in lipid metabolism, also contained depleted OCT1 peaks and increased DNMT3B binding in its enhancer region in response to PTS. A link between lipid homeostasis and tumor growth has been identified in several cancer types (Nath & Chan, 2016; Syafruddin et al., 2019). Most notably, a bioactive compound curcumin has been found to downregulate *SREBF1* and suppress liver tumor growth (You, Li, Xu, Chen & Ye, 2018).

We selected one of these oncogenes, namely *PRKCA*, for further investigation to better understand whether the proposed mechanistic players, OCT1 and DNMT3B, are affecting DNA methylation patterns and transcriptional activation of the gene. *PRKCA* is of particular interest as it regulates a network of cancer-driving genes and pathways.



**B** Genes that overlap from significant OCT1 peaks in regulatory regions (Ctrl>PTS) and significant DNMT3B peaks (Ctrl<PTS)

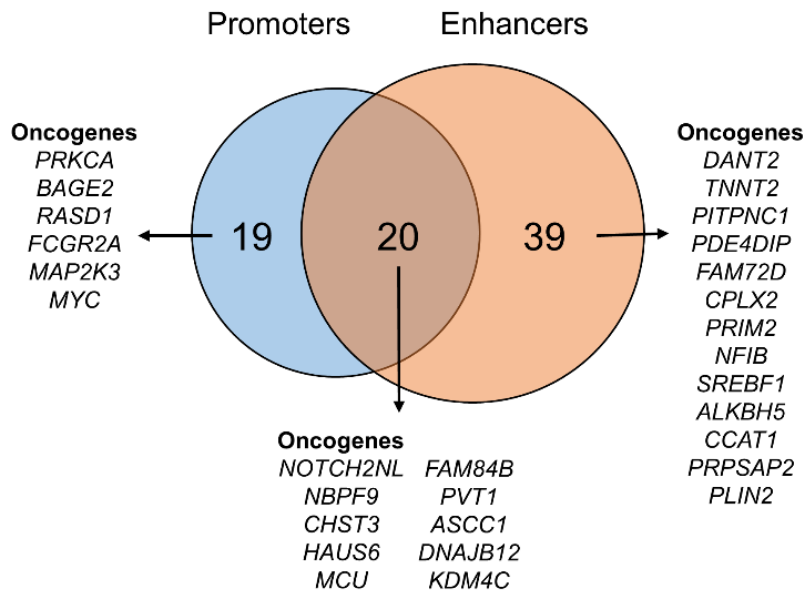


**Figure 3.2. Genes associated with reduced OCT1 peaks in regulatory regions overlap with genes exhibiting increased DNMT3B binding in response to PTS.** (A) Schematic of analysis of common genes associated with decreased OCT1 peaks (Ctrl>PTS) and enriched DNMT3B peaks (Ctrl<PTS) upon PTS treatment. (B) The 78 genes containing decreased OCT1 peaks in regulatory regions and enriched DNMT3B peaks in response to PTS were categorized into genes containing promoter peaks only, promoter and enhancer peaks, or enhancer peaks only as depicted by the Venn diagram. Genes with known or potential oncogenic role that are associated with those peaks are listed.

### **3.3.3 Protein kinase C alpha (PRKCA) modulates several oncogenic signaling pathways**

The protein kinase C alpha (*PRKCA*) gene encodes for an enzyme called PKC $\alpha$ . PKC $\alpha$  is a calcium-activated, serine/threonine protein kinase that is dependent on phospholipid and second messenger diacylglycerol (DAG). Initial activation of DAG and PKC $\alpha$  is through the phospholipase C (PLC)-mediated signal transduction pathway. This alpha type of PKC, specifically, requires interaction with cell membranes in order to derive a source of phospholipid for activation. PKC proteins phosphorylate numerous protein targets to modulate diverse signaling pathways in the cell (**Figure 3.3**). One of the most well-known functions of PKC $\alpha$  is its direct interaction with RAF1 to induce Ras/Raf/MEK/ERK signaling (Kolch et al., 1993). Activation of this pathway can lead to subsequent activation of AP-1 transcription factor which further upregulates other oncogenic transcription factors such as c-Myc, c-Fos and c-Jun (Fu et al., 2017; Kolch et al., 1993). The ERK/MAPK cascade can additionally lead to upregulation of NF $\kappa$ B (Schulze-Osthoff, Ferrari, Riehemann & Wesselborg, 1997). Non-canonical NF $\kappa$ B signaling can also be activated by PKC $\alpha$  directly (Leonard et al., 2015). ATF2 is activated via PKC $\alpha$ -mediated phosphorylation to coordinate cooperation between ATF2 and c-Jun to instigate transcription of downstream gene targets (Yamasaki, Takahashi, Pan, Yamaguchi & Yokoyama, 2009). Another important pathway modulated by PKC $\alpha$  is the PI3K-AKT pathway (Thorne, Jackson, Willis &

Bradford, 2013), which can ultimately induce mTOR signaling to regulate the cell cycle (Morrison et al., 2015). In addition, PKC $\alpha$  can interact with mTOR directly to amplify signal initially activated by EGFR (Fan et al., 2009). The kinase PKC $\alpha$  has also been found to enhance estrogen receptor  $\alpha$  (ER $\alpha$ )-associated transcription and cell proliferation in gynecological cancers (Thorne, Jackson, Willis & Bradford, 2013). It is also functionally linked to cell migration through regulation of the actin cytoskeleton (Larsson, 2006) and claudin expression (Leotlela et al., 2007; Schmitt, Horbach, Kubitz, Frilling & Haussinger, 2004). Collectively, PKC $\alpha$  has established oncogenic functions including induction of oncogenic signal transduction, regulation of the cell cycle, promotion of cell proliferation, migration and invasion, and altering tight junctions. In breast cancer, specifically, PKC $\alpha$  has been implicated in the metastatic phenotype and associated with poor prognosis in patients (Pham, Perez White, Zhao, Mortazavi & Tonetti, 2017).

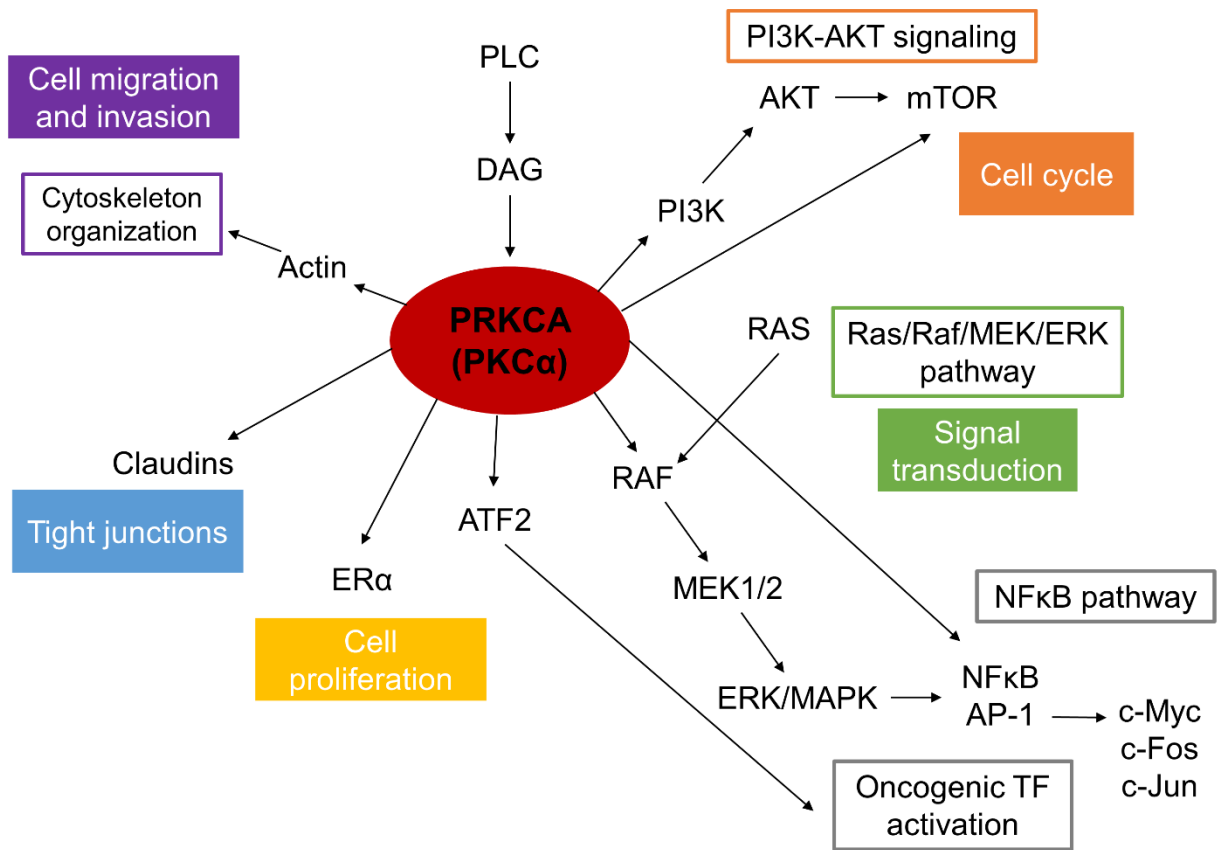


**Figure 3.3. Oncogenic roles of protein kinase C alpha (*PRKCA*).** A wide variety of pathways are activated by *PRKCA* ( $PKC\alpha$ ). Abbreviations: phospholipase C (PLC), diacylglycerol (DAG), phosphatidylinositol 3-kinase (PI3K), mechanistic target of rapamycin (mTOR), mitogen-activated protein kinase (MAPK), nuclear factor kappa B ( $NF\kappa B$ ), estrogen receptor alpha ( $ER\alpha$ ).

### 3.3.4 *PRKCA* silencing through hypermethylation in response to PTS is associated with decreased OCT1 binding at DNMT3B-occupied site

Fold enrichment (FE) within *PRKCA* derived from ChIP sequencing analysis corresponding to OCT1 and DNMT3B peaks in response to PTS is visualized in **Figure 3.4A** (blue = control-treated, red = PTS-treated). OCT1 binding upon PTS was depleted in this region, with a FE value of 4.45. The track region in **Figure 3.4A** represents the entire OCT1-depleted peak, a 340 base-

pair intronic region immediately following exon 1. This peak is considered to be within the promoter region and begins 224 nucleotides downstream of the transcription start site (+1). The OCT1 peak region encompasses a region occupied by DNMT3B in response to PTS (beginning of peak and end of peak, see red peaks in DNMT3B track). A map of the region of interest in the *PRKCA* promoter including the transcription start site (+1), exon 1 (orange) and intronic region containing OCT1 and DNMT3B peaks (blue) orients to the tested pyrosequencing and quantitative ChIP (qChIP) regions. Purple shaded area indicates the region assessed by pyrosequencing and the yellow shaded area indicates the region covered by qChIP validation (**Figure 3.4A**).

Validation of the differentially bound region established by ChIP sequencing was executed using qChIP. In line with ChIP sequencing, qChIP demonstrated lack of OCT1 binding in response to PTS. Similarly, qChIP confirmed significant enrichment of DNMT3B binding in the same region (yellow region in map) by 48% upon PTS treatment (**Figure 3.4B**). DNA methylation status was then measured using pyrosequencing (purple region in map). Within the OCT1 peak and immediately preceding the region with validated decrease in OCT1 and increase in DNMT3B binding by qChIP, DNA hypermethylation was observed upon exposure to PTS. Significant hypermethylation of 8 out of 9 CpGs sites within this region was confirmed, with methylation increasing by approximately 3-8% (**Figure 3.4C**). DNA hypermethylation in this region corresponds to decreased expression of *PRKCA* upon PTS treatment. A profound reduction in *PRKCA* expression to only 19% of expression level in control cells was observed (**Figure 3.4D**).

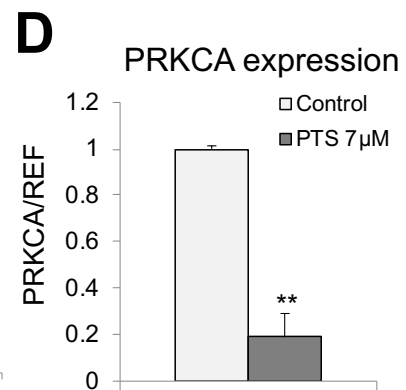
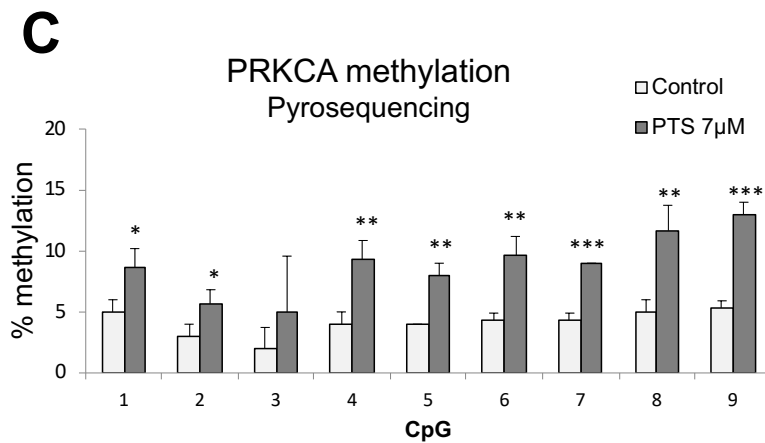
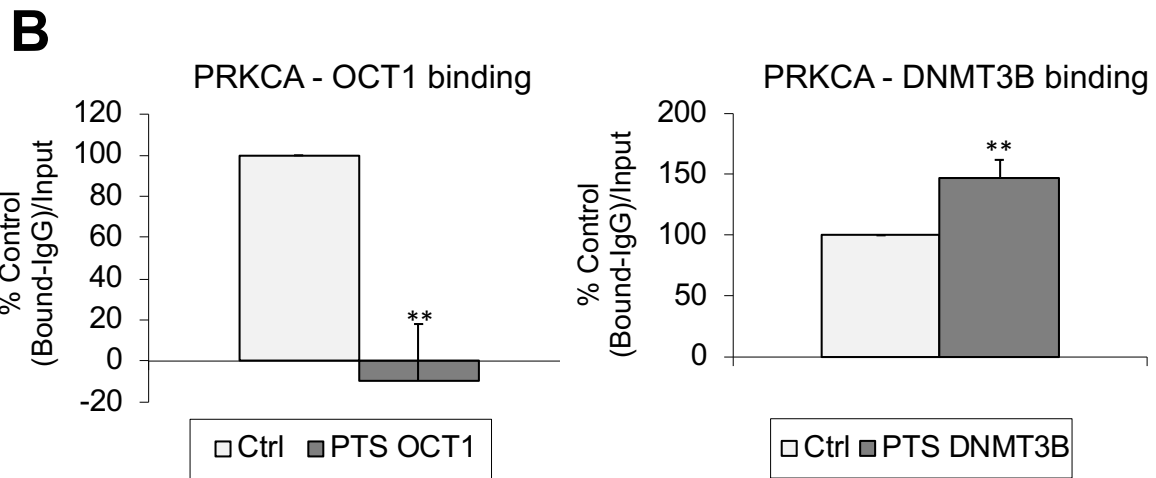
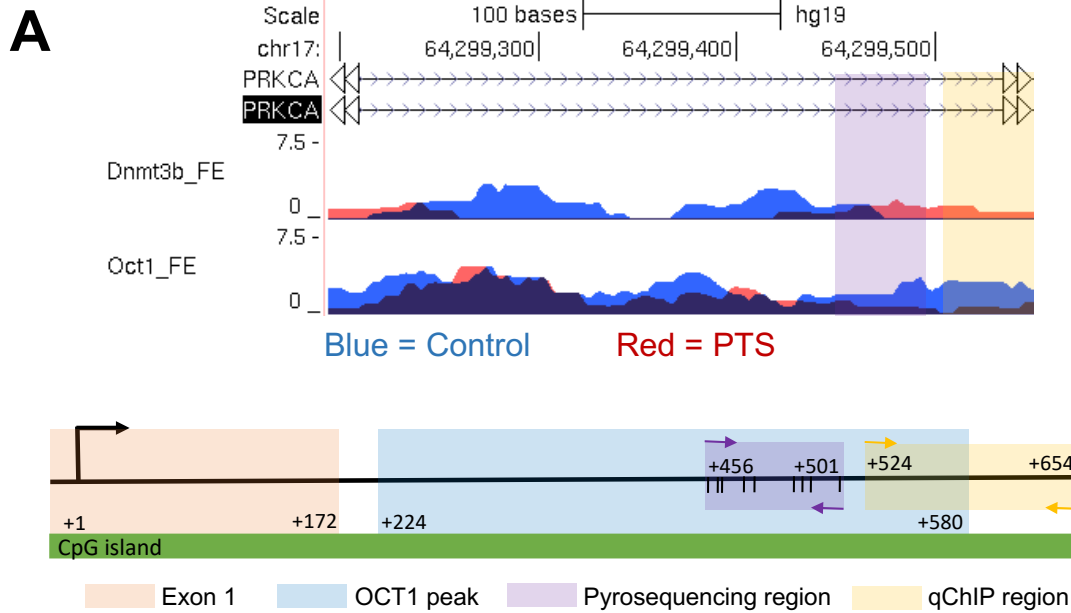


**Figure 3.4. DNMT3B-mediated hypermethylation is linked to transcriptional silencing of OCT-target genes in response to PTS in breast cancer cells.** (A) Genome browser tracks depicting DNMT3B and OCT1 fold enrichment in control-treated (blue) and PTS-treated (red) MCF10CA1a breast cancer cells. Below is a representative map of the OCT1 peak within the *PRKCA* promoter region. The entire region falls within a CpG island as shown in green. Transcription start site is indicated by +1 position, exon 1 is in orange, and OCT1 peak identified from ChIP sequencing is in blue. Within the OCT1 peak, the purple region represents the region assessed by pyrosequencing and the yellow region represents the region validated by qChIP. (B) Validation of lack of OCT1 and enrichment of DNMT3B binding within the OCT1 peak in response to 7  $\mu$ M PTS in MCF10CA1a invasive breast cancer cells. (C) Average methylation status of CpG sites in the OCT1 peak region within *PRKCA* as determined by pyrosequencing in MCF10CA1a invasive breast cancer cells treated for 9 days with 7  $\mu$ M PTS. (D) *PRKCA* gene expression upon 9-day treatment of MCF10CA1a invasive breast cancer cells with 7  $\mu$ M PTS as determined by qPCR. All results represent mean  $\pm$  SD of three independent experiments; \*\*\* $P < 0.001$ , \*\* $P < 0.01$ , \* $P < 0.05$ .

### 3.3.5 Knockout of *DNMT3B* indicates that PTS-mediated hypermethylation of *PRKCA* is DNMT3B-dependent

In order to determine whether or not the effects of PTS were specifically through modulation of DNMT3B, we generated a CRISPR-Cas9 knockout MCF10CA1a cell line for *DNMT3B* (DNMT3B KO). Knockout of *DNMT3B* was confirmed by qPCR of the targeted region early in the first exon of *DNMT3B* (**Figure 3.5A**). Robust effects on cell growth resulted from knockout of *DNMT3B* in MCF10CA1a breast cancer cells. In fact, DNMT3B KO cells grew at about 30% of original wild-type MCF10CA1a cells and had characteristics that resemble normal breast cells (i.e. growing in multi-layers, stronger anchorage-independent growth).

We treated DNMT3B KO cells for 9 days with PTS at doses ranging from 5  $\mu$ M to 10  $\mu$ M and including IC50 dose for MCF10CA1a cells of 7 $\mu$ M. We found that, despite the slowed growth characteristic of the DNMT3B KO cells, the IC50 dose of 7 $\mu$ M for MCF10CA1a cells was maintained in DNMT3B KO cells (**Figure 3.5B**).

Significant hypermethylation across the tested *PRKCA* region was diminished to just 3 out of 9 CpG sites in the DNMT3B KO cells (**Figure 3.5C**). Because minimal hypermethylation persists despite the lack of DNMT3B, we speculate that there may be a compensatory mechanism at play, perhaps involving DNMT3A, in the absence of DNMT3B. More interestingly, in response to PTS treatment, none of the CpG sites in the tested *PRKCA* region showed further hypermethylation in DNMT3B KO cells, supporting our hypothesis that PTS-mediated hypermethylation of regulatory regions of oncogenes occurs through a DNMT3B-controlled mechanism. Nevertheless, slowed cell growth and seemingly stepwise decrease in *PRKCA* expression is observed in DNMT3B KO cells compared to wild-type MCF10CA1a cells and in response to PTS treatment (**Figure 3.5D**), supporting the hypothesis that *PRKCA* is regulated by DNA methylation. The significant decrease in *PRKCA* expression despite the lack of increased methylation suggests that PTS is likely also working through other mechanisms to regulate *PRKCA* expression, such as histone modifications or indirectly through inhibition of oncogenic pathways, which could be subject to further study.

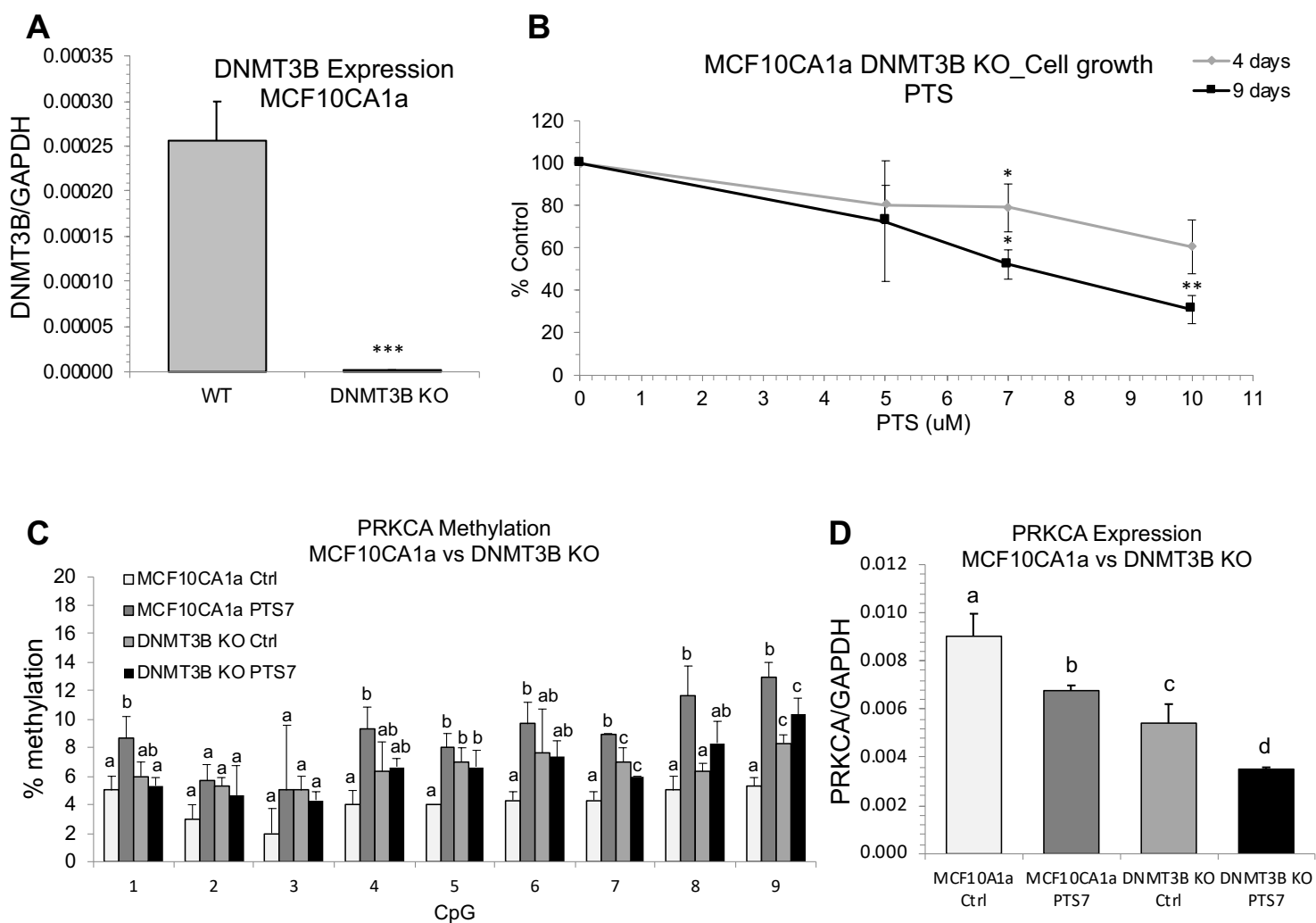


**Figure 3.5. DNMT3B-dependent regulation of PTS-mediated hypermethylation of *PRKCA*.**

(A) *DNMT3B* gene expression level in DNMT3B KO cells, as determined by qPCR. (B) Cell growth of DNMT3B KO cells in response to 4- and 9-day treatment with 5  $\mu$ M, 7  $\mu$ M, and 10  $\mu$ M PTS, as determined by trypan blue exclusion test. (C) Average methylation status of CpG sites within *PRKCA*, as determined by pyrosequencing in MCF10CA1a invasive breast cancer cells compared to DNMT3B KO cells treated for 9 days with 7  $\mu$ M PTS. (D) *PRKCA* gene expression upon 9-day treatment of MCF10CA1a invasive breast cancer cells and DNMT3B KO cells with 7  $\mu$ M PTS, as determined by qPCR. All results represent mean  $\pm$  SD of three technical replicates; \*\*\* $P$ <0.001. Letters (a, b, c, d) indicate significant differences between groups based on one-way ANOVA and Tukey's post-hoc test. If ab is indicated, there is no significant difference between compared groups.

### 3.4. Discussion

It has been shown that transcription factor binding activity can be associated with the dynamic changes in local DNA methylation state within and in proximity of binding motifs which is critical in gene regulation in both normal and cancerous cells (Luo, Hajkova & Ecker, 2018). The mechanisms by which dietary compounds induce modifications in DNA methylation patterns and subsequently change the expression of crucial genes involved in carcinogenesis is an area of great interest. The transcription factor, OCT1, is shown to be involved in upregulating numerous oncogenic targets which help drive the malignancy of a number of different cancers. However, how OCT1 is recruited to bind to its target regions is yet to be fully elucidated.

In this study, we show that regulatory regions with reduced OCT1 binding overlap with genes exhibiting increased DNMT3B binding upon PTS treatment in breast cancer cells. PTS treatment of MCF10CA1a breast cancer cells reduced OCT1 binding and increased DNMT3B in many regulatory regions of genes with potential oncogenic roles. Of those genes, we chose *PRKCA* as a gene candidate to explore a proposed PTS-mediated mechanism involving DNMT3B and OCT1 in regulation of DNA methylation and transcriptional activity. Various studies have indicated that *PRKCA* expression is elevated in breast cancer and is implicated with cancer aggressiveness and poor prognosis (Assender, Gee, Lewis, Ellis, Robertson & Nicholson, 2007; Lonne, Cornmark, Zahirovic, Landberg, Jirstrom & Larsson, 2010). In response to PTS treatment, OCT1 binding within the promoter region of *PRKCA* was abrogated while DNMT3B binding increased in the same region. Pyrosequencing revealed that PTS-treated cells exhibit a gain in methylation at the *PRKCA* promoter, indicating the role DNMT3B may have in the methylation state observed. Knockout of *DNMT3B* resulted in negating PTS-mediated

hypermethylation of the tested *PRKCA* region, further emphasizing the role of DNMT3B in PTS-modulated effects on DNA methylation at oncogenes. A key observation in our study is that the change in methylation status corresponds with a change in *PRKCA* gene expression upon PTS treatment in MCF10CA1a breast cancer cells. This clearly indicates that observed changes in epigenetic marks and DNA-protein interactions are biologically relevant, and complete disappearance of OCT1 enrichment upon PTS may play a pivotal role in PTS-mediated recruitment of DNMT3B and epigenetic silencing of *PRKCA* expression. However, downregulation of *PRKCA* expression that is observed in DNMT3B KO cells treated with PTS suggests that other mechanisms may also be at play in response to PTS.

The robust growth suppression and change in morphology of DNMT3B KO cells compared to parent MCF10CA1a cells indicates that DNMT3B plays an oncogenic role in these cells. Indeed, most studies in breast cancer observe upregulation of *DNMT3B* and consider *DNMT3B* overexpression as an independent and unfavorable prognostic factor (Jahangiri, Jamialahmadi, Gharib, Emami Razavi & Mosaffa, 2019; Tavakolian, Goudarzi & Faghihloo, 2019). However, in other cancers, DNMT3B has been shown to silence target oncogenes (Peralta-Arrieta, Hernandez-Sotelo, Castro-Coronel, Leyva-Vazquez & Illades-Aguiar, 2017). In addition, loss of *Dnmt3b* led to increased oncogenic functions in acute myeloid leukemia cells (Zheng et al., 2016), suggesting a context-dependent tumor suppressive role for DNMT3B.

DNA hypermethylation and silencing of *PRKCA* in response to PTS is associated with decreased OCT1 binding at a DNMT3B-occupied site. Here, we assess OCT1 and DNMT3B as mechanistic players in PTS-mediated changes in loci-specific DNA methylation and

transcriptional activity with the premise that upon PTS exposure DNMT3B may bind regulatory regions of oncogenes, methylate OCT1 binding sites, and as a result OCT1 cannot recognize its binding site and cannot participate in activation of transcription. Indeed, other studies have demonstrated that cells with loss of *de novo* DNMTs contain hypomethylated regulatory regions that are enriched with OCT1 binding motifs (Haney et al., 2016). It has also been shown that the use of DNMT inhibitors such as 5-aza-2'-deoxycytidine decreases the methylation status of OCT1-targeted gene regulatory regions, such as the *STAT4* promoter region containing OCT1 binding motifs, which directly upregulates gene expression (Shin et al., 2005). An increase in DNMT3B binding could therefore precede hypermethylation of regions that then dictate the affinity of OCT1 to bind to its recognized motifs and promote transcriptional activity. However, it could also be possible that OCT1, in fact, regulates where DNMT3B binds and acts to methylate DNA. DNMTs are shown to recognize and associate with the dimethylated state of histone 3 at lysine residue 9 (H3K9) in order to methylate nearby CpG dinucleotide sequences (Lehnertz et al., 2003). In malignant cells, OCT1 has been found to recruit a cofactor, Jmjd1a, which is known for its role as a histone demethylase enzyme that targets H3K9 to remove the histone methyl mark (Maddox et al., 2012). Studies have suggested an association between OCT1 and Jmjd1a that impacts DNMTs ability to recognize the demethylated histone state and therefore cause decrease in DNA methylation near the OCT1 binding site upstream of the human *CDX2* promoter (Jafek et al., 2019). Therefore, the timeline of events involving binding of OCT1 and DNMT3B is an interesting aspect that remains to be explored in future experiments.

Altogether, our results demonstrate a potential mechanistic link between OCT1 and DNMT3B in hypermethylation of regulatory regions of genes with potential cancer-promoting functions in

response to PTS treatment. Our findings suggest that PTS leads to epigenetic silencing of oncogenes which contributes to the anti-cancer action of stilbenoid polyphenols. Insights into the mechanistic underpinnings of bioactive compounds eliciting anti-cancer effects have the potential to be used in cancer prevention and support of therapeutic strategies.

## **Chapter 4: Epigenetic activation of oncogenes in rat hepatocellular carcinoma triggered by choline-deficiency is attenuated by pterostilbene supplementation**

### **4.1 Introduction**

DNA methylation and transcriptional machinery, including DNA methyltransferases (DNMTs) and transcription factors (TFs) as discussed in previous chapters, are important for maintaining normal DNA methylation and gene expression patterns, and are commonly dysregulated in cancers. Another crucial factor that regulates the DNA methylation machinery is availability of nutrients involved in proper functioning of one carbon metabolism (OCM), where the universal methyl donor called S-adenosyl-methionine (SAM) is synthesized (OCM nutrients). The Western diet containing high fat (mostly saturated and monounsaturated), high simple sugar content, low protein, and generally low micronutrients (with sodium as an exception) is also relatively low in OCM nutrients, such as folate, B12, B6, and choline, all of which are involved in SAM synthesis (Hintze, Benninghoff, Cho & Ward, 2018; Lipkin, Reddy, Newmark & Lamprecht, 1999; Newmark et al., 2001). OCM nutrients, including choline, are essential for human health. OCM nutrients are important during pregnancy and fetal development to ensure offspring health. Low levels of methyl donors can lead to metabolic and neurological disease development (Wiedeman, Barr, Green, Xu, Innis & Kitts, 2018). Choline, in particular, is vital for liver health throughout the lifespan. Liver diseases of varying severity can arise from diets deficient in choline (Buchman et al., 2001). Experimental studies to replenish OCM nutrients, including choline, have been promising in combating development of pathologies such as cancer and cardiovascular disease (Debrececi & Debrececi, 2014; Mahmoud & Ali, 2019; Torres, Guevara-Cruz, Velazquez-

Villegas & Tovar, 2015). However, the underlying mechanisms behind the link between methyl-donor deficiency (MDD) and disease, particularly cancer, are poorly understood. In order to study the pathogenesis of cancer associated with MDD, we turned to a rodent model of MDD that is characterized by choline depletion from the diets of Fischer-344 rats to trigger hepatocellular carcinoma (HCC), one of the most common and deadly types of liver cancer. More specifically, this model of MDD, established decades ago, utilizes a choline deficient L-amino acid-defined diet (CDAA) that leads to the development of hyperplastic nodules and liver cirrhosis within 6 months of exposure, which progresses to fully developed HCC tumors within further 6 months. Seminal papers using the CDAA diet began surfacing in the early 1990s with the first reports of the relationship between MDD and HCC development (Nakae et al., 1992). Shorter duration of the CDAA diet has also been used to study non-alcoholic fatty liver disease.

Aberrations in the epigenome have been widely studied and implicated as a driving factor in many cancer types including liver cancer (Stefanska et al., 2011). Although epigenetic alterations, mainly DNA methylation changes, have been observed as a consequence of MDD, studies are mostly limited to global changes and candidate genes and lack mechanistic insights (Pogribny, Poirier & James, 1995; Shimizu et al., 2007). To date in the CDAA rat model, only one study has reported DNA methylation changes in an oncogene (*c-Myc*) upon consumption of the CDAA diet (Tsujiuchi, Tsutsumi, Sasaki, Takahama & Konishi, 1999). Another study identified upregulation of oncogenic microRNAs in response to the CDAA diet but did not investigate a role for DNA methylation (Wang et al., 2009). Rather, most studies focus on more general OCM alterations or hypermethylation and silencing of tumor suppressor genes, a well-characterized phenomenon during carcinogenesis. Short-term feeding of the CDAA diet (4 days, 8 days, or 3 weeks) resulted

in promoter hypermethylation of tumor suppressor genes *E-cadherin*, *Cx26*, and *Rassfla*. At those early time-points, increased methylation of regulatory regions was not associated with gene repression (Shimizu et al., 2007). Other MDD diets such as folate/methyl deficiency report loss of methyl marks within promoter regions of tumor suppressor genes such as *p53* that may contribute to HCC by exposing regions for DNA-damaging agents leading to DNA strand breaks (Pogribny, Basnakian, Miller, Lopatina, Poirier & James, 1995).

In the present study, we aim to characterize the pathogenesis of HCC development upon MDD using RNA sequencing to assess processes and pathways altered upon MDD. We discovered profound disruption of metabolism-related genes, including genes involved in OCM and lipid removal pathways in the liver. Based on disturbances in OCM and dysregulated methylation reactions, we hypothesized that the MDD diet may impact DNA methylation status within cancer-related genes. Due to the greater amount of upregulated genes and higher magnitude of changes in upregulated genes compared to downregulated genes in response to MDD along with the limited evidence for oncogenes related to MDD-driven carcinogenesis, we therefore evaluated DNA methylation-related alterations with a specific focus on regulatory regions of oncogenes. Our interest in DNA methylation in particular stemmed from observed changes during MDD indicating perturbations in methylation reactions. Therefore, we proceeded with analysis of epigenetic regulation of upregulated oncogenes using pyrosequencing. Specifically, following analysis of differential gene expression to identify candidates, we employed pyrosequencing to analyze DNA methylation status of regulatory regions of candidate oncogenes. Due to our previous studies defining reversal of aberrant DNA methylation patterns by dietary stilbenoid compounds, we evaluated the effects of pterostilbene (PTS) on silencing candidate oncogene expression through

changing DNA methylation patterns. PTS was shown to re-establish homeostasis in DNA methylation machinery that is very often dysregulated during carcinogenesis (Beetch, Lubecka, Kristofzski, Suderman & Stefanska, 2018; Beetch et al., 2019b; Lubecka et al., 2016). Other *in vivo* studies have also reported anti-cancer effects of PTS on cancer cell growth through various other epigenetic and anti-inflammation-related mechanisms (Guo, Tan, Wang & Zhang, 2016; Qian, Liu, Yan, Yuan, Levenson & Li, 2018; Qian, Liu, Zhang, Levenson & Li, 2018), but the present study is the first to show attenuation of HCC in an *in vivo* model. Evidence for RSV-mediated attenuation of HCC in *in vivo* models has surfaced (Bishayee, Barnes, Bhatia, Darvesh & Carroll, 2010; Luther et al., 2011), but the superior bioavailability of PTS makes it the more attractive stilbenoid to study and the reason why we focused on PTS.

## **4.2 Materials and Methods**

### **4.2.1 Rat model**

#### **4.2.1.1 Animals and experimental timeline**

Fischer-344 rats (n=6 per experimental group) were housed 2 per cage. Rats arrived at the animal facility at 4 weeks of age. During acclimation period, all rats were fed a choline sufficient L-amino acid defined (CSAA) diet for 1 week. Following acclimation, the 3 experimental groups were assigned to Group 1: CSAA, Group 2: choline deficient L-amino acid defined (CDAA), and Group 3: CDAA diet supplemented with PTS. Groups 1 and 2 consumed the CSAA diet for an additional 3 weeks (for a total of 4 weeks). Group 3 consumed the CSAA diet supplemented with PTS for those 3 weeks (CSAA diet for 4 weeks and PTS supplementation for 3 of those weeks prior to switch to CDAA diet). At week 8, Groups 2 and 3 were started on CDAA diet and CDAA diet supplemented with PTS, respectively. Food consumption and body weight was measured every

week throughout the 52-week timeline. All animal work was conducted in accordance with a protocol approved by the Purdue Animal Care and Use Committee (PACUC) and all animal procedures were carried out following the PACUC guidelines and overseen by the Laboratory Animal Program (LAP) at Purdue University.

#### **4.2.1.2 Diets**

CSAA diet and CDAA diet were purchased and pelleted by Dyets Inc., Bethlehem, PA, USA. Detailed ingredients in CSAA and CDAA diets in **Appendix C**. PTS was obtained from Biotang Inc, Albuquerque, NM, USA and incorporated into respective diets (Dyets Inc., Bethlehem, PA, USA). PTS was incorporated in CDAA diet formula at 134 mg/kg BW/day.

#### **4.2.1.3 Histopathological analysis**

Four micrometer tissue sections were stained with hematoxylin and eosin, and a board-certified veterinary pathologist microscopically examined the slides. The interpretations were based on standard histopathological morphologies. The pathologist was blinded to the diet treatment.

#### **4.2.2 RNA isolation and qPCR**

TRIzol (Invitrogen) was used to isolate total RNA which served as a template for cDNA synthesis with AMV reverse transcriptase (Roche Diagnostics), according to the manufacturer's protocol. Amplification reaction was performed in CFX96 Touch Real-Time PCR Detection System (Bio-Rad) using 2 µl of cDNA, 400 nM forward and reverse primers (please see **Table 4.1** for sequences), and 10 µl of SsoFast EvaGreen Supermix (Bio-Rad) in a final volume of 20 µl. The following cycles were used in the amplification reaction: denaturation at 95 °C for 10 min, amplification for 60 cycles at 95 °C for 10s, annealing temperature for 10s, 72 °C for 10s, and final

extension at 72 °C for 10 min. The CFX Maestro Software (Bio-Rad) was used to quantify gene expression with a standard curve-based analysis.

**Table 4.1.** Primer sequences used in expression analysis by qPCR and in methylation analysis by pyrosequencing.

<b>Table 4.1. Primer sequences used in qPCR and methylation analysis.</b>			
<b>Gene</b>	<b>Primer sequences</b>	<b>Annealing temperature [°C]</b>	<b>Amplicon length [bp]</b>
<b>qPCR</b>			
Gapdh	FW 5'-TCTCTGCTCCTCCCTGTTCT-3' RV 5'-TACGGCCAAATCCGTTTACA-3'	59	104
Bhmt	FW 5'-GCAATCGGTGCCATCTTTC-3' RV 5'-TCAAGCCTTTGCTGGAGAC-3'	59	85
Vldlr	FW 5'-CTGGAGATGCGATGGTAAA-3' RV 5'-ACTGGAGCAAGTGAACATC-3'	59	97
Lpl	FW 5'-CTATACCAAGCTGGTGGGAAATG-3' RV 5'-GCTCCAAGACTGTACCCTAAGA-3'	59	108
Apoa4	FW 5'-CATGCAGACCACAATACAAGAC-3' RV 5'-CCCTTGAGCCCTTCCATATT-3'	59	108
Apoa5	FW 5'-GACGACCTCTGGGAAGATATTG-3' RV 5'-GACAACGAGCTGCAGAGTTA-3'	59	98
Apoc2	FW 5'-CTCTATTCCTGGCTCTCCTAGT-3' RV 5'-CCTTGGCAGAGTTCCAGTAA-3'	59	126
Apoc3	FW 5'-GCAGGAGTCTGATATAGCTGTG-3' RV 5'-CCAGAGGCCAGTGAACCTTATC-3'	59	106
Aldh1l1	FW 5'-GTACCTTCCAACCCACTGTT-3' RV 5'-CTTCCTCAGCTGGCAGTAAA-3'	59	86
Gnmt	FW 5'-CAACTACGACTACATCCTCAGC-3' RV 5'-GTGGGCTTTGTTGTTTACTGTC-3'	59	118
Mat2a	FW 5'-TATCGCCCAAGGTGTTTCATC-3' RV 5'-CTTCAGTTTCATCAGTGGCATAAC-3'	59	95
Gstp1	FW 5'-ACACCATTGTGTACTTCCCA-3' RV 5'-ACTTGAGCGAGCCTTGAA-3'	59	126
Gpx2	FW 5'-ACCTTCCAGACCATCAACATC-3' RV 5'-CTTGGAGAAACAGTCGGAGATT-3'	59	103
Dnmt1	FW 5'-CACCATCACGTCTCACTTCA-3' RV 5'-AGCAGATTCATTTGCGTTTCC-3'	59	82

Dnmt3a	FW 5'-CGGAGATGGCAAATTCTCAGT-3' RV 5'-TACATGGGCTGCTTGTTGTAG-3'	59	102
Dnmt3b	FW 5'-AGGGAGACAGCAGACATCTTA-3' RV 5'-CCGAGGACTGGTCACTACA-3'	59	93
Tet1	FW 5'-CCAAAGATGGCTCTCCAGTT-3' RV 5'-GAGCTGAGTCAGTGCTTCTATG-3'	59	101
Tet2	FW 5'-CTGCCCTGTAGGATTTGTTAGA-3' RV 5'-GAGGGTAAGCTGCTGAATGT-3'	59	104
Tet3	FW 5'-TGGAGATTC AAGGCAGCTAAG-3' RV 5'-AGTCGGGCTTCTGGTCTA-3'	59	116
Mmp27	FW 5'-CAATATGGTTACACCCTCCCT-3' RV 5'-TCTGAATAGCCTCATCCACATC-3'	59	106
Mmp12	FW 5'-CTGGACACCTCAACTCTGAAA-3' RV 5'-GAGATACCGCTTCATCCATCTT-3'	59	108
Spp1	FW 5'-GAAGGCGCATTACAGCAAAC-3' RV 5'-GGGCTAGAAGATTCTGCTTCTG-3'	59	83
Lamc2	FW 5'-TCTCTGGACCCTGTGATTCT-3' RV 5'-GTTTGCCCTGTCCAGATGATA-3'	59	104
Thbs1	FW 5'-GAGCATCTTCACCAGGGATTT -3' RV 5'-GTTCCAAAGACAAACCTCACATTC-3'	59	111
Pdgfd	FW 5'-GCAGAGCGCATCCATCAA-3' RV 5'-CACCCGAATGTTCTCATCTCTC-3'	59	100
Myc	FW 5'-AGAGCTCCTCGCGTTATTTG-3' RV 5'-GAGTCGTAGTCGAGGTCATAGT-3'	59	119
Mmp2	FW 5'-GACGTAACCTCACTACGCTTT-3' RV 5'-AATGGGTATCCATCTCCATGC-3'	59	95
Map3k6	FW 5'-TCATGAATCTGCTTCTGTCATACC-3' RV 5'-ACATCACAGGTGGGCAAAG-3'	59	94
Jag1	FW 5'-GAGGCATGGGATTCCAGTAA-3' RV 5'-GCAATCCCTGTGTTCTGTTTC-3'	59	122
Epcam	FW 5'-AATGCCAGTGTACTTCCTATGG-3' RV 5'-TTCATCCTCCTCCCAGACTT-3'	59	115
Heyl	FW 5'-GACCGTGGATCACTTGAAGAT-3' RV 5'-TTACGACCTCAGTAAGGCATTC-3'	59	119
Rps6ka2	FW 5'-AGGTTCTTCTCCGTGTACCT-3' RV 5'-CTTCCTTCACATGGTTGCTAATG-3'	59	115
Smo	FW 5'-GCTTATTGTGGGAGGCTACTT-3' RV 5'-GCAGCATGGTCTCATTGATCT-3'	59	119
Wnt4	FW 5'-CACTCATGAACCTTCACAACAAC-3' RV 5'-CCAGCATGTCTTTACCTCACA-3'	59	113
Map4k4	FW 5'-TTCATTAAGAAGAGCCCTCCAG-3' RV 5'-CTTTGAGCGTGTCCCTTTG-3'	59	115
<b>Pyrosequencing</b>			
Jag1	FW 5'-ATAGAGTAGGGAGAGTAGAAGGTTTAA-3' RVBio 5'-TTCCAATCCTACATACTCCAATCCAC-3' Seq 5'-GGGAGAGTAGAAGGTTTAAGG -3'	52	212

Wnt4	FW 5'-TAGGGAGGGGTAGGATTATAGAAT-3' RVBio 5'-ACCCAATACTAAATCCC-3' Seq 5'-AGTTTAGAGAGTTAGTGATTAGG -3'	53.5	300
Smo	FW 5'-GGGTTTTTAGGGTTGAAGATAATTT-3' RVBio 5'-AACTCCCCCAAATCCCCTAAC-3' Seq 5'-GGTTTTTAGGGTTGAAGATAATTTT -3'	53.5	246
Mmp12	FW 5'-TGGGAAATATAGAGGTGTAGAGTTGAGT-3' RVBio 5'-ACAAATTCCTTAAAATCCCACCTTTATAT-3' Seq 5'-ATGATTTAGATAATGGTTTGAT-3'	50	174

### 4.2.3 RNA sequencing

Total RNA was extracted from rat tissue samples collected at the end of the 52-week study using TRIzol (Invitrogen). Quality check was performed using an Agilent Bioanalyzer prior to library preparation. Libraries were prepared from 4 rats from each diet group (CSAA, CDAA, CDAA+PTS) using the TruSeq Stranded kit (Illumina, San Diego, CA, USA) and sequenced 4 rats per lane using the HiSeq2500 on high-throughput mode (1x50 bp reads). Reads were quality trimmed and Illumina TruSeq adapter sequences were removed. FastQC and FastX were run to ensure quality of data before and after trimming (Andrews, 2010). Reads were aligned to the rat rn6 reference genome using Tophat2 (Kim et al., 2013). Bioconductor packages Cufflinks, DESeq2, and EdgeR were used for differential expression analysis (Trapnell et al., 2012; Love, Huber & Anders, 2014; Robinson, McCarthy & Smyth, 2010). Differentially expressed genes that appeared in results of all three packages were deemed robust and considered in our analyses.

### 4.2.4 Measurement of SAM/SAH levels by LC-MS

For quantification, stock solutions of SAM and SAH were prepared using powders from Sigma-Aldrich (cat. no. A9384 and A4377, respectively). The stocks were pooled and diluted in acetonitrile:water (ACN:H<sub>2</sub>O) (1:1, v/v) to a set of 8 calibration standards for interpolation of liver sample concentrations (**Appendix D**). Internal standards of deuterated versions, SAM-d<sub>3</sub>

and SAH-d4, were purchased from CDN Isotopes (product no. D-4093) and Cayman Chemical (item no. 9000372), respectively. Internal standard solutions were pooled at final concentrations of 50  $\mu$ M SAM-d3 and 75  $\mu$ M SAH-d4 in ACN:H<sub>2</sub>O (1:1, v/v).

For sample preparation, ~10 mg of liver tissue, 1 mL of methanol:water (4:1, v/v), 30  $\mu$ L of internal standard and ~0.4 g of 1.0 mm glass beads were added to a 2-mL screw-capped tube. The samples were homogenized with a Mini-Beadbeater-24 (Biospec, San Diego, CA) for 30 seconds. The homogenate was transferred to a clean tube, combined with washings from rinsing the glass beads (2 x 200  $\mu$ L of methanol), stored for 2 hours at -20 °C to extract metabolites, and centrifuged to extract supernatant. The supernatant was concentrated to 100  $\mu$ L in ACN:H<sub>2</sub>O (1:1, v/v) for analysis on LC-MS.

The analysis was performed on a Bruker Impact II™ Ultra-High Resolution Qq-Time-of-Flight Mass Spectrometer (Bruker Daltonics, Bremen, Germany) coupled with an Agilent 1290 Infinity Liquid Chromatography (Agilent Technologies, Palo Alto, CA) system. The mobile phases were 10 mM ammonium acetate at pH 4.8 in 5% ACN in H<sub>2</sub>O (MP A) and 5% H<sub>2</sub>O in ACN (MP B). With a flow rate of 0.150 mL/min, the LC gradient went from 95% MP B to 5% MP A over 20 minutes and held for 5 minutes. The gradient went back to 95% MP B over a minute and was allowed to equilibrate for 18 minutes before the next injection.

Samples were injected at 5  $\mu$ L each onto a ZIC-pHILIC column (200Å, 5  $\mu$ m particle size, 2.1 × 150 mm) (EMD Millipore), for hydrophilic interaction chromatography (HILIC) positive ionization mode analysis. For mass calibration, 5  $\mu$ L of 150 mM sodium formate was injected. Mass spectra peak areas were integrated for SAM, SAH, SAM-d3 and SAH-d4 in each calibration standard to generate calibration curve plots. The plots were of peak area ratios of

SAM/SAM-d3 and SAH/SAH-d4 against the concentrations in **Appendix D**, and used to back calculate the concentrations in liver samples.

#### **4.2.5 DNA isolation and pyrosequencing**

DNA, isolated using standard phenol:chloroform extraction protocol, was treated with sodium bisulfite as previously described (Colella, Shen, Baggerly, Issa & Krahe, 2003; Lubecka et al., 2016). HotStar Taq DNA polymerase (Qiagen) and biotinylated primers were used to amplify bisulfite converted promoter sequences of the selected genes (please see **Table 4.1** for sequences). Pyrosequencing of the biotinylated DNA strands was performed in the PyroMark Q48 Autoprep instrument (Qiagen). Percentage of methylation at a single CpG site resolution was calculated using PyroMark Q48 Autoprep software.

#### **4.2.6 Statistical analysis**

Two-tailed Mann-Whitney U test was used for statistical analysis of qPCR. Unpaired t-test with two-tailed distribution was used for statistical analysis of pyrosequencing. When more than 2 groups were compared, one-way ANOVA was used, followed by Tukey's post-hoc test. All results represent n=6 rats per group. qPCR data presented in boxplots depicts minimum, interquartile range (IQR), and maximum. Pyrosequencing is presented as mean  $\pm$  standard error of the mean (SEM). The results were considered statistically significant when  $P < 0.05$ .

### 4.3 Results

#### 4.3.1 CDAA diet leads to fully developed HCC after 52 weeks

Upon exposure to either CSAA or CDAA diet (n=6 rats per group) for a total of 52 weeks, the average body weight of healthy rats (CSAA rats) compared to rats on CDAA diet (CDAA rats) was significantly higher (**Figure 4.1A**). Final body weights at 52 weeks were approximately 495 g for CSAA rats compared to 361 g for CDAA rats (shown in right panel of **Figure 4.1A**). Interestingly, body weights of CDAA rats were significantly reduced by 12 weeks (210 g compared to 287 g) and were consistently lower throughout the experiment (**Figure 4.2A**). Other studies using MDD diets have observed similarly slowed weight gain (Nakae et al., 1992; Pogribny, Poirier & James, 1995). For example, Pogribny and colleagues found that by 9 weeks, choline deficient rats weighed 20% less than their choline sufficient counterparts (Pogribny, Poirier & James, 1995). Final liver weights were the same between the CSAA and CDAA rats. However, the relative liver weight of CDAA rats was higher compared to healthy CSAA rats due to the decrease in body weight of CDAA rats over the experimental timeline (**Figure 4.1B**).

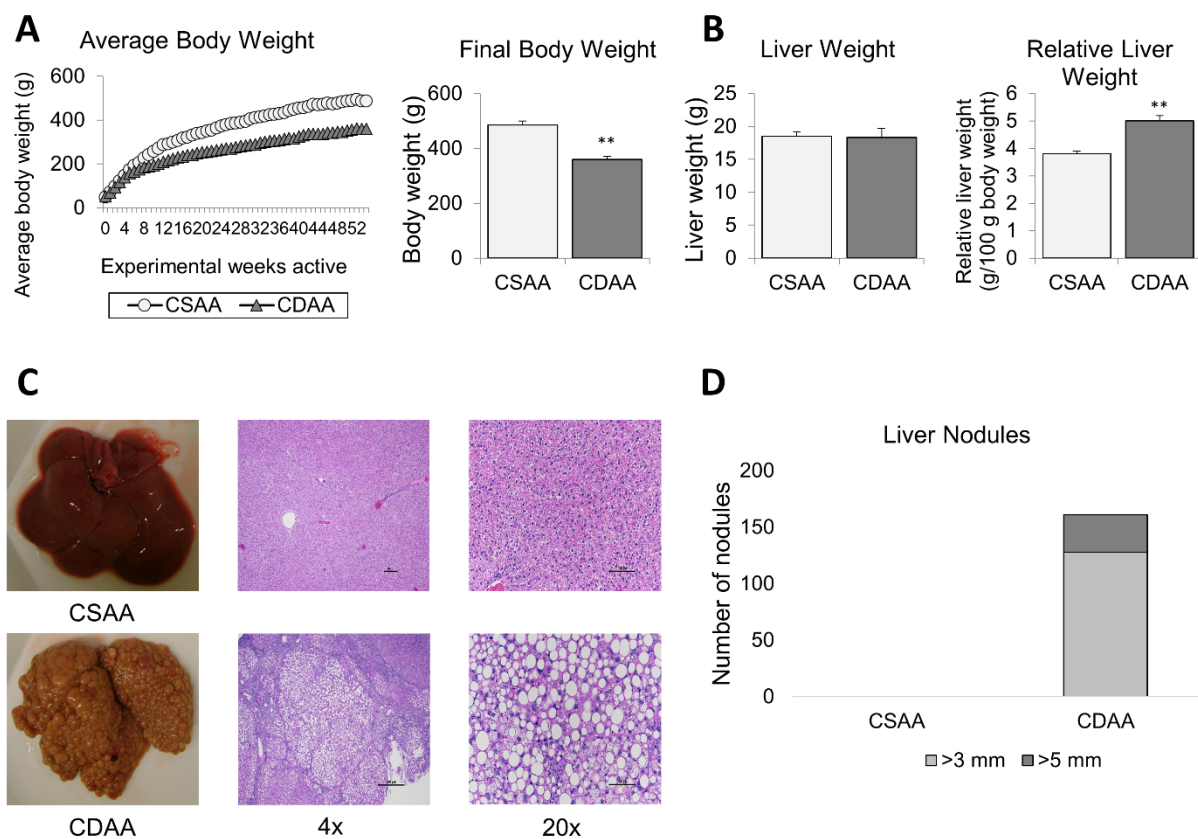


**Figure 4.1. Macroscopic and histopathological analyses of rat livers upon methyl donor deficient diets.** (A) Average body weights of CSAA and CDAA groups over 52-week experimental timeline. Bar graph represents average final body weights of CSAA and CDAA groups at the 52-week time-point. (B) Average liver weights and relative liver weights of CSAA and CDAA groups at the 52-week time-point. Results represent mean  $\pm$  SEM,  $n=6$  rats per group,  $**P < 0.01$ . (C) Representative images of whole CSAA and CDAA livers, as well as histopathological images at 4x and 20x magnification. (D) Analysis of liver nodules in CSAA and CDAA livers.

Macroscopic differences were observed when comparing the healthy livers from CSAA rats and livers with HCC from CDAA rats. CDAA livers appeared yellow and contained numerous HCC tumor nodules. Whole livers shown in **Figure 4.1C** are representative of livers from all rats from each group ( $n=6$  CSAA,  $n=6$  CDAA). Magnification at 4x and 20x revealed histopathological differences, namely lipidosis/steatosis manifesting as abundant fat globule accumulation in the

CDAA livers compared to CSAA livers (**Figure 4.1C**). Hyperplastic and HCC nodules did not develop in healthy CSAA livers, whereas upwards of 150 nodules on average were observed in CDAA livers. Tumor nodules in CDAA livers were defined as *solid* HCC containing large, vacuolated hepatocytes and absent of portal triads. Majority of the nodules observed in the CDAA livers were 3 mm or larger but a portion of the nodules were even larger, measuring more than 5 mm (**Figure 4.1D**). HCC nodules were evenly distributed among the median and lateral lobes of the CDAA livers (**Figure 4.2B**).

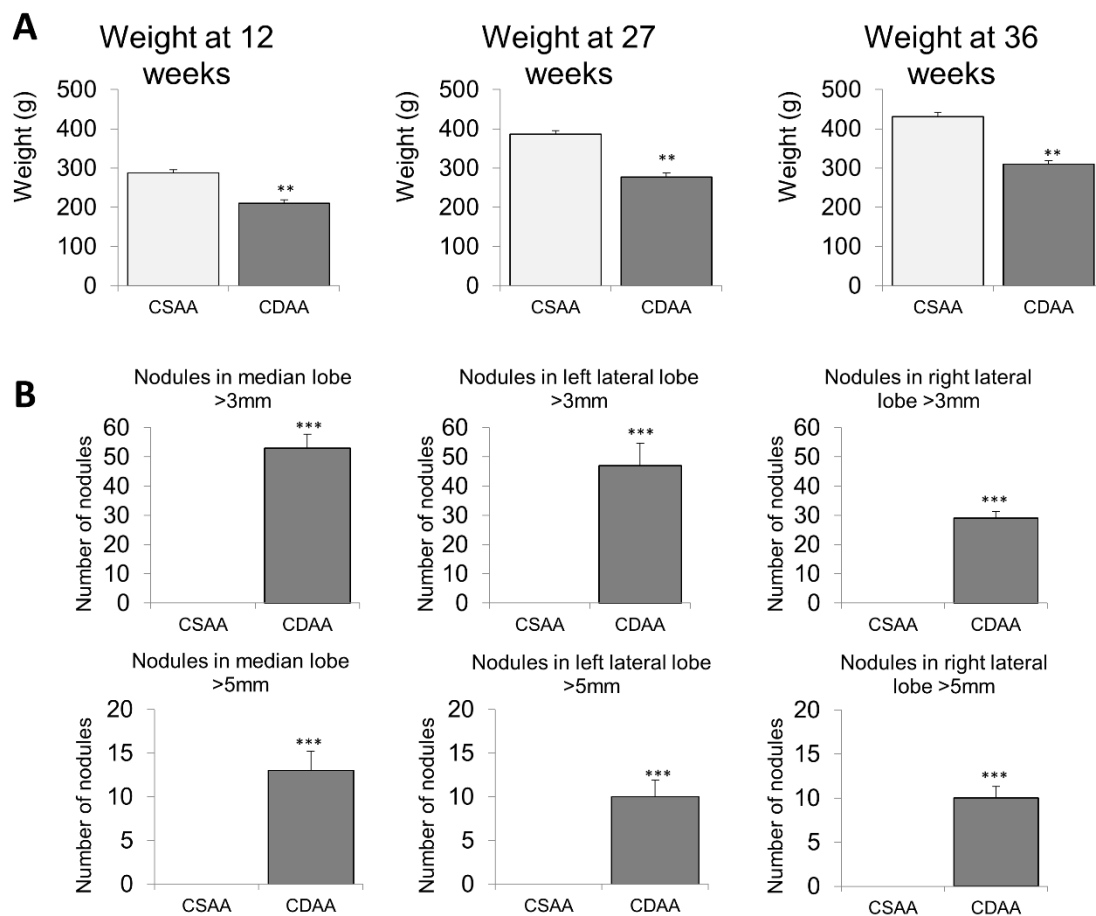


**Figure 4.2. Rat liver weights at earlier time-points and lobe-specific nodule analysis.** (A) Average body weights of CSAA and CDAA groups at 12-week, 27-week, and 36-week time-points. (B) Analysis of liver nodules per liver lobe. Data expressed as mean  $\pm$  SEM, n=6 rats per group, \*\* $P < 0.01$ , \*\*\* $P < 0.001$ .

### **4.3.2 Profound gene dysregulation occurs in the liver of rats exposed to the CDAA diet**

In order to understand CDAA-triggered liver carcinogenesis, we performed next generation RNA sequencing of healthy CSAA and HCC nodule-ridden CDAA liver tissues. We discovered 1,236 upregulated and 612 downregulated genes with statistically significant fold-change of 2 or higher. Chromosomal view of these changes is presented in **Figure 4.3A** using Integrative Genome Visualization (IGV) tool. Each red bar represents a gene that is upregulated and each blue bar represents a gene that is downregulated in CDAA livers compared to CSAA livers. Significantly upregulated and downregulated genes were functionally analyzed using GO and KEGG pathway analyses in DAVID Knowledgebase (Sherman et al., 2007). In general, upregulated genes were associated with classical cancer-related functions and pathways such as cell adhesion and migration, cell proliferation, signal transduction, immune and inflammatory response, cell cycle, and oncogenic signaling pathways like MAPK and Wnt signaling (**Figures 4.3B and C**). On the other hand, genes associated with myriad metabolic pathways were largely represented in the downregulated gene list. Genes involved in lipid processes such as homeostasis, localization, transport, and lipoprotein clearance were downregulated. In addition, expression of genes related to hormone and amino acid levels and functions surrounding utilization of carbohydrates were decreased in CDAA livers (**Figures 4.3B and C**).

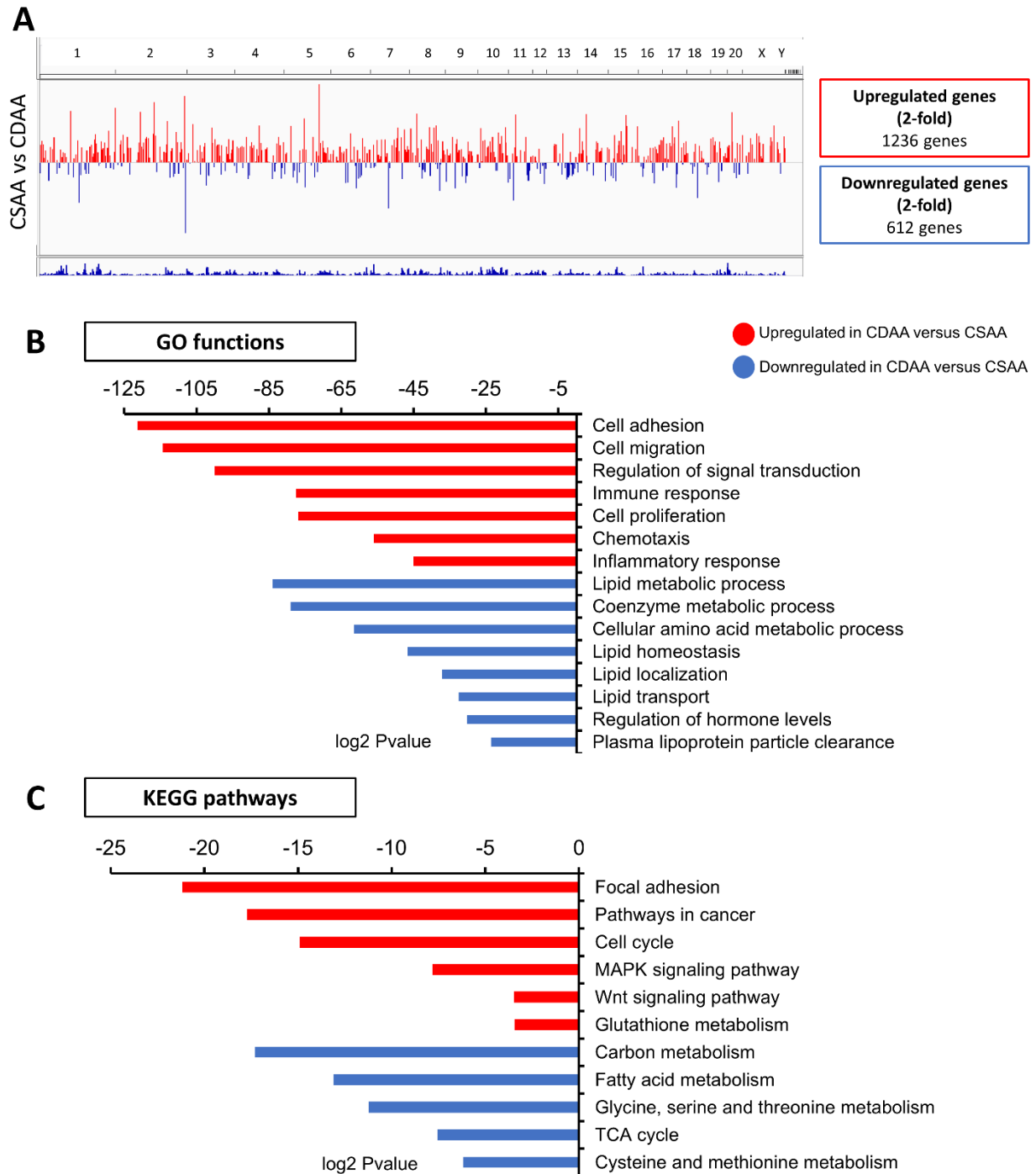


**Figure 4.3. Overview of RNA sequencing data: functional and pathway analysis.** (A) IGV map of differentially expressed genes upon MDD compared to a healthy CSAA diet. (B) GO function and KEGG pathway analyses of differentially expressed genes upon MDD compared to CSAA.

According to functional analysis, differentially expressed genes in response to MDD were most enriched with two broad functional categories, namely macronutrient metabolism and oncogenic processes and pathways. Altered expression of metabolism-related genes involved in carbohydrate, fatty acid, amino acid, vitamin, and other pathways is presented in **Figure 4.4**. Pyruvate kinase, liver and RBC (*Pklr*), pyruvate carboxylase (*Pc*), acetyl-CoA synthetase 2 (*Acss2*), and ATP citrate lyase (*Acly*) are downregulated genes with various roles in carbohydrate metabolism. For example, *Pklr* catalyzes the rate-limiting step of glycolysis, while *Pc* is involved in carboxylation of pyruvate to oxaloacetate. *Acss2* and *Acly* catalyze the synthesis of acetyl-CoA from short chain fatty acids (*Acss2*) or by cleavage of citrate (*Acly*). Furthermore, hexokinase 1 and 2 (*Hk1* and *Hk2*), involved in the essential first step of glucose and fructose metabolism, were found to be upregulated in the CDAA livers, whereas the catalytic subunit of glucose-6-phosphatase (*G6pc*) which hydrolyzes glucose-6-phosphate to glucose during gluconeogenesis and glycogenolysis was downregulated. *G6pc* downregulation has been associated with accumulation of lipid in the liver. In addition, expression of fatty acid metabolism and lipid removal genes were largely decreased in the CDAA livers. Acetyl-CoA acetyltransferase 2 (*Acat2*), acetyl-CoA carboxylase alpha (*Acaca*), fatty acid synthetase (*Fasn*), and ELOVL fatty acid elongase 5 (*Elovl5*) were among the downregulated fatty acid metabolism genes. Expression of several apolipoprotein genes, which are components of lipoproteins responsible for transporting lipids throughout the body, was reduced in CDAA livers. Another robustly downregulated gene that has been implicated in liver disease and HCC specifically was patatin-like phospholipase domain containing protein 3 (*Pnpla3*). *Pnpla3* has lipase activity toward triglycerides and its loss of function has been shown to promote fat accumulation in the liver (Trepo, Romeo, Zucman-Rossi & Nahon, 2016). *Pnpla5*, another member of the patatin-like phospholipase family, is a

novel gene that we discovered to be downregulated in CDAA livers. Unlike *Pnpla3*, *Pnpla5* has not been implicated in liver-related processes, but may play an important role similar to *Pnpla3*. Other novel downregulated genes that may play a part in metabolism alterations to drive MDD-associated carcinogenesis are kyphoscoliosis peptidase (*Ky*) (31.8-fold downregulated), which is in the trans-glutaminase superfamily and is associated with muscle growth and myopathy, as well as *Cyp2c11* (19.8-fold down) and *Cyp2c7* (19.7-fold down), which are cytochrome P450 subunits that catalyze many reactions in drug and nutrient metabolism. Novel upregulated genes may also participate in disturbed metabolism underlying MDD-triggered HCC. Some examples include the 5<sup>th</sup> highest upregulated gene *Slc5a9* (68.9-fold), which is an essential transporter of mannose and fructose, and aquaglyceroporin 7 (*Aqp7*) (34.9-fold) with implications in modulation energy metabolism. Together, established and novel alterations may underlie the observed fat accumulation and impairment of lipid removal from MDD-triggered HCC livers.

## Dysregulated metabolism-related pathways in CDAA livers

- Upregulated in CDAA versus CSAA
- Downregulated in CDAA versus CSAA

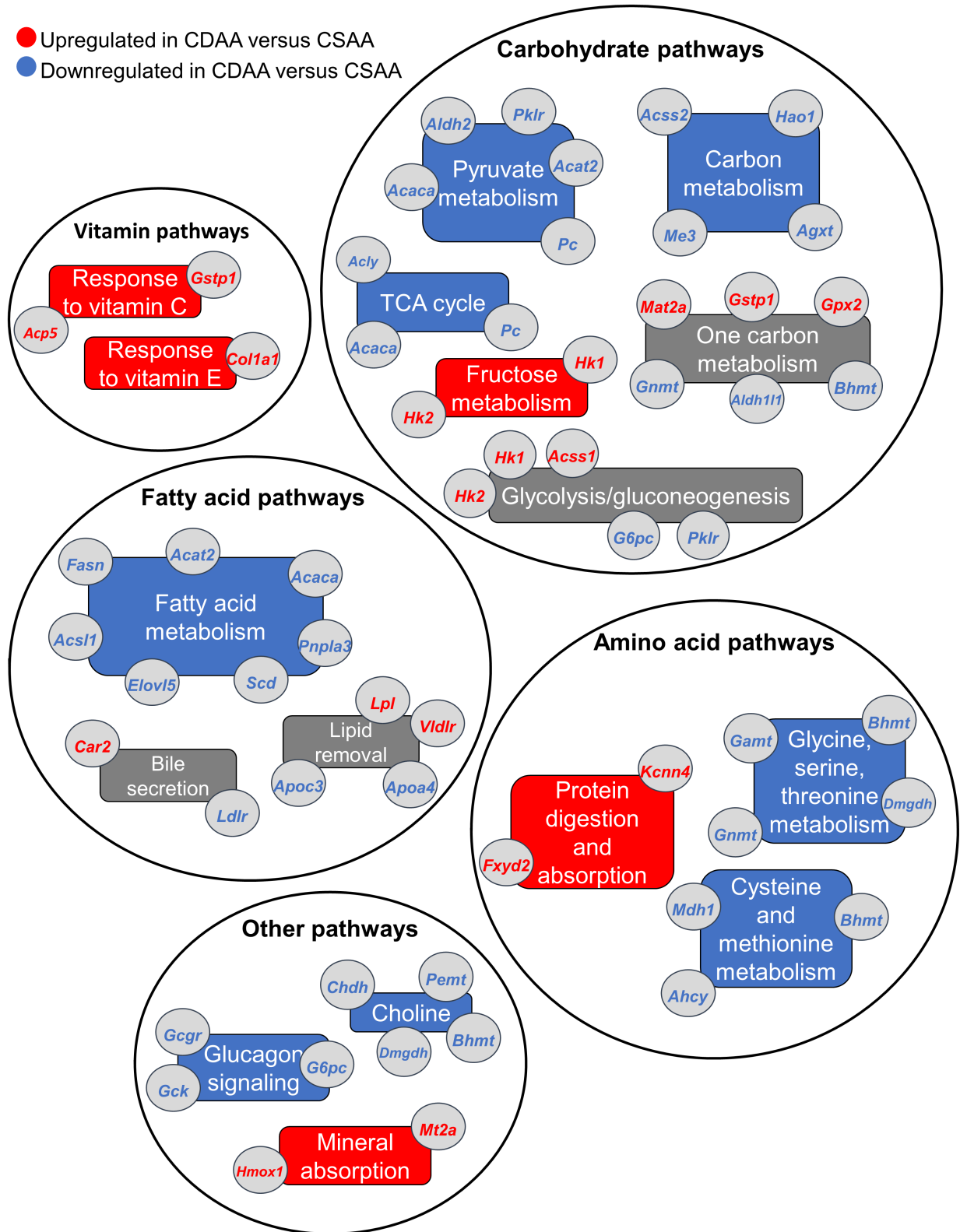


**Figure 4.4. Overview of genes involved in metabolism-related alterations in livers of CDAA rats.** Categories contain differentially expressed genes in CDAA versus CSAA livers. Red represents upregulated genes. Blue indicates downregulated genes. Grey boxes indicate categories with genes both upregulated and downregulated.

Genes active in metabolizing certain amino acids were also decreased in response to MDD. Specifically, glycine-N methyltransferase (*Gnmt*), dimethylglycine dehydrogenase (*Dmgdh*), adenosylhomocysteinase (*Ahcy*), and betaine-homocysteine S-methyltransferase (*Bhmt*) were downregulated genes associated with mainly glycine, cysteine and methionine metabolism. Notably, some of the amino acid metabolism genes (*Dmgdh* and *Bhmt*) are also crucial for choline metabolism. These genes, along with choline dehydrogenase (*Chdh*) and phosphotidylethanolamine N-methyltransferase (*Pemt*), were identified as significantly downregulated in our RNA sequencing data (**Figure 4.5A**). Decreased expression of *Dmgdh* was reported to be a potential diagnostic and prognostic marker for HCC, but *Dmgdh* has yet to be shown to be related to MDD (Liu, Hou, Li, Li, Zhou & Liu, 2016). The role of *Bhmt* has been of particular interest in studying HCC. *Bhmt* catalyzes the formation of methionine from betaine and homocysteine in the liver and kidney. Impairment of the *Bhmt* pathway has been observed in HCC. In human tissues, BHMT was decreased in 85% of HCC and low BHMT expression was associated with shorter overall survival (Jin et al., 2016). However, a clear link has not been established between MDD-triggered HCC and *Bhmt* levels. We used qPCR to validate gene expression changes of *Bhmt* (**Figure 4.5B**) as well as genes related to lipid removal in the healthy CSAA liver tissues and the HCC livers from CDAA rats (**Figure 4.5C**). Presence of choline and betaine to form phosphotidylcholine (PC) in the liver is vital for assembly of very low density lipoproteins (VLDL) that transport lipids out of the liver and into peripheral circulation. PC can be formed using exogenous (CDP-choline pathway) and endogenous choline pathways. The endogenous

choline pathway mainly involves *Chdh*, *Pemt*, and *Bhmt* (**Figure 4.5D**). Profound 8.8-fold downregulation of *Bhmt* in CDAA livers compared to CSAA livers was observed in RNA sequencing data (**Figure 4.5A**), which was further validated by qPCR showing 6.1-fold downregulation (**Figure 4.5B**). *Chdh* and *Pemt* showed only 1.7-fold downregulation in RNA sequencing data. Nonetheless, we were able to validate robust downregulation of choline metabolism-associated *Bhmt* and several apolipoproteins, as well as upregulation of lipid sensing genes (**Figure 4.5B and Figure 4.5C**).

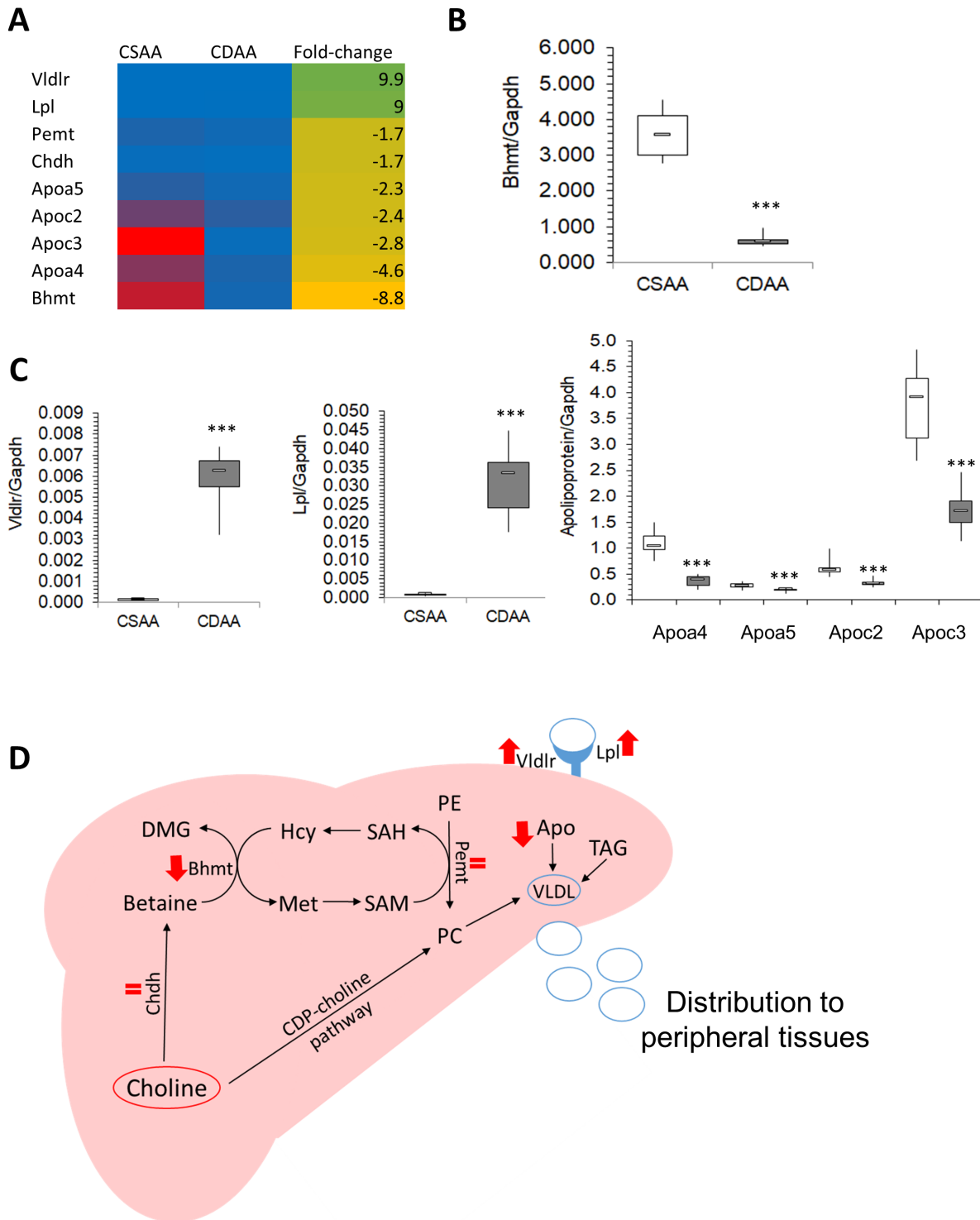


**Figure 4.5. Choline and associated lipid distribution pathways are dysregulated upon methyl donor deficiency. (A) Heat map based on RNA sequencing for genes associated with choline- and**

lipid distribution-related pathways; low expression marked in blue and high expression marked in red. Data from 4 rats per group. (B, C) Boxplots with mRNA expression data based on qPCR in CSAA and CDAA livers. Results expressed as min, IQR, and max; n=6 rats per group. \*\*\* $P < 0.001$ . (D) Schematic of disrupted choline metabolism and lipid distribution pathways in the liver.

### 4.3.3 One carbon metabolism and DNA methylation machinery are altered in CDAA rat livers

Considering changes in genes related to choline metabolism and the involvement of choline in one carbon metabolism (OCM), we next focused on alterations in OCM. Previously mentioned choline-related gene, *Bhmt*, is involved in OCM based on its role in forming methionine from homocysteine (**Figure 4.6A**). Methionine is then used to produce SAM via methionine adenosyltransferase (*Mat*) genes. We found that *Mat2a* was upregulated 2.4-fold, suggesting a compensatory mechanism whereby methionine detected in the CDAA livers is quickly converted to SAM for use in methylation reactions compared to healthy CSAA livers (**Figure 4.6B and 4.6C**). Upon donating a methyl group, SAM is converted to S-adenosyl-homocysteine (SAH) and further to homocysteine (**Figure 4.6A**). Another important pathway in OCM is the folate cycle, which plays a crucial role in converting homocysteine back to methionine (**Figure 4.6A**). We found that a gene called aldehyde dehydrogenase 1 family member 1 (*Aldh1l1*), which is responsible for converting 10-formyltetrahydrofolate to tetrahydrofolate in the folate cycle, was downregulated 2.5-fold in CDAA livers (**Figure 4.6B and 4.6C**). Indeed, depleted expression of *Aldh1l1* has been associated with cancer progression and disrupted OCM (Krupenko & Krupenko, 2019), but has never before been implicated in MDD-related carcinogenesis. We identified other genes involved in various methylation reactions to be downregulated such as previously mentioned *Bhmt*, *Pemt*, and *Gnmt* as well as RNA methyltransferase (*Mettl18*), catechol-O-methyltransferase

(*Comt*), and nicotinamide N-methyltransferase (*Nnmt*). Together, these findings suggest a dysregulated OCM that likely contribute to disturbances in subsequent methylation reactions.

We next measured SAM and SAH levels in liver tissues as an additional parameter indicative of any perturbations in OCM and methylation reactions. SAM and SAH levels were significantly lower in livers of CDAA rats, reflecting the contribution of the MDD diet to disturbances in OCM (**Figure 4.6D**). An average of 91.8 nmol/g SAM and 52.7 nmol/g SAH were measured in healthy CSAA rat livers, whereas CDAA livers had levels of 57.5 nmol/g SAM and 32.9 nmol/g SAH. Furthermore, *Gnmt* was significantly downregulated in CDAA rats according to RNA sequencing data (5.8-fold) and validated by qPCR (4.6-fold). *Gnmt* regulates the SAM:SAH ratio by using SAM to form a product with no known metabolic function (sarcosine) so that the SAM:SAH ratio can be maintained; thus, can be used as a proxy for indicating SAM and SAH levels (Luka, Mudd & Wagner, 2009). Therefore, downregulation of this gene is another indicator of reduced methyl donor availability and further suggests dysregulation of methylation reactions. Genes involved in OCM and differentially expressed in response to MDD-driven carcinogenesis are depicted in **Figure 4.6A**, with red arrows indicating up- and down-regulation.

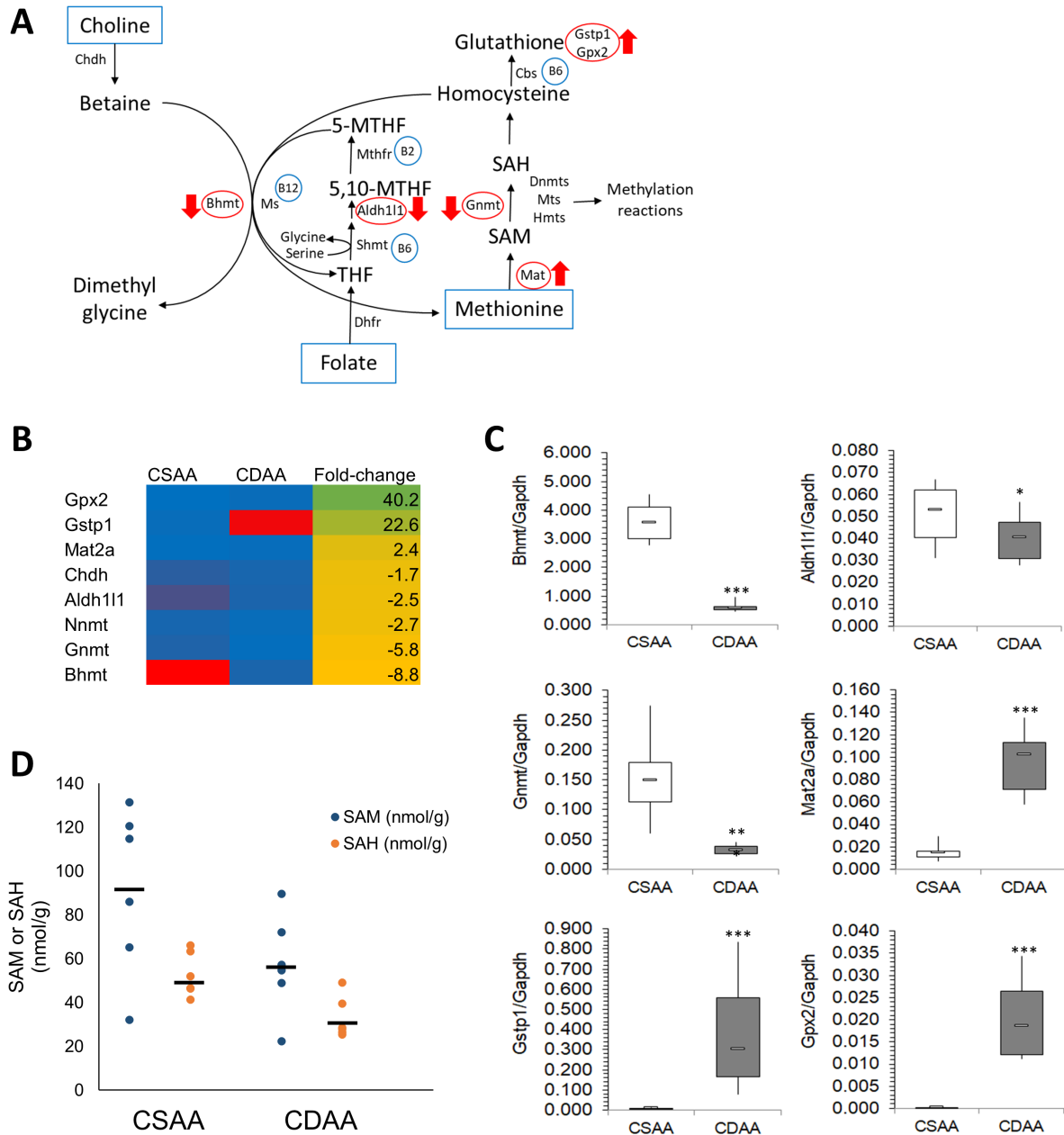


**Figure 4.6. Alterations in one carbon metabolism (OCM) in response to methyl donor deficiency-driven liver carcinogenesis.** (A) Schematic of disrupted one carbon metabolism. (B) Heat map based on RNA sequencing data from gene implicated in OCM; low expression marked in blue and high expression marked in red. Data from 4 rats per group. (C) Boxplots with mRNA expression data based on qPCR in CSAA and CDAA livers. Results expressed as min, IQR, and max; n=6 rats per group. \* $P < 0.05$ , \*\* $P < 0.01$ , \*\*\* $P < 0.001$ . (D) SAM and SAH levels measured by LC-MS-based method in CSAA and CDAA livers (n=6 rats per group).

Based on OCM perturbations induced by MDD, we considered the consequences of altered OCM on DNA methylation reactions. We sought to assess expression changes of *Dnmts* using qPCR and found that *Dnmt1* and *Dnmt3a* were significantly upregulated in CDAA livers, while *Dnmt3b* showed no statistically significant change in CDAA livers compared to healthy CSAA livers. These findings, accompanied by the previously discussed drop in SAM available for methylation reactions, suggest a deregulated state of DNA methylation. Potentially, the upregulation of *Dnmt1* and *Dnmt3a* is a compensatory response in order to upkeep DNA methylation reactions. In addition, significant upregulation of *Tet1*, *Tet2*, and *Tet3* expression in CDAA livers was observed (Figure 4.7). Such perturbations in expression of DNA methylation ‘writers’ (*Dnmts*) and ‘erasers’ (*Tets*) suggest dysregulation of the DNA methylation machinery, which may consequently lead to loci-specific changes in DNA methylation patterns and aberrations in gene transcription. We therefore proceeded with an assessment of DNA methylation states within regulatory regions of genes using pyrosequencing, as described in paragraphs below.

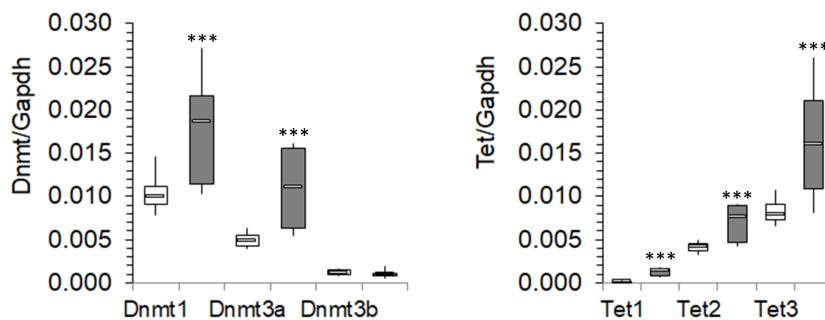


**Figure 4.7. *Dnmt* and *Tet* expression in CSAA versus CDAA livers.** Boxplots for each validated gene in CSAA and CDAA livers, as measured by qPCR. Results expressed as boxplots (min, IQR, max); n=6 rats per group. \* $P < 0.05$ , \*\* $P < 0.01$ , \*\*\* $P < 0.001$ .

#### 4.3.4 Robust upregulation of oncogenes accompanies dysregulation liver functions in CDAA rats

Upon scanning our RNA sequencing data, we observed more profound changes in gene expression in the upregulated genes compared to downregulated genes as evidenced by the greater number and higher magnitude of changes in the set of upregulated genes. A total of 1,236 significantly upregulated genes by 2-fold or higher was almost double the 612 significantly downregulated genes by 2-fold or higher. Maximum magnitude of fold-change reached 159-fold for upregulated genes, whereas the maximum fold-change was 46.6-fold for downregulated genes. Additionally, the amount of upregulated genes by 10-fold or higher was 116 compared to only 28 for downregulated genes. Therefore, we narrowed our analysis of cancer-related genes to those that were upregulated in CDAA livers compared to healthy CSAA livers. We discovered many genes from several oncogenic pathways to be robustly upregulated in HCC (**Figure 4.8A and 4.8B**). Browser tracks displaying RNA sequencing data generated using the WashU Epigenome Browser are presented in **Figure 4.8C** for some top upregulated oncogene candidates, namely jagged 1 (*Jag1*) from Notch signaling, *Myc*, and matrix metalloproteinase 12 (*Mmp12*). Upregulation of 16 top candidates was validated using qPCR, with the highest changes for *Mmp27* and *Mmp12* with fold-changes of 65.1-fold and 27.8-fold, respectively. Other established oncogenic players such as *Myc*, *Jag1*, and *Wnt4* had fold-changes ranging from 6.7-fold to 3-fold. Some less commonly considered genes with potential oncogenic functions included secreted phosphoprotein 1 (*Spp1*), thrombospondin 1 (*Thbs1*), and laminin C2 (*Lamc2*). These genes were some of the highest upregulated genes in response to MDD. (**Figure 4.9**).

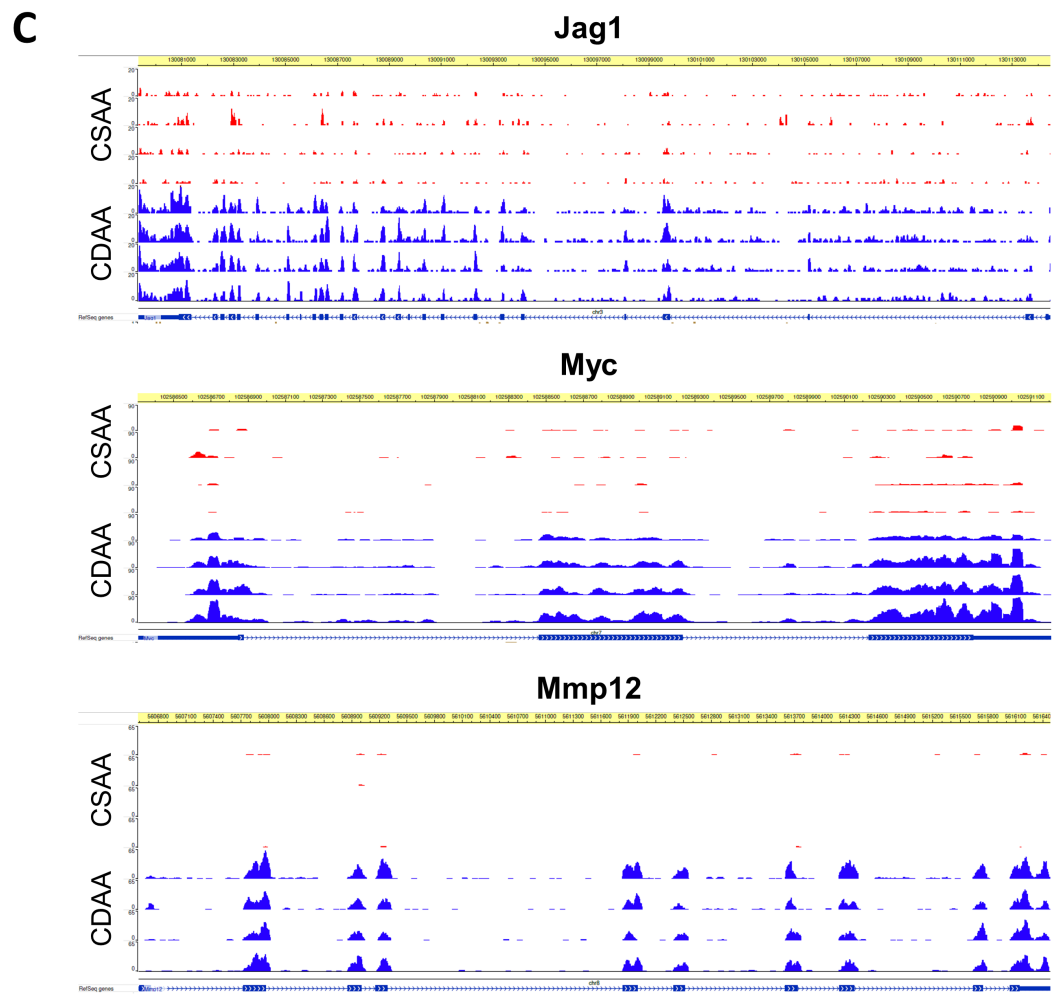
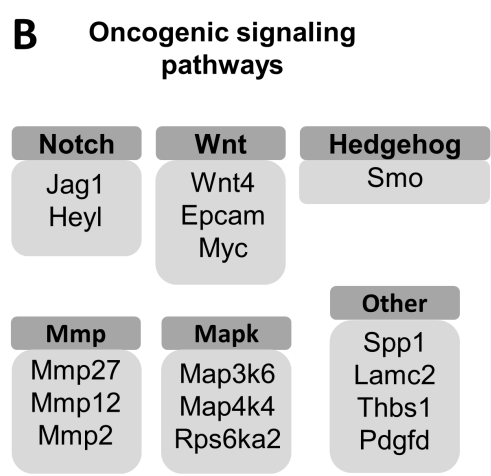
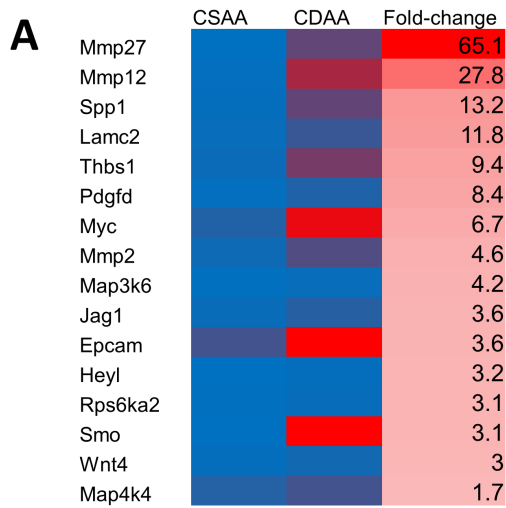


**Figure 4.8. Upregulated oncogenes and oncogenic pathways in CDAA livers.** (A) Heat map based on RNA sequencing data for genes with oncogenic functions; low expression marked in blue and high expression marked in red. Data from 4 rats per group. (B) Gene categorized in to oncogenic signaling pathways based on GO functions and KEGG pathways generated by DAVID Knowledgebase. (C) Tracks depicting RNA sequencing data for several top upregulated oncogene candidates generated by WashU Epigenome Browser. Red peaks indicate CSAA reads and blue peaks indicate CDAA reads from 4 rats analyzed by RNA sequencing.

#### **4.3.5 DNA hypomethylation in regulatory regions of candidate oncogenes corresponds with gene upregulation and may contribute to the potent HCC phenotype in CDAA livers**

Following qPCR, candidate oncogenes were selected for DNA methylation analysis by pyrosequencing. Because activation of signaling pathways is a hallmark of cancer (Hanahan & Weinberg, 2011) and highly upregulated genes fall into oncogenic signaling pathway category, we selected candidates considered to be upstream regulators of their respective pathways and whose alterations may have maximum downstream effect on their oncogenic pathway. We proceeded with *Jag1* from Notch signaling, *Wnt4* from Wnt signaling, smoothed (*Smo*) from the Hedgehog pathway and *Mmp12*. *Jag1* is a Notch ligand whose increased expression in cell membranes and cytoplasm of HCC tumor cells positively correlates with extrahepatic metastasis (Xue, Zou, Chen, Cui, Tang & Ye, 2014). *Wnt4* is a Wnt ligand that binds to its associated frizzled (Fzd) receptor to activate the Wnt/ $\beta$ -catenin signaling pathway. Accumulating evidence demonstrates a major role for aberrant Wnt signaling in HCC (Wang, Smits, Hao & He, 2019). *Smo* is a G-protein coupled receptor for Hedgehog proteins and an established proto-oncogene in human HCC (Sicklick et al., 2006). Several lines of evidence implicate high expression of *Mmp12* with HCC development and severity (Gao et al., 2019a; He et al., 2018). Because promoter regulatory regions are strongly associated with modulation of gene transcription, DNA methylation status of promoter regions of

these 4 genes was measured in CSAA and CDAA liver tissues. Pyrosequencing primers spanning each gene's promoter region were designed to cover as much of the region as possible in an attempt to capture differential DNA methylation that may be mediating upregulation of these genes.

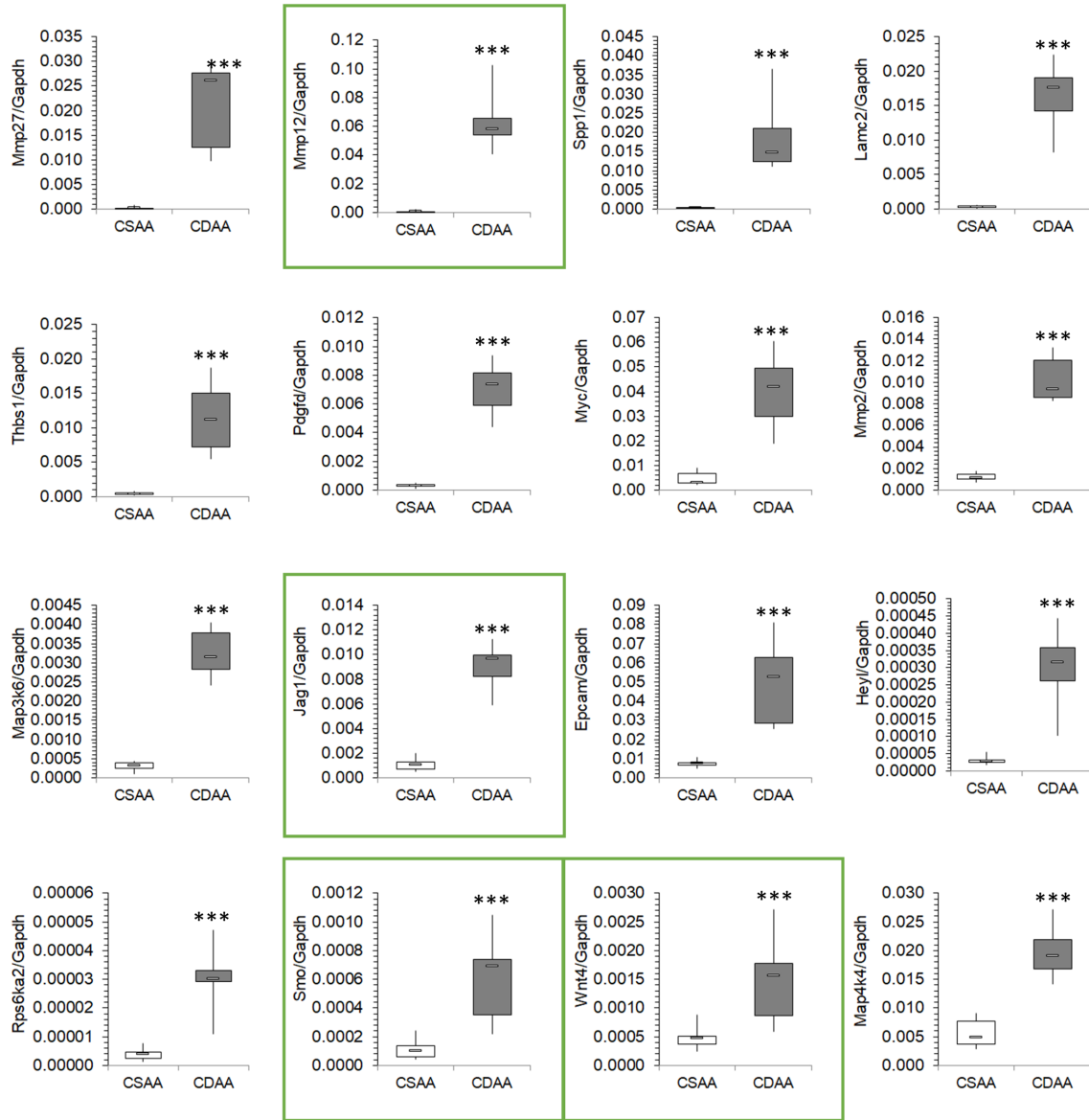


**Figure 4.9. Expression of candidate oncogenes that were found to be upregulated in CDAA livers.** Boxplots for each validated gene in CSAA and CDAA livers, as measured by qPCR. Green boxes indicate candidates for further investigation. Results expressed as min, IQR, and max; n=6 rats per group. \*\*\* $P < 0.001$ .

Among the 30 CpG sites measured surrounding the *Jag1* transcription start site (TSS) (+29 to -106), 4 were significantly hypomethylated while 12 showed a trend toward decreased DNA methylation (P<0.1), with differences reaching 9%. A region downstream of the *Wnt4* TSS (+96 to +271) contained 17 CpG sites, 10 of which were significantly hypomethylated by up to 19% in CDAAs livers compared to CSAA livers. Methylation differences, ranging from 3-5%, were significant or showed a trend toward hypomethylation for a region containing 7 CpGs preceding the TSS of *Smo* (-256 to -193). A region just upstream of the *Mmp12* TSS (-142 to -75) displayed robust hypomethylation of 3 CpG sites, with differential methylation as high as 67% for CpG 2 (Figure 10A and 10B).

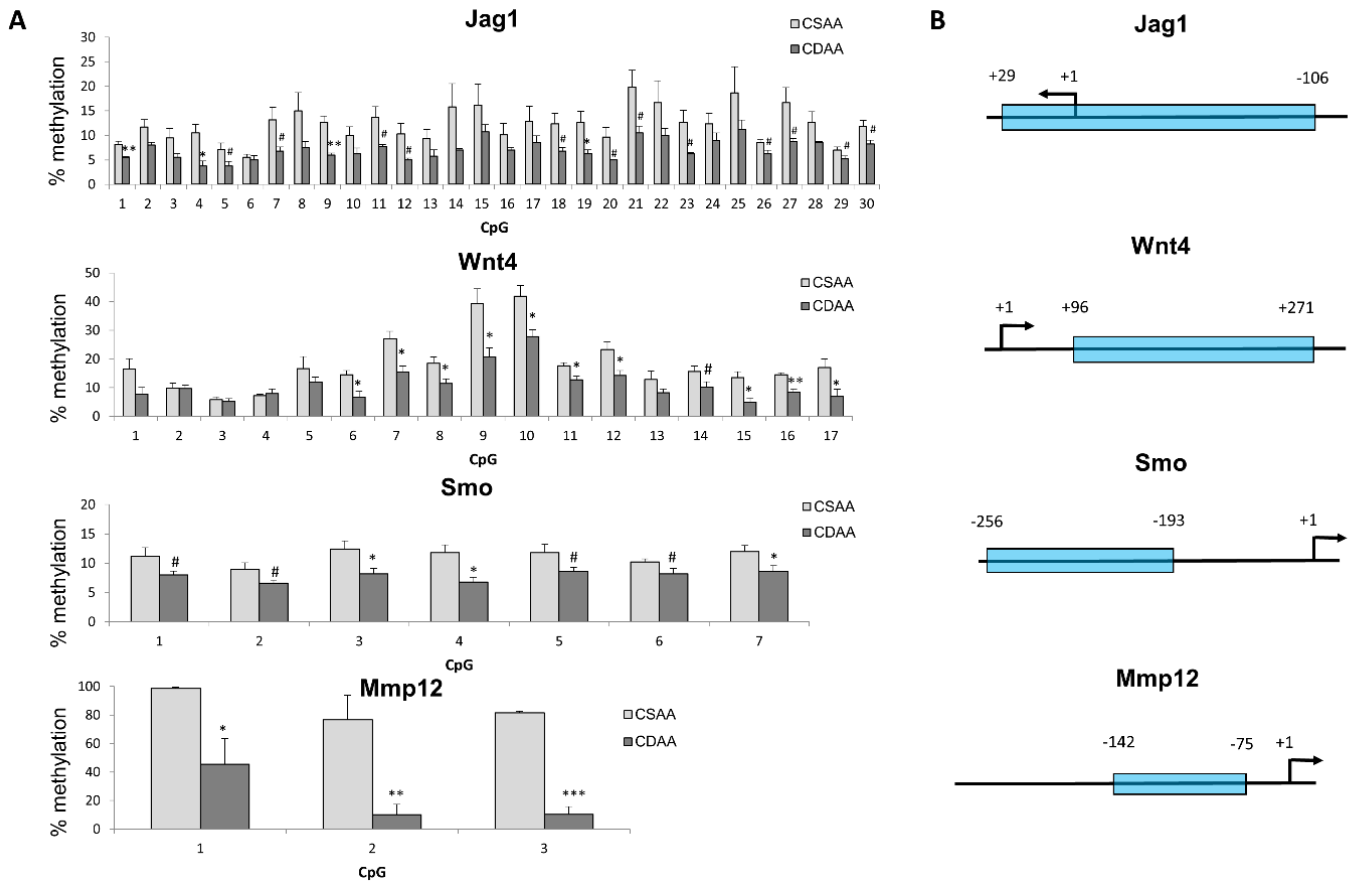


**Figure 4.10. DNA hypomethylation of promoter regions of candidate oncogenes evaluated by pyrosequencing.** (A) Hypomethylation of candidate oncogenes in CDAA livers compared to CSAA livers, as measured by pyrosequencing. (B) Maps of regions tested by pyrosequencing relative to transcription start site of respective gene. Numbers represent locations of first and last CpG sites relative to the TSS (+1) within the tested region. Data expressed as mean  $\pm$  SEM; n=6 rats per group. #  $P < 0.1$ , \* $P < 0.05$ , \*\* $P < 0.01$ , \*\*\* $P < 0.001$ .

#### **4.3.6 Supplementation of CDAA diet with pterostilbene leads to hypermethylation and reduced expression of *Mmp12* oncogene**

Based on our group's previous work aiming to understand anti-cancer mechanisms of dietary stilbenoids, an additional experimental group was analyzed which received the CDAA diet supplemented with PTS (CDAA+PTS) during the duration of the 52-week experiment. PTS has been shown to reactivate TSGs and silence oncogenes through modulating DNA methylation patterns at loci-specific sites in *in vitro* models of cancer (Beetch et al., 2019b; Lubecka et al., 2016). Therefore, we sought to discern the effect of PTS in our *in vivo* model of MDD-triggered liver carcinogenesis.

Average final body weight of the CDAA+PTS rats was similar to CDAA rats, both of which were significantly lower than body weight of the CSAA rats (**Figure 4.11A**). There was no difference in livers weights between groups but similar to CDAA rats, the CDAA+PTS rats had higher relative liver weights than CSAA rats (**Figure 4.11A**). Histopathological analysis revealed many hyperplastic nodules in the CDAA+PTS livers and fewer HCC nodules as compared with CDAA rats. In addition, smaller and less fat globules were present in the CDAA+PTS livers which would indicate potential attenuation or slowed development of HCC (**Figure 4.11B**).

Liver tissue from the CDAA+PTS rats was subjected to RNA sequencing. A comparison between CDAA and CDAA+PTS livers revealed a total of 708 genes that were significantly differentially expressed. Among 351 upregulated genes in response to PTS supplementation were *Bhmt* (4.5-fold), *G6pc* (3.1-fold), and *Aldh1l1* (2.6-fold). In earlier analyses of CSAA versus CDAA liver gene expression, these metabolism-related genes were shown to be significantly downregulated and implicated in MDD-associated HCC development. Therefore, reversal of the altered gene expression status could contribute to attenuation of HCC through modulation of metabolic processes. Among 357 genes found to be significantly downregulated in response to PTS were *Mmp12* (2-fold), *Myc* (1.9-fold) and *Mmp27* (1.8-fold). PTS reversed aberrant upregulation of these genes in livers upon MDD-driven HCC development.

Differentially expressed genes between CSAA and CDAA livers were then compared to differentially expressed genes between CDAA and CDAA+PTS livers. A total of 116 differentially expressed genes (2-fold or higher,  $P < 0.05$ ) from the CSAA/CDAA comparison were found to have a reversed expression pattern upon PTS supplementation (e.g., gene upregulated in CDAA compared to CSAA but downregulated upon PTS) (**Appendix E**). Many of these 116 genes were metabolism-related genes. We screened these 116 genes for our analyzed candidate oncogenes and discovered *Mmp12* to be a top upregulated gene in CDAA whose expression was decreased in response to PTS supplementation. We validated PTS-mediated expression changes using qPCR (**Figure 4.11C**) and analyzed the 3 CpG sites in the *Mmp12* promoter shown to be hypomethylated in CDAA livers. We found that DNA methylation status of 2 of 3 CpG sites was significantly increased by 43% upon PTS supplementation (**Figure 4.11D**), suggesting that PTS-mediated silencing of *Mmp12* may at least partially be controlled by DNA methylation.

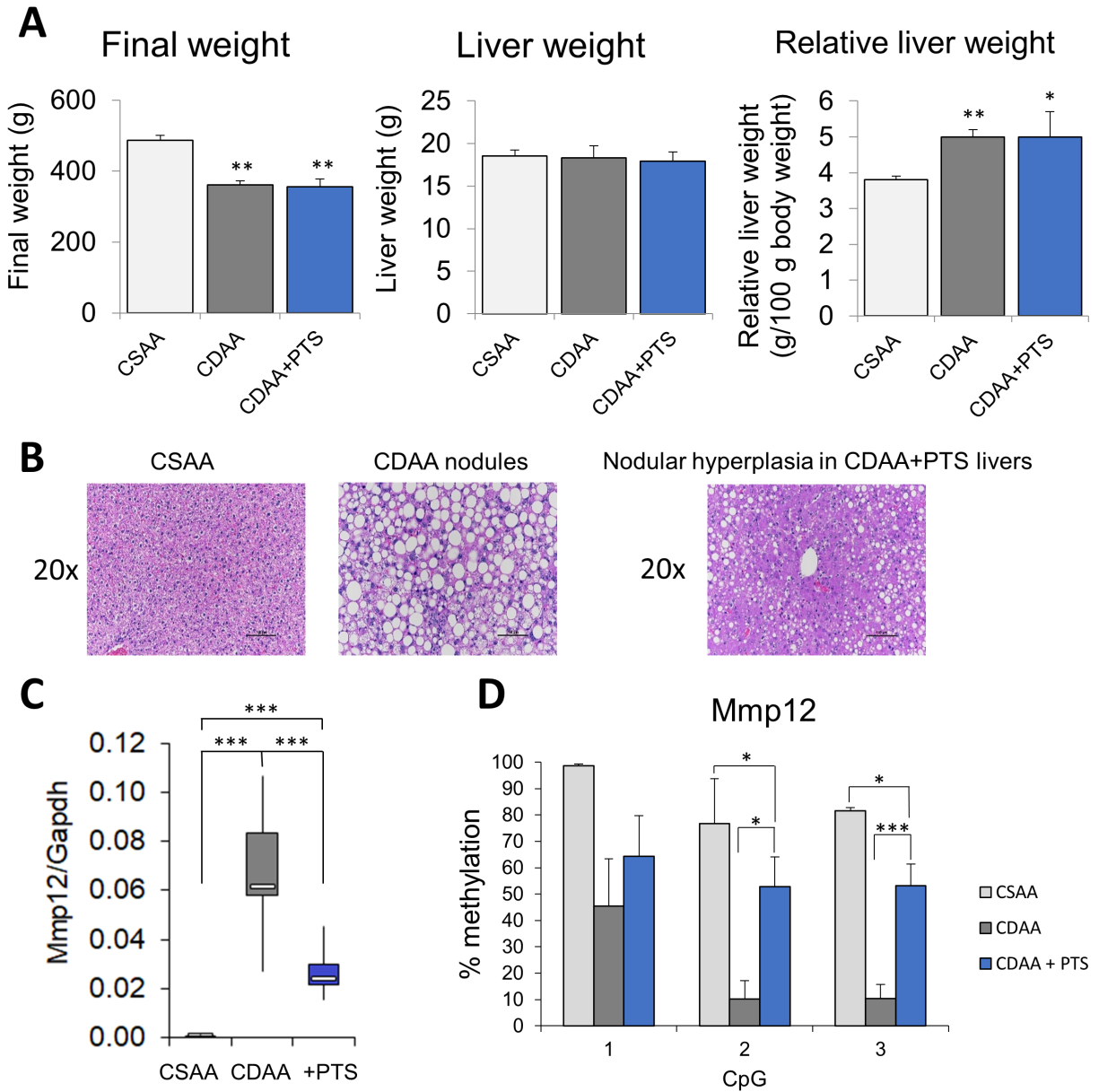


**Figure 4.11. Attenuation of HCC by PTS supplementation.** (A) Rat characteristics at 52-week time-point. (B) Representative image of hematoxylin and eosin staining depicting region of nodular hyperplasia in CDAA+PTS livers. (C) Mmp12 expression in CSAA, CDAA and CDAA+PTS livers (n=6 rats per group), as measured by qPCR. Results expressed as boxplots (min, IQR, max); n=6 rats per group. (D) Mmp12 methylation status in CSAA, CDAA and CDAA+PTS livers (n=6 per group), as measured by pyrosequencing. Data expressed as mean  $\pm$  SEM; n=6 rats per group; data were analyzed by one-way ANOVA followed by Tukey's post-hoc test. \* $P < 0.05$ , \*\* $P < 0.01$ , \*\*\* $P < 0.001$ .

#### 4.4 Discussion

Solid HCC nodules were detected in all CDAA rats compared to no nodule detection in livers of the healthy CSAA rats, reflecting the potency of MDD in development of HCC. Using RNA sequencing of CSAA and CDAA liver tissues, we observed impairment of lipid removal pathways and alterations in OCM in relation to HCC and have shed new light on the role of MDD in these perturbations. Genes previously found to be aberrantly expressed in HCC such as *Dmgdh* (Liu, Hou, Li, Li, Zhou & Liu, 2016) and *Aldh1l1* (Krupenko & Krupenko, 2019) were linked to MDD in this study. We also discovered several novel genes potentially related to MDD-driven HCC progression. *Pnpla5* is a gene that is related to *Pnpla3*. Loss of *Pnpla3* has previously been implicated in promoting lipid accumulation and contributing to liver disease (Trepo, Romeo, Zucman-Rossi & Nahon, 2016), whereas *Pnpla5* is simply known to be a lipid hydrolase with possible link to cardiovascular disease but no association with MDD or liver carcinogenesis. In addition, cytochrome P450 genes (*Cyp2c11* and *Cyp2c7*), glucose/mannose/fructose transporter *Slc5a9*, and a gene with a role in modulating energy metabolism *Aqp7* were some of the top differentially expressed genes (more than 20-fold) whose links to MDD-triggered HCC have never before been reported. Our finding of downregulation of methyltransferase genes such as *Mettl18* and *Nnmt* is also novel. The role of *Mettl18* has not yet been elucidated and contradictory findings for expression levels of *Nnmt* in HCC progression have surfaced (Kim et al., 2009; Li et al., 2019). We predicted that altered expression of these genes and others contribute to disturbances in OCM and subsequently DNA methylation reactions. For that reason, we delved further to address the consequences on DNA methylation machinery resulting from OCM dysregulation. Specifically, we assessed components of the DNA methylation machinery such as *Dnmt* and *Tet* expression, and SAM and SAH levels in healthy and HCC tissues. We next assessed the relationship between

altered DNA methylation machinery and observed differentially expressed genes in MDD-driven HCC carcinogenesis. We were particularly interested in upregulated genes based on the fact that there were double the amount of significantly upregulated genes compared to downregulated genes (1,236 up versus 612 down) and the magnitude of changes was substantially higher. Therefore, we analyzed DNA methylation patterns in regulatory regions of upregulated oncogenes in response to MDD. Following validation of upregulation of genes from several oncogenic pathways in the CDAA livers, we focused on upstream players from 4 pathways, namely Notch signaling, Wnt signaling, Hedgehog pathway, and Mmp. Significant DNA hypomethylation was detected in promoter regions of *Jag1*, *Wnt4*, *Smo*, and *Mmp12* in CDAA liver tissue compared to healthy CSAA livers. These findings support a mechanistic role of epigenetics in upregulation of cancer-promoting genes during HCC development upon MDD.

Furthermore, an additional group of CDAA rats were supplemented with PTS for the duration of the experimental timeline. RNA from liver tissues from those rats were sequenced and genes shown to be differentially expressed in CDAA versus CDAA+PTS livers were analyzed. We identified genes whose aberrant gene expression pattern was reversed upon PTS supplementation. Specifically, we found 116 differentially expressed genes whose expression pattern was reversed upon supplementation with PTS. One of those genes was *Mmp12*, an oncogene significantly upregulated in CDAA livers but downregulated in response to PTS. Several lines of evidence indicate that *Mmp12* expression is correlated with T-cell infiltration, tumor size, poor tumor cell differentiation, and poor prognosis (Gao et al., 2019a; He et al., 2018), thus, downregulation of this gene upon PTS supplementation may contribute to the anti-cancer effects of PTS. Most importantly, DNA methylation analysis by pyrosequencing provided evidence that PTS-mediated

increase in methylation within the *Mmp12* promoter may be at least partially responsible for decreased expression of this oncogene.

Several paths for further investigation stem from our findings. First, elucidation of the roles of novel candidates implicated in HCC development upon MDD is warranted. Novel candidates were found to be among the highest differentially expressed genes in this context, highlighting their potential involvement in MDD-driven carcinogenesis. Second, delving deeper into the contribution of each cell population comprising our analyzed liver lesions may uncover interesting findings and should be considered when interpreting our current findings. A detailed analysis of how cell populations might shift in response to MDD or supplementation with PTS could be pursued. Use of newly developed single cell technologies could provide more in-depth analysis of changes occurring in different cell populations that make up the HCC lesions. A third path for future studies may be to assess to what extent PTS plays in targeting lipid metabolism processes. Studies have shown that stilbenoid compounds, and PTS in particular, have dramatic effects on inhibiting lipogenic activity (Gomez-Zorita, Belles, Briot, Fernandez-Quintela, Portillo & Carpena, 2017). We found that of 116 genes with reversed expression in response to PTS, the majority of genes were related to metabolism. This suggests that PTS-mediated recovery of metabolic homeostasis may be at play during attenuation of MDD-triggered HCC development. Another aspect is whether modulation of lipid metabolism by PTS may indirectly impact DNA methylation of cancer-related genes. Interestingly, vitamin C and  $\alpha$ -ketoglutarate are related to Tet function, wherein they are required for catalytic activity of Tet demethylating enzymes (Yin et al., 2013). The changes seen in vitamin C-related functions and metabolic pathways in MDD-triggered HCC may explain, at least partially, dysregulation of Tet enzymes. Lastly, the concept of how PTS

may contribute to alleviating oxidative stress in MDD constitutes a thriving area of research. We found antioxidant-related genes (*Gstp1* and *Gpx2*) to be significantly upregulated in response to MDD. This finding falls in line with early papers that discuss oxidative injury in the CDAA model (Denda, Endoh, Tang, Tsujiuchi, Nakae & Konishi, 1998). Indeed, oxidative stress underlies many chronic diseases and its interrelatedness with DNA methylation is a topic of active investigation. PTS has been shown to have both antioxidant properties and DNA methylation-modifying properties (Beetch et al., 2019a). Therefore, the connection between those roles and the effects of PTS in combating disease should be thoroughly evaluated in future studies.

The present study sheds new light on MDD-triggered development of HCC with regard to metabolism-related alterations and novel gene candidates implicated in MDD-driven HCC carcinogenesis. Furthermore, aberrant DNA hypomethylation of oncogenes upon MDD-induced OCM and DNA methylation perturbations are explored. This work provides many new avenues for future research exploring mechanistic changes driving HCC pathogenesis.

## Chapter 5: Conclusions and Discussion

This thesis work provides evidence that supports the hypothesis that dietary stilbenoids modulate DNA methylation patterns and thereby gene transcription via modifying expression and activity of epigenetic enzymes such as DNMTs and transcriptional machinery such as TFs. In turn, reactivation of methylation-silenced TSGs and downregulation of epigenetically-activated oncogenes contribute, at least partially, to anti-cancer effects of stilbenoid compounds.

Chapters discussing *in vitro* studies highlight stilbenoid-mediated epigenetic reactivation of TSGs, with *SEMA3A* as an example, through a mechanism involving reduced DNMT3A and increased NF1C binding, whereas a mechanism implicating DNMT3B and OCT1 is shown to play a role in hypermethylation and silencing of oncogenes, such as *PRKCA*, in cancer cells exposed to stilbenoids. Genome-wide technologies facilitated the identification of candidate genes which were then elaborated upon using molecular techniques. These studies address in-depth epigenetic mechanisms underlying anti-cancer effects of stilbenoids that are lacking in the current literature. More specifically, there is adequate TSG-related research testing methylation status of candidates but mechanistic studies defining how TSGs become hypomethylated and reactivated in response to polyphenols are sparse. Research surrounding DNA methylation-modifying effects of polyphenols in relation to oncogenes is in its infancy. Therefore, the *in vitro* studies presented in this thesis assessing both sides of the bidirectional effect of stilbenoid compounds on DNA methylation patterns resolving mechanistic players involved in DNA hypomethylation and DNA hypermethylation events are novel. Importantly, these studies along with our earlier reports indicate that stilbenoid compounds exert their bidirectional effects on

DNA methylation in cancer cells without affecting normal cells which constitutes advantages over standard epigenetic therapies (Beetch, Lubecka, Kristofzski, Suderman & Stefanska, 2018; Beetch et al., 2019b; Lubecka et al., 2016). In addition, our work indicates that specific DNMTs regulate gene transcriptional activity depending on gene functions, with DNMT3A targeting TSGs and DNMT3B targeting oncogenes. It is evident from our studies that TFs may constitute important signals for such loci-specific recruitment of DNMTs. There are pieces of evidence suggesting that DNMT affinity to DNA sequences is regulated by covalent modifications of histone tails, which could be a result of cooperation between histone modifiers, chromatin-remodeling complexes, and possibly TFs (Gagliardi, Strazzullo & Matarazzo, 2018; Hervouet, Peixoto, Delage-Mourroux, Boyer-Guittaut & Cartron, 2018; Rinaldi et al., 2016). Indeed, OCT1 has been previously shown to recruit a co-factor called Jmjd1a, which demethylates H3K9, resulting in reduction of DNMT affinity to bind to DNA at given loci (Jafek et al., 2019). We speculate that different TFs co-localize with various histone modifying enzymes and thus regulate DNMT recruitment and subsequent transcriptional activity.

Upon proposing mechanistic players mediating methylation events in response to stilbenoids *in vitro*, we turned to an *in vivo* model of MDD to assess consequences of altering another important factor involved in regulation of DNA methylation reactions, namely the abundance of ubiquitous methyl donor SAM. Availability of SAM for use in methylation reactions throughout the body is an integral element of homeostasis in the DNA methylation machinery. We used RNA sequencing to understand foundational changes in gene expression patterns in MDD-driven liver carcinogenesis. Profound disruptions in several metabolic pathways including lipid removal from the liver and OCM were observed and explored. Indeed, reprogramming of energy

metabolism is a hallmark of cancer (Hanahan & Weinberg, 2011), making cancer a largely metabolic disorder. The complexity of energy metabolism and interrelatedness with other cancer hallmarks makes studying metabolism-associated changes important. Several differentially expressed genes in our dataset related to metabolism were not previously reported to be associated with MDD but were implicated in HCC, whereas some novel candidates were not previously shown to be involved in either MDD or liver-related diseases. Our findings support a recent hypothesis that metabolic changes occurring in cancer may be central to the disease (Coller, 2014). Interestingly, the epigenetic machinery responds to changes in cellular metabolism and certain metabolites are substrates for epigenetic enzymes that modify DNA, RNA, and histone tails (Sharma & Rando, 2017). For example, SAM, a direct metabolite of the essential amino acid methionine, is vital for the DNA methylation reaction acting as a methyl donor for DNMTs (Sharma & Rando, 2017). Furthermore, TET enzymes require alpha-ketoglutarate and ferrous iron along with vitamin C for their optimal activity in DNA demethylation reactions (Sharma & Rando, 2017; Yin et al., 2013).

OCM disturbances corresponded with dysregulated DNA methylation enzymes and altered DNA methylation status. Although, previous studies have reported DNA methylation alterations during MDD, they are limited to global DNA methylation and only few candidate genes. We are the first group to investigate genome-wide changes in gene expression upon MDD and consequences of these changes for cell functioning. Our detailed analysis unravels numerous genes along with novel candidates, such as *Pnpla5*, *Slc5a9*, *Nnmt*, *Mettl18*, and *Lamc2* that may be mechanistically involved in MDD-driven carcinogenesis. In addition, PTS supplementation led to attenuation of the cancer phenotype and reversal of aberrations in DNA methylation and

expression patterns of oncogenes potentially contributing to the anti-cancer action of this stilbenoid compound. In this context, utilization of PTS as a chemopreventive compound as opposed to a therapeutic was evaluated. Our MDD-driven HCC study and others support polyphenols as agents for cancer prevention. Stilbenoid compounds have been found to exert subtle effects on the DNA methylome of normal cells, with some changes within cancer-related genes that may aid in maintaining a healthy phenotype prior to cancer formation (Beetch, Lubecka, Kristofzski, Suderman & Stefanska, 2018). In addition, epigenetic alterations underlie early stages of cancer progression, thus stilbenoid exposure during initiation at sub-clinical stages of the disease may constitute an effective stage for targeting these changes. Moreover, polyphenols in support of anti-cancer therapy comprises another exciting application of these compounds. Upon establishing effective combinations of natural compounds and chemotherapy drugs, multiple levels within signaling pathways can be targeted by agents with different mechanistic targets. For example, use of stilbenoids in overcoming resistance to NOTCH oncogenic signaling inhibitors through targeting various points in the pathway holds promise. Currently, most developed NOTCH inhibitors are small molecule gamma secretase inhibitors (GSIs), which prevent cleavage and release of the NOTCH intracellular domain (NICD) from the plasma membrane so NICD cannot translocate into the nucleus to activate target genes. Combining existing Notch-targeted chemotherapies, such as GSIs, with stilbenoid compounds that have been shown to target other points in the NOTCH pathway, namely the transcriptional co-activator complex (Lubecka et al., 2016), has potential to alleviate side effects of wide-spectrum drugs and reduce resistance and cancer recurrence by requiring lower doses of chemotherapeutics to induce desired anti-cancer action. We speculate that in already-developed tumors, fast action with single-target drugs is needed to hinder cancer cell proliferation and

metastasis. Multi-target, often subtle, effects of stilbenoids could be insufficient to produce immediate anti-cancer effects. Thus, stilbenoid compounds would be most beneficial when used in cancer prevention and in support of anti-cancer therapy.

Many avenues for future research directions stem from these projects. The genome-wide analyses that were conducted provide a wealth of information regarding changes in DNA methylation at specific CpG sites in response to stilbenoids (Illumina DNA methylation microarray data), binding events of DNMT3B and OCT1 upon stilbenoid treatment (ChIP sequencing data), and gene expression changes during MDD-induced HCC and attenuation by stilbenoid supplementation (RNA sequencing data). Future projects could assess the temporal sequence of DNMT3B and OCT1 binding as proposed in Chapter 3 to understand how recruitment of these enzymes is modulated. In addition, future studies can investigate the involvement of histone marks or other epigenetic modifications in this process. Attenuation of MDD-triggered carcinogenesis by PTS is another path with many opportunities for future work to better understand epigenetic mechanisms of anti-cancer effects of dietary stilbenoids. For example, the relationship between the antioxidant role of stilbenoids and their DNA methylation-modifying role has been suggested but not yet fully elucidated (Beetch et al., 2019a). To date, a role for stilbenoids in activation of NRF2, master regulator of the antioxidant response, through DNA hypomethylation has been proposed (Singh et al., 2014). Genes altered in response to PTS supplementation in our MDD model constitute metabolism- and antioxidant-related genes. Further studies investigating the link between DNA methylation and antioxidant functions of stilbenoids, possibly through NRF2, could provide additional information on indirect effects of PTS.

There are several strengths of the *in vitro* and *in vivo* models used in these studies. The *in vitro* model of breast cancer is isogenic, meaning that these cell lines were engineered from the parental MCF10A breast cell line through transfection of the Harvey-*ras* oncogene. Transfected cells were then xenograft into mice and MCF10CA1h cell were isolated from highly differentiated tumors (non-invasive), whereas MCF10CA1a were isolated from poorly differentiated tumors (invasive) (Santner et al., 2001). Isogenic cell lines constitute an excellent model for investigating epigenetic changes occurring during progression of carcinogenesis, eliminating bias associated with differences in the genome. Additionally, we studied effects of prolonged exposure (9-day stilbenoid treatment) to mimic chronic exposure in humans. This is a strength because most studies assess exposures of only 48-72 hours, which reflect acute exposure. The DNMT3B KO model will continue to aid in our understanding of PTS-mediated hypermethylation with testing of other oncogenes. Future studies using the DNMT3B KO cells could address the proposed compensatory mechanism(s) occurring in response to knockout of *DNMT3B*. Additional ways to study DNMT3B-related mechanisms need to also be pursued that may incorporate bioactive compounds affecting DNMT3B binding in order to investigate regulation of DNMT3B activity and recruitment to specific DNA loci in cancer cells.

Utilization of the CDAA diet to model MDD is well-established. The CDAA diet has advantages over choline deficient (CD) and other models of MDD. In an early study comparing the CDAA diet with the CD diet, results showed that the CDAA diet conferred much more potent carcinogenicity after 52 weeks compared to the CD diet that does not take into account defined amino acid composition. In addition, the study indicated that 24 weeks on the CDAA diet is not be sufficient to induce fully developed HCC tumors (Nakae et al., 1992). Therefore, our use of

the CDAA diet to trigger MDD-induced HCC was warranted and performed for 52 weeks. A weakness of our CDAA study, however, is the number of time-points from which we collected liver tissue. Liver tissue from just one time-point is limiting for studying progression of MDD-triggered HCC and for studying preventive role of stilbenoids. Our study was meant to be more of a pilot study in nature. Therefore, future studies should ideally assess various time-points to gauge changes during progression and not just endpoint with potent HCC. Additionally, multiple time-points or shortening the experimental timeline could potentially capture the stage at which PTS supplementation may be safeguarding progression from hyperplastic nodules to formation of HCC. Nonetheless, many opportunities for exploring different pathways of gene misregulation in MDD-triggered HCC development are available from our existing RNA sequencing data of the CSAA and CDAA livers, as well as stilbenoid supplementation. For example, interesting questions that arise from our findings include: what indirect routes may PTS be affecting in relation to DNA methylation patterns or how hypermethylation is occurring in response to PTS despite the choline and SAM depleted environment.

Another strength of the research is the use of physiologically relevant doses of RSV (15  $\mu\text{M}$ ) and PTS (7  $\mu\text{M}$ ) in our *in vitro* studies. In humans, high absorption rates of RSV upon oral or intravenous administration, ranging from 50-85%, have been reported (Walle, 2011). A dose-escalation study administering single doses of 0.5, 1, 2.5, or 5 g RSV to healthy volunteers found that peak plasma concentration reached a maximum of 2.4  $\mu\text{M}$  in response to the highest dose level. RSV glucuronide and sulfate conjugates reached peak plasma concentrations as high as 14  $\mu\text{M}$  (Boocock et al., 2007). Because glucuronidation and sulfation facilitate clearance of stilbenoids from the body, future studies should investigate whether or not high concentrations of

these metabolites are beneficial. Interestingly, parent RSV was observed in resected colorectal cancer tissues following 8-day administration of RSV at higher levels than in the plasma (Patel et al., 2010). Pharmacokinetic studies of PTS in humans is lacking. Studies in mice and rats report higher plasma levels of PTS and PTS metabolites compared to RSV and RSV metabolites when given at equimolar doses (Kapetanovic, Muzzio, Huang, Thompson & McCormick, 2011). These findings indicate that the doses of RSV and PTS used in our preclinical studies are within the same orders of magnitude as physiologically attainable levels. More recently, attempts to encapsulate RSV and PTS to increase the time they remain in the bloodstream thus potentially reach target organs have been promising (Liu, Chen, Qin, Jiang & Zhang, 2019; Penalva et al., 2018).

The dose of PTS used in our *in vivo* study (134 mg/kg BW/day) of MDD-driven HCC is within range of doses of stilbenoids which were shown to be effective in attenuating cancer in previous studies in animal models, including liver cancer (Bishayee, Barnes, Bhatia, Darvesh & Carroll, 2010; Chen et al., 2012b; Luther et al., 2011; Paul et al., 2010). Studies performed in colon and lung cancers required 50-250 mg/kg BW/day of PTS to see profound reduction in tumor growth (Chen et al., 2012b; Paul et al., 2010). RSV at doses of 100-300 mg/kg BW/day was effective in reducing number and size of liver cancer nodules in rats (Bishayee, Politis & Darvesh, 2010; Luther et al., 2011). As for toxicity, administration of PTS at doses of 30, 300, 3000 mg/kg BW/day into mice for 28 days did not produce any toxic effects (Ruiz et al., 2009). In terms of translating *in vivo* doses into consumption in humans, 20 mg of PTS or RSV represents around 1000 or 100 times, respectively, the maximum amount of PTS or RSV found in 1 kg of dark-skinned grapes (Baur & Sinclair, 2006; Rimando, Cuendet, Desmarchelier, Mehta, Pezzuto &

Duke, 2002). Thus, the doses we used would have to be achieved from supplements rather than the diet. However, we cannot exclude the possibility that molecular changes we detected in rat livers can be triggered in humans upon years of consumption of diet-achievable doses of polyphenols.

Collectively, these findings provide evidence that dietary stilbenoids may exert their anti-cancer effects at least partially by impacting DNA methylation machinery, and as a result, this line of evidence has potential to be used in chemopreventive approaches and in support of existing anti-cancer strategies. As stilbenoids remodel and modulate many pathways and processes rather than have one directed effect, using them as drugs could be problematic. If cancer has already developed, fast action with distinct chemotherapeutic drugs should be taken. However, we can combine polyphenols with drugs to achieve better effect, overcome resistance, or potentially cut down on side effects of high doses of chemotherapeutic drugs. Accordingly, randomized clinical trials are needed before routine implementation of stilbenoid compounds in chemoprevention or support of anti-cancer therapy. Ideally, natural compounds should be administered at effective doses without off-target effects, but should modulate multiple pathways for optimal anti-cancer outcome. Progression from pre-clinical studies to clinical trials in humans has been insufficient due to several factors, including bioavailability, appropriate dosage, delivery of compounds, and conditions of participants (Carter, D'Orazio & Pearson, 2014). Future trials must consider variation in humans for metabolizing stilbenoid compounds including sex differences (Dellinger, Garcia & Meyskens, 2014) and the composition of the gut microbiota metabolizing stilbenoids. Along those same lines, the role of metabolites in biological effects elicited by stilbenoids is a largely understudied area. The field's current understanding is that 90% of the ingested

polyphenol pool becomes substrates for bacteria to convert to metabolites in the colon (Moco, Martin & Rezzi, 2012). Microbial metabolites then undergo fecal excretion or are absorbed via enterohepatic circulation into the liver where they are subjected to phase II metabolism before entering systemic circulation for distribution or excretion in urine. Microbial metabolites of polyphenols are believed to interact with the host epigenome by altering the pool of compounds used for epigenetic modifications or by directly inhibiting epigenetic machinery (Hullar & Fu, 2014; Qin & Wade, 2018). Specific molecular mechanisms by which microbial metabolites impact the host epigenome remain to be elucidated. Lastly, challenges in appropriately dosing individuals based on if they are healthy, high-risk, early-stage or late-stage, or receiving chemotherapies will certainly arise. Studies assessing pre-treatment versus co-treatment with stilbenoids will be important in determining the efficacy of RSV and PTS in the clinical setting. Pre-treatment with stilbenoids could induce changes in transcriptional activity of genes vital to the efficacy of a given chemotherapy agent prior to administration, possibly increasing initial sensitivity to the drug. On the other hand, co-treatment could be beneficial in maintaining a desired transcriptional state throughout drug treatment.

The limited human clinical trials that have come to fruition have strongly supported our speculation that stilbenoids may be more effective as chemopreventive agents as opposed to treating existing cancer (Nguyen et al., 2009; Zhu et al., 2012). For example, a phase 1 pilot study comparing effects of RSV or grape powder (GP) on the Wnt signaling pathway in normal colon mucosa versus colon cancer tissue found that RSV did not inhibit the Wnt pathway in colon cancer but did significantly inhibit Wnt activity in the normal colon mucosa. Expression of Wnt target genes was determined by gene microarray and validated by qPCR (Nguyen et al.,

2009). Zhu and colleagues conducted a randomized controlled trial assessing twice daily RSV administration (5 g or 50 g) for 12 weeks to pre-menopausal adult women with increased risk for breast cancer (Zhu et al., 2012). Increased risk for breast cancer was defined as having a first degree relative with breast cancer or having a personal history of atypical hyperplasia, ductal carcinoma *in situ*, or invasive breast cancer (currently free of disease). Detectable levels of free RSV and metabolites in serum increased over the study period and correlated with low versus high dosing. In mammary specimens collected at 12 weeks, DNA methylation levels of *RASSF1A*, an established TSG in breast cancer, showed a trend toward decreased methylation. The study concluded that in this population of women at high risk for breast cancer, administration of RSV may provide a chemopreventive effect through changes in DNA methylation (Zhu et al., 2012).

Despite the higher bioavailability of PTS compared to RSV, studies investigating PTS in relation to epigenetic mechanisms contributing to anti-cancer effects are severely lacking in the current literature. The findings from this thesis work will provide 3 additional pieces of evidence, each highlighting involvement of specific mechanistic players, pertaining to PTS-mediated mechanisms in this context, essentially doubling the amount of available studies on this topic. Encouragingly, in the last 5 years a larger portion of new research discussing anti-cancer effects of stilbenoids is also being dedicated to PTS. Overall, understanding epigenetic mechanisms of anti-cancer effects of these dietary bioactive compounds constitutes a promising strategy for chemoprevention and support of anti-cancer therapies.

## References

Adjakly M, Bosviel R, Rabiau N, Boiteux JP, Bignon YJ, Guy L, *et al.* (2011). DNA methylation and soy phytoestrogens: quantitative study in DU-145 and PC-3 human prostate cancer cell lines. *Epigenomics* 3: 795-803.

Almeida TC, Guerra CCC, De Assis BLG, de Oliveira Aguiar Soares RD, Garcia CCM, Lima AA, *et al.* (2019). Antiproliferative and toxicogenomic effects of resveratrol in bladder cancer cells with different TP53 status. *Environmental and molecular mutagenesis* 60: 740-751.

Andersen GB, & Tost J (2018). A Summary of the Biological Processes, Disease-Associated Changes, and Clinical Applications of DNA Methylation. *Methods in molecular biology* (Clifton, NJ) 1708: 3-30.

Andrews S (2010). FastQC: a quality control tool for high throughput sequence data.

Assender JW, Gee JM, Lewis I, Ellis IO, Robertson JF, & Nicholson RI (2007). Protein kinase C isoform expression as a predictor of disease outcome on endocrine therapy in breast cancer. *Journal of clinical pathology* 60: 1216-1221.

Baur JA, & Sinclair DA (2006). Therapeutic potential of resveratrol: the in vivo evidence. *Nature reviews drug discovery* 5: 493-506.

Baylin SB, & Jones PA (2011). A decade of exploring the cancer epigenome - biological and translational implications. *Nature reviews cancer* 11: 726-734.

Baylin SB, & Jones PA (2016). Epigenetic Determinants of Cancer. *Cold Spring Harbor perspectives in biology* 8: a019505.

Beetch M, Harandi-Zadeh S, Shen K, Lubecka K, Kitts DD, O'Hagan HM, *et al.* (2019a). Dietary antioxidants remodel DNA methylation patterns in chronic disease. *British journal of pharmacology* 177: 1382-1408.

Beetch M, Lubecka K, Kristofzski H, Suderman M, & Stefanska B (2018). Subtle Alterations in DNA Methylation Patterns in Normal Cells in Response to Dietary Stilbenoids. *Molecular nutrition & food research*: e1800193.

Beetch M, Lubecka K, Shen K, Flower K, Harandi-Zadeh S, Suderman M, *et al.* (2019b). Stilbenoid-Mediated Epigenetic Activation of Semaphorin 3A in Breast Cancer Cells Involves Changes in Dynamic Interactions of DNA with DNMT3A and NF1C Transcription Factor. *Molecular nutrition & food research*: e1801386.

Berkyurek AC, Suetake I, Arita K, Takeshita K, Nakagawa A, Shirakawa M, *et al.* (2014). The DNA methyltransferase Dnmt1 directly interacts with the SET and RING finger-associated (SRA) domain of the multifunctional protein Uhrf1 to facilitate accession of the catalytic center to hemi-methylated DNA. *The journal of biological chemistry* 289: 379-386.

Bhattacharyya S, Pradhan K, Campbell N, Mazdo J, Vasantkumar A, Maqbool S, *et al.* (2017). Altered hydroxymethylation is seen at regulatory regions in pancreatic cancer and regulates oncogenic pathways. *Genome research* 27: 1830-1842.

Bishayee A, Barnes KF, Bhatia D, Darvesh AS, & Carroll RT (2010). Resveratrol suppresses oxidative stress and inflammatory response in diethylnitrosamine-initiated rat hepatocarcinogenesis. *Cancer prevention research (Philadelphia, Pa)* 3: 753-763.

Bishayee A, Politis T, & Darvesh AS (2010). Resveratrol in the chemoprevention and treatment of hepatocellular carcinoma. *Cancer treat rev* 36: 43-53.

Bode LM, Bunzel D, Huch M, Cho GS, Ruhland D, Bunzel M, *et al.* (2013). In vivo and in vitro metabolism of trans-resveratrol by human gut microbiota. *The American journal of clinical nutrition* 97: 295-309.

Boocock DJ, Faust GE, Patel KR, Schinas AM, Brown VA, Ducharme MP, *et al.* (2007). Phase I dose escalation pharmacokinetic study in healthy volunteers of resveratrol, a potential cancer chemopreventive agent. *Cancer epidemiology, biomarkers & prevention : a publication of the American Association for Cancer Research, cosponsored by the American Society of Preventive Oncology* 16: 1246-1252.

Brill SS, Furimsky AM, Ho MN, Furniss MJ, Li Y, Green AG, *et al.* (2006). Glucuronidation of trans-resveratrol by human liver and intestinal microsomes and UGT isoforms. *The journal of pharmacy and pharmacology* 58: 469-479.

Brown SE, Suderman MJ, Hallett M, & Szyf M (2008). DNA demethylation induced by the methyl-CpG-binding domain protein MBD3. *Gene* 420: 99-106.

Buchman AL, Ament ME, Soheli M, Dubin M, Jenden DJ, Roch M, *et al.* (2001). Choline deficiency causes reversible hepatic abnormalities in patients receiving parenteral nutrition: proof of a human choline requirement: a placebo-controlled trial. *JPEN Journal of parenteral and enteral nutrition* 25: 260-268.

Carter LG, D'Orazio JA, & Pearson KJ (2014). Resveratrol and cancer: focus on in vivo evidence. *Endocrine-related cancer* 21: R209-225.

Cedar H, & Bergman Y (2009). Linking DNA methylation and histone modification: patterns and paradigms. *Nature reviews genetics* 10: 295-304.

- Cheishvili D, Boureau L, & Szyf M (2015). DNA demethylation and invasive cancer: implications for therapeutics. *British journal of pharmacology* 172: 2705-2715.
- Chen D, Sun Y, Wei Y, Zhang P, Rezaeian AH, Teruya-Feldstein J, *et al.* (2012a). LIFR is a breast cancer metastasis suppressor upstream of the Hippo-YAP pathway and a prognostic marker. *Nature medicine* 18: 1511-1517.
- Chen M, Zhu N, Liu X, Laurent B, Tang Z, Eng R, *et al.* (2015). JMJD1C is required for the survival of acute myeloid leukemia by functioning as a coactivator for key transcription factors. *Genes & development* 29: 2123-2139.
- Chen RJ, Tsai SJ, Ho CT, Pan MH, Ho YS, Wu CH, *et al.* (2012b). Chemopreventive effects of pterostilbene on urethane-induced lung carcinogenesis in mice via the inhibition of EGFR-mediated pathways and the induction of apoptosis and autophagy. *Journal of agricultural and food chemistry* 60: 11533-11541.
- Chen T, & Li E (2004). Structure and function of eukaryotic DNA methyltransferases. *Current topics in developmental biology* 60: 55-89.
- Chen X, Li W, Xu C, Wang J, Zhu B, Huang Q, *et al.* (2018). Comparative profiling of analog targets: a case study on resveratrol for mouse melanoma metastasis suppression. *Theranostics* 8: 3504-3516.
- Chuang LS, Ian HI, Koh TW, Ng HH, Xu G, & Li BF (1997). Human DNA-(cytosine-5) methyltransferase-PCNA complex as a target for p21WAF1. *Science (New York, NY)* 277: 1996-2000.
- Chung S, Yao H, Caito S, Huang J, Arunachalam G, & Rahman I (2010). Regulation of SIRT1 in cellular functions: role of polyphenols. *Archives of biochemistry and biophysics* 501: 79-90.
- Colella S, Shen L, Baggerly KA, Issa JP, & Krahe R (2003). Sensitive and quantitative universal Pyrosequencing methylation analysis of CpG sites. *BioTechniques* 35: 146-150.
- Coller HA (2014). Is cancer a metabolic disease? *The American journal of pathology* 184: 4-17.
- Dai Y, Wang M, Wu H, Xiao M, Liu H, & Zhang D (2017). Loss of FOXN3 in colon cancer activates beta-catenin/TCF signaling and promotes the growth and migration of cancer cells. *Oncotarget* 8: 9783-9793.
- Das S, Foley N, Bryan K, Watters KM, Bray I, Murphy DM, *et al.* (2010). MicroRNA mediates DNA demethylation events triggered by retinoic acid during neuroblastoma cell differentiation. *Cancer research* 70: 7874-7881.

de Larco JE, & Todaro GJ (1978). Growth factors from murine sarcoma virus-transformed cells. *Proceedings of the National Academy of Sciences of the United States of America* 75: 4001-4005.

Debrececi B, & Debrececi L (2014). The role of homocysteine-lowering B-vitamins in the primary prevention of cardiovascular disease. *Cardiovascular therapeutics* 32: 130-138.

Dellinger RW, Garcia AM, & Meyskens FL, Jr. (2014). Differences in the glucuronidation of resveratrol and pterostilbene: altered enzyme specificity and potential gender differences. *Drug metab pharmacokinet* 29: 112-119.

Denda A, Endoh T, Tang Q, Tsujiuchi T, Nakae D, & Konishi Y (1998). Prevention by inhibitors of arachidonic acid cascade of liver carcinogenesis, cirrhosis and oxidative DNA damage caused by a choline-deficient, L-amino acid-defined diet in rats. *Mutation research* 402: 279-288.

Ding JJ, Wang G, Shi WX, Zhou HH, & Zhao EF (2016). Promoter Hypermethylation of FANCF and Susceptibility and Prognosis of Epithelial Ovarian Cancer. *Reproductive sciences (Thousand Oaks, Calif)* 23: 24-30.

Domcke S, Bardet AF, Adrian Ginno P, Hartl D, Burger L, & Schubeler D (2015). Competition between DNA methylation and transcription factors determines binding of NRF1. *Nature* 528: 575-579.

Ernst J & Kellis M (2012). ChromHMM: automating chromatin-state discovery and characterization. *Nature methods* 28: 215-216.

Escudero-Esparza A, Bartoschek M, Gialeli C, Okroj M, Owen S, Jirstrom K, *et al.* (2016). Complement inhibitor CSMD1 acts as tumor suppressor in human breast cancer. *Oncotarget* 7: 76920-76933.

Esteller M (2008). Epigenetics in cancer. *The New England journal of medicine* 358: 1148-1159.

Fan QW, Cheng C, Knight ZA, Haas-Kogan D, Stokoe D, James CD, *et al.* (2009). EGFR signals to mTOR through PKC and independently of Akt in glioma. *Science signaling* 2: ra4.

Fane M, Harris L, Smith AG, & Piper M (2017). Nuclear factor one transcription factors as epigenetic regulators in cancer. *International journal of cancer journal international du cancer* 140: 2634-2641.

Fang MZ, Chen D, Sun Y, Jin Z, Christman JK, & Yang CS (2005). Reversal of hypermethylation and reactivation of p16INK4a, RARbeta, and MGMT genes by genistein and other isoflavones from soy. *Clinical cancer research : an official journal of the American Association for Cancer Research* 11: 7033-7041.

Fang MZ, Wang Y, Ai N, Hou Z, Sun Y, Lu H, *et al.* (2003). Tea polyphenol (-)-epigallocatechin-3-gallate inhibits DNA methyltransferase and reactivates methylation-silenced genes in cancer cell lines. *Cancer research* 63: 7563-7570.

Feinberg AP, & Vogelstein B (1983). Hypomethylation distinguishes genes of some human cancers from their normal counterparts. *Nature* 301: 89-92.

Fu Q, Song X, Liu Z, Deng X, Luo R, Ge C, *et al.* (2017). miRomics and Proteomics Reveal a miR-296-3p/PRKCA/FAK/Ras/c-Myc Feedback Loop Modulated by HDGF/DDX5/beta-catenin Complex in Lung Adenocarcinoma. *Clinical cancer research : an official journal of the American Association for Cancer Research* 23: 6336-6350.

Fudhaili A, Yoon NA, Kang S, Ryu J, Jeong JY, Lee DH, *et al.* (2019). Resveratrol epigenetically regulates the expression of zinc finger protein 36 in nonsmall cell lung cancer cell lines. *Oncology reports* 41: 1377-1386.

Gabay M, Li Y, & Felsher DW (2014). MYC activation is a hallmark of cancer initiation and maintenance. *Cold Spring Harbor perspectives in medicine* 4.

Gagliardi M, Strazzullo M, & Matarazzo MR (2018). DNMT3B Functions: Novel Insights From Human Disease. *Frontiers in cell and developmental biology* 6: 140.

Gao H, Zhou X, Li H, Liu F, Zhu H, Song X, *et al.* (2019a). Role of Matrix Metalloproteinase 12 in the Development of Hepatocellular Carcinoma. *Journal of investigative surgery : the official journal of the Academy of Surgical Research*: 1-7.

Gao P, Lin S, Cai M, Zhu Y, Song Y, Sui Y, *et al.* (2019b). 5-Hydroxymethylcytosine profiling from genomic and cell-free DNA for colorectal cancers patients. *Journal of cellular and molecular medicine* 23: 3530-3537.

Gao Q, Yuan Y, Gan HZ, & Peng Q (2015). Resveratrol inhibits the hedgehog signaling pathway and epithelial-mesenchymal transition and suppresses gastric cancer invasion and metastasis. *Oncology letters* 9: 2381-2387.

Gao Y, & Tollefsbol TO (2018). Combinational Proanthocyanidins and Resveratrol Synergistically Inhibit Human Breast Cancer Cells and Impact Epigenetic(-)Mediating Machinery. *International journal of molecular sciences* 19: E2204.

Gendrel AV, & Heard E (2014). Noncoding RNAs and epigenetic mechanisms during X-chromosome inactivation. *Annual review of cell and developmental biology* 30: 561-580.

Gomez-Zorita S, Belles C, Briot A, Fernandez-Quintela A, Portillo MP, & Carpena C (2017). Pterostilbene Inhibits Lipogenic Activity similar to Resveratrol or Caffeine but Differently Modulates Lipolysis in Adipocytes. *Phytotherapy research : PTR* 31: 1273-1282.

- Gracia A, Elcoroaristizabal X, Fernandez-Quintela A, Miranda J, Bediaga NG, M MdP, *et al.* (2014). Fatty acid synthase methylation levels in adipose tissue: effects of an obesogenic diet and phenol compounds. *Genes & nutrition* 9: 411.
- Gravina GL, Ranieri G, Muzi P, Marampon F, Mancini A, Di Pasquale B, *et al.* (2013). Increased levels of DNA methyltransferases are associated with the tumorigenic capacity of prostate cancer cells. *Oncology reports* 29: 1189-1195.
- Greenberg MVC, & Bourc'his D (2019). The diverse roles of DNA methylation in mammalian development and disease. *Nature reviews molecular cell biology* 20: 590-607.
- Gruenbaum Y, Stein R, Cedar H, & Razin A (1981). Methylation of CpG sequences in eukaryotic DNA. *FEBS letters* 124: 67-71.
- Guo L, Tan K, Wang H, & Zhang X (2016). Pterostilbene inhibits hepatocellular carcinoma through p53/SOD2/ROS-mediated mitochondrial apoptosis. *Oncology reports* 36: 3233-3240.
- Guo M, Alumkal J, Drachova T, Gao D, Marina SS, Jen J, *et al.* (2015). CHFR methylation strongly correlates with methylation of DNA damage repair and apoptotic pathway genes in non-small cell lung cancer. *Discovery medicine* 19: 151-158.
- Han W, Shi M, & Spivack SD (2013). Site-specific methylated reporter constructs for functional analysis of DNA methylation. *Epigenetics* 8: 1176-1187.
- Hanahan D, & Weinberg RA (2011). Hallmarks of cancer: the next generation. *Cell* 144: 646-674.
- Haney SL, Upchurch GM, Opavska J, Klinkebiel D, Hlady RA, Roy S, *et al.* (2016). Dnmt3a Is a Haploinsufficient Tumor Suppressor in CD8+ Peripheral T Cell Lymphoma. *PLoS genetics* 12: e1006334.
- He MK, Le Y, Zhang YF, Ouyang HY, Jian PE, Yu ZS, *et al.* (2018). Matrix metalloproteinase 12 expression is associated with tumor FOXP3(+) regulatory T cell infiltration and poor prognosis in hepatocellular carcinoma. *Oncology letters* 16: 475-482.
- Herman JG, & Meadows GG (2007). Increased class 3 semaphorin expression modulates the invasive and adhesive properties of prostate cancer cells. *International journal of oncology* 30: 1231-1238.
- Hervouet E, Peixoto P, Delage-Mourroux R, Boyer-Guittaut M, & Cartron PF (2018). Specific or not specific recruitment of DNMTs for DNA methylation, an epigenetic dilemma. *Clinical epigenetics* 10: 17.
- Hintze KJ, Benninghoff AD, Cho CE, & Ward RE (2018). Modeling the Western Diet for Preclinical Investigations. *Advances in nutrition (Bethesda, Md)* 9: 263-271.

Huang Y, Khor TO, Shu L, Saw CL, Wu TY, Suh N, *et al.* (2012). A gamma-tocopherol-rich mixture of tocopherols maintains Nrf2 expression in prostate tumors of TRAMP mice via epigenetic inhibition of CpG methylation. *The journal of nutrition* 142: 818-823.

Hullar MA, & Fu BC (2014). Diet, the gut microbiome, and epigenetics. *Cancer journal (Sudbury, Mass)* 20: 170-175.

Hwang-Verslues WW, Chang PH, Jeng YM, Kuo WH, Chiang PH, Chang YC, *et al.* (2013). Loss of corepressor PER2 under hypoxia up-regulates OCT1-mediated EMT gene expression and enhances tumor malignancy. *Proceedings of the National Academy of Sciences of the United States of America* 110: 12331-12336.

Izquierdo-Torres E, Hernandez-Oliveras A, Meneses-Morales I, Rodriguez G, Fuentes-Garcia G, & Zarain-Herzberg A (2019). Resveratrol up-regulates ATP2A3 gene expression in breast cancer cell lines through epigenetic mechanisms. *The international journal of biochemistry & cell biology* 113: 37-47.

Jafek JL, Shakya A, Tai PY, Ibarra A, Kim H, Maddox J, *et al.* (2019). Transcription factor Oct1 protects against hematopoietic stress and promotes acute myeloid leukemia. *Experimental hematology* 76: 38-48.e32.

Jahangiri R, Jamialahmadi K, Gharib M, Emami Razavi A, & Mosaffa F (2019). Expression and clinicopathological significance of DNA methyltransferase 1, 3A and 3B in tamoxifen-treated breast cancer patients. *Gene* 685: 24-31.

Jang HS, Shin WJ, Lee JE, & Do JT (2017). CpG and Non-CpG Methylation in Epigenetic Gene Regulation and Brain Function. *Genes* 8: E148.

Jeyabalan J, Aqil F, Munagala R, Annamalai L, Vadhanam MV, & Gupta RC (2014b). Chemopreventive and therapeutic activity of dietary blueberry against estrogen-mediated breast cancer. *Journal of agricultural and food chemistry* 62: 3963-3971.

Jeziorska DM, Murray RJS, De Gobbi M, Gaentzsch R, Garrick D, Ayyub H, *et al.* (2017). DNA methylation of intragenic CpG islands depends on their transcriptional activity during differentiation and disease. *Proceedings of the National Academy of Sciences of the United States of America* 114: E7526-e7535.

Jiang X, Yu Y, Yang HW, Agar NY, Frado L, & Johnson MD (2010). The imprinted gene PEG3 inhibits Wnt signaling and regulates glioma growth. *The journal of biological chemistry* 285: 8472-8480.

Jin B, Gong Z, Yang N, Huang Z, Zeng S, Chen H, *et al.* (2016). Downregulation of betaine homocysteine methyltransferase (BHMT) in hepatocellular carcinoma associates with poor

prognosis. *Tumour biology : the journal of the International Society for Oncodevelopmental Biology and Medicine* 37: 5911-5917.

Jones PA (2012). Functions of DNA methylation: islands, start sites, gene bodies and beyond. *Nature reviews genetics* 13: 484-492.

Jones PA, Issa JP, & Baylin S (2016). Targeting the cancer epigenome for therapy. *Nature reviews genetics* 17: 630-641.

Kala R, Shah HN, Martin SL, & Tollefsbol TO (2015). Epigenetic-based combinatorial resveratrol and pterostilbene alters DNA damage response by affecting SIRT1 and DNMT enzyme expression, including SIRT1-dependent gamma-H2AX and telomerase regulation in triple-negative breast cancer. *BMC cancer* 15: 672.

Kala R, & Tollefsbol TO (2016). A Novel Combinatorial Epigenetic Therapy Using Resveratrol and Pterostilbene for Restoring Estrogen Receptor-alpha (ERalpha) Expression in ERalpha-Negative Breast Cancer Cells. *PloS one* 11: e0155057.

Kalamohan K, Periasamy J, Bhaskar Rao D, Barnabas GD, Ponnaiyan S, & Ganesan K (2014). Transcriptional coexpression network reveals the involvement of varying stem cell features with different dysregulations in different gastric cancer subtypes. *Molecular oncology* 8: 1306-1325.

Kamal M, Holliday DL, Morrison EE, Speirs V, Toomes C, & Bell SM (2017). Loss of CSMD1 expression disrupts mammary duct formation while enhancing proliferation, migration and invasion. *Oncology reports* 38: 283-292.

Kapetanovic IM, Muzzio M, Huang Z, Thompson TN, & McCormick DL (2011). Pharmacokinetics, oral bioavailability, and metabolic profile of resveratrol and its dimethylether analog, pterostilbene, in rats. *Cancer chemotherapy and pharmacology* 68: 593-601.

Khan MA, Hussain A, Sundaram MK, Alalami U, Gunasekera D, Ramesh L, *et al.* (2015). (-)-Epigallocatechin-3-gallate reverses the expression of various tumor-suppressor genes by inhibiting DNA methyltransferases and histone deacetylases in human cervical cancer cells. *Oncology reports* 33: 1976-1984.

Kim D, Pertea G, Trapnell C, Pimentel H, Kelley R, & Salzberg SL (2013). TopHat2: accurate alignment of transcriptomes in the presence of insertions, deletions and gene fusions. *Genome biology* 14:R36.

Kim GD, Ni J, Kelesoglu N, Roberts RJ, & Pradhan S (2002). Co-operation and communication between the human maintenance and de novo DNA (cytosine-5) methyltransferases. *The EMBO journal* 21: 4183-4195.

- Kim J, Hong SJ, Lim EK, Yu YS, Kim SW, Roh JH, *et al.* (2009). Expression of nicotinamide N-methyltransferase in hepatocellular carcinoma is associated with poor prognosis. *Journal of experimental & clinical cancer research* : CR 28: 20.
- Kisliouk T, Cramer T, & Meiri N (2017). Methyl CpG level at distal part of heat-shock protein promoter HSP70 exhibits epigenetic memory for heat stress by modulating recruitment of POU2F1-associated nucleosome-remodeling deacetylase (NuRD) complex. *Journal of neurochemistry* 141: 358-372.
- Kolch W, Heidecker G, Kochs G, Hummel R, Vahidi H, Mischak H, *et al.* (1993). Protein kinase C alpha activates RAF-1 by direct phosphorylation. *Nature* 364: 249-252.
- Komatsu H, Kakehashi A, Nishiyama N, Izumi N, Mizuguchi S, Yamano S, *et al.* (2013). Complexin-2 (CPLX2) as a potential prognostic biomarker in human lung high grade neuroendocrine tumors. *Cancer biomarkers : section A of Disease markers* 13: 171-180.
- Koval OM, Nguyen EK, Santhana V, Fidler TP, Sebag SC, Rasmussen TP, *et al.* (2019). Loss of MCU prevents mitochondrial fusion in G1-S phase and blocks cell cycle progression and proliferation. *Science signaling* 12: eaav1439.
- Krupenko SA, & Krupenko NI (2019). Loss of ALDH1L1 folate enzyme confers a selective metabolic advantage for tumor progression. *Chemico-biological interactions* 302: 149-155.
- Larsson C (2006). Protein kinase C and the regulation of the actin cytoskeleton. *Cellular signalling* 18: 276-284.
- Lee HK, Lee DS, & Park JC (2015). Nuclear factor I-C regulates E-cadherin via control of KLF4 in breast cancer. *BMC cancer* 15: 113.
- Lee WJ, Shim JY, & Zhu BT (2005). Mechanisms for the inhibition of DNA methyltransferases by tea catechins and bioflavonoids. *Molecular pharmacology* 68: 1018-1030.
- Lee WJ, & Zhu BT (2006). Inhibition of DNA methylation by caffeic acid and chlorogenic acid, two common catechol-containing coffee polyphenols. *Carcinogenesis* 27: 269-277.
- Lehnertz B, Ueda Y, Derijck AA, Braunschweig U, Perez-Burgos L, Kubicek S, *et al.* (2003). Suv39h-mediated histone H3 lysine 9 methylation directs DNA methylation to major satellite repeats at pericentric heterochromatin. *Current biology* : CB 13: 1192-1200.
- Leonard B, McCann JL, Starrett GJ, Kosyakovskiy L, Luengas EM, Molan AM, *et al.* (2015). The PKC/NF-kappaB signaling pathway induces APOBEC3B expression in multiple human cancers. *Cancer research* 75: 4538-4547.

Leotlela PD, Wade MS, Duray PH, Rhode MJ, Brown HF, Rosenthal DT, *et al.* (2007). Claudin-1 overexpression in melanoma is regulated by PKC and contributes to melanoma cell motility. *Oncogene* 26: 3846-3856.

Li J, You S, Zhang S, Hu Q, Wang F, Chi X, *et al.* (2019). Elevated N-methyltransferase expression induced by hepatic stellate cells contributes to the metastasis of hepatocellular carcinoma via regulation of the CD44v3 isoform. *Molecular oncology* 13: 1993-2009.

Li W, Ma X, Li N, Liu H, Dong Q, Zhang J, *et al.* (2016). Resveratrol inhibits Hexokinases II mediated glycolysis in non-small cell lung cancer via targeting Akt signaling pathway. *Experimental cell research* 349: 320-327.

Link A, Balaguer F, Shen Y, Lozano JJ, Leung HC, Boland CR, *et al.* (2013). Curcumin modulates DNA methylation in colorectal cancer cells. *PloS one* 8: e57709.

Lipkin M, Reddy B, Newmark H, & Lamprecht SA (1999). Dietary factors in human colorectal cancer. *Annual review of nutrition* 19: 545-586.

Lister R, Pelizzola M, Dowen RH, Hawkins RD, Hon G, Tonti-Filippini J, *et al.* (2009). Human DNA methylomes at base resolution show widespread epigenomic differences. *Nature* 462: 315-322.

Liu G, Hou G, Li L, Li Y, Zhou W, & Liu L (2016). Potential diagnostic and prognostic marker dimethylglycine dehydrogenase (DMGDH) suppresses hepatocellular carcinoma metastasis in vitro and in vivo. *Oncotarget* 7: 32607-32616.

Liu HT, & Gao P (2016). The roles of microRNAs related with progression and metastasis in human cancers. *Tumour biology* 37: 15383-15397.

Liu Q, Chen J, Qin Y, Jiang B, & Zhang T (2019). Encapsulation of pterostilbene in nanoemulsions: influence of lipid composition on physical stability, in vitro digestion, bioaccessibility, and Caco-2 cell monolayer permeability. *Food & function* 10: 6604-6614.

Liu X, Gao Q, Li P, Zhao Q, Zhang J, Li J, *et al.* (2013). UHRF1 targets DNMT1 for DNA methylation through cooperative binding of hemi-methylated DNA and methylated H3K9. *Nature communications* 4: 1563.

Liu Y, Amin EB, Mayo MW, Chudgar NP, Bucciarelli PR, Kadota K, *et al.* (2016). CK2alpha' Drives Lung Cancer Metastasis by Targeting BRMS1 Nuclear Export and Degradation. *Cancer research* 76: 2675-2686.

Liu Y, Zhou J, Hu Y, Wang J, & Yuan C (2017). Curcumin inhibits growth of human breast cancer cells through demethylation of DLC1 promoter. *Molecular and cellular biochemistry* 425: 47-58.

- Liu Z, Xie Z, Jones W, Pavlovicz RE, Liu S, Yu J, *et al.* (2009). Curcumin is a potent DNA hypomethylation agent. *Bioorganic & medicinal chemistry letters* 19: 706-709.
- Lonne GK, Cornmark L, Zahirovic IO, Landberg G, Jirstrom K, & Larsson C (2010). PKC $\alpha$  expression is a marker for breast cancer aggressiveness. *Molecular cancer* 9: 76.
- Lou XD, Wang HD, Xia SJ, Skog S, & Sun J (2014). Effects of resveratrol on the expression and DNA methylation of cytokine genes in diabetic rat aortas. *Archivum immunologiae et therapiae experimentalis* 62: 329-340.
- Love MI, Huber W, & Anders S (2014). Moderated estimation of fold change and dispersion for RNA-seq data using DESeq2. *Genome biology* 15:550.
- Lubecka K, Kurzava L, Flower K, Buvala H, Zhang H, Teegarden D, *et al.* (2016). Stilbenoids remodel the DNA methylation patterns in breast cancer cells and inhibit oncogenic NOTCH signaling through epigenetic regulation of MAML2 transcriptional activity. *Carcinogenesis* 37: 656-668.
- Luka Z, Mudd SH, & Wagner C (2009). Glycine N-methyltransferase and regulation of S-adenosylmethionine levels. *The journal of biological chemistry* 284: 22507-22511.
- Luo C, Hajkova P, & Ecker JR (2018). Dynamic DNA methylation: In the right place at the right time. *Science (New York, NY)* 361: 1336-1340.
- Luther DJ, Ohanyan V, Shamhart PE, Hodnichak CM, Sisakian H, Booth TD, *et al.* (2011). Chemopreventive doses of resveratrol do not produce cardiotoxicity in a rodent model of hepatocellular carcinoma. *Investigational new drugs* 29: 380-391.
- Ly D, Forman D, Ferlay J, Brinton LA, & Cook MB (2013). An international comparison of male and female breast cancer incidence rates. *International journal of cancer* 132: 1918-1926.
- Ma L, Li W, Wang R, Nan Y, Wang Q, Liu W, *et al.* (2015). Resveratrol enhanced anticancer effects of cisplatin on non-small cell lung cancer cell lines by inducing mitochondrial dysfunction and cell apoptosis. *International journal of oncology* 47: 1460-1468.
- Ma Z, Zhang X, Xu L, Liu D, Di S, Li W, *et al.* (2019). Pterostilbene: Mechanisms of its action as oncostatic agent in cell models and in vivo studies. *Pharmacological research* 145: 104265.
- Maddox J, Shakya A, South S, Shelton D, Andersen JN, Chidester S, *et al.* (2012). Transcription factor Oct1 is a somatic and cancer stem cell determinant. *PLoS genetics* 8: e1003048.
- Mahmoud AM, & Ali MM (2019). Methyl Donor Micronutrients that Modify DNA Methylation and Cancer Outcome. *Nutrients* 11: E608.

- Maiga A, Lemieux S, Pabst C, Lavallee VP, Bouvier M, Sauvageau G, *et al.* (2016). Transcriptome analysis of G protein-coupled receptors in distinct genetic subgroups of acute myeloid leukemia: identification of potential disease-specific targets. *Blood cancer journal* 6: e431.
- Majid S, Dar AA, Shahryari V, Hirata H, Ahmad A, Saini S, *et al.* (2010). Genistein reverses hypermethylation and induces active histone modifications in tumor suppressor gene B-Cell translocation gene 3 in prostate cancer. *Cancer* 116: 66-76.
- Makuuchi R, Terashima M, Kusahara M, Nakajima T, Serizawa M, Hatakeyama K, *et al.* (2017). Comprehensive analysis of gene mutation and expression profiles in neuroendocrine carcinomas of the stomach. *Biomedical research (Tokyo, Japan)* 38: 19-27.
- Maurano MT, Wang H, John S, Shafer A, Canfield T, Lee K, *et al.* (2015). Role of DNA Methylation in Modulating Transcription Factor Occupancy. *Cell reports* 12: 1184-1195.
- Mayol G, Martin-Subero JI, Rios J, Queiros A, Kulis M, Sunol M, *et al.* (2012). DNA hypomethylation affects cancer-related biological functions and genes relevant in neuroblastoma pathogenesis. *PloS one* 7: e48401.
- McCormack D, & McFadden D (2012). Pterostilbene and cancer: current review. *The journal of surgical research* 173: e53-61.
- Medina-Aguilar R, Perez-Plasencia C, Marchat LA, Gariglio P, Garcia Mena J, Rodriguez Cuevas S, *et al.* (2016). Methylation Landscape of Human Breast Cancer Cells in Response to Dietary Compound Resveratrol. *PloS one* 11: e0157866.
- Michailidi C, Theocharis S, Tsurouflis G, Pletsas V, Kouraklis G, Patsouris E, *et al.* (2015). Expression and promoter methylation status of hMLH1, MGMT, APC, and CDH1 genes in patients with colon adenocarcinoma. *Experimental biology and medicine (Maywood, NJ)* 240: 1599-1605.
- Miksits M, Maier-Salamon A, Aust S, Thalhammer T, Reznicek G, Kunert O, *et al.* (2005). Sulfation of resveratrol in human liver: evidence of a major role for the sulfotransferases SULT1A1 and SULT1E1. *Xenobiotica; the fate of foreign compounds in biological systems* 35: 1101-1119.
- Minor EA, Court BL, Young JI, & Wang G (2013). Ascorbate induces ten-eleven translocation (Tet) methylcytosine dioxygenase-mediated generation of 5-hydroxymethylcytosine. *The journal of biological chemistry* 288: 13669-13674.
- Mirza S, Sharma G, Parshad R, Gupta SD, Pandya P, & Ralhan R (2013). Expression of DNA methyltransferases in breast cancer patients and to analyze the effect of natural compounds on DNA methyltransferases and associated proteins. *Journal of breast cancer* 16: 23-31.

- Mishra R, Thorat D, Soundararajan G, Pradhan SJ, Chakraborty G, Lohite K, *et al.* (2015). Semaphorin 3A upregulates FOXO 3a-dependent MelCAM expression leading to attenuation of breast tumor growth and angiogenesis. *Oncogene* 34: 1584-1595.
- Moco S, Martin FP, & Rezzi S (2012). Metabolomics view on gut microbiome modulation by polyphenol-rich foods. *Journal of proteome research* 11: 4781-4790.
- Mohapatra P, Satapathy SR, Siddharth S, Das D, Nayak A, & Kundu CN (2015). Resveratrol and curcumin synergistically induces apoptosis in cigarette smoke condensate transformed breast epithelial cells through a p21(Waf1/Cip1) mediated inhibition of Hh-Gli signaling. *The international journal of biochemistry & cell biology* 66: 75-84.
- Morris J, Moseley VR, Cabang AB, Coleman K, Wei W, Garrett-Mayer E, *et al.* (2016). Reduction in promotor methylation utilizing EGCG (epigallocatechin-3-gallate) restores RXRalpha expression in human colon cancer cells. *Oncotarget* 7: 35313-35326.
- Morrison MM, Young CD, Wang S, Sobolik T, Sanchez VM, Hicks DJ, *et al.* (2015). mTOR Directs Breast Morphogenesis through the PKC-alpha-Rac1 Signaling Axis. *PLoS genetics* 11: e1005291.
- Murayama A, Sakura K, Nakama M, Yasuzawa-Tanaka K, Fujita E, Tateishi Y, *et al.* (2006). A specific CpG site demethylation in the human interleukin 2 gene promoter is an epigenetic memory. *The EMBO journal* 25: 1081-1092.
- Nakae D, Yoshiji H, Mizumoto Y, Horiguchi K, Shiraiwa K, Tamura K, *et al.* (1992). High incidence of hepatocellular carcinomas induced by a choline deficient L-amino acid defined diet in rats. *Cancer research* 52: 5042-5045.
- Nath A, & Chan C (2016). Genetic alterations in fatty acid transport and metabolism genes are associated with metastatic progression and poor prognosis of human cancers. *Scientific reports* 6: 18669.
- Nestor CE, Ottaviano R, Reddington J, Sproul D, Reinhardt D, Dunican D, *et al.* (2012). Tissue type is a major modifier of the 5-hydroxymethylcytosine content of human genes. *Genome research* 22: 467-477.
- Newmark HL, Yang K, Lipkin M, Kopelovich L, Liu Y, Fan K, *et al.* (2001). A Western-style diet induces benign and malignant neoplasms in the colon of normal C57Bl/6 mice. *Carcinogenesis* 22: 1871-1875.
- Nguyen AV, Martinez M, Stamos MJ, Moyer MP, Planutis K, Hope C, *et al.* (2009). Results of a phase I pilot clinical trial examining the effect of plant-derived resveratrol and grape powder on Wnt pathway target gene expression in colonic mucosa and colon cancer. *Cancer management and research* 1: 25-37.

- Ooi SK, Qiu C, Bernstein E, Li K, Jia D, Yang Z, *et al.* (2007). DNMT3L connects unmethylated lysine 4 of histone H3 to de novo methylation of DNA. *Nature* 448: 714-717.
- Papoutsis AJ, Borg JL, Selmin OI, & Romagnolo DF (2012). BRCA-1 promoter hypermethylation and silencing induced by the aromatic hydrocarbon receptor-ligand TCDD are prevented by resveratrol in MCF-7 cells. *The journal of nutritional biochemistry* 23: 1324-1332.
- Patel KR, Brown VA, Jones DJ, Britton RG, Hemingway D, Miller AS, *et al.* (2010). Clinical pharmacology of resveratrol and its metabolites in colorectal cancer patients. *Cancer research* 70: 7392-7399.
- Paul S, DeCastro AJ, Lee HJ, Smolarek AK, So JY, Simi B, *et al.* (2010). Dietary intake of pterostilbene, a constituent of blueberries, inhibits the beta-catenin/p65 downstream signaling pathway and colon carcinogenesis in rats. *Carcinogenesis* 31: 1272-1278.
- Penalva R, Morales J, Gonzalez-Navarro CJ, Larraneta E, Quincoces G, Penuelas I, *et al.* (2018). Increased Oral Bioavailability of Resveratrol by Its Encapsulation in Casein Nanoparticles. *International journal of molecular sciences* 19: E2816.
- Peng D, Ge G, Gong Y, Zhan Y, He S, Guan B, *et al.* (2018). Vitamin C increases 5-hydroxymethylcytosine level and inhibits the growth of bladder cancer. *Clinical epigenetics* 10: 94.
- Peng GH, & Chen S (2013). Double chromatin immunoprecipitation: analysis of target co-occupancy of retinal transcription factors. *Methods in molecular biology* 935: 311-328.
- Peralta-Arrieta I, Hernandez-Sotelo D, Castro-Coronel Y, Leyva-Vazquez MA, & Illades-Aguilar B (2017). DNMT3B modulates the expression of cancer-related genes and downregulates the expression of the gene VAV3 via methylation. *American journal of cancer research* 7: 77-87.
- Pfaffl MW, Horgan GW, & Dempfle L (2002). Relative expression software tool (REST) for group-wise comparison and statistical analysis of relative expression results in real-time PCR. *Nucleic acids research* 30: e36.
- Pfeifer GP (2018). Defining Driver DNA Methylation Changes in Human Cancer. *International journal of molecular sciences* 19: E1166.
- Pham TND, Perez White BE, Zhao H, Mortazavi F, & Tonetti DA (2017). Protein kinase C alpha enhances migration of breast cancer cells through FOXC2-mediated repression of p120-catenin. *BMC cancer* 17: 832.
- Pogribny IP, Basnakian AG, Miller BJ, Lopatina NG, Poirier LA, & James SJ (1995). Breaks in genomic DNA and within the p53 gene are associated with hypomethylation in livers of folate/methyl-deficient rats. *Cancer research* 55: 1894-1901.

- Pogribny IP, Poirier LA, & James SJ (1995). Differential sensitivity to loss of cytosine methyl groups within the hepatic p53 gene of folate/methyl deficient rats. *Carcinogenesis* 16: 2863-2867.
- Qian YY, Liu ZS, Yan HJ, Yuan YF, Levenson AS, & Li K (2018). Pterostilbene inhibits MTA1/HDAC1 complex leading to PTEN acetylation in hepatocellular carcinoma. *Biomedicine & pharmacotherapy = Biomedecine & pharmacotherapie* 101: 852-859.
- Qian YY, Liu ZS, Zhang Z, Levenson AS, & Li K (2018). Pterostilbene increases PTEN expression through the targeted downregulation of microRNA-19a in hepatocellular carcinoma. *Molecular medicine reports* 17: 5193-5201.
- Qin T, Castoro R, El Ahdab S, Jelinek J, Wang X, Si J, *et al.* (2011). Mechanisms of resistance to decitabine in the myelodysplastic syndrome. *PLoS one* 6: e23372.
- Qin W, Zhang K, Clarke K, Weiland T, & Sauter ER (2014). Methylation and miRNA effects of resveratrol on mammary tumors vs. normal tissue. *Nutrition and cancer* 66: 270-277.
- Qin Y, & Wade PA (2018). Crosstalk between the microbiome and epigenome: messages from bugs. *Journal of biochemistry* 163: 105-112.
- Rabello Ddo A, de Moura CA, de Andrade RV, Motoyama AB, & Silva FP (2013). Altered expression of MLL methyltransferase family genes in breast cancer. *International journal of oncology* 43: 653-660.
- Rao X, Evans J, Chae H, Pilrose J, Kim S, Yan P, *et al.* (2013). CpG island shore methylation regulates caveolin-1 expression in breast cancer. *Oncogene* 32: 4519-4528.
- Rasmussen KD, & Helin K (2016). Role of TET enzymes in DNA methylation, development, and cancer. *Genes & development* 30: 733-750.
- Rauf A, Imran M, Butt MS, Nadeem M, Peters DG, & Mubarak MS (2018). Resveratrol as an anti-cancer agent: A review. *Critical reviews in food science and nutrition* 58: 1428-1447.
- Rezk YA, Balulad SS, Keller RS, & Bennett JA (2006). Use of resveratrol to improve the effectiveness of cisplatin and doxorubicin: study in human gynecologic cancer cell lines and in rodent heart. *American journal of obstetrics and gynecology* 194: e23-26.
- Rimando AM, Cuendet M, Desmarchelier C, Mehta RG, Pezzuto JM, & Duke SO (2002). Cancer chemopreventive and antioxidant activities of pterostilbene, a naturally occurring analogue of resveratrol. *Journal of agricultural and food chemistry* 50: 3453-3457.
- Rinaldi L, Datta D, Serrat J, Morey L, Solanas G, Avgustinova A, *et al.* (2016). Dnmt3a and Dnmt3b Associate with Enhancers to Regulate Human Epidermal Stem Cell Homeostasis. *Cell stem cell* 19: 491-501.

- Robinson MD, McCarthy DJ, & Smyth GK (2010). EdgeR: a Bioconductor package for differential expression analysis of digital gene expression data. *Bioinformatics* 26:139-140.
- Ruiz MJ, Fernandez M, Pico Y, Manes J, Asensi M, Carda C, *et al.* (2009). Dietary administration of high doses of pterostilbene and quercetin to mice is not toxic. *Journal of agricultural and food chemistry* 57: 3180-3186.
- Saghafinia S, Mina M, Riggi N, Hanahan D, & Ciriello G (2018). Pan-Cancer Landscape of Aberrant DNA Methylation across Human Tumors. *Cell reports* 25: 1066-1080.e1068.
- Santner SJ, Dawson PJ, Tait L, Soule HD, Eliason J, Mohamed AN, *et al.* (2001). Malignant MCF10CA1 cell lines derived from premalignant human breast epithelial MCF10AT cells. *Breast cancer research and treatment* 65: 101-110.
- Sarver AL, Murray CD, Temiz NA, Tseng YY, & Bagchi A (2016). MYC and PVT1 synergize to regulate RSPO1 levels in breast cancer. *Cell cycle (Georgetown, Tex)* 15: 881-885.
- Saunier E, Antonio S, Regazzetti A, Auzeil N, Laprevote O, Shay JW, *et al.* (2017). Resveratrol reverses the Warburg effect by targeting the pyruvate dehydrogenase complex in colon cancer cells. *Scientific reports* 7: 6945.
- Schmitt M, Horbach A, Kubitz R, Frilling A, & Haussinger D (2004). Disruption of hepatocellular tight junctions by vascular endothelial growth factor (VEGF): a novel mechanism for tumor invasion. *Journal of hepatology* 41: 274-283.
- Schulze-Osthoff K, Ferrari D, Riehemann K, & Wesselborg S (1997). Regulation of NF-kappa B activation by MAP kinase cascades. *Immunobiology* 198: 35-49.
- Sengelaub CA, Navrazhina K, Ross JB, Halberg N, & Tavazoie SF (2016). PTPRN2 and PLCbeta1 promote metastatic breast cancer cell migration through PI(4,5)P2-dependent actin remodeling. *The EMBO journal* 35: 62-76.
- Shao C, Sun W, Tan M, Glazer CA, Bhan S, Zhong X, *et al.* (2011). Integrated, genome-wide screening for hypomethylated oncogenes in salivary gland adenoid cystic carcinoma. *Clinical cancer research : an official journal of the American Association for Cancer Research* 17: 4320-4330.
- Shao X, Chen X, Badmaev V, Ho CT, & Sang S (2010). Structural identification of mouse urinary metabolites of pterostilbene using liquid chromatography/tandem mass spectrometry. *Rapid communications in mass spectrometry : RCM* 24: 1770-1778.
- Sharma U, & Rando OJ (2017). Metabolic Inputs into the Epigenome. *Cell metabolism* 25: 544-558.

Sherman BT, Huang da W, Tan Q, Guo Y, Bour S, Liu D, *et al.* (2007). DAVID Knowledgebase: a gene-centered database integrating heterogeneous gene annotation resources to facilitate high-throughput gene functional analysis. *BMC bioinformatics* 8: 426.

Shikauchi Y, Saiura A, Kubo T, Niwa Y, Yamamoto J, Murase Y, *et al.* (2009). SALL3 interacts with DNMT3A and shows the ability to inhibit CpG island methylation in hepatocellular carcinoma. *Molecular and cellular biology* 29: 1944-1958.

Shimizu K, Onishi M, Sugata E, Sokuza Y, Mori C, Nishikawa T, *et al.* (2007). Disturbance of DNA methylation patterns in the early phase of hepatocarcinogenesis induced by a choline-deficient L-amino acid-defined diet in rats. *Cancer science* 98: 1318-1322.

Shin HJ, Park HY, Jeong SJ, Park HW, Kim YK, Cho SH, *et al.* (2005). STAT4 expression in human T cells is regulated by DNA methylation but not by promoter polymorphism. *Journal of immunology (Baltimore, Md : 1950)* 175: 7143-7150.

Sicklick JK, Li YX, Jayaraman A, Kannangai R, Qi Y, Vivekanandan P, *et al.* (2006). Dysregulation of the Hedgehog pathway in human hepatocarcinogenesis. *Carcinogenesis* 27: 748-757.

Siegel RL, Miller KD, & Jemal A (2015). *Cancer statistics, 2015*. CA: a cancer journal for clinicians 65: 5-29.

Singh B, Shoulson R, Chatterjee A, Ronghe A, Bhat NK, Dim DC, *et al.* (2014). Resveratrol inhibits estrogen-induced breast carcinogenesis through induction of NRF2-mediated protective pathways. *Carcinogenesis* 35: 1872-1880.

Soll JM, Brickner JR, Mudge MC, & Mosammamarast N (2018). RNA ligase-like domain in activating signal cointegrator 1 complex subunit 1 (ASCC1) regulates ASCC complex function during alkylation damage. *The journal of biological chemistry* 293: 13524-13533.

Stefanska B, Bouzelmat A, Huang J, Suderman M, Hallett M, Han ZG, *et al.* (2013). Discovery and Validation of DNA Hypomethylation Biomarkers for Liver Cancer Using HRM-Specific Probes. *PloS one* 8: e68439.

Stefanska B, Cheishvili D, Suderman M, Arakelian A, Huang J, Hallett M, *et al.* (2014). Genome-wide study of hypomethylated and induced genes in liver cancer patients unravels novel anticancer targets. *Clinical cancer research* 20: 3118-3132.

Stefanska B, Huang J, Bhattacharyya B, Suderman M, Hallett M, Han ZG, *et al.* (2011). Definition of the landscape of promoter DNA hypomethylation in liver cancer. *Cancer research* 71: 5891-5903.

Stefanska B, Rudnicka K, Bednarek A, & Fabianowska-Majewska K (2010). Hypomethylation and induction of retinoic acid receptor beta 2 by concurrent action of adenosine analogues and natural compounds in breast cancer cells. *European journal of pharmacology* 638: 47-53.

Stefanska B, Salame P, Bednarek A, & Fabianowska-Majewska K (2012). Comparative effects of retinoic acid, vitamin D and resveratrol alone and in combination with adenosine analogues on methylation and expression of phosphatase and tensin homologue tumour suppressor gene in breast cancer cells. *The British journal of nutrition* 107: 781-790.

Stefanska B, Suderman M, Machnes Z, Bhattacharyya B, Hallett M, & Szyf M (2013). Transcription onset of genes critical in liver carcinogenesis is epigenetically regulated by methylated DNA binding protein MBD2. *Carcinogenesis* 34: 2738-2749.

Sun Y, Wu X, Cai X, Song M, Zheng J, Pan C, *et al.* (2016). Identification of pinostilbene as a major colonic metabolite of pterostilbene and its inhibitory effects on colon cancer cells. *Molecular nutrition & food research* 60: 1924-1932.

Sunahori K, Juang YT, & Tsokos GC (2009). Methylation status of CpG islands flanking a cAMP response element motif on the protein phosphatase 2Ac alpha promoter determines CREB binding and activity. *Journal of immunology (Baltimore, Md : 1950)* 182: 1500-1508.

Suzuki IK, Gacquer D, Van Heurck R, Kumar D, Wojno M, Bilheu A, *et al.* (2018). Human-Specific NOTCH2NL Genes Expand Cortical Neurogenesis through Delta/Notch Regulation. *Cell* 173: 1370-1384.e1316.

Syafruddin SE, Rodrigues P, Vojtasova E, Patel SA, Zaini MN, Burge J, *et al.* (2019). A KLF6-driven transcriptional network links lipid homeostasis and tumour growth in renal carcinoma. *Nature communications* 10: 1152.

Tang N, Ma L, Lin XY, Zhang Y, Yang DL, Wang EH, *et al.* (2015). Expression of PHF20 protein contributes to good prognosis of NSCLC and is associated with Bax expression. *International journal of clinical and experimental pathology* 8: 12198-12206.

Tang T, Guo C, Xia T, Zhang R, Zen K, Pan Y, *et al.* (2019). LncCCAT1 Promotes Breast Cancer Stem Cell Function through Activating WNT/beta-catenin Signaling. *Theranostics* 9: 7384-7402.

Tavakolian S, Goudarzi H, & Faghihloo E (2019). E-cadherin, Snail, ZEB-1, DNMT1, DNMT3A and DNMT3B expression in normal and breast cancer tissues. *Acta biochimica Polonica* 66: 409-414.

Taylor SC, Nadeau K, Abbasi M, Lachance C, Nguyen M, & Fenrich J (2019). The Ultimate qPCR Experiment: Producing Publication Quality, Reproducible Data the First Time. *Trends in biotechnology* 37: 761-774.

- Thomas R, Thomas S, Holloway AK, & Pollard KS (2017). Features that define the best ChIP-seq peak calling algorithms. *Briefings in bioinformatics* 18:441-450.
- Thorne AM, Jackson TA, Willis VC, & Bradford AP (2013). Protein Kinase C alpha Modulates Estrogen-Receptor-Dependent Transcription and Proliferation in Endometrial Cancer Cells. *Obstetrics and gynecology international* 2013: 537479.
- Tian F, DaCosta Byfield S, Parks WT, Yoo S, Felici A, Tang B, *et al.* (2003). Reduction in Smad2/3 signaling enhances tumorigenesis but suppresses metastasis of breast cancer cell lines. *Cancer research* 63: 8284-8292.
- Torres N, Guevara-Cruz M, Velazquez-Villegas LA, & Tovar AR (2015). Nutrition and Atherosclerosis. *Archives of medical research* 46: 408-426.
- Toska E, Osmanbeyoglu HU, Castel P, Chan C, Hendrickson RC, Elkabets M, *et al.* (2017). PI3K pathway regulates ER-dependent transcription in breast cancer through the epigenetic regulator KMT2D. *Science* 355: 1324-1330.
- Tost J, & Gut IG (2007). DNA methylation analysis by pyrosequencing. *Nature protocols* 2: 2265-2275.
- Trapnell C, Roberts A, Goff L, Pertea G, Kim D, Kelley DR, Pimentel H, Salzberg SL, Rinn JL, & Pachter L (2012). Differential gene and transcript expression analysis of RNA-seq experiments with TopHat and Cufflinks. *Nature protocols* 7:562-578.
- Trepo E, Romeo S, Zucman-Rossi J, & Nahon P (2016). PNPLA3 gene in liver diseases. *Journal of hepatology* 65: 399-412.
- Tsai HC, & Baylin SB (2011). Cancer epigenetics: linking basic biology to clinical medicine. *Cell research* 21: 502-517.
- Tsujiuchi T, Tsutsumi M, Sasaki Y, Takahama M, & Konishi Y (1999). Hypomethylation of CpG sites and c-myc gene overexpression in hepatocellular carcinomas, but not hyperplastic nodules, induced by a choline-deficient L-amino acid-defined diet in rats. *Japanese journal of cancer research : Gann* 90: 909-913.
- Vazquez-Arreguin K, & Tantin D (2016). The Oct1 transcription factor and epithelial malignancies: Old protein learns new tricks. *Biochimica et biophysica acta* 1859: 792-804.
- Vizoso M, Ferreira HJ, Lopez-Serra P, Carmona FJ, Martinez-Cardus A, Girotti MR, *et al.* (2015). Epigenetic activation of a cryptic TBC1D16 transcript enhances melanoma progression by targeting EGFR. *Nature medicine* 21: 741-750.
- Walle T (2011). Bioavailability of resveratrol. *Annals of the New York Academy of Sciences* 1215: 9-15.

- Wallerius M, Wallmann T, Bartish M, Ostling J, Mezheyeuski A, Tobin NP, *et al.* (2016). Guidance Molecule SEMA3A Restricts Tumor Growth by Differentially Regulating the Proliferation of Tumor-Associated Macrophages. *Cancer research* 76: 3166-3178.
- Wang B, Majumder S, Nuovo G, Kutay H, Volinia S, Patel T, *et al.* (2009). Role of microRNA-155 at early stages of hepatocarcinogenesis induced by choline-deficient and amino acid-defined diet in C57BL/6 mice. *Hepatology (Baltimore, Md)* 50: 1152-1161.
- Wang P, & Sang S (2018). Metabolism and pharmacokinetics of resveratrol and pterostilbene. *BioFactors (Oxford, England)* 44: 16-25.
- Wang T, Li J, Ding K, Zhang L, Che Q, Sun X, *et al.* (2017). The CpG Dinucleotide Adjacent to a kappaB Site Affects NF-kappaB Function through Its Methylation. *International journal of molecular sciences* 18: E528.
- Wang W, Smits R, Hao H, & He C (2019). Wnt/beta-Catenin Signaling in Liver Cancers. *Cancers* 11: E926.
- Wang Y, Zhou J, Wang Z, Wang P, & Li S (2017). Upregulation of SOX2 activated LncRNA PVT1 expression promotes breast cancer cell growth and invasion. *Biochemical and biophysical research communications* 493: 429-436.
- Wang YP, Cheng ML, Zhang BF, Mu M, & Wu J (2010). Effects of blueberry on hepatic fibrosis and transcription factor Nrf2 in rats. *World journal of gastroenterology : WJG* 16: 2657-2663.
- Wen W, Lowe G, Roberts CM, Finlay J, Han ES, Glackin CA, *et al.* (2017). Pterostilbene, a natural phenolic compound, synergizes the antineoplastic effects of megestrol acetate in endometrial cancer. *Scientific reports* 7: 12754.
- Wiedeman AM, Barr SI, Green TJ, Xu Z, Innis SM, & Kitts DD (2018). Dietary Choline Intake: Current State of Knowledge Across the Life Cycle. *Nutrients* 10: E1513.
- Wilhelm-Benartzi CS, Koestler DC, Karagas MR, Flanagan JM, Christensen BC, Kelsey KT, *et al.* (2013). Review of processing and analysis methods for DNA methylation array data. *British journal of cancer* 109: 1394-1402.
- Wossidlo M, Nakamura T, Lepikhov K, Marques CJ, Zakhartchenko V, Boiani M, *et al.* (2011). 5-Hydroxymethylcytosine in the mammalian zygote is linked with epigenetic reprogramming. *Nature communications* 2: 241.
- Wu WF, Maneix L, Insunza J, Nalvarte I, Antonson P, Kere J, *et al.* (2017). Estrogen receptor beta, a regulator of androgen receptor signaling in the mouse ventral prostate. *Proceedings of the National Academy of Sciences of the United States of America* 114: E3816-E3822.

- Xie Q, Bai Q, Zou LY, Zhang QY, Zhou Y, Chang H, *et al.* (2014). Genistein inhibits DNA methylation and increases expression of tumor suppressor genes in human breast cancer cells. *Genes, chromosomes & cancer* 53: 422-431.
- Xu T, Park SS, Giaimo BD, Hall D, Ferrante F, Ho DM, *et al.* (2017). RBPJ/CBF1 interacts with L3MBTL3/MBT1 to promote repression of Notch signaling via histone demethylase KDM1A/LSD1. *The EMBO journal* 36: 3232-3249.
- Xue TC, Zou JH, Chen RX, Cui JF, Tang ZY, & Ye SL (2014). Spatial localization of the JAG1/Notch1/osteopontin cascade modulates extrahepatic metastasis in hepatocellular carcinoma. *International journal of oncology* 45: 1883-1890.
- Yamasaki T, Takahashi A, Pan J, Yamaguchi N, & Yokoyama KK (2009). Phosphorylation of Activation Transcription Factor-2 at Serine 121 by Protein Kinase C Controls c-Jun-mediated Activation of Transcription. *The Journal of biological chemistry* 284: 8567-8581.
- Yin R, Mao SQ, Zhao B, Chong Z, Yang Y, Zhao C, *et al.* (2013). Ascorbic acid enhances Tet-mediated 5-methylcytosine oxidation and promotes DNA demethylation in mammals. *Journal of the American Chemical Society* 135: 10396-10403.
- Yin Y, Morgunova E, Jolma A, Kaasinen E, Sahu B, Khund-Sayeed S, *et al.* (2017). Impact of cytosine methylation on DNA binding specificities of human transcription factors. *Science* 356.
- You Z, Li B, Xu J, Chen L, & Ye H (2018). Curcumin suppress the growth of hepatocellular carcinoma via down-regulating SREBF1. *Oncology research* doi: 10.3727/096504018X15219173841078
- Yu J, Peng Y, Wu LC, Xie Z, Deng Y, Hughes T, *et al.* (2013). Curcumin down-regulates DNA methyltransferase 1 and plays an anti-leukemic role in acute myeloid leukemia. *PloS one* 8: e55934.
- Yu J, Qin B, Moyer AM, Nowsheen S, Liu T, Qin S, *et al.* (2018). DNA methyltransferase expression in triple-negative breast cancer predicts sensitivity to decitabine. *The journal of clinical investigation* 128: 2376-2388.
- Yun H, Damm F, Yap D, Schwarzer A, Chaturvedi A, Jyotsana N, *et al.* (2014). Impact of MLL5 expression on decitabine efficacy and DNA methylation in acute myeloid leukemia. *Haematologica* 99: 1456-1464.
- Zappe K, Pointner A, Switzeny OJ, Magnet U, Tomeva E, Heller J, *et al.* (2018). Counteraction of Oxidative Stress by Vitamin E Affects Epigenetic Regulation by Increasing Global Methylation and Gene Expression of MLH1 and DNMT1 Dose Dependently in Caco-2 Cells. *Oxidative medicine and cellular longevity* 2018: 3734250.

Zhang P, Li H, Yang B, Yang F, Zhang LL, Kong QY, *et al.* (2014). Biological significance and therapeutic implication of resveratrol-inhibited Wnt, Notch and STAT3 signaling in cervical cancer cells. *Genes & cancer* 5: 154-164.

Zhang Y, Liu T, Meyer CA, Eeckhoute J, Johnson DS, Bernstein BE, Nusbaum C, Myers RM, Brown M, Li W, & Liu XS (2008). Model-based analysis of ChIP-Seq (MACS). *Genome biology* 9: R137.

Zhao FQ (2013). Octamer-binding transcription factors: genomics and functions. *Frontiers in bioscience (Landmark edition)* 18: 1051-1071.

Zheng Y, Zhang H, Wang Y, Li X, Lu P, Dong F, *et al.* (2016). Loss of Dnmt3b accelerates MLL-AF9 leukemia progression. *Leukemia* 30: 2373-2384.

Zhu W, Qin W, Zhang K, Rottinghaus GE, Chen YC, Kliethermes B, *et al.* (2012). Trans-resveratrol alters mammary promoter hypermethylation in women at increased risk for breast cancer. *Nutrition and cancer* 64: 393-400.

## Appendices

### Appendix A

#### 116 CpG sites hypomethylated in response to 9-day RSV exposure in MCF10CA1h and MCF10CA1a cells

CpG #	UCSC_REFGENE_NAME	lowly invasive MCF10CA1h 9-day RSV		highly invasive MCF10CA1a 9-day RSV	
		methylation difference	P.Value	methylation difference	P.Value
cg00303429		-0.0602	0.0144	-0.0502	0.0118
cg00564737		-0.0583	0.0092	-0.0830	0.0035
cg00661205	KIAA0564;KIAA0564	-0.0673	0.0014	-0.0720	0.0021
cg00690903	C2orf56;C2orf56	-0.0867	0.0005	-0.0703	0.0075
cg00927494	ANO1	-0.0542	0.0263	-0.0676	0.0153
cg01202731	TMEM182	-0.0643	0.0051	-0.0545	0.0091
cg01287342	TTPA	-0.0624	0.0045	-0.0769	0.0170
cg01903440		-0.0583	0.0010	-0.0685	0.0317
cg01915885	NCRNA00171	-0.0807	0.0026	-0.0661	0.0207
cg01952313	MIR548F5;NBEA;MAB21L1	-0.0895	0.0016	-0.0819	0.0021
cg01963059	C1orf161	-0.1191	0.0000	-0.1116	0.0001
cg02286623	RAI2;RAI2	-0.0659	0.0118	-0.0678	0.0004
cg02306639	ZNF860	-0.0523	0.0002	-0.1075	0.0104
cg02670637		-0.0832	0.0001	-0.0648	0.0001
cg02688903	SRP19	-0.0544	0.0083	-0.0521	0.0025
cg02862516		-0.1281	0.0057	-0.0912	0.0046
cg03655395		-0.0789	0.0000	-0.0690	0.0148
cg03737629	FAM73A	-0.0705	0.0141	-0.0613	0.0480
cg03927037	ARHGAP20	-0.0510	0.0091	-0.0638	0.0009
cg04016485		-0.0531	0.0017	-0.0904	0.0001
cg04468334	KRBA1	-0.0542	0.0062	-0.0716	0.0001
cg04950342		-0.0550	0.0140	-0.1317	0.0001
cg05105016	PIAS1	-0.0609	0.0038	-0.0800	0.0008
cg05308293	RPS2P32	-0.1117	0.0073	-0.0622	0.0116

cg05457998	DST;DST;DST;DST	-0.0551	0.0039	-0.1303	0.0002
cg06034708	DTWD1;DTWD1	-0.0817	0.0003	-0.0811	0.0273
cg06082141	C17orf48	-0.0628	0.0008	-0.0526	0.0020
cg06579338	ERI2;ERI2	-0.1089	0.0012	-0.0589	0.0026
cg06620353	SEC63	-0.0754	0.0027	-0.0654	0.0009
cg06810490		-0.1343	0.0000	-0.0672	0.0100
cg06963672	SNORD114-23;SNORD114-24	-0.0561	0.0080	-0.1052	0.0009
cg06971044		-0.0725	0.0282	-0.0835	0.0007
cg07091529	FAM49A	-0.0775	0.0017	-0.1129	0.0001
cg07321237	PCLO;PCLO	-0.0679	0.0004	-0.0793	0.0086
cg07416364		-0.0508	0.0019	-0.0545	0.0266
cg07801516	ZNF461	-0.1303	0.0002	-0.0798	0.0025
cg07813628		-0.0736	0.0002	-0.0513	0.0003
cg07982740	WFDC3	-0.1377	0.0000	-0.1079	0.0000
cg08017956	METTL3	-0.0718	0.0040	-0.0555	0.0024
cg08128444		-0.0518	0.0362	-0.0762	0.0224
cg08628584	SLC35F1	-0.0589	0.0035	-0.0826	0.0028
cg08692175		-0.0738	0.0053	-0.0519	0.0036
cg08697689	SLITRK1	-0.0514	0.0345	-0.0647	0.0077
cg09089913		-0.0893	0.0001	-0.0571	0.0031
cg09442613		-0.0595	0.0021	-0.0658	0.0092
cg09501717		-0.0547	0.0044	-0.0579	0.0269
cg09524613	UST	-0.0952	0.0000	-0.1189	0.0001
cg09856869	S100PBP;S100PBP	-0.0644	0.0029	-0.0592	0.0011
cg09903879	EMP1	-0.0739	0.0008	-0.0715	0.0003
cg10702227		-0.0923	0.0242	-0.0956	0.0029
cg10979364		-0.1408	0.0001	-0.0701	0.0003
cg11062168	AQR	-0.0762	0.0392	-0.0527	0.0310
cg11206067	PHYHIPL;PHYHIPL	-0.0925	0.0011	-0.0557	0.0357
cg11328303	GAD2;GAD2;GAD2;GAD2	-0.0705	0.0017	-0.0634	0.0030
cg12970937	CALCR;CALCR;CALCR	-0.0607	0.0093	-0.0542	0.0017

cg13375518		-0.0826	0.0011	-0.0548	0.0256
cg13736811	TMEM91	-0.1252	0.0000	-0.1112	0.0000
cg14069088	CDKN2BAS	-0.0729	0.0001	-0.0804	0.0024
cg14082959		-0.0958	0.0001	-0.0609	0.0051
cg14114546	LHFPL2	-0.0533	0.0003	-0.0530	0.0351
cg14123942	GRIN3A;GRIN3A	-0.0519	0.0015	-0.0741	0.0080
cg14334147		-0.0705	0.0260	-0.0639	0.0024
cg14489199	SNORD114-26;SNORD114-27	-0.0592	0.0099	-0.0544	0.0043
cg14496314	PTPRG	-0.0930	0.0004	-0.0601	0.0086
cg14550910		-0.0914	0.0035	-0.0746	0.0121
cg14801158	ZNF506;ZNF506	-0.0837	0.0002	-0.0584	0.0146
cg14877502		-0.0545	0.0095	-0.0541	0.0126
cg15650209		-0.0541	0.0018	-0.0534	0.0335
cg15686216	KCTD3	-0.0699	0.0260	-0.0849	0.0008
cg15978039	MEIS1	-0.1055	0.0000	-0.0720	0.0426
cg16476639	RBM25	-0.0864	0.0120	-0.0705	0.0003
cg16530981		-0.0892	0.0000	-0.0816	0.0033
cg16580499	SALL3	-0.0746	0.0185	-0.0539	0.0101
cg17014647	ATXN1;ATXN1	-0.0551	0.0211	-0.0510	0.0119
cg17097119	DEFB133	-0.0602	0.0006	-0.0940	0.0039
cg17343671	RASA2	-0.0573	0.0050	-0.0596	0.0002
cg17417618		-0.0727	0.0093	-0.1156	0.0104
cg17513789	XIST	-0.0567	0.0059	-0.0587	0.0009
cg17546721	TGFBR2;TGFBR2	-0.0806	0.0009	-0.0564	0.0477
cg17652616		-0.0502	0.0120	-0.0527	0.0005
cg17811323	RUFY1;RUFY1;RUFY1	-0.0532	0.0272	-0.0634	0.0036
cg17949403	SLC22A23;SLC22A23	-0.0655	0.0019	-0.0515	0.0150
cg18017082		-0.0597	0.0472	-0.0682	0.0026
cg18172516	RBMS1;RBMS1	-0.1223	0.0001	-0.1157	0.0001
cg18539325	DSCR8;DSCR8;DSCR8;DSCR4	-0.0592	0.0098	-0.0523	0.0438
cg18740872	FYB;FYB	-0.0573	0.0029	-0.0610	0.0034

cg18764240	FAM47C	-0.0600	0.0034	-0.0536	0.0027
cg19593229	ZNF92;ZNF92	-0.0766	0.0004	-0.0841	0.0024
cg20265360		-0.0841	0.0003	-0.0636	0.0228
cg20970886	C3orf59	-0.1183	0.0000	-0.0598	0.0087
cg21518151		-0.0751	0.0016	-0.0537	0.0144
cg21573231	SDCCAG8	-0.0790	0.0098	-0.0865	0.0069
cg21843114	RBPJ;RBPJ;RBPJ;RBPJ	-0.0561	0.0183	-0.0659	0.0252
cg22280402	FAM115A	-0.0709	0.0272	-0.0650	0.0027
cg22403811	RALYL;RALYL;RALYL;RALYL	-0.0900	0.0004	-0.0611	0.0457
cg22582187		-0.0927	0.0025	-0.0530	0.0070
cg22805813	DENR	-0.0726	0.0038	-0.0869	0.0006
cg22819952	PCNX	-0.0566	0.0070	-0.0707	0.0398
cg23242697		-0.0618	0.0126	-0.0886	0.0000
cg23391288		-0.0839	0.0000	-0.1143	0.0000
cg23523755		-0.0514	0.0188	-0.0580	0.0263
cg23732483	ARIH2	-0.0511	0.0290	-0.0577	0.0001
cg23736695		-0.0500	0.0011	-0.0502	0.0122
cg24087039	LPHN3	-0.1024	0.0000	-0.0696	0.0105
cg24149455	GPC6	-0.0772	0.0042	-0.0751	0.0142
cg24509398	EYA3	-0.0843	0.0021	-0.0501	0.0080
cg24641829		-0.0510	0.0003	-0.0562	0.0420
cg24907569	OSGIN2;OSGIN2	-0.0519	0.0066	-0.0711	0.0070
cg24983383	IL18R1	-0.0526	0.0342	-0.0504	0.0151
cg25558440		-0.0602	0.0016	-0.0521	0.0112
cg25680105		-0.0653	0.0068	-0.0610	0.0069
cg25772365		-0.0550	0.0000	-0.0773	0.0250
cg26309511		-0.0910	0.0003	-0.0700	0.0110
cg26664528	MIR548H4;NOX5	-0.0638	0.0073	-0.0970	0.0000
cg27183454	SCAND3	-0.0611	0.0047	-0.0518	0.0170
cg27486624	POLH;XPO5	-0.0545	0.0074	-0.0781	0.0001

## Appendix B

### Genes hypomethylated in response to resveratrol in lowly invasive MCF10CA1h and highly invasive MCF10CA1a breast cancer cells

UCSC_REFGENE_NAME		
ACSL4	DEFB133	LPHN3
AKAP13	DENR	MDGA2
ANO1	DLX6AS	MEIS1
AQR	DSC2	METTL3
ARHGAP10	DSCR8	MIR548F5
ARHGAP20	DST	MIR548H4
ARIH2	DTWD1	NCRNA00171
ASAP2	EMP1	OSGIN2
ASCC3	EPHA3	PALLD
ATXN1	ERI2	PARD3
BMPER	EYA3	PCLO
BTBD3	FAM115A	PCNX
C17orf48	FAM190A	PDE7B
C1orf161	FAM47C	PHYHIPL
C2orf56	FAM49A	PIAS1
C3orf59	FAM73A	POLH
CALCR	FHIT	PPP2R2A
CAMTA1	FYB	PRDM16
CBLN1	GAD2	PTPRG
CDH6	GPC6	RAI2
CDKN2BAS	GRIN3A	RALYL
CLIC6	IL18R1	RASA2
CPA5	INPP4B	RB1CC1
CREB3L2	KCTD3	RBM25
CSMD1	KIAA0564	RBMS1
CTNNA2	KIAA1217	RBPJ
CYB5R4	KRBA1	RPS2P32
	LHFPL2	RUFY1

S100PBP
SALL3
SCAND3
SDCCAG8
SDK1
SEC63
SEMA3A
SLC22A23
SLC35F1
SLC5A7
SLITRK1
SNORD114-23
SNORD114-26
SRP19
TFPI2
TGFBR2
TMEM182
TMEM91
TTPA
TUBGCP3
UST
VPS53
WFDC3
XIST
YTHDC1
ZFHX4
ZNF461
ZNF506
ZNF860
ZNF92

## Appendix C

### Choline-sufficient L-amino acid defined (CSAA) and choline-deficient L-amino acid defined (CDAA) rat diet ingredients

Commercially available from Dyets Inc., Bethlehem, PA, USA (Diet #518753 and #518754)

L- Alanine	5.1 g/kg		
L-Arginine	12.7 g/kg		
L-Aspartic Acid	15.8 g/kg		
L-Cystine	3.7 g/kg		
L-Glutamic Acid	28.9 g/kg		
Glycine	6.2 g/kg		
L-Histidine	3.4 g/kg		
L-Isoleucine	6.1 g/kg		
L-Leucine	10.5 g/kg		
L-Lysine HCl	9.1 g/kg		
L-Methionine	1.7 g/kg		
L-Phenylalanine	7.3 g/kg		
L-Proline	7.6 g/kg		
L-Serine	7.2 g/kg		
L-Threonine	4.6 g/kg		
L-Tryptophan	1.8 g/kg		
L-Tyrosine	5.7 g/kg		
L-Valine	6.3 g/kg		

Total L-AA	143.7 g/kg	4 kcal/g	574.8 kcal/g total
Cornstarch	100 g/kg	3.6 kcal/g	360 kcal/g total
Dextrin	100 g/kg	3.63 kcal/g	363 kcal/g total
Sucrose*	406.67 g/kg	4 kcal/g	1626.7 kcal/g total
Cellulose	50 g/kg	0 kcal/g	0 kcal/g total
Corn Oil	50 g/kg	9 kcal/g	450 kcal/g total
Salt Mix #215001	35 g/kg	0.47 kcal/g	16.45 kcal/g total
Sodium Bicarbonate	4.3 g/kg	0 kcal/g	0 kcal/g total
Vitamin Mix #300050	10 g/kg	3.92 kcal/g	39.2 kcal/g total
Choline Bitartrate**	14.48 g/kg	0 kcal/g	0 kcal/g total
Ferric Citrate, U.S.P	0.33 g/kg	0	0
Total CSAA	1000 g/kg		4329.63 kcal/kg
Total CDAA	1000 g/kg		4271.71 kcal/kg
*CDAA Sucrose	392.19 g/kg	4 kcal/g	1568.76 kcal/kg
**only in CSAA			

## Appendix D

### Concentrations of SAM & SAH calibration standards

Calibration Standard	Initial Stock Vol (μL)	ACN:H <sub>2</sub> O Vol (μL)	Total Vol (μL)	Final Vol (μL)	SAM		SAH	
					Initial Conc (μM)	Final Conc (μM)	Initial Conc (μM)	Final Conc (μM)
1	1800	0	1800	900	320	320	320	320
2	900	900	1800	900	320	160	320	160
3	900	900	1800	900	160	80	160	80
4	900	900	1800	900	80	40	80	40
5	900	900	1800	900	40	20	40	20
6	900	900	1800	900	20	10	20	10
7	900	900	1800	1350	10	5	10	5
8	450	1350	1800	1800	5	1.25	5	1.25

\*vol = volume, conc = concentration

## Appendix E

### List of 116 genes with PTS-mediated reversal of HCC-driven altered gene expression.

	CSAA vs CDAA	CDAA vs CDAA+PTS	Srxn1	2.554152	-0.964354
Gene name	log2FoldChange	log2FoldChange	Mybl1	2.538832	-0.920628
Cyp2c24	7.312453	-1.118050	Erich5	2.538212	-1.131929
LOC100361492	7.112578	-1.313806	Lgals3	2.501289	-0.542499
Mmp12	4.798066	-0.787882	Irgax	2.498076	-0.797757
Gucy2c	4.368692	-0.962052	Tnfrsf12a	2.495242	-0.735242
LOC100365112	4.280487	-0.906345	Wee1	2.411799	-0.790489
Cd276	4.240440	-0.636270	Hist1h2ak	2.349871	-0.787593
Fabp4	3.968000	-0.729161	Cyp2b1	2.326420	1.169869
Pde5a	3.442820	-0.649640	Cyp3a62	2.222965	-0.737286
Maff	3.413100	-1.005233	Samd9l	2.117251	-0.804162
Syt13	3.290631	-0.598915	Popdc2	2.111653	0.825975
Tnfrsf21	3.254444	-0.717128	Hdc	2.049234	-1.277224
Neurl3	3.159657	-0.962928	Slc1a6	2.043346	-1.534635
Dusp8	2.832624	-0.858806	Gfra1	2.025856	-0.596727
Atf3	2.828379	-1.027260	Liph	1.912874	0.749294
Rnd1	2.713696	-1.074013	Bcl3	1.911120	-0.751835
Bmp7	2.618707	-0.832096	Fcnb	1.821433	-0.922225
Synpo	2.586120	-0.557315	Tox3	1.754972	-0.829928
			Cyp2b2	1.749886	0.855666

Erc2	1.724027	-0.739329	Ceacam1	-0.857399	0.520894
Magee1	1.654096	-0.728130	Fads2	-0.914768	-0.859835
Gbp2	1.651341	-0.601493	Etv6	-0.923066	0.561975
Tyro3	1.624787	-0.940465	Papss2	-1.101182	0.561495
Fmo2	1.538682	0.810712	Pyroxd2	-1.125209	0.461977
Vnn1	1.508606	-0.942525	Akr1c2	-1.178559	0.817177
Dusp16	1.426484	-0.813015	Exph5	-1.182026	0.782159
Mfge8	1.400060	-0.565872	Bphl	-1.235274	0.703000
Rhob	1.387562	-0.825486	Fndc4	-1.282520	0.971710
Ajuba	1.357395	-0.910346	Pik3c2g	-1.298105	0.915647
Sesn3	1.203774	-0.502541	Efna1	-1.298580	0.552653
Rab30	1.180396	-0.754556	Hal	-1.309102	0.662942
Vasp	1.097977	-0.566055	Ass1	-1.316969	0.765118
Sat1	1.096653	-0.543502	Dhtkd1	-1.321770	0.680755
Cpsf2	1.068665	-0.922588	Aldh1l1	-1.330770	1.220682
Hmox1	1.038732	-0.539464	LOC103691744	-1.370198	0.634337
Ifrd1	0.886591	-0.697073	Car3	-1.372381	-0.807697
Limk2	0.825365	-0.583464	Arrdc3	-1.377895	0.738621
Tmem120a	0.758138	-0.680580	Pcsk5	-1.387549	0.587632
Ypel2	-0.767025	0.535537	Aamdc	-1.394851	0.778916
Cyp4v3	-0.840116	0.777611	Rmdn2	-1.408058	0.789949
Pbld1	-0.841824	0.515233	Rnf125	-1.425954	0.744028

Hebp1	-1.475568	0.526627	Fam198a	-2.292033	0.807976
Adssl1	-1.570539	0.767793	Adck3	-2.325713	0.694946
Pipox	-1.585626	0.590161	Slc19a2	-2.341722	0.610144
AABR07021096.1	-1.589132	0.465763	Ethe1	-2.401831	0.715613
Clpx	-1.600049	1.056036	Crp	-2.421550	0.921991
Pm20d2	-1.611736	0.795340	Aass	-2.505786	1.367834
Kmo	-1.665842	0.585628	Slc45a3	-2.530880	0.782046
Atp2b2	-1.682653	0.857448	Ilf17rb	-2.625660	0.833125
Gckr	-1.719350	0.828456	G6pc	-2.812138	1.427770
Bhmt2	-1.857821	0.692982	Slc16a10	-2.844468	1.041908
Pdk4	-1.860872	0.671656	Bhmt	-3.144815	1.481671
Cyp1a2	-1.877171	2.431341	Avpr1a	-3.618270	0.934930
Olr36	-1.965373	0.967167	Rgs16	-5.093291	0.773639
Arntl	-2.005372	1.401101			
Gpam	-2.030714	0.696141			
Notum	-2.059743	0.741511			
Cldn1	-2.061198	0.782381			
Kynu	-2.074551	0.855453			
Fmo3	-2.162232	0.872196			
Apcs	-2.210230	0.505809			
Hacl1	-2.275854	0.851487			
Rn50_10_0892.1	-2.285184	0.887782			

## Appendix F

### Gene name abbreviations

Acaca: acetyl-CoA carboxylase alpha

Acat2: acetyl-CoA acetyltransferase 2

ACVR1: serine/threonine-protein kinase  
receptor R1

Acly: ATP citrate lyase

Acss2: acetyl-CoA synthetase 2

AGTPBP1: ATP/GTP binding protein 1

Ahcy: adenosylhomocysteinase

Aldh1l1: aldehyde dehydrogenase 1 family  
member 1

ANKHD1: ankyrin repeat and KH domain  
containing 1

ANP32E: acidic nuclear phosphoprotein 32  
family member E

APC: APC regulator of WNT signaling  
pathway

Aqp7: aquaglyceroporin 7

ASCC1: activating signal cointegrator 1  
complex subunit 1

ATF2: activating transcription factor 2

ATM: ATM serine/threonine kinase

ATP2A3: ATPase

sarcoplasmic/endoplasmic reticulum Ca<sup>2+</sup>  
transporting 3

BAX: BCL2 associated X, apoptosis  
regulator

BCL2: BCL2 apoptosis regulator

Bhmt: betaine-homocysteine S-  
methyltransferase

BRAF: B-Raf proto-oncogene

BRCA: breast cancer

BRMS1: breast cancer metastasis suppressor 1

BRUNOL4: CUGBP elav-like family  
member 4

CACNA: calcium voltage-gated channel  
subunit alpha

CDA: cytidine deaminase

CDH: cadherin

CDKN: cyclin dependent kinase inhibitor

CDX2: caudal type homeobox 2

CHD: chromodomain helicase DNA binding  
protein

Chdh: choline dehydrogenase

CHFR: checkpoint with forkhead and ring finger domains

COMT: catechol-O-methyltransferase

CPLX2: complexin 2

CRABP2: cellular retinoic acid binding protein 2

CREB: CAMP responsive element binding protein

CSMD1: CUB and sushi multiple domains 1

CTCF: CCCTC-binding factor

CTNNB1: catenin beta 1

CXXC5: CXXC finger protein 5

Cyp: cytochrome P450 family

DAPK: death associated protein kinase

DCK: deoxycytidine kinase

DDX46: DEAD-box helicase 46

Dmgdh: dimethyl glycine dehydrogenase

DNAJB12: DnaJ heat shock protein family member B12

EPN2: epsin 2

ER $\alpha$ : estrogen receptor alpha

Elovl5: ELOVL fatty acid elongase 5

FAK: focal adhesion kinase

FAM49A: family with sequence similarity 49 member A

FANCF: FA complementation group F

FASN: fatty acid synthetase

FBXW11: F-box and WD repeat domain containing 11

FCGR2A: Fc fragment of IgG receptor IIa

FOXN3: forkhead box N3

FRMPD1: FERM and PDZ domain containing 1

Fzd: frizzled

G3BP1: G3BP stress granule assembly factor 1

G6pc: catalytic subunit of glucose-6-phosphatase

Gnmt: glycine-N methyltransferase

GLI: GLI family zinc finger

HAT1: histone acetyltransferase 1

HAUS6: HAUS augmin like complex subunit 6

HES1: Hes family BHLH transcription factor 1

HEY1: Hes related family BHLH transcription factor with YRPW motif

HIST1H2BK: H2B clustered histone 12

Hk: hexokinase

HOXA9: homeobox A9

HSPA2: heat shock protein family A member 2

IL2: interleukin 2

JADE2: Jade family PHD finger 2

Jag1: jagged 1

JMJD1: jumonji domain containing 1

KDM4C: lysine demethylase 4C

Ky: kyphoscoliosis peptidase

Lamc2: laminin C2

LAMTOR2: late endosomal/lysosomal adaptor, MAPK and MTOR activator 2

LIFR: LIF receptor subunit alpha

LPHN: adhesion G protein-coupled receptor

MAML2: mastermind like transcriptional coactivator 2

MAPK: mitogen-activated protein kinase

Mat2a: methionine adenosyltransferase 2A

MBD: methyl binding domain

MCU: mitochondrial calcium uniporter

MeCP2: methyl-CpG binding protein 2

METTL3: methyltransferase like 3

Mettl18: methyltransferase like 18

MGMT: O-6-methylguanine-DNA methyltransferase

MICU1:mitochondrial calcium uptake 1

MLH1: MutL homolog 1

MLL5: mixed lineage leukemia 5

MLLT3: MLLT3 super elongation complex subunit

MPZL1: myelin protein zero like 1

MYC: MYC proto-oncogene

MYT1L: myelin transcription factor like 1

NANOG: Nanog homeobox

NF1C: nuclear factor 1C

Nnmt: nicotinamide N-methyltransferase

NOS1AP: nitric oxide synthase 1 adaptor protein

NR3C1: nuclear receptor subfamily 3 group C member 1

NRF1: nuclear respiratory factor 1

NRF2: nuclear factor erythroid 2

OCT1: octamer-binding transcription factor 1	RASSF1A: Ras association domain family member 1
PAX9: paired box 9	RB: retinoblastoma
PBRM1: polybromo 1	RBPJ: recombination signal binding protein for immunoglobulin kappa J
Pc: pyruvate carboxylase	REST: RE1-silencing transcription factor
PEG3: paternally expressed 3	RPS6KA3: ribosomal protein S6 kinase A3
Pemt: phosphatidylethanolamine N-methyltransferase	RPTOR: regulatory associated protein of mTOR complex 1
PHF20: PHD finger protein 20	RRAGA: Ras related GTP binding A
Pklr: pyruvate kinase, liver and RBC	S100A5: S100 calcium binding protein A5
PLAU: plasminogen activator, urokinase	SALL3: sal-like 3
Pnpla: patatin-like phospholipase domain containing protein	SEMA3A: semaphorin 3A
PRDM16: PR/SET domain 16	SH3RF2: SH3 domain containing ring finger 2
PRDX6: peroxiredoxin 6	SHMT1: serine hydroxymethyltransferase 1
PRKCA: protein kinase C alpha	SIGMAR1: sigma non-opioid intracellular receptor 1
PTEN: phosphatase and tensin homolog	SIRT1: sirtuin 1
PTPRN2: protein tyrosine phosphatase receptor	Slc5a9: solute carrier family 5 member 9
PVT1: PVT1 oncogene	SMARCA4: SWI/SNF related, matrix associated, actin dependent regulator of chromatin
RACK1: receptor for activated C kinase 1	
RAR $\beta$ 2: retinoic acid receptor beta 2	
RASD1: Ras related dexamethasone induced 1	

SMCR8: SMCR8-C9orf72 complex subunit

Smo: smoothened

Spp1: secreted phosphoprotein 1

SRC: SRC proto-oncogene, non-receptor tyrosine kinase

SREBF1: sterol regulatory element binding transcription factor 1

STAT4: signal transducer and activator of transcription 4

SUV39H1: suppressor of variegation 3-9 homolog 1

TCF15: transcription factor 15

TERT: telomerase reverse transcriptase

Thbs1: thrombospondin 1

TLE1: TLE family member 1, transcriptional corepressor

TMEM91: transmembrane protein 91

UACA: uveal autoantigen with coiled-coil domains and ankyrin repeats

UBE2B: ubiquitin conjugating enzyme E2 B

UHRF1: ubiquitin like with PHD and ring finger domains 1

ZBTB20: zinc finger and BTB domain containing 20

ZNF36: zinc finger 36